CHEMICAL REVIEWS

pubs.acs.org/CR

Review

Zwitterionic Biomaterials

Qingsi Li,[○] Chiyu Wen,[○] Jing Yang,[○] Xianchi Zhou,[○] Yingnan Zhu, Jie Zheng, Gang Cheng, Jie Bai, Tong Xu, Jian Ji, Shaoyi Jiang,* Lei Zhang,* and Peng Zhang*

Cite This: *Chem. Rev.* 2022, 122, 17073−17154

Read Online

ACCESS | Metrics & More | Article Recommendations

ABSTRACT: The term "zwitterionic polymers" refers to polymers that bear a pair of oppositely charged groups in their repeating units. When these oppositely charged groups are equally distributed at the molecular level, the molecules exhibit an overall neutral charge with a strong hydration effect via ionic solvation. The strong hydration effect constitutes the foundation of a series of exceptional properties of zwitterionic materials, including resistance to protein adsorption, lubrication at interfaces, promotion of protein stabilities, antifreezing in solutions, etc. As a result, zwitterionic materials have drawn great attention in biomedical and engineering applications in recent years. In this review, we give a comprehensive and panoramic overview of zwitterionic materials, covering the fundamentals of hydration and nonfouling behaviors, different types of zwitterionic surfaces and polymers, and their biomedical applications.

CONTENTS

Received: May 25, 2022
Published: October 6, 2022

1. INTRODUCTION

Nonspecific adsorption of biomacromolecules onto material surfaces has remained a major issue in many biomedical applications, ranging from macroscale medical devices to nanoscale therapeutic/diagnostic materials.[1] For example, biofilm formation is believed to start with the adsorption of organic molecules onto the surface, followed by the attachment of bacteria and matrix formation, which further result in the failure of medical devices.[2,3] For biosensing and detection, nonspecific protein adsorption results in decreased signal/noise ratio and lower sensitivity.[4] In nanomedicine, proteins in the biological milieu tend to adsorb onto the surfaces of nanoparticles, forming a protein corona, which changes the physical–chemical properties and the *in vivo* fate of these particles.[5−7] Prevention of nonspecific adsorption by forming a nonfouling surface is key to overcoming these challenges.

Many hydrophilic surfaces are found to reduce nonspecific protein adsorption; however, only a few of them can prevent adsorption to the desired extent and be classified as nonfouling surfaces.[8] Even a small number of proteins adsorbed on a surface can lead to the propagation of unwanted fouling.[9] Nonfouling surfaces generally have strong interactions with water. Although there are other potential mechanisms, strong hydration effects are now considered as the main factor which determines the resistance to the protein adsorption.[10,11] Note that contact angle is not a good indicator for predicting the nonfouling property of a surface. Poly(ethylene glycol) (PEG) and its derivatives are the most well-studied nonfouling materials.[12] However, due to the intrinsic shortcomings of PEG, such as structural instability and immunogenicity, its applications in long-term and *in vivo* applications are greatly limited.[8,13,14] Zwitterionic polymers, containing both positively and negatively charged groups in their repeating units and exhibiting overall neutral charge, have drawn tremendous attention in the past two decades as the new generation of nonfouling materials. Different from PEG and PEG-like materials which bind water through hydrogen bonding, zwitterionic materials hold water more strongly through ionic solvation.[1,15−17] Moreover, there exist diversified zwitterionic molecular structures to accommodate various properties and applications.

Several types of zwitterionic materials have been extensively studied, including polybetaines, amino acid derived zwitterionic polymers, and mixed-charge/pseudozwitterionic polymers.[18−21] These polymers exhibit strong hydration capacities and have been applied in a wide range of biomedical applications, including biosensors, medical devices, cell encapsulations, drug delivery, protein modifications, etc.[8,22−29] Several excellent reviews already exist to introduce the basics of zwitterionic materials, including their synthesis and solution behavior,[21] surface hydration,[30] early applications,[31] and interaction with biomolecules.[32] This review aims to provide a comprehensive and panoramic overview of zwitterionic materials and to highlight their important developments and biomedical applications. We start in section 2 with an introduction of the basics of nonspecific protein adsorption. Next, we discuss the principles of the hydration phenomenon of zwitterionic materials and the related properties such as nonfouling, lubricative, and antifreezing. In section 3 we provide a discussion of different types of zwitterionic surfaces and polymers. Finally, in section 4 we showcase the representative, innovative cases of zwitterionic materials used in different biomedical applications. We conclude the review in section 5 with remarks on the potential for future development and challenges faced by this field of research.

2. NONSPECIFIC PROTEIN ADSORPTION, NONFOULING, AND HYDRATION

2.1. Protein Adsorption

Proteins are a type of biomacromolecule condensed from plenty of amino acids, and they are abundant in various biological environments. Nonspecific protein adsorption can occur on almost all surfaces that are in direct contact with protein-containing environments. However, this universal phenomenon has been a troublesome issue for many

https://doi.org/10.1021/acs.chemrev.2c00344
Chem. Rev. 2022, 122, 17073−17154

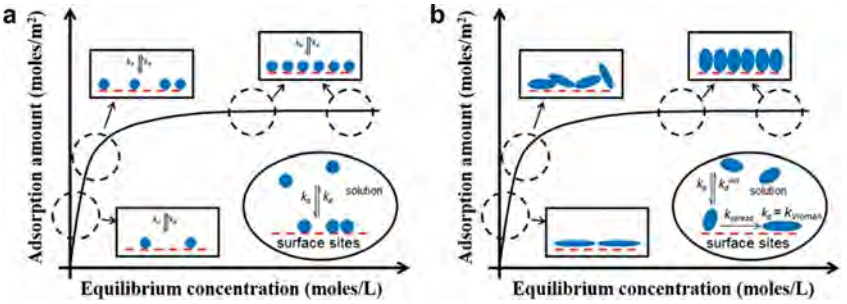

Figure 1. (a) Langmuir adsorption isotherm. (b) Protein adsorption with Langmuir-like behavior. k_a (L mol^{-1} s^{-1}) is the adsorption rate constant, k_d (s^{-1}) is the desorption rate constant, k_d^{init} (s^{-1}) is the initial desorption rate constant, k_{spread} is the spreading rate constant of adsorbed protein, and k_{Vroman} is the displacement rate constant of adsorbed protein by another protein from solution via the Vroman effect. Adapted with permission from ref 40. Copyright 2020 Academic Press.

biomedical and industrial applications, including sensors, medical implants, drug delivery vehicles, nanodiagnostic agents, blood purification materials, ship hulls, etc.[8,23,33−37] The reason is that protein adsorption is key and is the first step to initiating various severe biofouling events, including biofilm formation, thrombosis, foreign body reaction (FBR), protein corona and opsonization, marine fouling, etc. For example, even a small amount of adsorbed fibrinogen (7−10 ng cm^{-2}) can cause an unsatisfactory hemocompatibility, which can increase the morbidity and mortality rates of certain patients.[9,36] Therefore, the elimination of protein adsorption has been a crucial research topic.

It is generally acknowledged that the investigation of the protein adsorption mechanism contributes to overcoming the protein adsorption phenomenon. Protein adsorption often occurs in a very rapid manner (half of the equilibrium adsorption can be achieved within 1 s).[38] Once adsorbed, a protein can unfold its structure, change its conformation, and form a preferred orientation that can generate more favorable interaction with the surface. For example, fibrinogen prefers to expose its nonpolar/hydrophobic residues to a CH_3-terminated self-assembled monolayer (SAM) or expose its positively charged side chains to a COOH-terminated SAM.[39] The conformational changes of adsorbed proteins, even a small difference, can often cause changes in biological activity, thus determining different fates of biological responses.[40] For example, once fibrinogen is adsorbed on the polystyrene surface, its conformation can be changed to expose fragment D for antibody binding, which is correlated with platelet adhesion. In contrast, fibrinogen does not bind antibodies in the solution phase.[40] Hydrophobic−hydrophobic and electrostatic interaction have been considered as two major types of driving forces for protein adsorption.[41] Accompanied by these interactions, the surface releases its bound water molecules, largely increasing the system entropy. This dehydration and entropy gain can be considered as the intrinsic essence of protein adsorption mechanisms.[42,43]

Fundamental adsorption studies with single or complex protein solutions have found that, with the increase of protein concentration, the adsorption amount initially increases sharply but then typically achieves a plateau value of ∼0.1 to ∼0.5 μg cm^{-2} (Figure 1).[40,44,45] This observation means that the protein adsorption process typically presents a monolayer behavior. It should be noted that, although the monolayer adsorption behaves like Langmuir adsorption, it is not true Langmuir adsorption because the protein−protein interaction and protein unfolding should be considered.[40] Therefore, using the Langmuir model to investigate the protein adsorption mechanisms is erroneous. The monolayer adsorption mechanism is probably attributed to that the hydration layer of adsorbed proteins prevents the nonspecific adsorption of other proteins.[1] In certain experimental scenarios, proteins, such as albumin and casein, are used as blocking agents to decrease nonspecific adsorption.[1] This phenomenon indicates that adsorbed protein molecules themselves own reasonable protein resistance ability due to the retention of water molecules in their interface.

Apart from the monolayer feature, protein adsorption also shows a competitive behavior. Protein affinity and concentration are two factors affecting the competitive adsorption and the final composition of adsorbed protein on a surface. For example, the protein concentration in the plasma is in the order albumin > fibrinogen, but the protein affinity to the surface typically shows an inverse order (fibrinogen > albumin). As a result, the amount of adsorbed albumin is usually similar to that of fibrinogen once the equilibrium adsorption is reached.[40] In addition, the competitive process is dynamic. Usually, according to the law of mass action, the protein with the higher concentration tends to arrive at and attach to the surface first. Then, these protein molecules are gradually displaced by later proteins with higher surface affinities. This dynamic and competitive protein adsorption process is known as the "Vroman effect".[40] The Vroman effect indicates that protein molecules prefer to scramble for the sites on the material surface instead of nonspecifically attaching to the layer of the first adsorbed protein. The reason probably is that the bound water molecules are more easily released from the material surface but are more retentive on the adsorbed protein layer. As a result, the protein concentration and complexity also determine protein adsorption on surfaces.[46]

In addition to the protein characteristics, surface properties are another major factor influencing protein adsorption. It is well-known that a hydrophobic surface is more prone to adsorb proteins, whereas protein adsorption on a hydrophilic surface is usually relatively weak.[1,47] In addition, a hydrophobic surface tends to induce a higher degree of protein conformational change compared with a neutral hydrophilic surface.[40] The greater level of protein unfolding may initiate a more severe cell adhesion event. For example, a SAM surface with a terminal $-CH_3$ results in a higher degree of loss of α-helix in adsorbed fibrinogen than a surface with −OH, and it shows a stronger platelet adhesion.[48] Apart from the hydrophobic surface, a positively/negatively charged surface can also

https://doi.org/10.1021/acs.chemrev.2c00344
Chem. Rev. 2022, 122, 17073−17154

strongly adsorb proteins with negative/positive charges driven by ion−ion Coulombic interactions.[1]

2.2. Nonfouling Mechanisms

Protein adsorption is the first step of many biofouling events, including thrombosis, foreign body reaction (FBR), biofilm formation, etc. Therefore, the key to "nonfouling" is to inhibit the "origin" of biofouling: protein adsorption. Ostuni et al. has summarized four common properties of many nonfouling structures after a survey of their structure−property relationships: hydrophilicity, electric neutrality, and containing hydrogen-bond acceptors but not hydrogen-bond donors.[49] While the first three factors are well-recognized, hydrogen-bond donors are more complicated as many hydroxyl group rich materials demonstrate good nonfouling properties. A typical example of nonfouling material is PEG, which is neutral and hydrophilic. The repeating unit of PEG (−C−O−C−) binds water molecules via hydrogen bonding. The nonfouling mechanism of PEG is considered to be "osmotic repulsion" (resistance of PEG molecule to release both bound and free water molecules from its polymer coil) and "elastic network resistance" (or called "entropic repulsion", which describes the resistance of the PEG coil to compression due to its tendency to keep a more expanded state).[1] Later, it was demonstrated that chain conformational flexibility was not required for nonfouling surfaces with a strong hydration effect.[11] As a general rule, the entropic gain of released water from the surface (dehydration) and the enthalpy loss due to cation−anion attractive interactions between ionic protein groups and surface groups are the main factors in favor of protein adsorption. The retention of water molecules on the hydrophilic surface (hydration), as well as entropic and osmotic repulsion of the polymer coils, contributes to protein adsorption resistance.[1]

Different from PEG, zwitterionic material interacts with water molecules through electrostatically induced hydration (or ionic solvation), forming a strong hydration layer on the material surface.[15,17] A study on phosphorylcholine (PC) SAMs showed that strong resistance to protein adsorption could be achieved even on a rigid surface, proving that strong hydration capacity via electrostatic interactions is the key factor for the nonfouling property of zwitterionic materials.[10] Although positively or negatively charged surfaces can also bind water through ionic solvation, they adsorb charged proteins through electrostatic attractions. As a result, balanced charge and minimized dipole are two prerequisites for polyelectrolytes to have nonfouling behavior. In addition, a more recent study emphasized that the antipolyelectrolyte effect (APE) of zwitterionic materials could increase hydration and improve nonfouling performance.[50] To validate the theoretical explanation of the protein resistance effect induced by surface hydration of zwitterionic materials, both experimental and computational studies were extensively conducted.

2.3. Experimental Studies of Surface Hydration

Many analytical tools have been used to study the hydration effect of zwitterionic materials, including X-ray photoelectron spectroscopy (XPS),[10] contact angle (CA) goniometry,[51] atomic force microscopy (AFM),[51] differential scanning calorimetry (DSC),[52,53] Raman spectroscopy,[54] infrared (IR) spectroscopy,[53−56] and sum frequency generation (SFG) vibrational spectroscopy.[57] These techniques characterize the water/material/protein interaction directly or indirectly by measuring the changes in both chemical and physical properties, providing evidence to elucidate the mechanism of nonfouling behavior.

Contact angle measurement is the easiest way to characterize the hydrophilicity of a surface. For example, the SAMs prepared from phosphorylcholine showed a low water contact angle of only ∼17°.[10] However, this measurement does not reflect the binding strength and the structure of water on the hydrated surface. When characterizing the PC SAMs using XPS, it was found that the oxygen contents were much higher than the theoretical value, indicating that tightly associated water molecules remained even under a high vacuum. Morisaku et al. used DSC to study the hydration phenomenon of poly(2-methacryloyloxyethyl phosphorylcholine (PMPC) hydrogels.[52] From the results of the enthalpy change associated with the ice-to-water transitions, the water in the hydrogels can be classified into two states: freezable and nonfreezable water. The nonfreezable water corresponds to the water molecules that bonded to the polymer chains via electrostatic interaction as well as hydrogen bonds. Compared with poly(methoxy oligo(ethylene glycol)-monomethacrylate (p(Me(EG)$_n$MA)) hydrogels, PMPC hydrogel possessed higher contents of nonfreezable water, indicating its stronger hydration ability. The higher nonfreezable water content was also correlated with a better nonfouling performance.

Raman, attenuated total reflection infrared (ATR-IR), and transmission IR spectroscopies have been used to study the water structure in the vicinity of zwitterionic materials, including PMPC, poly(sulfobetaine) (PSB), poly(carboxybetaine)s (PCBs), polyampholytes, etc.[54−56,58−61] Results suggested that the hydrogen-bonded network of water molecules in the hydration shell was not significantly disturbed by zwitterionic materials. In contrast, the network structures of water in the neighborhood of hydrophobic poly(methyl methacrylate) (PMMA) and poly(*n*-butyl methacrylate) (PBMA) were significantly perturbed.[56,61] The studies also demonstrated a strong correlation between biofouling and the perturbation of water structure in the hydration layer.

SFG vibrational spectroscopy is an intrinsically surface-sensitive method that provides information about chemical structures at a molecular level. Leng et al. used SFG vibrational spectroscopy combined with isotopic dilution to measure the surface hydration of three zwitterionic polymers, i.e. poly(carboxybetaine acrylamide) with one carbon spacer between the two opposite charges (PCBAA1), PCBAA with two carbon spacers (PCBAA2), and poly(sulfobetaine methacrylate) (PSBMA), in comparison with that of PEG, poly(ethylene terephthalate) (PET), and poly(methyl methacrylate) (PMMA) (Figure 2a).[62] Isotopic dilution enabled interfacial SFG water spectra to be better interpreted. Water peaks in SFG measurements could appear around 3200 and 3400 cm^{-1}, representing the strongly and weakly hydrogen-bonded water molecules, respectively. The zwitterionic polymers mainly showed a peak around 3200 cm^{-1} (Figure 2b, left).[57] In contrast, the SFG spectra of PEG showed not only a strong peak around 3200 cm^{-1} but also a shoulder around 3400 cm^{-1} (Figure 2b, left).[57] These results indicated that zwitterionic polymers formed stronger hydration than PEG because the electrostatic attraction could enhance the hydrogen bonds between water molecules and hydrophilic charged groups in zwitterionic materials.[62] This strong hydration of zwitterionic materials is key to their nonfouling properties. For the relatively hydrophobic PET and PMMA that are not

https://doi.org/10.1021/acs.chemrev.2c00344
Chem. Rev. 2022, 122, 17073−17154

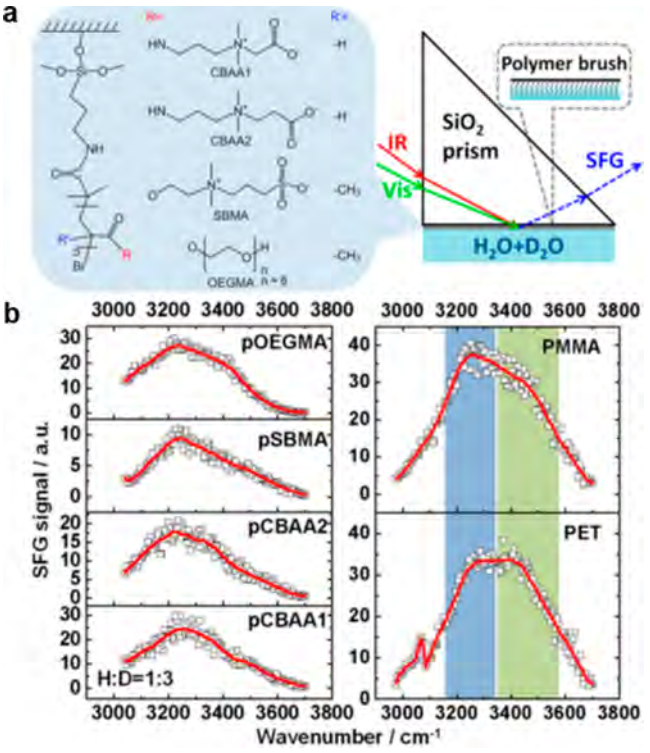

Figure 2. Study of hydration effects of zwitterionic surfaces using SFG vibrational spectroscopy combined with isotopic dilution. (a) Schematic illustration of SFG measurement and chemical structures of polymers. Reproduced from ref 62. Copyright 2015 American Chemical Society. (b) SFG spectra of pOEGMA, pSBMA, pCBAA2, pCBAA1, PMMA, and PET surfaces. Reproduced with permission from ref 57. Copyright 2016 Elsevier.

nonfouling, the weakly hydrogen-bonded interfacial water molecules generated strong SFG signals around 3400 cm^{-1} (Figure 2b, right).[57]

SFG is a powerful tool for studying the *in situ* and real-time interaction between protein, water, and materials.[57] In a real-time assessment of the surface hydration of the PSBMA and poly(oligo(ethylene glycol) methacrylate) (POEGMA) polymer brushes in contact with proteins, a majority of strongly hydrogen-bonded water was observed at both PSBMA and POEGMA surfaces.[63] However, upon contact with proteins, the water ordering at the POEGMA surface was disturbed, while the surface hydration of PSBMA remained unaffected. The effects of free sulfobetaine (SB) and PEG on the hydration layer of protein molecules were also investigated. The results demonstrated that free SB molecules could strengthen the protein hydration layer, but free PEG chains greatly disrupt the protein hydration layer and likely directly interact with the protein surfaces. This direct evidence demonstrates that ionic-solvation-induced hydration is stronger than hydrogen-bonding-induced hydration, and this superior hydration property results in excellent nonfouling properties of zwitterionic materials.[63]

2.4. Computational Studies of Surface Hydration and Data-Driven Design

While extensive experimental studies have claimed that the interactions between zwitterionic materials and foulants are key to understanding nonfouling mechanisms and are likely caused by the hydration structure and dynamics of zwitterionic materials, it still remains a great challenge to quantify the changes in the dynamic and interactive behaviors of zwitterionic materials, interfacial water, and protein conformation/orientation at the polymer/water/protein interface by experiments. Parallel to experimental works, a large number of computational studies, including quantum mechanics, molecular dynamics (MD), Monte Carlo (MC) simulations, and molecular docking, enable revealing the interaction, dynamic, and structural changes of proteins, surfaces, waters, and ions for a wide variety of zwitterionic material−protein systems at electronic, atomic, and coarse-grained (CG) resolution levels.[64] Generally speaking, MD simulations enable exploration of the interaction, structural, and dynamic changes of all components (e.g., proteins, surfaces, water, ions) at the local energy minimum under different conditions in relation to nonfouling mechanisms. MC simulations are used to determine the optimal orientations of proteins upon adsorption on surfaces. Both MD and MC simulations allow the study of the individual zwitterionic materials systems in a "one-at-a-time" manner, thus lacking a data-driven capacity for rapid prediction of a large number of zwitterionic materials from a given database or for building a broad data set by examining enough materials, due to high computational expense. Molecular docking allows the achievement of rapid and large-scale screening of the most energy favorable adsorption ensembles of proteins on surfaces, but it lacks the dynamic details and environmental effects on binding complexes.

While the time scale and length scale of the current simulations are still common roadblocks to directly mimicking realistic nonfouling experiments for zwitterionic materials and surfaces, the continuous innovations, advances, and integration of both algorithms and hardware make it possible to bridge this gap. From a hardware viewpoint, the high degree of implementation of graphics processing unit (GPU) accelerated algorithms in different simulation packages (CHARMM, GROMACS, and NAMD) greatly speeds up the massively parallel computing for the above-mentioned simulation techniques, leading to a performance gain of 10−100 times faster than the conventional CPU implementations. Apart from hardware innovations, different accelerated simulation algorithms, including (i) enhanced sampling protocols (steered MD, replica-exchange MD), (ii) multiscale models integrating the information from atomic, CG, and theoretical simulations, and (iii) integration of specific simulation codes into computer chips (Anton supercomputer), have been continuously developed, evolved, and applied to study different aspects of protein interactions with zwitterionic materials in solution and on surfaces.

2.4.1. Mechanical Understanding of Zwitterionic Materials from Molecular Simulations. Different from direct observation and qualification of protein adsorption on any nonfouling surface (not only limited to zwitterionic surfaces) by experiments, molecular simulations, from a different angle, enable the quantitative capture of subtle structural, dynamic, and interaction changes of a given zwitterionic material/surface under different conditions, with the goals of better understanding the component- or structure-dependent nonfouling properties at atomic length and time scales. Current molecule simulations (quantum mechanics, MD, and MC) of zwitterionic materials can be generally grouped into two families by studying (i) the zwitterionic monomers, oligomers, or polymers themselves in aqueous solutions and (ii) zwitterionic material coated surfaces in the

https://doi.org/10.1021/acs.chemrev.2c00344
Chem. Rev. 2022, 122, 17073−17154

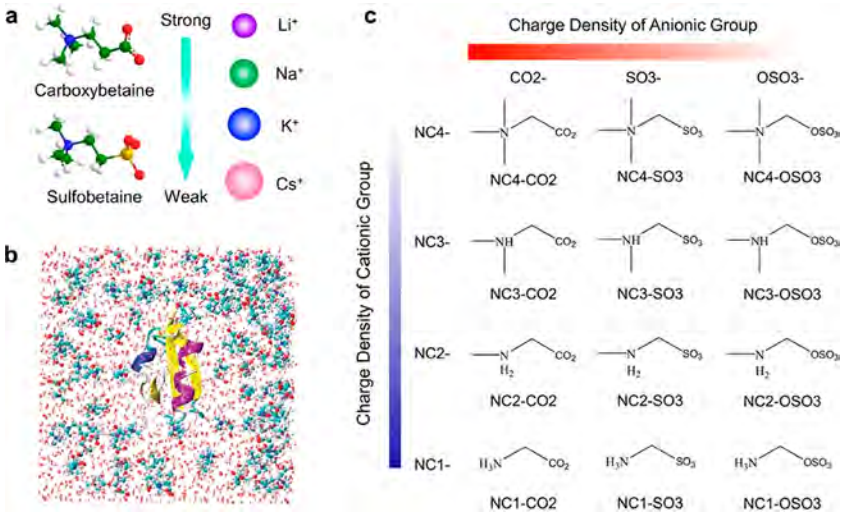

Figure 3. Molecular simulations of zwitterionic materials in aqueous solution. (a) Highly hydrated carboxybetaine (CB) and sulfobetaine (SB) monomers with different association strengths with different ions. Adapted from ref 66. Copyright 2011 American Chemical Society. (b) CB monomer interactions with a chymotrypsin inhibitor 2 protein. Reproduced with permission from ref 68. Copyright 2012 AIP Publishing. (c) Twelve zwitterionic monomers as constructed from different combinations of anionic and cationic groups, each with distinct hydration free energy, structure, and dynamics. Adapted from ref 67. Copyright 2014 American Chemical Society.

absence and presence of proteins. Given diverse zwitterionic materials being simulated in bulk solution and on surfaces, it is not a surprise that they have different modes to interact with water, proteins, and organisms; i.e., the commonality and differences between bulk and surface hydrations, as derived from both types of simulations, allows the collection of a comparative benchmarking data set for better assessing the component−structure−property−performance relationship of zwitterionic polymers under different conditions.

2.4.1.1. Molecular Simulations of Zwitterionic Materials in Aqueous Solution. Starting from simulating small zwitterionic monomers and oligomers in aqueous solution,[15] representative MD simulations of zwitterionic carboxybetaine (CB) and SB monomers showed that both CB and SB monomers exhibited lower hydration free energies than typical nonfouling OEG monomers.[65] They also showed differential hydration behaviors: (i) CB monomers attracted fewer water molecules but with a much stronger binding affinity than SB monomers and (ii) CB monomers tended to interact strongly with smaller kosmotropic cations (Li^+ and Na^+) while SB monomers associated more strongly with large chaotropic cations (K^+ and Cs^+) (Figure 3a),[66] indicating that the distinct ionic solvation can greatly improve the hydration property to different extents. Later, a more systematic simulation study was carried out to assess and compare the hydration structures, dynamics, and free energies of 12 zwitterionic monomers derived from anionic groups (carboxylic, sulfonate, and sulfate) and four cationic groups (quaternary ammonium, tertiary ammonium, secondary ammonium, and primary ammonium) (Figure 3c).[67] Overall, all 12 zwitterionic monomers (−238 to −303 kJ/mol) had lower hydration free energies than ethylene glycol (EG4) monomers (−180 kJ/mol), indicating that ionic-induced hydration in these zwitterionic monomers has more favorable interactions with water molecules than hydrogen-bond-induced hydration in the hydrophilic monomer. More importantly, due to different chemical structures and ionic pairs, both anionic and cationic groups displayed different trends in their hydration free energies; i.e., anionic groups were ranked in the decreasing order OSO_3 > SO_3 > CO_2, while cationic groups did not show any obvious trend. Regarding the hydration structural and dynamic properties of these zwitterionic monomers, overall hydration properties of zwitterionic monomers were more sensitive to anionic groups than to cationic groups. Finally, NC4-CO2 and NC3-CO2 monomers were found to have the highest hydration and the least self-association properties, both demonstrating their strong but unfavorable interactions with a model protein. This information provides critical design guidance for zwitterionic materials; i.e., engineering/modifications of anionic groups would be more effective in optimizing hydration free energy and nonfouling efficacy than those of cationic groups.

One further step is to expand the simulation systems from zwitterionic monomers in bulk solution to zwitterionic material−protein systems and zwitterionic surfaces in an aqueous solution. Accordingly, a 64-residue CI2 protein was introduced to a monomeric CB solution, with a specific focus on CB−protein interactions by considering the hydration effect of CB and the folding structure of chymotrypsin inhibitor 2 (CI2) (Figure 3b).[68] Results showed that highly hydrated CB had repulsive interactions with CI2 as evidenced by nonobservable adsorption of CB on the CI2 surface. The presence of CB monomers did not alter the biologically activated CI2 structure, another indicator of the inertness of CB. Moreover, CB brushes with varying carbon spacer length (CSL) between the quaternary ammonium cation and carboxylic anion were constructed and studied for their hydration properties by using a combination of quantum mechanics and MD simulations.[69] Simulations showed a strong structural-dependent hydration property of CB brushes; i.e., an optimal CSL of 6−8 was observed to achieve the strongest hydration, while a too short or too long CSL led to significant and sudden dehydration of CB brushes, indicating that the strong hydration of zwitterionic groups and the dehydration of hydrocarbon backbones are the two dominant but competing factors to control the overall hydration property at different CSL values. Simulation results also provided additional design guidance that subtle structural changes in zwitterionic pendant

https://doi.org/10.1021/acs.chemrev.2c00344
Chem. Rev. 2022, 122, 17073−17154

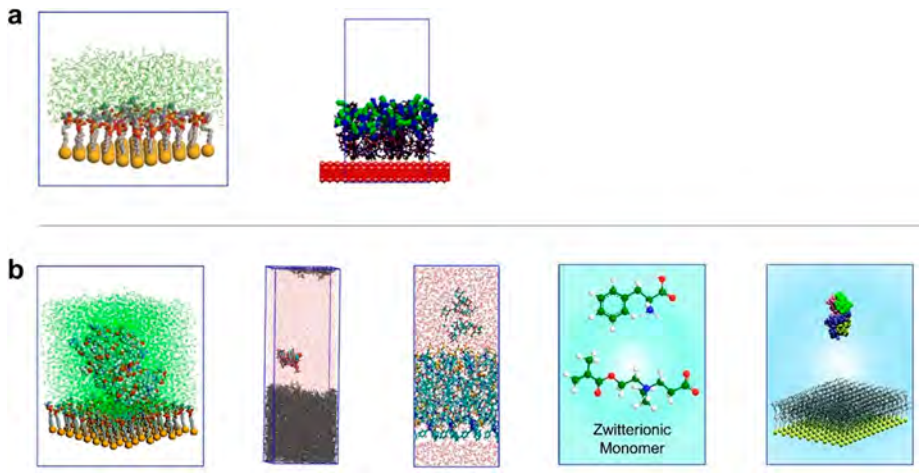

Figure 4. Typical simulation models and molecular simulations of zwitterionic-materials-coated surfaces. (a) MD simulations of phosphorylcholine SAMs,[70] and PSKE (lysine and glutamic acid inserted polysarcosine) brush,[72] without any foulant (protein). Adapted with permission from ref 70. Copyright 2006 AIP Publishing. Adapted from ref 72. Copyright 2019 American Chemical Society. (b) MD simulations of phosphorylcholine SAMs with lysozyme,[76] PVDF-*g*-DMAPS with sodium alginate,[77] SB brush with alginate gel,[78] CB-derived CMB surface with different amino acids,[79] and poly(CBMA) brush with a lysozyme.[80] Adapted from ref 76. Copyright 2008 American Chemical Society. Adapted from ref 77. Copyright 2019 American Chemical Society. Adapted from ref 78. Copyright 2018 American Chemical Society. Adapted from ref 79. Copyright 2012 American Chemical Society. Adapted with permission from ref 80. Copyright 2020 Royal Society of Chemistry.

groups but the same polymer backbone can greatly enhance the nonfouling performance.

2.4.1.2. Molecular Simulations of Zwitterionic-Materials-Coated Surfaces. The early molecular simulations in the 2000s mainly focused on the interfacial water behaviors on short PC-terminated self-assembled monolayers (PC-SAMs) in the absence of proteins (Figure 4a, left),[70] partially due to the simplicity of simulation systems and less computational cost. MD simulations showed that PC-SAMs can strongly interact with water molecules around their zwitterionic head groups to form a tightly bound, structured water layer, suggesting that such a strong hydration layer would produce a physical and energetic barrier to resist protein adsorption. Later, apart from PC-SAMs, CB- and SB-terminated SAMs were constructed and studied for the structure and dynamics of interfacial water near the zwitterionic SAMs.[71] The three types all formed two hydration layers near the zwitterionic SAM surfaces via strong ionic interactions, which were more stable than a thin and single layer via weaker hydrogen bonding on the hydrophilic PVA surface.

To expand the surface hydration hypothesis from short-chain SAMs to long-chain polymer-grafted surfaces, molecular modeling methods were further evolved to study the much more complex polymer-grafted surfaces with or without a foulant or a protein. Different from ideal SAM surfaces formed by well-ordered, short, and rigid chains with almost no conformational changes, polymer-grafted surfaces formed by long-chain polymers usually undergo large conformational changes, which are affected by grafting density, chain length, and end-group hydrophobicity of grafting polymers. Starting with pure polymer-grafting surfaces, several MD simulations were set up and conducted to study the hydration properties of different polymer-grafted surfaces/brushes in response to chain length, conformation, flexibility, grafting density, and end-group hydrophobicity without a foulant.[72−75] MD simulations of zwitterionic peptoid polymer brushes showed that the low or intermediate grafting density not only facilitated the extended chain conformations and flexibility that promote water density around peptoid brush, but also minimized the surface dipoles that suppress electrostatic interactions with proteins, each of which is a key contribution to the nonfouling efficacy of surfaces (Figure 4a, right).[72] However, high grafting density caused the reduction of surface hydration and chain flexibility, due to the steric effect. Consistently, another set of MD simulations of methyl- and ethyl-substituted poly(2-oxazoline) (MPOX and EPOX) brushes grafted on silica surfaces revealed that both MPOX and EPOX brushes with low grafting density exhibited significantly higher levels of surface hydration than PEG brushes,[73] as indicated by the higher chain flexibility, more hydrogen bonds formed at the interface, and low water contact angles. Instead, higher grafting densities of MPOX and EPOX brushes caused a decrease in chain dynamics and an increase in surface hydrophobicity, rendering the brushes to be more prone to fouling as explained by Kitano theories.

While the above-mentioned simulations highlight the importance of the dynamics and structure of grafted polymer chains in surface hydration, different simulation studies do not adequately explain the surface hydration as caused by different grafting densities. On the other hand, these simulations do not directly study protein adsorption on zwitterionic surfaces due to the absence of proteins. Thus, further investigation of protein adsorption on these surfaces is necessary to reconcile the structure−property relationship between the structural characteristics of grafting polymers and the dynamics of the hydration layer at polymer/water interfaces. The presence of a protein in zwitterionic surface systems allows for computational examination of the protein-induced entropic changes in interfacial water molecules and polymer chains, which have not been considered in nonfouling simulations without proteins but are important for the nonfouling efficacy associated with the direct surface resistance to proteins.

To better simulate the protein resistance to any zwitterionic surfaces by MD simulations in a more efficient and realistic way, two computational strategies are often used to construct protein−surface systems in the presence of water and ions and to simulate the systems using different algorithms. The first strategy is to construct a preadsorption of protein on a surface

https://doi.org/10.1021/acs.chemrev.2c00344
Chem. Rev. 2022, 122, 17073−17154

by placing the protein right above the surface with a separation distance of less than the van der Waals cutoff value (<10−12 Å). This protein preadsorption model allows identifying a surface with a strong protein resistance ability if the protein rapidly desorbs from the surface within a typical time scale of MD simulations (∼100 ns). As an early example, a lysozyme was introduced and preadsorbed onto PC-SAMs for studying the surface hydration effect on protein interactions with PC-SAMs (Figure 4b).[76] The results showed that (i) the tightly bound water layer above the PC-SAM surface generated a strong repulsive force on the protein to prevent its adsorption on the surface and (ii) the strong repulsive force mainly stemmed from a tightly bound water layer (90%), instead of from the surface.

The use of conventional MD simulations in the first strategy cannot directly and adequately simulate the protein adsorption process due to time scale and length scale issues. To address this issue, the second strategy is to use state-of-the-art potential-mean-force MD (PMF-MD) simulations, combining the adaptive biasing force method and umbrella sampling protocol, to probe a complete adsorption process of a protein on polymer brushes. During this adsorption process, a harmonic potential with an adaptive biasing force is applied to the center of mass (COM) of the protein, but still allowing it to rotate freely, to pull it from the bulk solution toward the polymer brush. PMF profiles are calculated to assess free energy barriers using the effective umbrella sampling at every distance between the COM of the protein and the polymer brush, in which a complete protein−surface energy landscape is mapped out to determine different surface adsorption/resistance scenarios. Due to the complex and time-consuming natures of PMF-MD simulations for multicomponent zwitterionic−protein−water−ion systems, only several PMF-MD simulations were reported to study the adsorption of a foulant or protein on different SAMs and polymer-grafted surfaces. PMF-MD simulations of zwitterionic-modified PVDF membranes (PVDF-*g*-DMAPS) in the presence of sodium alginates showed that the increase of grafting density of zwitterionic DMAPS triggered the two synergistic effects of a stable hydration layer and strong electrostatic repulsion at the membrane interfaces to enhance surface resistance to sodium alginates (SAs) (Figure 4b).[77] Specifically, at the membrane interface, the stable ionic hydration layer prevents hydrophobic groups of SAs from adhering to the hydrophobic backbone of PVDF near the membrane surface, while two cationic layers around the membrane surface and SA further induce additional energy barriers to repel SAs from the membrane surface via strong electrostatic repulsion. Another set of typical PMF-MD simulations was conducted to study the surface resistance and hydration of SB and PEG brushes at different grafting densities in the presence of a foulant of alginate gel (Figure 4b).[78,81] Comparative PMF profiles showed that, when the alginate gel approached SB brushes, repulsive forces not only increased dramatically but also depended on SB grafting densities. The high grafting density led the surface-induced repulsive force to appear earlier and stronger due to the compression of this hydration layer. Similar PMF profiles but with fewer energy barriers confirm the existence of the hydration layer at the water/membrane interface for generating strong repulsive forces, regardless of surface chemistry and grafting density. Consistently, another PMF-MD study reported the free energy profiles of different amino acids (glycine, phenylalanine, asparaginic acid, and lysine) approaching zwitterionic surfaces made of CB derivatives (CMB) (Figure 4b).[79] It was found that, when the four types of residue approached a CMB surface, they all displayed similar flat PMF profiles, regardless of their hydrophobicity, acidity, and size, indicating a high free energy barrier at the water/CMB interface to prevent the residues from adsorption. Recently, a combination of molecular mechanics (MM), MC, MD and steered MD (SMD) simulations were performed to study the packing structures, surface hydration, and nonfouling properties of three zwitterionic poly(carboxybetaine methacrylate) (PCBMA), PSBMA, and PMPC brushes with and without a lysozyme (Figure 4b).[80] While all three zwitterionic brushes exhibited stronger interactions with water molecules and higher surface resistance to a protein than the PEG brush, repulsive forces acting on a lysozyme from the brushes were shown in the decreasing order PCBMA > PMPC > PSBMA > PEG, consistent with the surface hydration order. Simulations also revealed that both the CSL between zwitterionic groups and the nature of the anionic groups play major roles in electrostatic potentials, hydrogen bonding, structuring, and stability of water around the surfaces, explaining different surface resistant properties (nonfouling efficacy).

Both computational strategies enabled circumventing the time scale of conventional MD simulations, thus leading to one more step toward better mimicking nonfouling experiments. The above-mentioned simulations, despite their differences in zwitterionic materials and simulation setups, showed similar interfacial water behaviors on different zwitterionic surfaces. Apart from strong interactions with zwitterionic surfaces, the interfacial water molecules exhibited structural and dynamic properties that were completely different from those of bulk water. Dynamically, interfacial water molecules significantly slowed down their movements as evidenced by a large decrease in residence time and self-diffusion coefficient. Structurally, while it is generally accepted that competition between water and protein for occupying the interface is critical for reducing the free energy of protein adsorption at solid−liquid interfaces, structured water at interfaces can also mediate protein adsorption. High amounts of interfacial water molecules around these zwitterionic groups reoriented themselves to accommodate the ionic solvation nature around zwitterionic head groups. As a result, these water molecules involving strong ionic solvation on zwitterionic surfaces preferred to stay longer and are bound stronger at the interface. Taken together, all of these computational studies have shown that, while these zwitterionic materials are highly hydrated, their local hydration properties are different from each other, leading to their different interactions with proteins. This indicates that surface hydration is attributed to multiple factors from the physicochemical properties of materials (i.e., chemical structure, hydrophobicity, charge distribution, molecular weight), surface properties (i.e., packing density, film thickness and roughness, chain conformation), and interfacial properties (i.e., interfacial water structures and dynamics of interfacial waters, materials, and ions). Moreover, it is worth noting that zwitterionic and electrolyte monomers/polymers are often reported to have a tendency to associate with each other via charge and dipole interactions, which can compete with ionic solvation. Thus, the self-association of zwitterionic materials can further influence their ionic hydration (e.g., SB-based materials).[15]

2.4.2. Data-Driven Design of Zwitterionic Materials from Machine Learning. Despite significant progress in the

https://doi.org/10.1021/acs.chemrev.2c00344
Chem. Rev. 2022, 122, 17073−17154

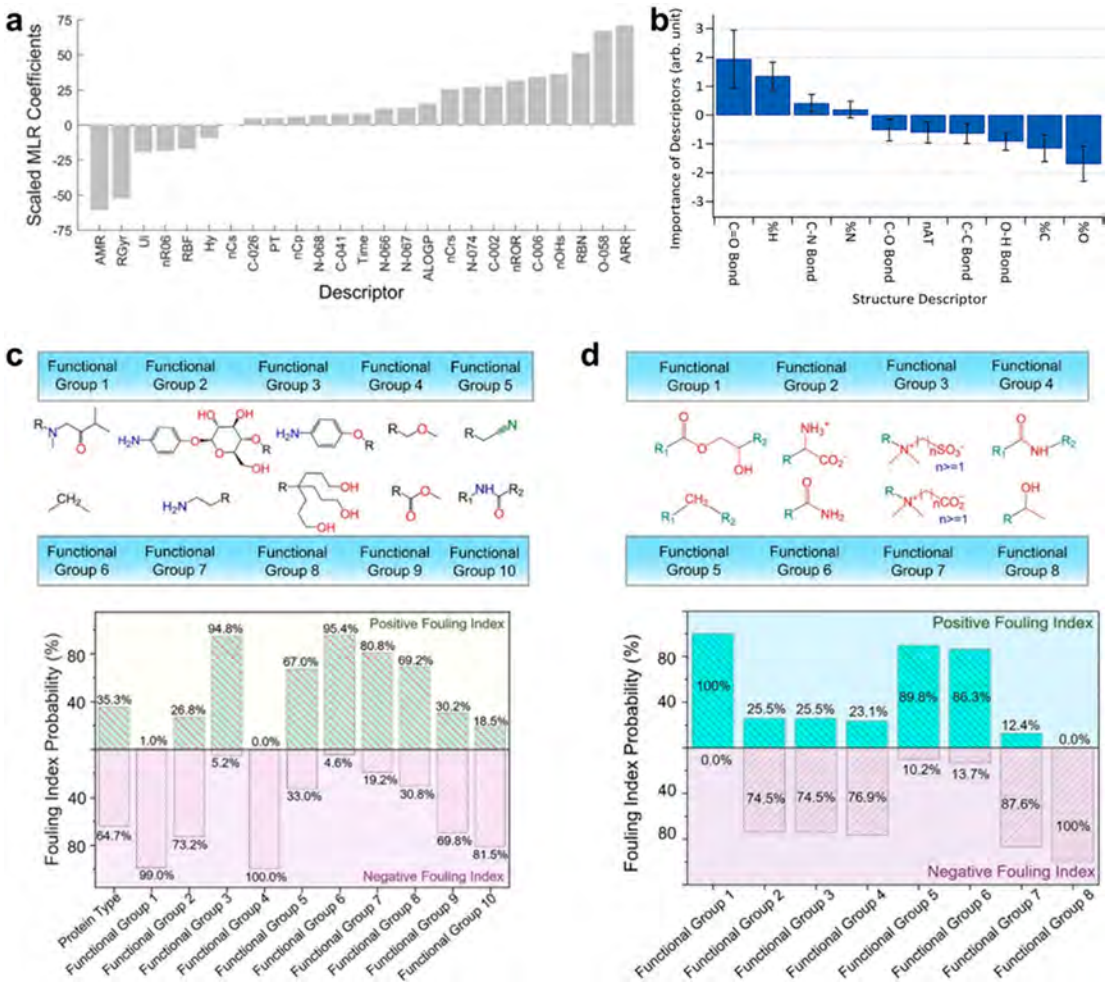

Figure 5. Different machine-learning models for assessing protein adsorption ability of existing and new nonfouling SAMs and polymer brushes. (a) The most relevant descriptors for their contributions to the predicted protein adsorption (%ML) on SAMs by an MLREM model. Reproduced with permission from ref 95. Copyright 2019 Springer Nature. (b) Important structural descriptors to predict fibrinogen adsorption on SAMs by an ANN model. Adapted from ref 96. Copyright 2020 American Chemical Society. Fouling index probability (%) of functional groups for predicting protein resistance and protein adsorption (c) on SAMs by an FAFG−ANN model[97] and (d) on polymer brushes by an SVR model.[98] Adapted from ref 97. Copyright 2021 American Chemical Society. Adapted with permission from ref 98. Copyright 2021 Elsevier.

synthesis, applications, and understanding of different zwitterionic materials, the most effective zwitterionic materials are still largely derived from three common CB-, SB-, and PC-based motifs. On the one hand, different zwitterionic polymers are different in chemistries and structures, but all of them are highly hydrated and resistant to different foulants. On the other hand, even small changes in the structures (e.g., CSL, pendant group, and charge type/pair/distribution) of zwitterionic materials can lead to large property changes in hydration structures, hydration dynamics, and degrees of interactions with water molecules and foulants, showing a strong structural dependence on nonfouling efficacy. Major challenges still remain to achieve a rational or structural-based design of new effective nonfouling materials. While the machine-learning-based or data-driven-based methods have been commonly used for drug discovery,[82,83] disease diagnosis,[84] solid functional materials (batteries,[85,86] catalysts,[87] nanoparticles,[88] and semiconductors[89,90]), very few studies, until recently, have been reported to develop data-driven models for the rational design of soft materials (not limited to zwitterionic materials), mainly due to the lack of high-quality data at both structure and property levels.

Currently, since there are no existing nonfouling databases available for nonfouling materials, it requires collecting experimental data from the literature to construct nonfouling databases for different data-driven models. But the multilab data set often contains some erroneous or inconsistent entries due to the variation of the experimental conditions and measurements. To address this issue, a very limited number of quantitative structure−property/activity relationship (QSPR or QSAR) studies,[91] as assisted by machine-learning algorithms, have been reported to assess the nonfouling properties of different materials and coatings, including (i) QSPR models to assess the overall antisettlement activity of chalcone derivatives against *Mytilus galloprovincialis* larvae,[92] (ii) QSAR models to evaluate the inhibition activity of gramine compounds against *E. coli* growth,[93] and (iii) genetic algorithm−multiple linear regression based QSAR models to predict the fouling-release activity of amphiphilic polysiloxane-based polymer coatings for different marine fouling organisms (bacteria, algae, and barnacles).[94] The above-mentioned QSAR/QSPR studies, despite being very few to date, are exclusively built on very few compounds (i.e., five to nine data sets) with similar structures and chemistry; thus it is difficult to

https://doi.org/10.1021/acs.chemrev.2c00344
Chem. Rev. 2022, 122, 17073−17154

derive or extrapolate the composition−structure−property relationship of different or new nonfouling materials.

Until very recently in 2019−2021, three different QSAR models, including (i) descriptor-based linear (MLREM) and nonlinear (BRANNGP and BRANNLP) models,[95] (ii) descriptor-based artificial neural network (ANN) models,[96] and (iii) functional-group-based ANN models, were developed with the use of the same protein adsorption data set of SAMs from the Whitesides group,[49] and they were used to evaluate protein adsorption on both existing and newly designed SAMs.[97] As compared to previously mentioned small data sets, the Whitesides data set contains a total of 96 protein adsorption data, i.e., two different proteins of lysozyme and fibrinogen being adsorbed on 48 SAMs terminated by hydrophilic groups of hydroxyl, amide, acrylate, ether, and ethylene glycol and zwitterionic groups of carboxylic, sulfonate, sulfate, and quaternary/tertiary/secondary/primary ammonium. In this data set, the large structural diversity of SAMs and the highly reliable protein adsorption data from the same lab make them a robust source developing machine-learning models for studying and understanding the adsorption of proteins on surfaces. The first two machine-learning models,[95,96] built on conventional descriptors, mainly focus on the evaluation of the nonfouling property of any given material and surface, instead of the design of original nonfouling materials and surfaces. For instance, in the MLREM, BRANNGP, and BRANNLP models in 2019,[95] ARR (assigning to aromatic groups), N-074 (nitriles), nOHs (hydrogen-bond-donating secondary alcohols), and N-066 and N-067 (NHR_2 groups) descriptors were considered as positive contributors to promote protein adsorption, while AMR (associated with ligand size and polarizability), RGyr and RBF (conformational flexibility of chains), nR06 (number 6 aromatic ring), and nonzero unsaturation indices were identified to suppress protein adsorption (Figure 5a). The second ANN modeling in 2020 used different descriptors to predict both water contact angle and protein adsorption on SAMs and to determine the importance of each structural parameter for the water contact angle and protein adsorption.[96] For instance, C═O bond in the terminal COOH group, C−N bond and %N in the terminal NH_2 group, and %H in a hydrogen-bond-donating group were critical factors for promoting protein adsorption, while C−O bond representing the number of sites for hydrogen bonding with water molecules, nAT as the total number of atoms, C−C bond representing the length of the alkyl chain, O−H bond in hydroxyl groups, %C in nonpolar methyl and alkyl chains, and %O representing proton acceptors acted as the important descriptors to reduce protein adsorption (Figure 5b). However, the descriptor-based models often lack a physical or chemical basis, making the design of original nonfouling materials not straightforward.

In 2021, a new data-driven, machine-learning model (FAFG−ANN), combining factor analysis of functional group (FAFG) with ANN algorithms, was developed to predict protein resistance on existing and newly designed SAMs.[97] Different from the descriptor-based models above, this model provided the functional-group-based design principle, making the design of new nonfouling materials very straightforward, e.g., the functional groups 1 (tertiary amine derivative), 4 (methyl-alkoxy ether), 9 (carboxy), and 10 (amide) were predicted to be the most promising groups for nonfouling materials (Figure 5c). More importantly, as guided by the model, we designed three new monomers with both fouling and nonfouling indexes and used them to prepare nonfouling coatings in the form of SAMs and polymer brushes. The resultant coatings with nonfouling indexes exhibited strong surface resistance to protein adsorption from undiluted blood serum and plasma, while the coating with fouling indexes promoted protein adsorption, validating the model predictions. Later, the Zheng lab improved and expanded the FAFG−ANN model from SAMs to polymer brushes.[98] They first assembled experimental data from the literature to construct this nonfouling polymer brush database, which can also be used for other purposes and researchers. Then, they developed two distinct machine-learning approaches for discovering the nonfouling potentials of any existing polymer brush by the descriptor-based ANN model and designing the new nonfouling polymer brushes by the group-based supporting vector regression (SVR) model (Figure 5d). Finally, as guided by both machine-learning models, they synthesized three different repurposed and two newly designed polymer brushes, all of which exhibited excellent surface resistance to protein adsorption from undiluted human blood serum and plasma, highly consistent with the predicted values from the models. It can be envisioned that these early and pioneering machine-learning studies will provide a basis to encourage more collaborations from both experimental and computational researchers to accelerate the discovery and understanding of functional materials (not only limited to zwitterionic materials). The ongoing efforts need to continuously and iteratively collect more reliable experimental data, incorporate more structural properties of materials/coatings, and train and optimize machine-learning models for high prediction accuracy and design efficacy of zwitterionic nonfouling materials.

From a computational viewpoint, significant advances in computer powers and simulation methodologies allow computational probing of the long-time and large-scale behaviors of protein−surface systems that are considered as some of the most complicated simulation systems. Considering that protein adsorption on zwitterionic surfaces involves the diverse structural and dynamic changes of proteins, surfaces, and water molecules and the complex adsorption/desorption pathways of proteins in solution and on surfaces, graph theory, which has been used in protein folding and aggregation on the cell membrane, can be transferred to study protein adsorption on surfaces. During the adsorption process, any intermediate state defines a structural and energetic node, while any edge connecting the two neighboring nodes defines an energy barrier for structural transitions or adsorption pathways. In this way, an ensemble of all possible intermediate states enables mapping out the multiple protein adsorption pathways with different probabilities from multiple atomistic or CG simulations. Currently, there has not been any report on such a computational approach combining graph theory and MD simulations. Different from atomic simulations, CG models and implicit solvent models provide a reasonable trade-off between accuracy and computational efficiency to explore the whole protein adsorption process at microsecond to millisecond time scales.[99−101] However, it still remains a state-of-art challenge to develop an accurate and transferrable CG force field to different protein−surface systems, because different simulation systems may require different CG resolutions, specific potential energy functions, and even biased sampling.[102] More importantly, recent advances in

https://doi.org/10.1021/acs.chemrev.2c00344
Chem. Rev. 2022, 122, 17073−17154

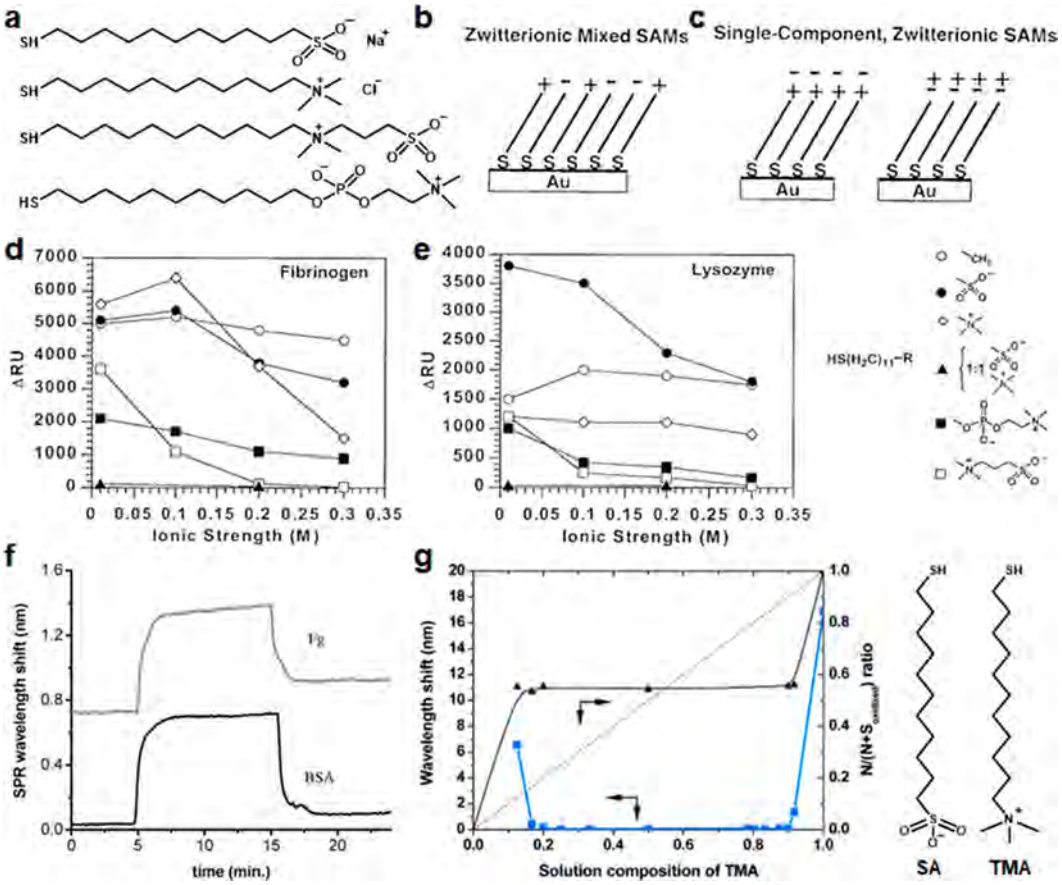

Figure 6. Resistance to nonspecific protein adsorptions of zwitterionic SAMs. (a–c) Molecular structures of the single component zwitterionic SAMs (SB-SAM, MPC-SAM) and mixed-charge SAM. Irreversible adsorption of (d) fibrinogen and (e) lysozyme to different SAMs as a function of the ionic strength of the buffer. Adapted from ref 104. Copyright 2001 American Chemical Society. (f) Adsorption of Fg and BSA on the PC SAM. Reproduced from ref 10. Copyright 2005 American Chemical Society. (g) Correlation between protein adsorption on (blue) mixed SA/TMA SAM and (black) TMA SAM as a function of TMA solution composition. Adapted from ref 11. Copyright 2006 American Chemical Society.

artificial intelligence (AI) and rapid increase of nonfouling data provide powerful tools for accelerated prediction, design, and repurposing of existing and new nonfouling materials.

2.5. Mechanistic Studies Using Zwitterionic Self-Assembled Monolayers

Self-assembled monolayers (SAMs) built on gold surfaces are excellent models to study the protein adsorption phenomenon, as well-defined surfaces capable of presenting a wide range of groups can be easily prepared and the protein adsorption on a gold chip can be readily monitored by surface plasmonic resonance (SPR) spectroscopy.[103] More than two decades ago, Whitesides and co-workers pioneered the *in situ* measurement of protein adsorption on SAMs using SPR sensors.[49,103,104] For instance, by measuring protein adsorption on a wide range of SAM surfaces, they summarized the four principles for building nonfouling surfaces: hydrophilicity, electric neutrality, and containing hydrogen-bond acceptors but not hydrogen-bond donors.[49] In a study of protein fouling on charged SAM surfaces, they found that surfaces presenting single charges adsorbed nearly a full monolayer of protein, while mixed SAMs formed from a 1:1 combination of a thiol terminated in a trimethylammonium group and a thiol terminated in a sulfonate group showed strong resistance to protein adsorption (Figure 6).[104] Single-component SAMs formed from thiols terminating in zwitterionic groups were also found effective in resisting the adsorption of proteins, with comparable efficacy to the best known nonfouling systems at that time. In addition, the protein adsorption repelling ability of zwitterionic SAMs was sensitive to the ionic strength and pH of the buffer, as these factors could affect the ionization and self-association of these charged groups.

In the above-mentioned study, the SAM surface with a phosphorylcholine head group did not show a satisfactory antiadsorption property (adsorbed ∼23% of a monolayer, tested using fibrinogen) compared with other tested zwitterionic SAMs (<1% of a monolayer).[104] A similar phenomenon was also reported in two other studies, showing 18 and 35% of the fibrinogen adsorption compared with that on the methyl-terminated SAMs.[10,105,106] Jiang and co-workers revisited the problem in a following study with a new synthetic route in the preparation of PC-SAMs.[10] They found that PC-terminated SAM could also demonstrate strong resistance to fibrinogen adsorption (∼1% of a monolayer) (Figure 6f), but only when the N/P ratio was very close to 1:1. It should be noted that the preparation condition of the PC-SAM significantly affected the resulting N/P ratio of the surface. The PC-SAM formed in acidic ethanol solution had an N/P ratio of 0.87:1, while fibrinogen adsorption on the PC-SAM was 3.5% of a monolayer. The relatively higher protein adsorption observed in previous studies might originate from unbalanced charges, as the N/P ratio was observed to be around 0.59:1, resulting in unbalanced surface charges.[105,106]

https://doi.org/10.1021/acs.chemrev.2c00344
Chem. Rev. 2022, 122, 17073−17154

The balanced surface charge is key to nonfouling behavior, which has been proved on both single-component zwitterionic SAMs and mixed SAMs consisting of 1:1 positively and negatively charged head groups.[10,104] Nonfouling surfaces with mixed SAMs could be easily prepared with negatively charged monovalent sulfonic acid (SA), carboxylic acid (CA), and methyl phosphonate (PM) terminated alkanethiols, with positively charged trimethylammonium chloride terminated alkanethiols (TMAs).[11,104] Chen et al. showed that there was a strong tendency to form 1:1 mixed SAMs with balanced charges when they were formed from a solution containing positively and negatively charged (monovalent) components.[11] Interestingly, the formation of 1:1 mixed SAMs was insensitive to the thiol solution composition (Figure 6g). For instance, a strong nonfouling surface could be achieved with an SA/TMA pair with a solution composition of TMA in the range 0.2−0.9, and a CA/TMA pair with a solution composition of TMA in the range 0.8−0.9. Further characterizations suggested that the packing structure of mixed-charge SAMs was directed by strong charge−charge interactions of the terminal groups instead of S−Au and chain−chain interactions. The single layer of the balanced charged groups formed a crystalline structure, which did not possess conformational flexibility but demonstrated strong resistance to nonspecific protein adsorption. This observation suggested that tightly bound water molecules on the topmost part of the mixed SAMs determined their nonfouling behavior.

Encouraged by the performance of zwitterionic SAMs, zwitterionic small-molecule ligands have been extensively studied as nonfouling coatings for various surfaces and nanoparticles.[107] Betaine, amino acid, and mixed charge based ligands can be anchored onto surfaces via specific or nonspecific bindings, such as thiol−Au bonds, siloxanes, and catechol groups. The modification of nanoparticles with zwitterionic ligands could stabilize them in the biological milieu by inhibiting aggregation and protein adsorption through the surface hydration layer.[108] Natural amino acids present both cationic and anionic groups in their structures, and they have been studied as popular ligands for various metallic and inorganic nanoparticles. The typical example is cysteine, which enables facile surface immobilization via its thiol group.[109,110] Cysteine single layer modified gold nanoparticles were shown to have zero protein adsorption in undiluted FBS.[110] Attributed to the small ligand size, cysteine coated quantum dots could reach a very tiny size of ∼5 nm, thus allowing effective renal clearance in biomedical usage.[111] Moreover, small nanoparticles with hydrodynamic size (<6 nm) were also shown to traffic rapidly from the lungs to lymph nodes and the bloodstream, potentially enabling inhaled drug formulations.[112]

Zwitterionic SAMs exhibit strong resistance to protein adsorption when tested in single protein solutions. However, it is challenging to resist the adsorption of undiluted blood with very complex compositions in real-world applications. Ladd et al. showed that, although mixed-charge SAMs exhibited ultralow fouling property from single protein solutions, they failed when challenged by undiluted human serum and plasma.[46] In addition, zwitterionic SAMs can not exhibit complete long-term inhibition to the attachment of bacteria and mammalian cells. For example, when placed in bacteria suspensions, large numbers of *Staphylococcus epidermidis* and *Staphylococcus aureus* adhered onto the SB-SAMs, although these SAMs reduced the adsorption of fibrinogen and lysozyme to ≤6 and <1% of a fibrinogen/lysozyme monolayer in single protein solutions, respectively.[104,113] The mixed SAM was "nonfouling" in single protein solutions with adsorption densities lower than 0.3 ng cm^{-2}. However, when applied with human blood plasma and serum, large amounts of protein over 300 and 100 ng cm^{-2} were adsorbed on mixed SAMs, respectively (Figure 7a,b).[46,114] The SAM surface also failed

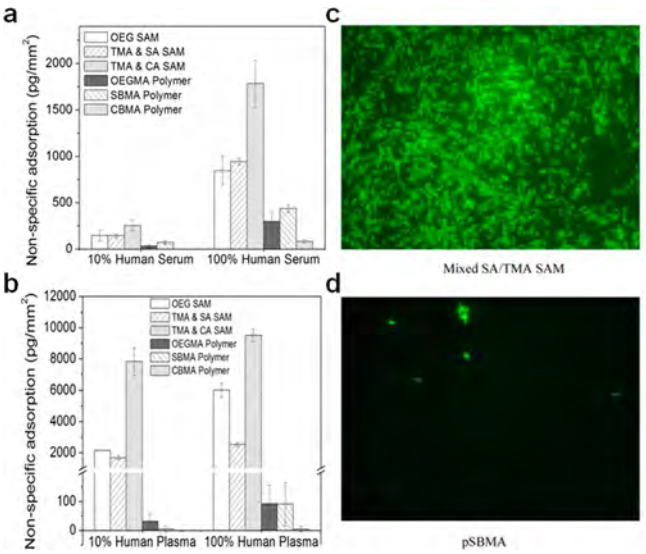

Figure 7. Nonfouling behavior of zwitterionic SAMs in complex mediums. SPR sensor response for nonspecific adsorption of surfaces in (a) 10% human serum and 100% human serum and nonspecific adsorption of surfaces in (b) 10% human plasma and 100% human plasma. Adapted from ref 46. Copyright 2008 American Chemical Society. Representative fluorescence microscopy images of *Pseudomonas aeruginosa* attachment on (c) mixed SA/TMA SAM and (d) PSBMA coated surface at 24 h. Adapted with permission from ref 115. Copyright 2007 Elsevier.

when challenged with bacterial attachment (Figure 7c,d).[115] The failure of SAMs in the real biological milieu may result from their insufficient film stability and the thickness of the hydration layer, which is not strong enough to resist adsorptions in complex media. By contrast, surface grafted zwitterionic polymers with higher packing density and a steric repulsion demonstrated superior antiadsorption performance in human blood.[46,115]

2.6. Hydration and Antifreezing

Zwitterionic polymers are derived from naturally occurring zwitterions, which are able to strongly bind water molecules. These zwitterions play many roles in nature such as osmolytes and can be used for applications such as antifreezing.[116−122] As is well-known, ice nucleation and growth are well correlated with the aggregation of water molecules via hydrogen bonds to form infinitely well-organized networks. During the freezing process, the phase transition first requires a crystallite formation via reduced thermal fluctuation (ice nucleation). Then, water molecules must overcome the electrostatic interactions and van der Waals forces from the surrounding molecules in the liquid, to thus become a regular crystal arrangement.[123] It is not hard to see that ice formation is a dual process of enthalpy change and entropy change.

The superhydrophilic zwitterionic molecules or segments are able to strongly bind water molecules via long-range electrostatic interaction. Zwitterionic small molecules, such as

https://doi.org/10.1021/acs.chemrev.2c00344
Chem. Rev. 2022, 122, 17073−17154

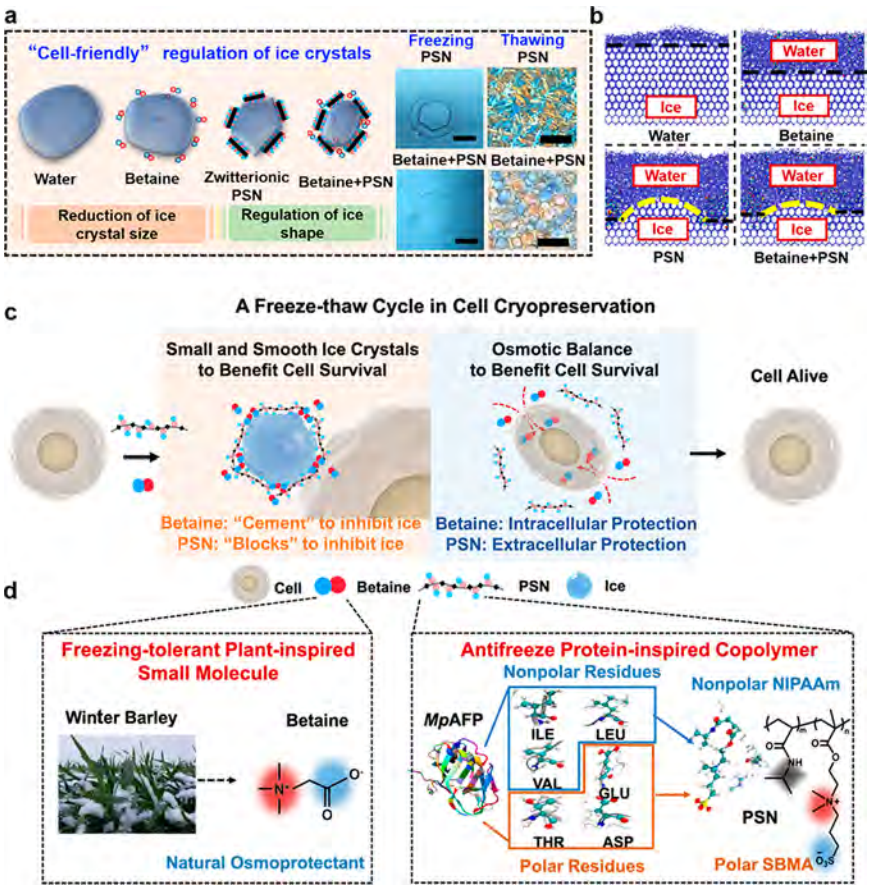

Figure 8. Antifreezing mechanism of zwitterionic materials. (a) Experimental and (b) MD simulation analysis results of the synergistic effects of betaine and PSN on ice crystal inhibition. (c) Schematics of cell-friendly regulation of ice crystals and osmotic balance during cell cryopreservation. (d) Small molecule, zwitterionic betaine inspired by freeze-tolerant plants, and copolymer PSN mimicking the bacterial antifreeze protein. Adapted with permission from ref 125. Copyright 2022 John Wiley and Sons.

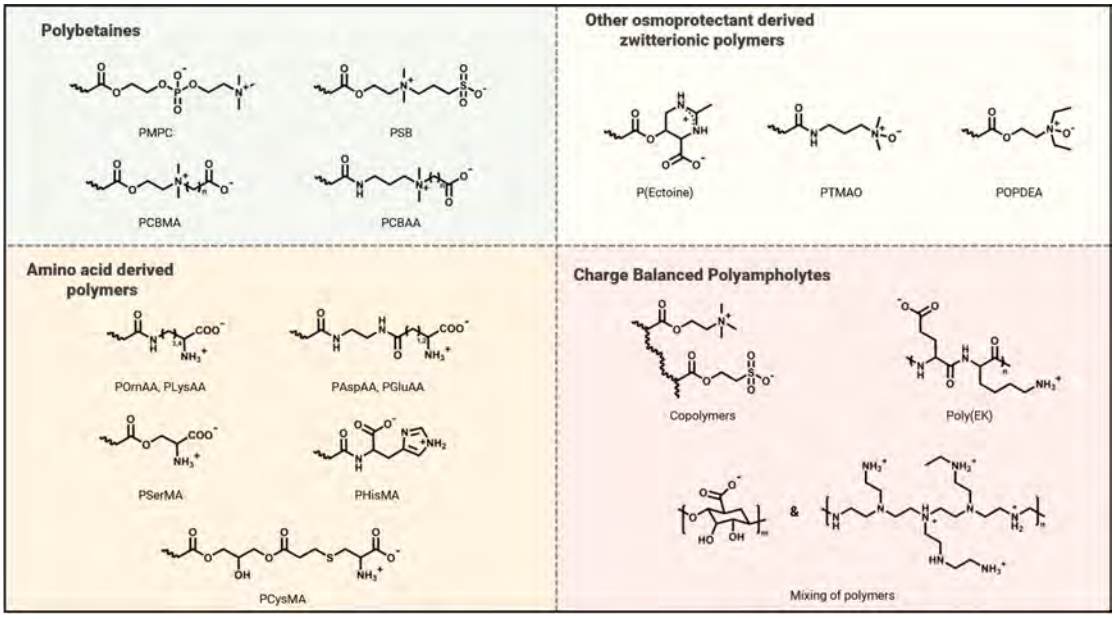

Figure 9. Chemical structures of zwitterionic polymers.

betaine, proline, TMAO, and L-carnitine, were all demonstrated to inhibit ice formation during the freezing process, attributable to the prevention of enthalpy and entropy reduction in a water−zwitterion system.[116−118] In 2016, Zhang et al. first studied the cryoprotection ability of zwitterionic small molecules to cryopreserve mammalian cells including somatic and red blood cells.[116,117,124] It was presented that zwitterionic molecules resulted in a smaller

https://doi.org/10.1021/acs.chemrev.2c00344
Chem. Rev. 2022, 122, 17073−17154

endothermic peak compared with traditional cryoprotectants (DMSO and glycerol) in DSC tests, indicating a lower enthalpy reduction and a stronger freezing point depression. From a molecular-level insight, zwitterionic molecules with high diffusivities can break the spatial arrangement of ice-like water to prevent ice nucleation, as well as increase the force barrier of water molecules when attaching to crystals to prevent ice growth.

Zwitterionic copolymers, such as poly(SBMA-*co*-NIPAAm) (PSN), have been reported to mimic the natural antifreeze proteins (AFPs) for antifreezing applications (Figure 8). Although PSN exhibited a high ice recrystallization inhibition (IRI) activity by resisting ice crystal face growth through ice crystal binding sites, PSN induces different-direction ice growth rates in a crystal, resulting in small but sharp-edged ice crystals during freeze−thaw cycles, disrupting cell structural integrity in cell cryopreservation (Figure 8a). To protect cells in cryopreservation, small betaine molecules with high diffusivity can be applied together with PSN, as they can smooth the sharp-edged shape of the ice crystals owing to the Gibbs−Curie−Wulff theorem (Figure 8b,c).[125] The synergistic cryoprotection effect from small and large zwitterionic materials was verified with several human cell lines, achieving up to 90% cryopreservation efficiency.[126]

3. ZWITTERIONIC POLYMERS

Zwitterionic polymers refer to polymers that bear a pair of oppositely charged groups in their repeating units, such as polybetaines and amino acid derived zwitterionic polymers. The equal amounts of positively and negatively charged groups are uniformly distributed at the molecular level, ensuring the overall balanced charge. Although ionic functional groups usually have strong hydration capacities, it is also well-known that cationic proteins bind to anionic surfaces and vice versa.[1] Thus, the two key criteria to identify a nonfouling zwitterionic material are (1) equal amounts of oppositely charged groups (charge balance) and (2) uniform distribution at the molecular level (minimized dipole). The structures of the most commonly seen zwitterionic polymers are shown in Figure 9.

3.1. Polybetaines

"Betaine" refers to a neutral compound with a positively charged quaternary ammonium or phosphonium cation and a negatively charged functional group. The most widely studied polybetaines are poly(2-methacryloyloxyethyl phosphorylcholine) (PMPC), poly(sulfobetaine) (PSB), and poly(carboxybetaine)s (PCBs) with repeat units simultaneously bearing a quaternary ammonium moiety and a phosphate, a sulfonate, or a carboxylate moiety, respectively.

3.1.1. Poly(2-methacryloyloxyethyl phosphorylcholine). The synthesis of PMPC was first reported in the late 1970s by Kadoma et al., aiming to mimic the structural lipid of cell membranes—phosphatidylcholine.[127] However, their original synthetic approach of MPC monomer was rather difficult and complex, which restricted further studies on its properties and applications. In the following decade, Nakaya et al. developed an alternative synthetic approach, while Ishihara et al. further refined the process for the synthesis and purification of MPC monomer, enabling its production on an industrial scale.[128−130] With the improved accessibility, the physical−chemical properties of PMPC polymers have been intensively studied by Ishihara and others. For example, PMPC was found to reduce protein adsorption from human plasma, endowing the surface with excellent hemocompatibility.[131−133] The hydration phenomenon of PMPC was further characterized to explain its nonfouling behavior.[134] In addition, the outstanding lubricating property was also reported for PMPC modified surfaces.[135,136]

Advances in polymerization techniques significantly facilitate the fundamental and applied studies of zwitterionic polymers. Atom transfer radical polymerization (ATRP) of MPC was realized by the Armes group through the optimization of reaction conditions.[137] Feng et al. systematically studied protein adsorption on PMPC functionalized surfaces by varying the polymer grafting density in the range 0.06−0.39 chains nm^{-2} and the chain length from 5 to 200 monomer units.[138] All surfaces were prepared in a "grafting from" manner with the use of the surface-initiated ATRP (SI-ATRP) approach. The study showed that grafting density had a more prominent effect on protein adsorption than chain length. The PMPC modified surface could resist 98% of the protein fouling from 1.0 mg mL^{-1} fibrinogen solution. Protein adsorption reached a level of less than 10 ng cm^{-2} when the degree of polymerization was larger than 100 and the MPC graft density was more than 0.29 chains nm^{-2}. In addition, the repellency of protein on the PMPC functionalized surface was not dependent on the charge or size of the proteins.[139]

Over the development of the past half-centrury, PMPC has been successfully industrialized and translated into cosmetics and medical applications. The most widely applied form of PMPC is the copolymer system with a hydrophobic component, which has been approved by the regulatory agencies in the 2000s and has been used on many medical devices. In addition, PMPC grafted artificial joints and PMPC-based contact lenses are also available on the market. The successful translation of PMPC was thoroughly reviewed by Ishihara and co-workers,[140−142] and some of the typical examples are also listed in the sections below.

3.1.2. Poly(sulfobetaine). PSB is another type of well-studied zwitterionic polymer. The first synthesized PSB analogue dates back to the 1950s, when the synthesis of poly(4-vinylpyridine *N*-butyl sulfobetaine) was reported by Hart and Timmerman.[143] The early usage of PSB was in petroleum exploration as a surfactant. PSB has later been shown to be ultralow fouling, and it has been used in a range of biomedical and engineering applications. Now the most commonly studied sulfobetaine analogue is sulfobetaine methacrylate (SBMA), which mimics the structure of taurine, a natural betaine highly abundant in the human body.[144] High grafting density is needed to achieve an ultralow fouling surface with PSB coating. When grafted onto a surface via ATRP, the PSB surface exhibited undetectable nonspecific protein adsorption (<0.3 ng cm^{-2}) from single protein solutions by SPR sensor measurements.[145] Due to its biomimetic nature, ultralow fouling properties, thermal stability, and commercial availability, PSB is widely used as a nonfouling material for a range of applications.

Different from other polybetaines, PSB exhibits significantly higher dipole moment leading to strong inter- and intramolecular dipolar interactions in aqueous solutions, which further result in reversible self-association of the polymer chains.[51,146,147] Such reversible self-association endows PSB with some unusual phase behavior and properties. For instance, the surface wettability of a PSB polymer brush was found to depend on its thickness.[147] Counterintuitively, the thin PSB brush is hydrophilic while the thick PSB brush is

https://doi.org/10.1021/acs.chemrev.2c00344
Chem. Rev. 2022, 122, 17073−17154

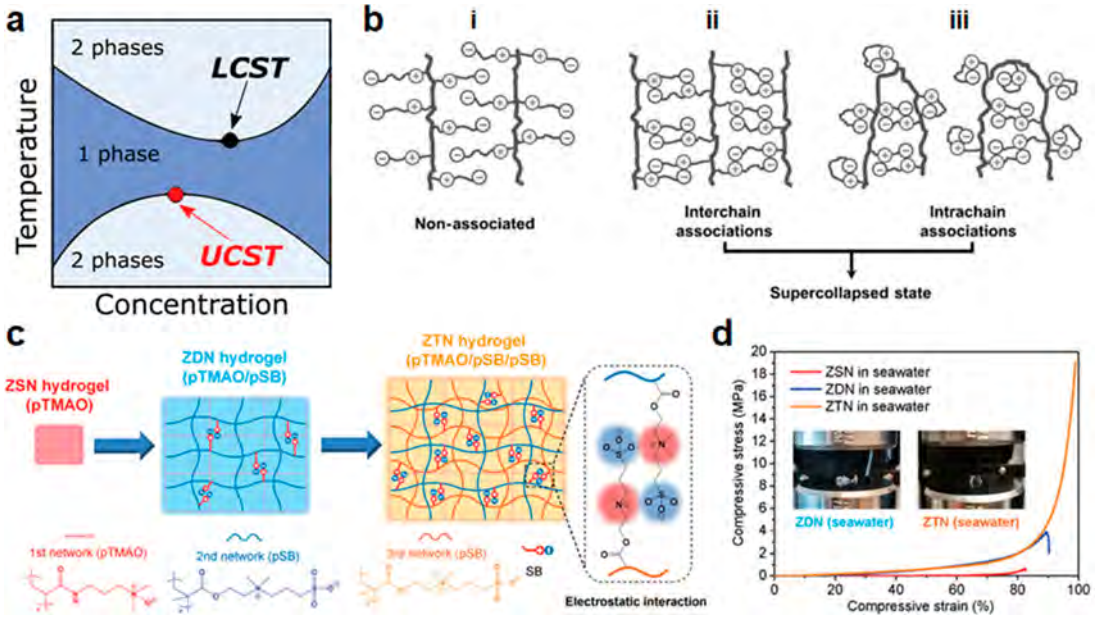

Figure 10. (a) Phase diagram showing the (red) UCST and (black) LCST points for a thermoresponsive polymer. Reproduced with permission from ref 151. Copyright 2017 Royal Society of Chemistry. (b) Illustration of (i) nonassociated, (ii) interchain associations, (iii) and intrachain associations. Adapted with permission from ref 51. Copyright 2006 John Wiley and Sons. (c) PSB enhances the strength of hydrogels by electrostatic interactions. (d) Compression tests of pTMAO/pSB/pSB ZTN hydrogel. Adapted with permission from ref 152. Copyright 2021 John Wiley and Sons.

hydrophobic, and the transition suddenly occurs at a critical thickness. The polymer chain grafting density affects the critical thickness, suggesting the role of the interplay between intrachain and interchain associations. Self-association between the zwitterionic moieties can be interrupted by elevated temperature or ionic strength of the solution, causing the PSB polymers to have an upper critical solution temperature (UCST) in water solution, resulting in both temperature and ionic strength induced stimuli responses.[15,21,148−150]

The phase behavior and aqueous solution properties of free PSB polymers were first studied by Schulz et al., determining the phase diagrams of PSB solutions.[148] An UCST and an "apparent inverted" lower critical solution temperature (LCST) were reported for PSB in H_2O, and such unusual phase behavior was attributed to the interplay of intra- and intermolecular associations (Figure 10a).[151] The presence of salts has a prominent influence on the phase behavior of PSB solutions, as the addition of salts breaks the molecular associations and promotes solubility. Moreover, the aqueous solubility of PSB is a function of its molecular weight as well as the concentration and type of the added salts. "Soft" salt anions and cations are more effective solubilizers than "hard" anions and cations. Finally, the PSB solution exhibits an "anti-polyelectrolyte effect"; i.e., polymer solution viscosities increase with increasing salt concentrations. In addition to free polymer solutions, PSBMA polymer brushes grafted on surfaces also demonstrated thermoresponsiveness, enabling the controlled surface wettability via temperature stimuli (Figure 10b).[51] The self-association of sulfobetaine moieties can be regulated by varying the chemical and topological structures of the zwitterionic moieties and the polymers. The effects of alkyl substituents on the nitrogen atom,[153,154] spacer length between two charged centers,[155] complexations with other polyelectrolytes,[156] and topological structures[155] on the thermoresponsive behavior of sulfobetaine polymers were also well-documented.

The self-association phenomenon of sulfobetaine moieties can be used to prepare physically cross-linked hydrogels[157] as well as to strengthen weak hydrogels by a "locking" mechanism.[152,158] For example, although zwitterionic hydrogels exhibit extraordinary potential for many applications, they suffer from weak mechanical strength in physiological environments. PSB can be integrated into other zwitterionic hydrogels as the secondary and tertiary networks.[152,158] The strong electrostatic interaction and network entanglement within the double- or triple-PSB network structure can effectively dissipate energy to toughen the hydrogel and achieve high strength, toughness, and stiffness. With a PSB double network, the hydrogel made from PCB/PSB exhibited a large tensile strain of 169.9% with a fracture stress close to 1 MPa.[158] A triple-network hydrogel with two PSB networks demonstrated a high compression fracture stress of around 18.2 MPa, which can even be maintained in salt solutions such as PBS and seawater (Figure 10c,d).[152] The salt-responsiveness and thermoresponsiveness of PSB could also be utilized to design environmental stimuli-responsive materials, such as hydrogels,[159] microgels,[160] and nanogels[161] for controlled drug release.

The reversible intermolecular association of sulfobetaine provides a physical mechanism for the material to self-heal after damage. Hydrogels with self-healing properties were prepared by incorporating PSB with various components.[162−171] The self-healing behavior of PSB hydrogels made them attractive candidates for constructing self-repairable nonfouling or antifogging coatings, which can easily recover after wearing or upon mechanical damage.[172−174] When immersed in water, the scratches on a PSBMA coating fully recovered within 1 min, and the fast self-healing property can even be achieved for nanoscale thick coatings.[175] In addition to hydrogels, the incorporation of sulfobetaine moieties into elastomeric materials also endowed them with self-healing properties upon contact with water.[176,177]

https://doi.org/10.1021/acs.chemrev.2c00344
Chem. Rev. 2022, 122, 17073−17154

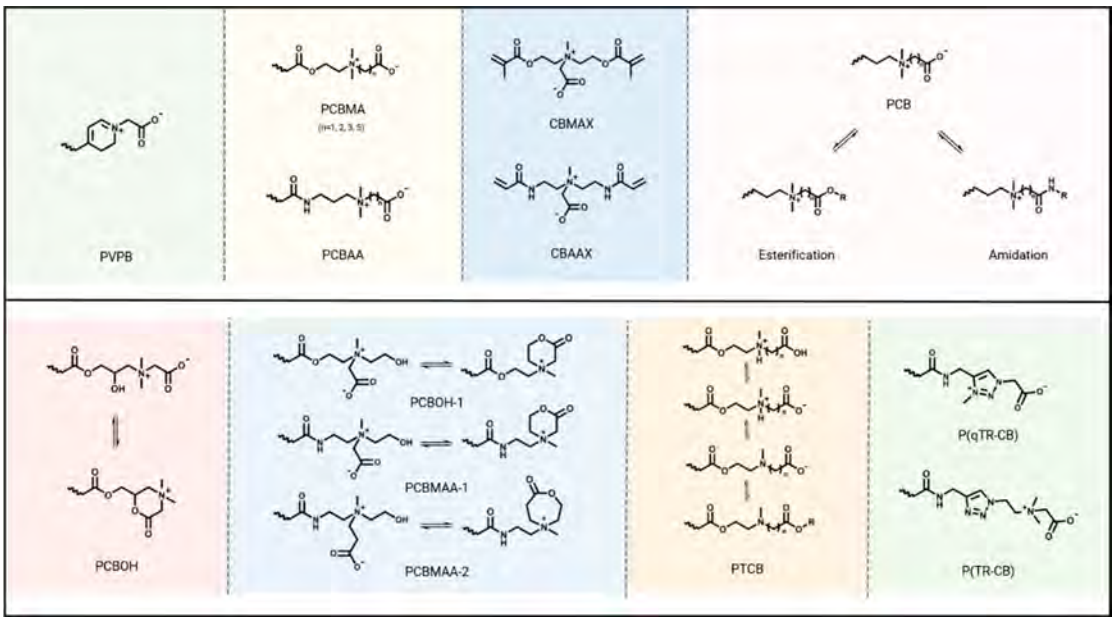

Figure 11. Chemical structures of PCB derivatives.

3.1.3. Poly(carboxybetaine)s. *3.1.3.1. Nonfouling Behavior of PCBs.* Polybetaines with negatively charged carboxyl groups constitute the family of PCBs. The first synthesized PCB analogue was poly(4-vinylpyridine betaine), which was reported by Ladenheim and Morawetz in 1957.[178] Now the most commonly seen PCB constitutes a quaternary amine with the carboxyl group, mimicking the structure of glycine betaine, which is an osmoprotectant widely presented in biological systems. Different from phosphoryl and sulfo groups, the carboxyl group has a much higher pK_a and its protonation can be modulated by the chemical environment. The hydration of the zwitterions is greatly affected by the alkyl spacer between the two opposite charge centers.[69] To understand the structure−property relationship of PCBs, Zhang et al. synthesized a series of CB polymers varying the length of the carbon spacer between the quaternary ammonium group and the carboxy group from one to five (PCB-1 to PCB-5).[145] These PCB polymers were grafted onto gold surfaces by surface initiated ATRP, and their nonfouling properties against fibrinogen under different pHs and ionic strengths were evaluated with SPR measurements. It was found that all PCB polymers are highly resistant to fibrinogen adsorption at higher pH values and higher ionic strength, while PCBs with shorter spacer length tend to have better performance. PCB with a longer spacer is easier to protonate at lower pH values,[179] exhibiting pH-dependent nonfouling behavior. Vaisocherová et al. tested the protein adsorption from human blood plasma and serum on PCB-1, PCB-2, and PCB-3 coated SPR sensor chips.[180] The PCB-1 and PCB-2 surfaces exhibited ultralow (<5 ng cm^{-2}) protein adsorption from 100% human serum and plasma. In contrast, the protein adsorption on PCB-3 was about 70 ng cm^{-2}, suggesting that the optimal spacers for nonfouling PCB polymers are methylene and ethylene. With its exceptional nonfouling behavior in complex media, surface coatings or hydrogels made from PCB could effectively inhibit many interfacial biological responses, including bacteria/cell attachment, foreign body reaction, stem cell differentiation, etc. The detailed discussions of these applications can be found in section 4.

3.1.3.2. Functionalizable and Hydrolyzable PCB. Benefiting from the ease of synthesis, many functional PCB analogues were developed (Figure 11). For instance, the spacer between amine and the methacrylate group of carboxybetaine methacrylate can be functionalized to derive PCB analogues. Cao et al. synthesized a carboxybetaine derived monomer with a hydroxyl group, which can switch reversibly between an open carboxylate form (CB-OH) and a six-membered lactone ring.[181] PCB-OH can switch between sticky and nonsticky states simply by acidic treatment and aqueous hydrolysis. The lactone ring of PCB-OH presents a positive charge, making it a functional material that can switch between bacteria-attacking and bacteria-releasing states repeatedly.[182]

In addition to the spacer, the functional carboxybetaine analogues can also be made by manipulation of the positively charged amine group. The positive charge center of a classic carboxybetaine monomer is a quaternary amine substituted by two methyl groups. Various structures can be derived from the carboxybetaine structure by varying the degree of nitrogen substitution or the substituted group. For instance, the tertiary amine can be used as the positive group to construct a zwitterionic polymer that has a dual-pH responsive behavior. Sundaram et al. synthesized a CBMA-1-TAM monomer, which consisted of a tertiary amine, a carboxyl group, and a methylene spacer in between.[183] The monomer showed two pK_a values of ∼2.6 and ∼8.7 for the carboxyl and amino groups, respectively. Due to the synergistic protonation and deprotonation, the PCBMA-1-TAM reversibly switched between cationic/zwitterionic/anionic states in response to solution pH. Substitution of the nitrogen by functional alkyl groups provides more flexibility for the design of novel PCB analogues. A bifunctional zwitterionic cross-linker carboxybetaine dimethacrylate was made by substitution of two methacrylate groups onto the nitrogen atom, enabling the preparation of pure zwitterionic hydrogels.[184] Cao et al. synthesized *N*-hydroxyethyl substituted PCB derivatives, which can also form bactericidal cationic ring structures in acidic conditions, and change into zwitterionic forms after hydrolysis in basic or neutral conditions.[185,186] Liu et al. developed a

https://doi.org/10.1021/acs.chemrev.2c00344
Chem. Rev. 2022, 122, 17073−17154

triazole zwitterionic polymer by replacing the positive charge center of PCB with a quaternized triazole group, which significantly enhanced the mechanical property of PCB hydrogels.[187]

A unique property of PCB is that further functionalization can be realized through esterification or amidation of the carboxyl group, providing more possibilities for the design of functional materials. Affected by the electron-withdrawing effect of the positive charge center, the carboxyl group of PCB with an ethylene spacer has higher reactivity, and the products are stabler than the analogue with a methylene spacer.[180] By the simple EDC/NHS coupling chemistry, PCB can be easily functionalized with targeting ligands and antibodies, enabling specific interactions on a nonfouling surface, which is highly desired for biosensors[188] and drug delivery carriers.[189] Carboxylate functionalized PCB derivatives can also be synthesized via CB ester monomers. These PCB esters can be hydrolyzed, resulting in a charge switch from positive to neutral.[190] In the ester form, the material interacts with negatively charged biomacromolecules via electrostatic interactions; upon hydrolyzation, they become zwitterionic and repel the adsorbed molecules via hydration effects. Such a characteristic has been utilized to develop pH- or light-responsive materials, which can be used for antimicrobial[191−193] and gene delivery (enabling the triggered release for gene cargos) applications.[194−196] Furthermore, coupling a tertiary amine with a carboxylic ester can make hydrophobic precursors, which can generate zwitterionic surfaces on demand by simple hydrolysis, enabling stand-alone nonfouling elastomers that do not require surface coatings.[197,198]

3.2. Other Osmoprotectant Derived Zwitterionic Polymers

Osmoprotectants, also known as compatible solutes, are organic compounds with neutral charge and low toxicity at high concentrations that help cells maintain osmotic pressure and structural integrity.[199] One characteristic property of osmoprotectants is the strong hydration ability that enables them to keep water and protect protein structures. Betaines, polyols, sugars, and amino acids constitute the majority of osmoprotectants. The key mechanism of a nonfouling surface is to form a strong hydration layer; thus, osmoprotectants provide a natural pool for the exploration of new nonfouling materials.

3.2.1. Poly(ectoine). Ectoine (1,4,5,6-tetrahydro-2-methyl-4-pyrimidinecarboxylic acid) is a compatible solute that presents in halophilic organisms to help them survive high-temperature, high-salinity, extreme pH environments, and even exposure to chemical agents by improving the stabilities of cell membranes, nucleic acids, and proteins.[200] It can also protect cells from the damage of ultraviolet (UV) radiation, cytotoxins, and osmotic stress.[200−203] The delocalized π-bonding in the N−C−N group of the ectoine ring results in a permanent positive charge center due to the mesomeric stabilization of the N−H protons, thus forming a zwitterionic structure with the carboxyl group. Its zwitterionic character induces a strong affinity to water.[202] Ectoine has been used as a superior moisturizer to enhance the skin barrier function.[202]

Due to the promising characteristics of ectoine, the preparation of ectoine-based polymers shows biomedical significance. To obtain a polymerizable ectoine, the Jiang group synthesized an ectoine methacrylate monomer using the reaction between hydroxyectoine and methacryloyl chloride.[204] Ectoine methacrylate was thermally polymerized and cross-linked by *N*′,*N*′-methylenebis(acrylamide) (MBAA) to form an nonfouling poly(ectoine) hydrogel. Enzyme-linked immunosorbent assay (ELISA) analysis revealed that poly(ectoine) hydrogel resisted at least 95% of fibrinogen adsorption compared with the PP surface. The cell attachment test indicated that NIH-3T3 was not adhesive to poly(ectoine) hydrogel and tended to aggregate before rinsing. After rinsing, all the cell aggregations were easily removed from the poly(ectoine) hydrogel. The hydration and mechanical properties of poly(ectoine) were also studied. It showed a high equilibrium water content (EWC) ranging from 85% to ∼94% depending on different cross-link ratios, indicating its strong hydration induced by ionic solvation. The compressive break stress of poly(ectoine) hydrogels is higher than that of other types of zwitterionic methacrylate monomer polymerized hydrogels with the same cross-link ratio. The better mechanical strength could be attributed to the ring structure of ectoine.[204]

3.2.2. Trimethylamine *N*-Oxide Derived Polymer (PTMAO). Trimethylamine *N*-oxide (TMAO) is another protective osmolyte solute naturally occurring in marine animals such as fishes, sharks, skates, and rays.[205,206] It is well-known to stabilize proteins and protect living cells against high urea and salt concentrations.[205−208] Unlike conventional betaines which possess at least a one-carbon spacer, TMAO has a negatively charged oxygen directly connected to the positively charged quaternary amine group, with no spacer in between. A rule of thumb of zwitterionic materials is that the hydration ability as well as the nonfouling property increases with the decrease of CSL between the cationic and anionic moieties. The synthesis of TMAO derived polymer (PTMAO) is of particular interest due to its special zwitterionic structure.

The Jiang group reported the synthesis of a zwitterionic TMAO derived methacrylate monomer via oxidizing *N*,*N*-dimethylaminopropylacrylamide (DMAPA) using 50% hydrogen peroxide (H_2O_2).[206] The PTMAO hydrogel showed a 97.6% reduction of fibrinogen adsorption with respect to polypropylene surface in 10 mg mL^{-1} fibrinogen solution, displayed a much lower complement activation than poly(vinyl alcohol) (PVA), and exhibited a remarkable fibroblast attachment resistance. SPR analysis of PTMAO polymer brush showed less than 3 ng/cm^2 protein adsorption when contact with undiluted human blood serum, demonstrating an ultralow fouling characteristic. The MD simulations suggested that PTMAO oxygen accepted an average of 2.5 hydrogen bonds from water, forming a contiguous hydration shell around its head groups. In contrast, the oxygen in a PEG structure can only accept one hydrogen bond from the surrounding water. In addition to the classic properties possessed by zwitterionic polymers, Shen and co-workers reported that *N*-oxide derived polymers interacted weakly with phospholipids on cell membranes, enabling adsorption-mediated transcytosis and making them highly attractive for drug applications.[209]

A unique property of PTMAO is that its surface hydration can tolerate higher salt concentrations compared with other zwitterionic polymers. Using SFG and computer simulations at quantum and atomistic scales, Huang et al. demonstrated that the highly concentrated salt solutions such as seawater showed a low influence on the surface hydration as well as the nonfouling properties of PTMAO brush.[207] In seawater, the presence of proteins showed minimal impacts on the surface hydration of PTMAO, indicating the complete repulsion of protein adsorption. This superb resistance to the salt effect

https://doi.org/10.1021/acs.chemrev.2c00344
Chem. Rev. 2022, 122, 17073−17154

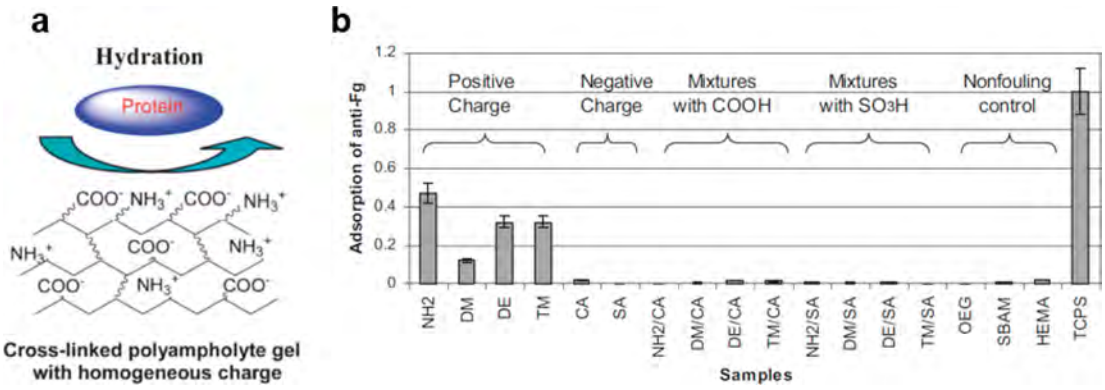

Figure 12. Charge balanced polyampholyte hydrogels and their protein resistant properties. (a) Schematic illustration of charge balanced polyampholyte hydrogels. (b) HRP conjugated antifibrinogen adsorption on various hydrogels. All charge balanced polyampholyte hydrogels could efficiently resist protein adsorption, whereas the cationic polyelectrolyte hydrogels (NH_2, DM, DE, TM) showed high protein adsorption. Adapted with permission from ref 223. Copyright 2008 John Wiley and Sons.

could be attributed to the very short distance between N^+ and O^-, which resulted in a smaller dipole and stronger hydration around the TMAO zwitterion.

3.3. Amino Acid Derived Polymers

Amino acids, with a carboxyl group and a primary amine group directly linked to the central α-carbon, are well-known to be zwitterionic within a wide pH range.[107] For example, cysteine and lysine have been used as small ligands to stabilize quantum dots[109] and gold nanoparticles,[110] rendering them to resist nonspecific protein adsorptions from blood serum. The traditional polymerization approach of amino acids consumes both carboxyl and amino groups to form polypeptides. To preserve the zwitterionic moieties, vinyl monomers were made from amino acids with reactive side chains, including cysteine,[210] serine,[211] aspartic acid,[212] glutamic acid,[212] lysine[213] and ornithine.[213−215] These monomers can be polymerized via SI-ATRP or photoiniferter-mediated polymerization (PIMP) to form poly(amino acid) brushes. For instance, serine can be methacrylated on its hydroxyl group to make polymerizable monomers. The poly(serine methacrylate) (PSerMA) polymer brush exhibited reduced protein adsorption of 1.8, 9.2, and 12.9 ng cm^{-2} in 1 mg mL^{-1} BSA solution, 100% human serum, and 100% human plasma, respectively.[211] The amino acids possessing cationic side groups, e.g., histidine, can also be amidated on their backbone amine to introduce the polymerizable vinyl groups. Wang et al. synthesized a zwitterionic poly(histidine methacrylamide) (PHisMA), which exhibited good protein resistance in single protein solutions.[216]

The structure of the amino acid affects the nonfouling performance of the derived polymer. Two amino acid derived polymers, poly(ornithine methacrylamide) (POrnAA) and poly(lysine methacrylamide) (PLysAA), were compared for their protein adsorption.[214] The POrnAA surface exhibited protein adsorption of 1.8 ng cm^{-2} in pure human serum, while the PLysAA had a higher adsorption of 3.9 ng cm^{-2}, due to the longer alkyl chain of lysine. Li et al. compared the nonfouling performances of a series of amino acid derived polymers against human serum and plasma, including serine, lysine, ornithine, glutamic acid, and aspartic acid.[213] Generally, the tested polymer brushes all exhibited ultralow fouling characteristics under physiological pH. However, PSerMA had higher protein adsorption compared with the acrylamide type of amino acid derived polymers, possibly due to the lower hydrophilicity of an ester bond than that of an amide bond.

Due to pH-dependent protonation and deprotonation of both carboxyl and amino groups, the amino acid derived polymers exhibit pH-responsive behavior, showing either cationic or anionic character at low or high pH values while maintaining zwitterionic around physiological pH.[210] In addition, both of the carboxyl and amino groups can be conjugated to introduce further functionalities, which facilitates their biomedical applications.

3.4. Mixed-Charge/Pseudozwitterionic Materials

As discussed above, the two key criteria of zwitterionic nonfouling materials are equal charge stoichiometry and uniform distribution of charge groups at the molecular level. Therefore, the negatively and positively charged groups are not necessarily present in the same repeating unit of a polymer. They can be distributed in different units in a polymer molecule, or even in different polymer molecules, as long as the charge is balanced at the molecular level. These polymers are named "mixed-charge polymers" or "pseudozwitterionic polymer", also called "charge balanced polyampholytes".[217−221]

Various cationic or anionic monomers/polymers have been explored to design and synthesize charge balanced polyampholytes. Similar to polyzwitterions, charge balanced polyampholytes also show pH-responsive, salt-responsive, thermoresponsive, and self-coacervation behaviors in solution. In addition, their structures including sequence, type of charged groups, etc., can also affect their behaviors on charged surfaces. These behaviors have been discussed in detail in a previous review.[21] Therefore, in this section, we will focus on the nonfouling behavior of these materials.

3.4.1. Charge Balanced Polyampholyte Polymers. Motivated by the studies of protein-resistant mixed-charge SAMs, the investigation of charge balanced polyampholyte polymers as nonfouling materials has begun to attract researchers' attention.[222] The combination of different positively and negatively charged monomers could possibly result in a wide spectrum of new nonfouling materials. It is expected that charge balanced polyampholyte polymers can more efficiently resist nonspecific protein adsorption than mixed-charge SAMs due to their thicker hydration layers. The pioneering work on nonfouling mixed-charge polymers was reported by Chen et al., in which they prepared a series of polyampholyte hydrogels and compared their protein

https://doi.org/10.1021/acs.chemrev.2c00344
Chem. Rev. 2022, 122, 17073−17154

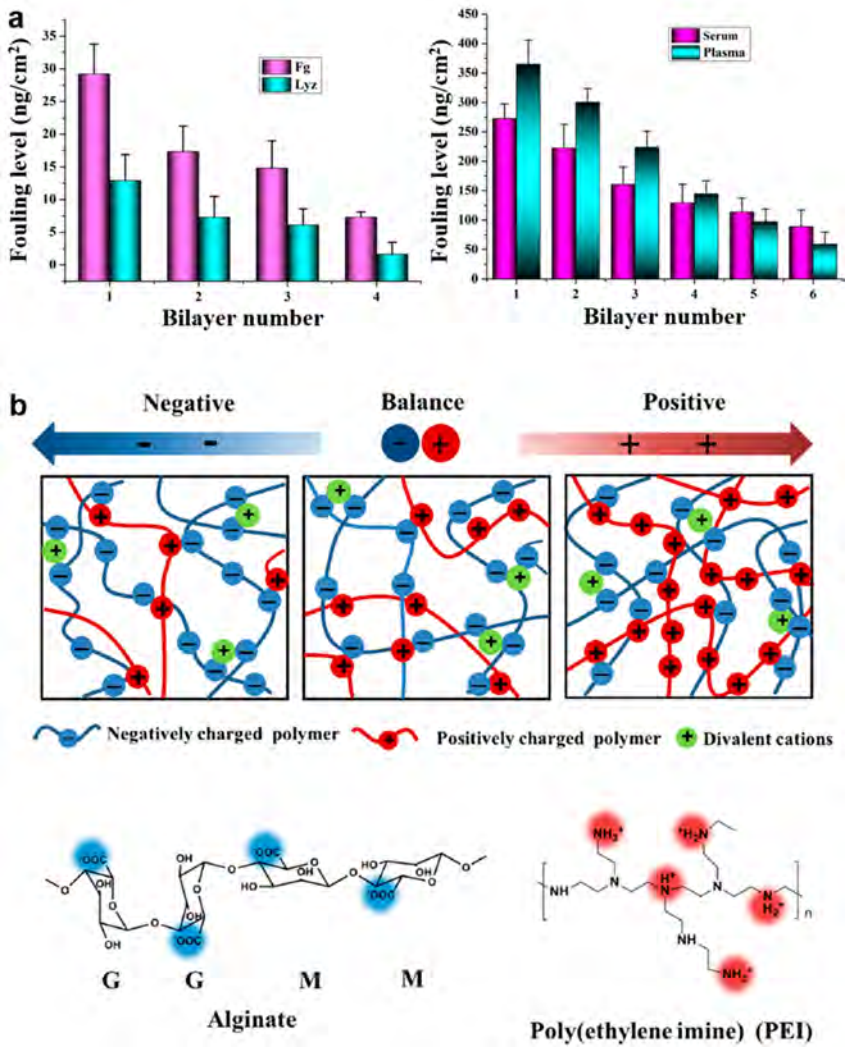

Figure 13. Nonfouling materials obtained by mixing balanced cationic and anionic polymers. (a) Nonfouling surfaces fabricated by LBL of diethylaminoethyl-dextran (CD) hydrochloride and alginate (ALG). The fouling level of CD/ALG (12−80 kDa) as a function of bilayer numbers in (left) single protein solutions of fibrinogen (Fg) and lysozyme (Lyz) and (right) undiluted human blood serum and plasma. Adapted with permission from ref 225. Copyright 2016 Elsevier. (b) Schematic illustration of PEI/alginate polyampholyte hydrogel. Adapted from ref 226. Copyright 2018 American Chemical Society.

adsorptions (Figure 12).[223] The hydrogels were made from the combination of cationic monomers including aminoethyl methacrylate hydrochloride (NH_2), 2-(dimethylamino) ethyl methacrylate (DM), 2-(diethylamino) ethyl methacrylate (DE), 2-(methacryloyloxy) ethyl trimethylammonium chloride (TM), and anionic monomers including 2-carboxyethyl acrylate (CA) and 3-sulfopropyl methacrylate potassium salt (SA). All charge balanced polyampholyte hydrogels showed strong resistance to nonspecific adsorptions of immunoglobulin G (IgG) and fibrinogen, suggesting that nonfouling materials could be facilely prepared from the combination of many oppositely charged monomers. The uniform self-organization of cationic and anionic groups at the molecular scale in the hydrogels leads to the nonfouling property (Figure 12).

Following the previous work, Bernards et al. showed that nonfouling surfaces could also be prepared by grafting mixed-charge polymer brushes.[224] In this study, cationic TM and anionic SA monomers were used to prepare a series of polyampholyte polymer brush coatings with different charge biases on a gold surface via SI-ATRP. The feeding molar ratios of TM to SA were chosen as 1:0, 2:1, 1:1, 1:2, and 0:1, and protein resistance ability was tested using fibrinogen, BSA, and lysozyme. It was found that the protein resistance got stronger when the charge stoichiometry was closer to being equal. Polyampholyte polymerized from 1:1 TM and SA showed the best nonfouling performance, with protein adsorptions of less than 4 ng/cm^2 in all tested single protein solutions.

In addition to copolymerization of oppositely charged monomers, the nonfouling property could also be achieved by mixing of different cationic and anionic polymers. Wei et al. first demonstrated that low-fouling surfaces could be built with oppositely charged polysaccharides via layer-by-layer (LBL) assembly. With the use of positively and negatively charged polysaccharides as the model system, it was found that the assembled LBL films eventually reached very low fouling when they were sufficiently far from the substrate surface, where the substrate surface effect was minimized and oppositely charged marcromolecules were uniformly mixed (Figure 13a).[225] Zhang et al. prepared a polyampholyte hydrogel using

https://doi.org/10.1021/acs.chemrev.2c00344
Chem. Rev. 2022, 122, 17073−17154

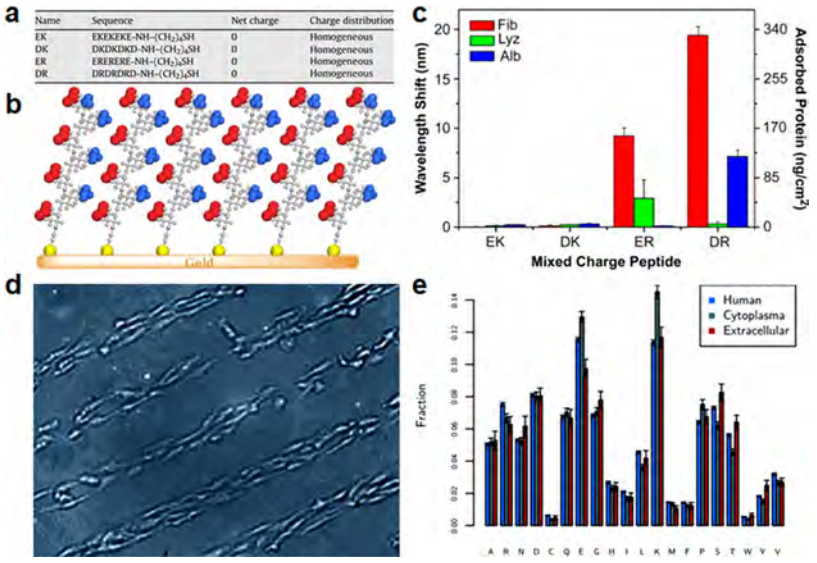

Figure 14. (a) Sequence of four mixed-charge zwitterionic peptides: EK, DK, ER, and DR. (b) Illustration of EK alternating peptide SAM. (c) Protein adsorption on EK, DK, ER, and DR SAMs. (d) Cell attachment on pattern surface with EK and 1-dodecanethiol alternating lines. Reproduced with permission from ref 233. Copyright 2009 Elsevier. (e) Fraction of amino acids on surfaces of proteins found in three different locations in humans. Reproduced with permission from ref 234. Copyright 2012 Royal Society of Chemistry.

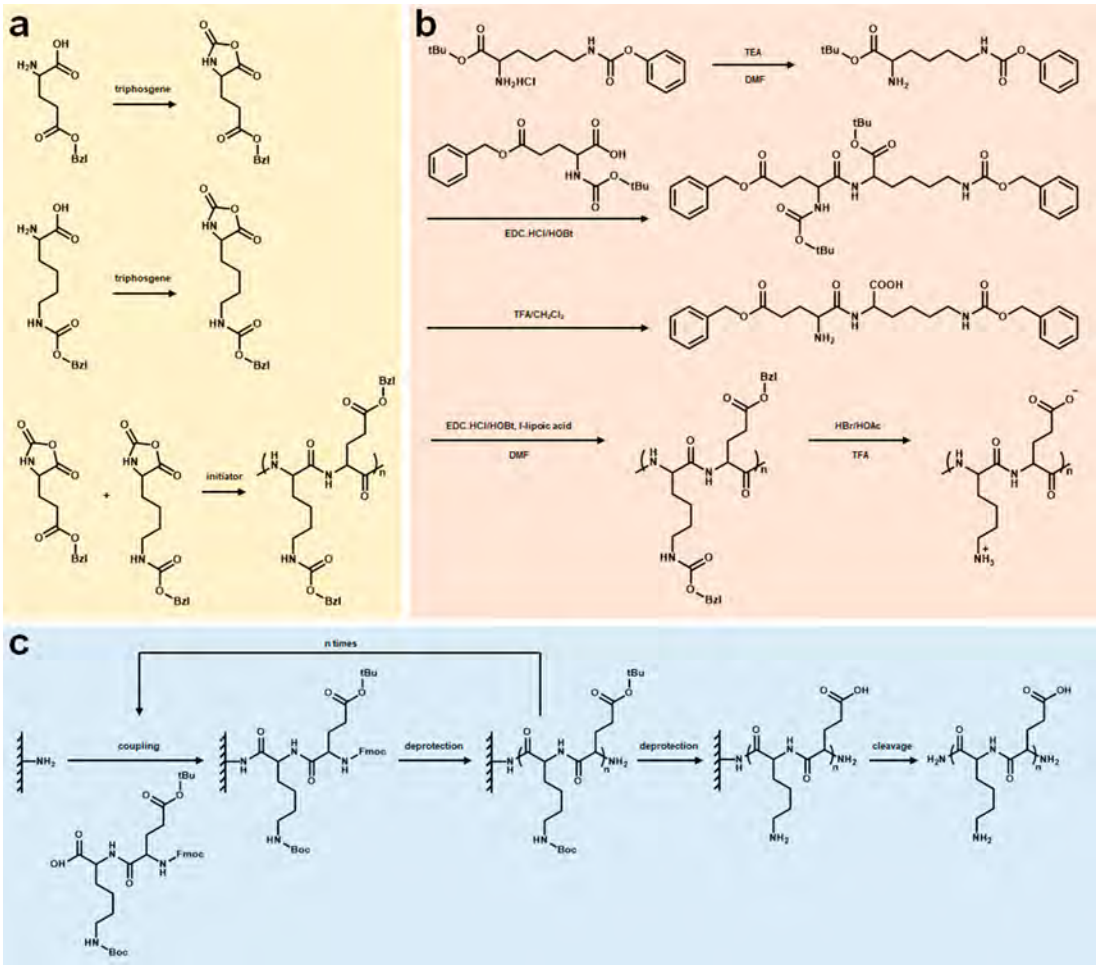

Figure 15. Preparation of poly(EK) peptides. (a) Ring-opening polymerization of Glu-NCA and Lys-NCA.[235] (b) Polycondensation of EK dimers.[237] (c) Solid-phase peptide synthesis using EK dimers.[29]

positively charged polyethylenimine (PEI) with negatively charged alginate (Figure 13).[226] Different from other non-fouling polyampholyte hydrogels, oppositely charged groups were separately distributed in different polymer chains in this

https://doi.org/10.1021/acs.chemrev.2c00344
Chem. Rev. 2022, 122, 17073−17154

alginate/PEI hydrogel. The net charge of the hydrogel can be fine-tuned by adjusting the ratio of the two polymers. The hydrogel exhibited neutral charge at the alginate/PEI weight ratio of 1:0.045, showing strong resistance to BSA adsorption, as well as cell and blood adhesions.

Mixed-charge polymers exhibit many advantages as nonfouling materials, including the simplicity of synthesis, ease of applicability, abundance of raw materials, and availability of functional groups. Because of these advantages, various charge balanced polyampholytes have been used as coatings for devices and nanoparticles to reduce the adsorption from proteins, cells, and bacteria.[227−230] It should be noted that strong electrostatic interactions exist between oppositely charged polyampholytes, providing them with an ion-responsive property.[231] The strong interactions were also explored for physically cross-linked hydrogels with high mechanical strength. Sun et al. designed a series of charge balanced polyampholyte physical hydrogels cross-linked by both strong and weak ionic bonds.[232] These hydrogels showed biocompatibility and nonfouling properties and also exhibited many excellent mechanical properties, including stiffness, strength, toughness, damping, fatigue resistance, and self-healing. The strong ionic bonds in the gel provided permanent cross-linking and elasticity, while the weak ionic bonds were dynamic, which dissipated energy during the deformation process.

3.4.2. Mixed-Charge Zwitterionic Peptides. A special type of zwitterionic material, mixed-charge polypeptides, can be prepared when natural amino acids are used as the building blocks. Following the mixed-charge principle, polypeptides composed of uniformly distributed oppositely charged amino acids at a 1:1 molar ratio will show zwitterionic characteristics. Chen et al. studied the protein resistance of peptides made from four amino acids: positively charged lysine (K) and arginine (R) as well as negatively charged glutamic acid (E) and aspartic acid (D).[233] Pairing of these four amino acids resulted in four peptide sequences: EK, DK, ER and DR, and in each sequence the positive and negative residues were distributed alternatively (Figure 14a,b). Among these four peptides, EK and DK SAMs showed strong resistance to protein fouling, while ER and DR SAMs showed high protein adsorptions (Figure 14c). It has been speculated that three reasons might cause the high fouling of ER and DR surfaces: (1) high pK_a (12.48) of the guanidinium group; (2) the positive charge of R is delocalized, enabling it to form multiple hydrogen bonds with biofoulants; (3) the hydration of R is weak, favoring the interactions between R and many amino acid residues. The EK surface showed the best performance, with undetectable (<0.3 ng cm^{-2}) protein adsorption from the tested single protein solutions. On a patterned surface with alternating lines of EK and 1-dodecanethiol, the cells only aligned on the 1-dodecanethiol-covered lines, while no cells can be observed on EK-covered lines (Figure 14d). In addition, random poly(EK) polymer film also demonstrated ultralow protein adsorption.[233] Interestingly, E and K are the most abundant residues equally presented on the surface of human albumin protein, making up 34 and 34% of the surface charged residues, respectively. Subsequent structural bioinformatics study showed that E and K are also the most abundant residues across over 1000 human extracellular and cytoplasm proteins, which are randomly distributed at a 1:1 ratio (Figure 14e).[234] All this evidence suggests that rich E and K might be the strategy adopted by nature to address the undesired nonspecific protein interactions.

As a nature-inspired nonfouling material, EK-based peptides and polymers are of particular interest for biomedical applications due to their superior biocompatibility and degradability. The synthesis of random EK copolypeptides via ring-opening polymerization of *N*-carboxyanhydrides (NCAs) is relatively easy (Figure 15a), while the synthesis of long EK polymer with alternative residue distribution remains difficult.[233,235,236] The classic solid phase peptide synthesis method is restricted by the peptide length and high cost.[29] Chen and co-workers developed a polycondensation approach to synthesize alternative EK polypeptides (Figure 15b).[237] The alternative distribution of E and K residues was ensured by using presynthesized EK dimer as the monomer in condensation polymerization; however, the molecular weight and distribution cannot be controlled. Yuan et al. used EK dimer as the building block in solid phase synthesis, which can double the length limit of the synthesized EK peptide (Figure 15c).[29] Although it is tough to make a controlled long EK peptide via chemical synthesis, it is possible to produce the peptide via synthetic biology. EK polymer conjugated proteins have been prepared by genetic engineering methods.[238,239] It would be possible to produce well-defined long EK peptide polymers by eco-friendly and sustainable microbial fermentation technology.

4. APPLICATIONS OF ZWITTERIONIC BIOMATERIALS

4.1. Blood-Contacting Devices

Many medical devices and biomaterials need to contact blood to fulfill their functions, such as intravascular stents, catheters, hemodialysis membranes, and extracorporeal membrane oxygenation (ECMO).[22,240−245] Unfortunately, the performances of these devices and biomaterials are limited by unsatisfied hemocompatibility, which also impairs patient health.[246−248]

4.1.1. Thrombosis. Thrombosis is a typical biological response caused by low hemocompatibility. It usually results in pulmonary embolism, ischemic stroke, unstable angina, deep-vein thrombosis, acute myocardial infarction, and even death.[249] For example, vascular thrombosis caused by device contact is a significant cause of morbidity for patients suffering end-stage renal failure during hemodialysis. Worse still, natural coagulation inhibitors in cancer patients are deficient, leading to a greater possibility of thrombus formation, which limits the implantation operation on these patients.[250]

The hemostatic phenomenon is a host-defense mechanism to arrest bleeding from wounds. However, the same process can induce undesired thrombosis on blood-contacting biomaterials.[251] Blood protein adsorption is the first event during thrombus formation. These proteins land and form a "conditioning film" on the surface with a thickness of 2−10 nm, and the protein concentration can be 1000-fold higher than that in plasma.[252] After protein adsorption occurs, its conformation is changed to expose signal factors for recognizing platelets via binding to various receptors on their external surface, such as glycoprotein Ib and IIb/IIIa.[253] After the initiating binding between proteins and platelets, adhesion between platelets and surface and aggregation between platelets occur. Then, adhered platelets are activated and cause a conformational change of glycoprotein IIb/IIIa, mediating clotting events and finally leading to thrombus formation.

https://doi.org/10.1021/acs.chemrev.2c00344
Chem. Rev. 2022, 122, 17073−17154

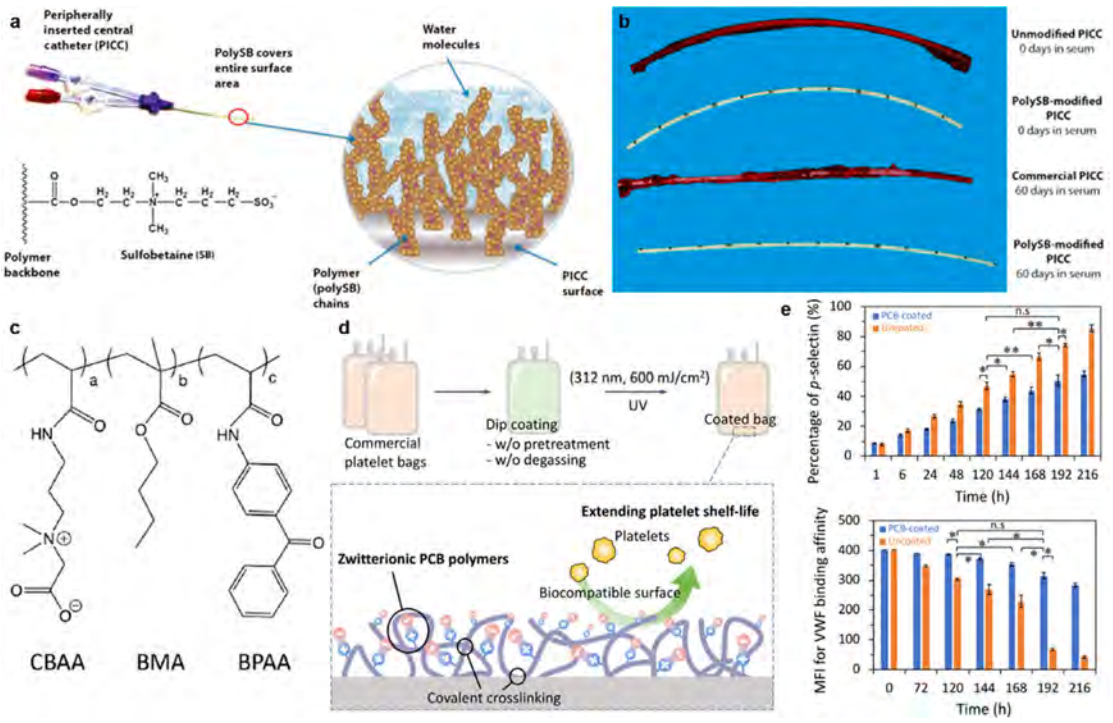

Figure 16. Zwitterionic polymer modified catheters and bags. (a) Schematic illustration of PSB modified peripherally inserted central catheters (PICCs). (b) Thrombus accumulation on PSB-modified and unmodified PICCs after exposure to bovine blood in a flow loop system. Adapted with permission from ref 22. Copyright 2012 The American Association for the Advancement of Science. (c) Structure of poly(CBAA-*co*-BMA-*co*-BPAA). (d) Schematic illustration of surface modification of commercial platelet bags with poly(CBAA-*co*-BMA-*co*-BPAA). (e) Quality assessment of platelets stored in poly(CBAA-*co*-BMA-*co*-BPAA)-coated and uncoated bags. (top) Percentage of P-selectin indicating the platelet activation level. (bottom) Von Willebrand factor (VWF) binding affinity indicates the platelet function. Adapted with permission from ref 265. Copyright 2020 Elsevier.

Anticoagulation agents such as heparin are commonly used to prevent thrombosis.[254] Unfortunately, the control of heparin dosage is difficult. For example, bleeding induced by an overdose of heparin and thrombosis caused by insufficient anticoagulation have become the most common reasons for mortality and morbidity in ECMO treatment.[255,256] Thus, how to prevent thrombus formation by controlling the device/material itself becomes a key question.

4.1.2. Superior Hemocompatibility of Zwitterionic Materials. As blood protein adsorption is required to initiate thrombus formation, it can be inferred that endowing the devices and implants with nonfouling surfaces could be a potential solution to solve the thrombosis issue. The majority of pioneering studies for nonfouling surfaces mainly focused on single protein buffer solutions. However, the nonfouling surfaces demonstrated in these solutions might lose their protein resistance abilities when tested in undiluted serum/plasma/blood, because these real blood fluids were complex and contained hundreds of proteins.[46,114] For example, oligo(ethylene glycol) (OEG) SAMs could efficiently resist fibrinogen adsorption from single fibrinogen buffer solutions, but they adsorbed large amounts of proteins from plasma and serum.[257] Therefore, the key to preventing thrombosis is to efficiently resist nonspecific protein adsorption in real blood environments.

As discussed in previous sections, zwitterionic polymers have been shown to maintain superior nonfouling properties in undiluted serum and plasma. The highly protein resistant properties indicate the great potential of zwitterionic materials to own high hemocompatibility. Therefore, Zhang et al. directly investigated the hemocompatibility of zwitterionic surfaces with superlow protein adsorption.[114] They found that the surfaces with zwitterionic polymer brushes (pSBMA and pCBMA) or zwitterionic SAMs (PC, oligo(phosphorylcholine) (OPC), 11-mercaptoundecylsulfonic acid (SA)/11-mercapto-*N*,*N*,*N*- trimethylammonium chloride (TMA), 12-mercapto-dodecanoic acid (CA)/TMA), all showed very low platelet adhesion after incubation in the platelet-suspension buffer and did not reduce the clotting time of recalcified platelet-poor plasma (PPP). Apart from the zwitterionic surfaces, they also studied the influences of free zwitterionic polymers on the clotting time of PPP. Results showed that pSBMA and pCBMA polymers did not shorten the clotting time. Interestingly, pCBMA polymers significantly prolonged the clotting time, indicating their anticoagulant activity. Chang et al. also demonstrated that pSBMA surface could avoid platelet adhesion and activation in the platelet-rich plasma.[258] In addition, the pSBMA and charge balanced polyampholyte (poly(TMA-*co*-SA)) surfaces could resist blood cell adhesion and activation in human whole blood.[218] The same tendency, i.e., platelet adhesion and activation reduction, was observed on the zwitterionic PC-containing surfaces.[259−262] The poly-(MPC-*co*-*n*-butyl methacrylate (BMA)) with 30 mol % MPC unit, named PMB30, is a well-developed hemocompatible polymer, and it has been approved by the U.S. Food and Drug Administration (FDA) under Master Access File LIPIDURE-CM5206.[141] With superior hemocompatibility, zwitterionic materials have been applied to improve the hemocompatibility of various blood-contacting devices.

https://doi.org/10.1021/acs.chemrev.2c00344
Chem. Rev. 2022, 122, 17073−17154

4.1.3. Blood-Contacting Tubes/Containers. Blood-contacting tubes and containers are the simplest forms of medical devices that are commonly used for transportation or storage in the clinic and are generally made of poly(vinyl chloride) (PVC), polyurethane (PU), silicone rubber (SR), and other materials. Zwitterionic materials can be used to modify all these plastic or elastomeric materials to improve their hemocompatibility.[22,263−266] For example, Kuo et al. developed a series of copolymers composed of SBMA and acrylic acid.[263] These copolymers were coated onto various polymeric substrates, including tissue culture polystyrene (TCPS), PU, and PDMS, via a layer-by-layer polyelectrolyte deposition method, and significantly improved their hemocompatibility. To obtain a stable coating via a simple procedure, Lin et al. designed a photoreactive zwitterionic copolymer, poly(CBAA-*co*-*N*-(4-benzoylphenyl) acrylamide (BPAA)), which could be covalently attached to the surface of medical-grade PVC through dip coating followed by light illumination.[264] With such a simple procedure, the zwitterionic coating prevented protein adsorption and platelet and complement activation, and it effectively inhibited plasticizer leaching from PVC, showing the potential for industrial production.

The catheter is a type of blood-contacting medical device that needs to be inserted into blood vessels. For example, peripherally inserted central catheters (PICCs) are inserted through the vein to a deep position, such as the superior vena cava or right atrium, for the prolonged delivery of drugs and nutrition.[22] However, thrombosis and infection are commonly seen for PICCs, resulting in complications with substantial morbidity and cost.[267] Zwitterionic coatings fabricated by both graft-from and graft-to methods have been shown to successfully solve these issues.[22,266] As a typical example, Smith et al. from Semprus BioSciences Corp. modified PU-based PICCs with PSB through a surface-initiated redox polymerization process (Figure 16a).[22] Compared with commercial catheters, the nonleaching PSB-modified PICCs could effectively repel protein and mammalian cell attachment *in vitro* and *in vivo*. They showed an over 98% reduction in the adhesion and activation of platelets, lymphocytes, monocytes, and neutrophils after blood perfusion. After exposure to serum *in vitro* for 60 days, the formation of thrombotic substances on PSB modified PICC surface was decreased by over 99% compared with the commercial ones (Figure 16b). Moreover, these modified PICCs could reduce device- and vessel-associated thrombus by 99% in a highly thrombogenic canine model *in vivo*, indicating the effectiveness of the zwitterionic coating.[22] The PSB-coated PICC was granted clearance from the FDA in 2012.

Therapeutic transfusion requires storing platelets in proper containers. The quality of stored platelets is depressed by the unfavorable interactions between the platelets and the hydrophobic surfaces of common storage bags (made from PVC), known as platelet storage lesion (PSL). Hemocompatibility improvement of the storage bags is highly desired to inhibit PSL and increase the platelet quality. For this purpose, Lin et al. synthesized a zwitterionic copolymer, poly(CBAA-*co*-BMA-*co*-BPAA), from CBAA, *n*-butyl methacrylate (BMA), and BPAA via a conventional free-radical polymerization (Figure 16c).[265] This copolymer could be stably coated onto the PVC platelet storage bag by a simple yet efficient dip-coating and light-irradiation method without leaching issues (Figure 16d). The shelf life of platelets stored in the zwitterion-coated bag was extended to 8 days, beyond the current FDA standard (5 days) (Figure 16e).

4.1.4. Blood Purification Devices. Blood purification is a therapy based on the extracorporeal treatment of blood and has been widely used for the treatment of many disorders that are refractory to conventional therapies. It works by direct removal of toxins or pathogenic agents from blood circulation through bioseparation techniques, including dialysis, filtration, and adsorption. During treatment, blood from the patients will be directly purified by the membranes or adsorbents and then circulated back to the body. Ameliorating the hemocompatibility of the core devices is of particular importance for the improvement of patient safety. In addition, the biofouling issue results in occlusion of membrane pores which reduces the toxin removal performance of membranes. Over two decades ago, Ishihara and co-workers attempted to use MPC to solve those issues.[268−273] In their work, several MPC-based copolymers were blended with polysulfone (PSf) or cellulose acetate (CA) to prepare zwitterionic membranes for blood purification. The MPC copolymer blended membranes showed reduced protein adsorption, decreased blood cell adhesion, and improved permeability against toxins. For example, PMB30 blended CA membrane showed strong resistance to platelet adhesion and activation.[273] More importantly, the blended membrane exhibited steady real-time permeability and clearance of cytochrome C (targeted toxin) over time from an albumin/cytochrome C mixture during a simulated hemofiltration process. In contrast, the performance of the pure CA membrane drastically decreased with time on account of membrane fouling. The enhanced durability could make the membrane suitable for long-term continuous blood purification therapy. In addition to direct blending, surface coating of zwitterionic moieties onto the surfaces of the membranes also showed improved hemocompatibility and purification efficacy.[274,275]

Hemoperfusion is another type of blood purification technique that can remove water-insoluble, large, or high protein binding toxins by adsorbents. Similar to dialysis membranes, hemoadsorbents also face the issues of low hemocompatibility and high biofouling. Zhang and co-workers reported a series of coating methods for various hemodesorbent materials using PCB hydrogels.[33,276,277] For example, PCB hydrogel has been coated onto powdered activated carbon (PAC).[276] The coated hemoadsorbent showed high stability without leakage of carbon debris. Moreover, the PCB gel coating resisted protein fouling and avoided the risk of hemolysis. With the use of methylene blue (MB) as the model toxin, the coated adsorbent maintained full adsorption capacity even in 100% FBS. In contrast, uncoated PAC lost 50% adsorption capacity in the same test because of biofouling. Following this work, PCB hydrogel was also applied to encapsulate polystyrene resin (H103) and metal−organic framework (MOF) MIL-101(Cr), and it successfully improved their hemocompatibility, mechanical stability, and adsorption performance.[33,277]

4.1.5. Extracorporeal Membrane Oxygenation. Extracorporeal membrane oxygenation (ECMO) is a device for respiratory support which is capable of supporting patients from weeks to a few months. ECMO works by pumping the blood through an artificial lung outside the body and then back into the bloodstream. The core component of ECMO—the artificial lung, also called an oxygenator—presents a large surface area to facilitate gas exchange but induces rapid surface

https://doi.org/10.1021/acs.chemrev.2c00344
Chem. Rev. 2022, 122, 17073−17154

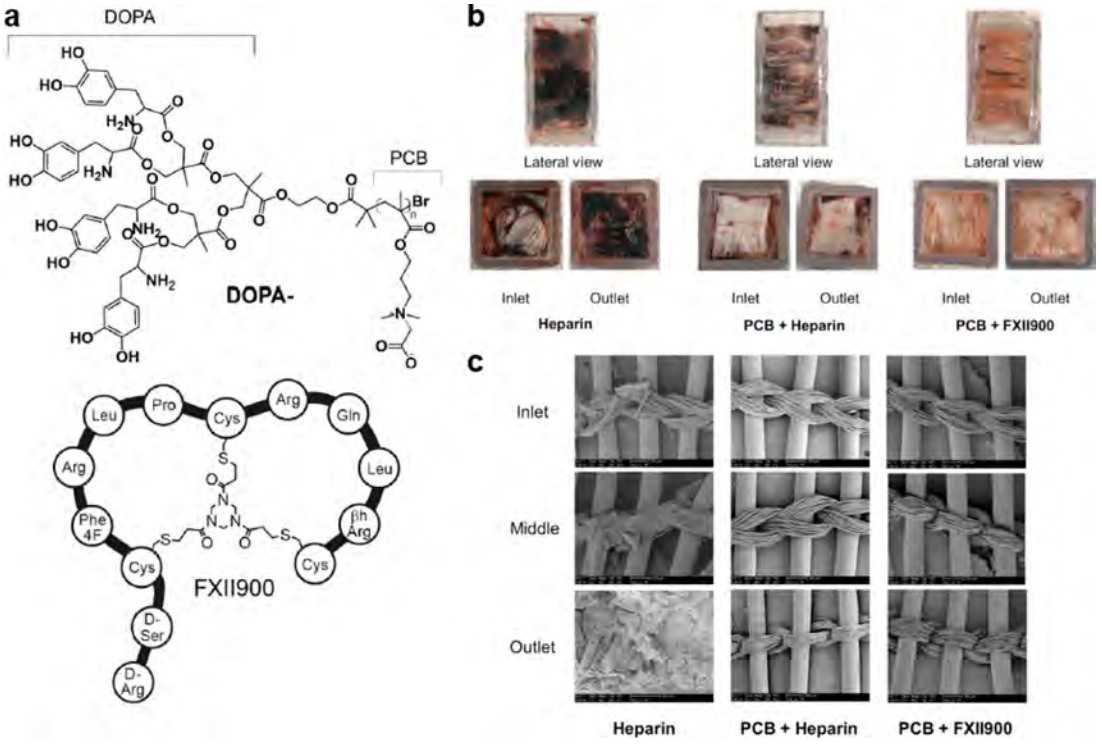

Figure 17. DOPA-PCB coated oxygenator combined with FXII900 treatment. (a) Molecular structures of DOPA-PCB and FXII900. (b, c) Blood coagulation on sham oxygenators with different treatments after ECLS testing. (b) Photographs of oxygenator from lateral, inlet, and outlet views. (c) SEM images of fiber bundle's inlet, middle, and outlet. Heparin: uncoated oxygenator with heparin treatment. PCB + Heparin: DOPA-PCB coated oxygenator with heparin treatment. PCB + FXII900: DOPA-PCB coated oxygenator with FXII900 treatment. Adapted with permission from ref 246. Copyright 2021 Elsevier.

coagulation.[246] Systemic anticoagulation is used to slow device failure, but the associated bleeding and thrombotic complications are common, and they cause significant reductions in survival.[248] Anticoagulant coating is crucial for an ECMO system to maintain its function.

MPC-based coating was developed by Iwasaki et al. for gas-permeable porous membranes.[278] In their work, a copolymer composed of MPC and dodecyl methacrylate (DMA), named PMD, was synthesized and coated on the surface of polyethylene (PE) porous membrane by simple solvent evaporation. The PMD coating effectively resisted protein adsorption and platelet adhesion from human plasma without affecting the permeation of oxygen gas. Therefore, the authors concluded that the PMD-coated PE porous membrane was suitable as a membrane oxygenator. The MPC coating was successfully applied to a series of commercialized oxygenators, including Dideco D901 (Sorin Biomedica, Italy), Monolyth (Sorin Biomedica, Italy), and Oxia ICN (Legacoat, JMS, Japan), etc.[142,279] To further increase the coating density and stability of the MPC polymer coating, Wang et al. synthesized a cross-linkable polymer by the copolymerization of MPC with 3-(trimethoxysilyl)propyl methacrylate (TSMA) and *n*-butyl methacrylate (BMA).[280] The poly(MPC-*co*-BMA-*co*-TSMA) (PMBT) was tested as an anticoagulation coating on hollow fiber membranes. Stability tests showed that the cross-linked PMBT coating could resist dissolution by ethanol or SDS aqueous solution, while the poly(MPC-*co*-BMA) (PMB) control coating was washed away. Subsequent *in vitro* and *in vivo* tests confirmed the improved effectiveness of the PMBT coating in reducing protein adsorption and thrombosis, suggesting its potential in the development of advanced oxygenator systems.[280,281]

Recently, PCB-based coatings were also developed for artificial lungs. Ukita et al. investigated the *in vivo* hemocompatibility of artificial lungs coated by three different methods.[245] The artificial lung was constructed by encapsulation of a polysiloxane-coated PP fiber bundle in PETG housing. The three coating strategies included two graft-to approaches using DOPA conjugated PCB (DOPA-PCB), the copolymer of PCB and hydrophobic groups, and a graft-from approach using activators regenerated by the electron transfer method of ATRP (ARGET-ATRP). Notably, the end group of the DOPA-PCB was designed to have four DOPA moieties to facilitate its anchoring on the surface. The head-to-head comparison showed that the DOPA-PCB coating performed best in reducing artificial lung thrombosis of the artificial lung in sheep and rabbit models.[245] The DOPA-PCB coating showed the minimum increase of blood flow resistance and lowest incidence of device failure when tested in a 36 h veno−venous sheep extracorporeal life support (ECLS) model without continuous anticoagulation. It decreased the formation of fibrin and gross thrombus by 59% in a 4 h rabbit model of ECLS. A recent study showed that combining DOPA-PCB coating with a factor XII inhibitor reduced clot formation to 4% of that in the heparin infusion group while preserving normal tissue coagulation during extracorporeal life support in a rabbit model (Figure 17).[246]

4.1.6. Cardiovascular Devices. *4.1.6.1. Ventricular Assist Device (VAD).* A VAD is an implantable mechanical pump that helps pump blood from the ventricles to the rest of the body and is used as a life-saving device for heart failure patients.

https://doi.org/10.1021/acs.chemrev.2c00344
Chem. Rev. 2022, 122, 17073−17154

However, VADs are underutilized due to low hemocompatibility. Zwitterionic polymer coatings have been developed to solve this issue. Ishihara et al. used PMB30 to coat a diaphragm-type blood pump made by segmented polyurethane (SPU) and tested its hemocompatibility in aminal experiments.[141,282] After implantation into a sheep as a VAD attachment, the PMB30-coated blood pump resisted thrombus formation for at least 27 days. In contrast, the uncoated pump showed severe thrombus formation 4 days after implantation. Similarly, the PMB30-coated SunMedical EVAHEART VAD, a centrifugal blood pump made of titanium, exhibited improved hemocompatibility in preclinical tests.[283,284] In 2005, the PMB30-coated EVAHEART VAD was successfully applied to 18 patients in a pilot clinical study. In 2011, the PMB30-coated EVAHEART VAD was approved by the regulatory agency in Japan. Up to 2017, the PMB30-coated EVAHEART VAD has been implanted in more than 160 patients, demonstrating the effectiveness of the zwitterionic copolymer. Recently, a new version of the PMB30-coated VAD, named EVAHEART 2 Left Ventricular Assist System, has been approved in Japan and is undergoing a clinical trial in the United States (ClinicalTrials.gov/, identifier NCT01187368).[141]

4.1.6.2. Endovascular Stents. Similar to VAD, MPC-based copolymers have also been used to improve the unsatisfactory hemocompatibility faced by endovascular stents, leading to several clinically translated stent products, including BiodivYsio and Dexamet (Biocompatibles), TriMaxx (Abbott Laboratories), and Endeavor (Medtronic).[141] An early version of MPC-based copolymer for stent coating, poly(MPC-*co*-*n*-dodecyl methacrylate) (PMD), was developed by Biocompatibles.[285,286] When implanted in the coronary arteries of pigs, PMD-coated metallic stents did not cause stent thrombosis and prevented excessive neointimal growth up to 12 weeks.[286] To enhance the coating stability, a cross-linkable MPC-based copolymer, poly(MPC-*co*-DMA-*co*-2-hydroxypropyl methacrylate (HPMA)-*co*-3-(trimethoxysilyl)propyl methacrylate (TSMA)) with a molar reaction feed ratio of 23:47:23:5, called PC100B or PC1036, was subsequently developed.[287,288] PC100B could form a uniform cross-linked polymer coating with improved mechanical properties, and this coating could substantially reduce protein adsorption and show excellent hemocompatibility.[287,288] Based on the PC100B coating, Biocompatible Ltd. developed the BiodivYsio coronary stents, which have been approved in the United States and the European Union.[142] From March 1999 to July 2000, 106 BiodivYsio ministents (2.0 mm) were implanted in 97 patients, and the safety and efficacy in the treatment of complex coronary lesions were confirmed.[289] Lewis et al. demonstrated that the coatings of BiodivYsio stents showed long-term stability after implantation in porcine or human patient for 6 months.[290,291] Between August 2001 and April 2003, the first trial of the BiodivYsio stents in Japan was carried out to treat 130 patients with native coronary artery lesions, and the follow-up results comfirmed their safety and efficacy.[292] Followed by BiodivYsio, PC100B coating was also used in the development of Dexamet (Biocompatibles), TriMaxx (Abbott Laboratories), and Endeavor (Medtronic).[142]

Besides PMPC, sulfobetabine-based polymers have also been studied as coating materials for stents. Wang et al. used graft-from methods to prepare ahyperbranched PSB coated bare metal stents (BMSs).[293,294] The coated stents displayed excellent resistance to platelet adhesion, prolonged plasma recalcification time, and negligible complement activation in the *in vitro* tests. To improve the stability and tolerance to high temperature, Chou et al. reported a thermosettable poly(vinylpyrrolidone)-*co*-polySBMA coating for a stainless steel (SS) stent.[295] The thermosettable coating maintained stable nonfouling properties, including resistance to platelet adhesion and erythrocyte attachment after treatment under 200 °C. Degradable metallic stents are drawing more interest as an alternative to traditional metallic stents but face challenges in controlling the corrosion rate and thrombosis. Ye et al. developed a series of sulfobetaine-bearing polyurethanes with tunable degradation behavior for the coating of the biodegradable Mg alloy AZ31 stent.[296] The coated stent not only showed the desired thromboresistance but also resulted in controlled rates of coating degradation and underlying alloy corrosion.

Endothelialization is a promising strategy for stents to prevent thrombosis and restenosis. To achieve endothelialization on an nonfouling background, endothelial cells targeting bioligands can be conjugated on the zwitterionic coating.[297,298] For example, Chen et al. coated a zwitterionic copolymer made of SBMA and acrylic acid onto BMS and conjugated the polymer with specific antibody targeting endothelial progenitor cells (EPCs).[298] The coated BMS showed good resistance to platelet adhesion but specific interaction with EPCs. After implantation in the carotid artery of rabbit for 4 weeks, a smooth endothelium surface was formed on the stent. Apart from bioligand conjugation, local generation of nitric oxide (NO) can also facilitate endothelialization. Zhu et al. grafted a block copolymer brush coating consisting of zwitterionic SBMA and NO generating NONOate onto a 316L SS stent.[299] The SBMA modified and NO-supplied stent showed high cytocompatibility and improved anticoagulation, antirestenosis, and endothelialization effects in a rabbit model.

4.1.6.3. Vascular Grafts. Vascular grafts are used to replace damaged blood vessels for the recovery of blood supply in revascularization or bypass procedures in patients.[241] Zwitterionic materials have been used to improve the hemocompatibility of artificial vascular grafts. An early study of zwitterionic coatings for vascular grafts was reported by Yoneyama et al.[300] In this study, poly(MPC-*co*-2-ethylhexyl methacrylate (EHMA)) with 30 mol % MPC, called PMEH, was blended with segmented poly(etherurethane) (SPU) at a weight percentage of 7.5%. Dacron vascular grafts with 2 mm inner diameter (Sumitomo Electronics Co., Ltd., Osaka, Japan) were dip-coated in the polymer blend solution and tested in a rabbit model. After implantation at the interposition of carotid arteries for 5 days, no thrombus and pseudointima were formed on the surface of the MPC blend polymer coated vascular grafts. In contrast, a massive thrombus was attached to the SPU coated counterpart surface after implantation for 90 min.[300] Although the short-term *in vivo* hemocompatibility was excellent, pseudointima was observed on the SPU/PMEH(7.5) coated vascular graft after implantation in rabbits for 4 weeks.[301] Therefore, Yoneyama et al. further increased the content of PMEH in the SPU/PMEH blend to 10 wt % and prepared the SPU/PMEH(10) coated vascular graft, which showed no thrombus and pseudointima formation 8 weeks after implantation.[302]

Following MPC, other zwitterionic polymers have also been developed as coatings for artificial vascular grafts, such as SBMA copolymers[303] and SB modified starch,[304] which all showed improved hemocompatibility compared with uncoated grafts. Yao et al. further conjugated REDV peptide to the SB-

https://doi.org/10.1021/acs.chemrev.2c00344
Chem. Rev. 2022, 122, 17073−17154

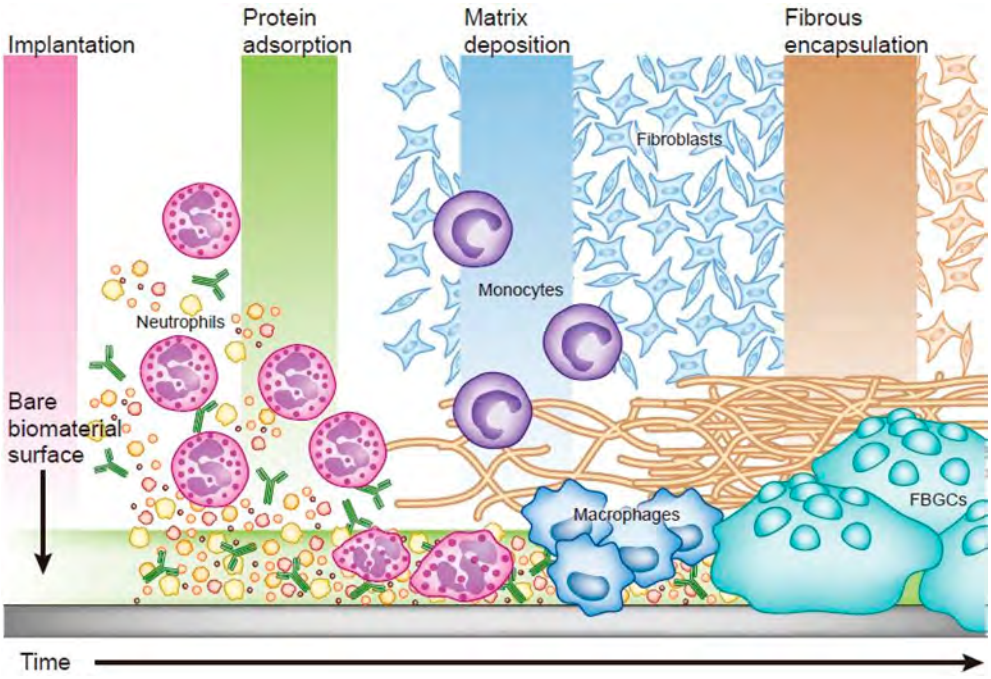

Figure 18. Schematic illustration of the FBR process. Reproduced with permission from ref 323. Copyright 2013 Springer Nature.

starch coating via thiol−ene click chemistry, which facilitated the adhesion, proliferation, and migration of human umbilical vein endothelial cells (HUVECs) onto the vascular grafts.[304] In addition to synthetic polymers, Zheng et al. designed two triblock functional proteins, cofp-MZY and cofp-MZR, as the coating materials.[305] Both of the functional proteins contained an adhesive domain (DOPA-containing peptide), a nonfouling domain (zwitterionic EK peptide), and an EC-specific affinity domain (YIGSR and REDV peptides, respectively) and were produced through a synthetic biology technique. These two proteins were dip-coated onto PTFE and showed resistance to protein and platelet adhesion, remarked cytocompatibility and hemocompatibility, and selective adhesion of ECs over smooth muscle cells (SMCs).

In addition to coatings, zwitterionic polymers have also been blended into a biodegradable vascular scaffold for improved hemocompatibility. Hong et al. reported a vascular scaffold made by blending poly(ester urethane) urea (PEUU) and poly(MPC-*co*-methacryloyloxyethyl butylurethane (MEBU)) (PMBU).[306] In their formulations, PMBU contained 30 mol % MPC. The integrated MPC component successfully inhibited thrombogenesis and the attachment of SMCs, while the degradability of PEUU allowed an autologous tissue replacement. The grafts with 15% PMBU blending showed higher potency than pure PEUU after implantation in rat abdominal aorta for 8 weeks. Importantly, a neointimal layer with endothelial coverage and good anastomotic tissue integration was formed on the PEUU/PMBU vascular grafts.

4.1.6.4. Artificial Heart Valves. Artificial heart valves are used in the treatment of structural heart diseases, such as end-stage valvular disease and aortic valve stenosis. Thrombosis and calcification are the major issues faced by bioprosthetic heart valves. Yang et al. reported a zwitterionic polymer/tissue hybrid (PSBMA-PP) synthesized by *in situ* copolymerization of SBMA and methacrylated porcine pericardium (MA-PP).[307] The hybrid material met the high requirements in terms of chemical stability, mechanical strength, and durability for a transcatheter aortic valve. Importantly, it showed remarkable antithrombogenicity through the evaluations of platelet adhesion, *in vitro* thrombus formation, and *ex vivo* arteriovenous shunt. The *in vitro* pulsatile flow test showed that the effective orifice area (EOA) and regurgitant fraction followed the ISO 5480 Standard after 300 million cycles, indicating its excellent hydrodynamic performance and durability. After it was subcutaneously implanted in rats for 120 days, the improved valve could efficiently resist the leaflet calcification.[307] In another study, a cross-linked PEGDA−PSBMA network was used to modify decellularized porcine heart valves.[308] Both *in vitro* and *in vivo* tests confirmed that the PSB-modified artificial heart valve efficiently resisted calcification and inflammatory responses. Similar to the previously discussed cardiovascular devices, endothelization of the artificial heart valves can also be enhanced by coating them with signaling peptide conjugated zwitterionic polymer coatings.[309]

4.2. Implants with Mitigated Foreign Body Reaction

Numerous medical devices and biomaterials need to be implanted into the host body to achieve their functions, such as intraocular lens (IOL), artificial vitreous body, continuous glucose monitor (CGM), artificial islet, neuroprosthetic device, and breast implant. However, these implantable devices and biomaterials are troubled by the foreign body reaction (FBR), a cascade of host immune reactions including various inflammatory responses and fibrosis. These immune reactions can disturb the functions or even cause failure of the implants. For example, early/acute inflammation responses can generate significant signal noise or signal quality degradation to sensors, such as CGM and neural probes.[310,311] For long-term implantation, fibrosis is the main factor that affects device functions. Fibrosis can isolate implants from the host by forming an avascular, collagenous, and fibrotic capsule.[8] Such a fibrotic capsule is impermeable to most molecules in the surrounding microenvironments, thus inhibiting signal communication and disturbing implant functions.[8] For patients,

https://doi.org/10.1021/acs.chemrev.2c00344
Chem. Rev. 2022, 122, 17073−17154

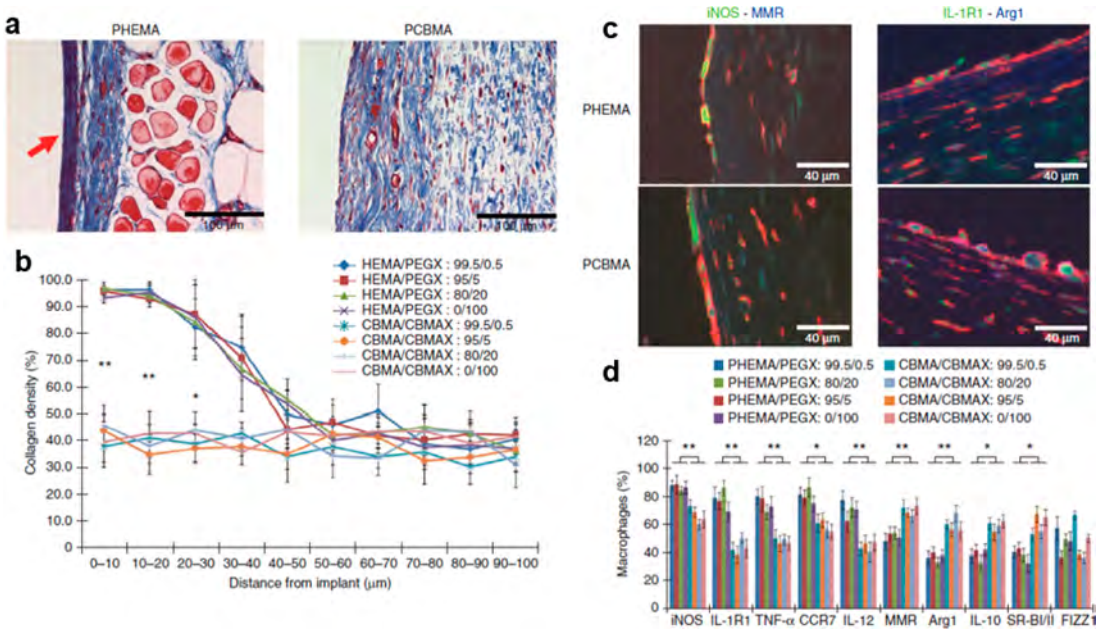

Figure 19. Anti-FBR property of zwitterionic PCBMA hydrogel. (a) Masson's trichome staining images of tissues around PHEMA and PCBMA hydrogel after implantation for 3 months. (b) Collagen density close to implant quantified by measuring the percentage of blue-pixel coverage in the Masson's trichome staining images. (c) Macrophage phenotypes in the tissue surrounding implants. Green, pro-inflammatory biomarkers (iNOS and IL-1R1); blue, anti-inflammatory biomarkers (MMR and Arg1). (d) Percentage of pro-inflammatory and anti-inflammatory macrophages. Pro-inflammatory biomarkers: iNOS, IL-1R1, TNF-α, CCR7, and IL-12. Anti-inflammatory biomarkers: MMR, Arg-1, IL-10, SR-BI/II, and FIZZ1. Adapted with permission from ref 8. Copyright 2013 Springer Nature.

FBR can induce various harmful risks, such as pain, tissue distortion, and tissue necrosis.[8,312] Therefore, it is crucially essential to explore efficient strategies for FBR mitigation, which is beneficial for the development of ideal implantable devices and biomaterials.

4.2.1. FBR Mechanisms. It is well-reasoned that understanding the mechanisms and processes of FBR should contribute to the development of highly efficient anti-FBR strategies and the design of next-generation biomedical implants. Until now, although the immune-mediated FBR is extremely complicated and not yet fully understood,[313] a consensus on the general orchestration of FBR events has been reached (Figure 18). The first step of FBR is protein adsorption. Upon implantation, proteins released from ruptured vessels are rapidly adsorbed onto implants within seconds to minutes.[314,315] Initiated by protein adsorption, a provisional matrix is formed and then releases various chemoattractants to attract polymorphonuclear neutrophils.[314,316,317] Neutrophils are the first type of cells arriving at the implantation site within a few hours, and they are also the primary cell type in the acute inflammation phase (usually within 1 week).[313,314,318] They can release a "sticky network" composed of histones, chromatin DNA, neutrophil elastase, and granular proteins, called neutrophil extracellular traps (NETs),[319−321] which can facilitate the fibrotic encapsulation process.[322] Also, neutrophils can secrete potent chemoattractants to recruit the next wave of cells, including monocytes and macrophages.[321] The monocytes can differentiate into macrophages, and they can also secrete a series of chemokines to induce more monocytic infiltration and activate macrophages.[313]

Over time, the mononuclear cells, including monocytes and macrophages, become predominant, identifying the beginning of the chronic inflammation phase, which usually fades within 3 weeks after implantation.[324−327] In this phase, many macrophages appear at the implantation site.[324] Macrophages play an important role in determining the outcomes of FBR. They can polarize into a spectrum of phenotypes based on local cues, including pro-inflammatory M1 macrophages at one end of the spectrum and anti-inflammatory M2 macrophages at another end.[328] The implanted stimuli result in a prolonged presence of M1 macrophages and an imbalance of M1 over M2 macrophages.[325] The M1 macrophages attempt to phagocytose the foreign materials but are frustrated because the materials are too large for them.[8,325] Therefore, they further differentiate and eventually fuse into foreign body giant cells (FBGCs), huge cells containing abundant cytoplasm and up to 100 nuclei.[313] FBGCs can secrete high levels of protons, enzymes (elastase, protease, lysozymes, etc.), and reactive oxygen species (ROS) to degrade implants.[325] If the FBGCs fail to digest the implants, they send out signals to recruit fibroblasts.[329] As a result of chronic inflammation, abundant fibroblasts infiltrate and proliferate at the implant surface and begin to deposit collagens, forming the granulation tissue, a precursor of the fibrous capsule.[8,314] Next, fibroblasts continually excrete excessive collagens, constituting a dense, aligned, and avascular fibrous capsule. The capsule isolates the implant from surrounding tissues and severely impairs its performance due to mass transfer limitation and nutrient consumption.

4.2.2. Superior Anti-FBR Property of Zwitterionic Materials. As discussed above, FBR is initiated by surface protein adsorption. Due to the strong nonfouling capacity, zwitterionic polymers have been explored as anti-FBR materials.[19,158,187,226,330−334] Zhang et al. first reported the complete inhibition of foreign body capsule formation against implanted PCB hydrogels in a mice model for at least 3 months.[8] The zwitterionic cross-linker CBMAX was used in

https://doi.org/10.1021/acs.chemrev.2c00344
Chem. Rev. 2022, 122, 17073−17154

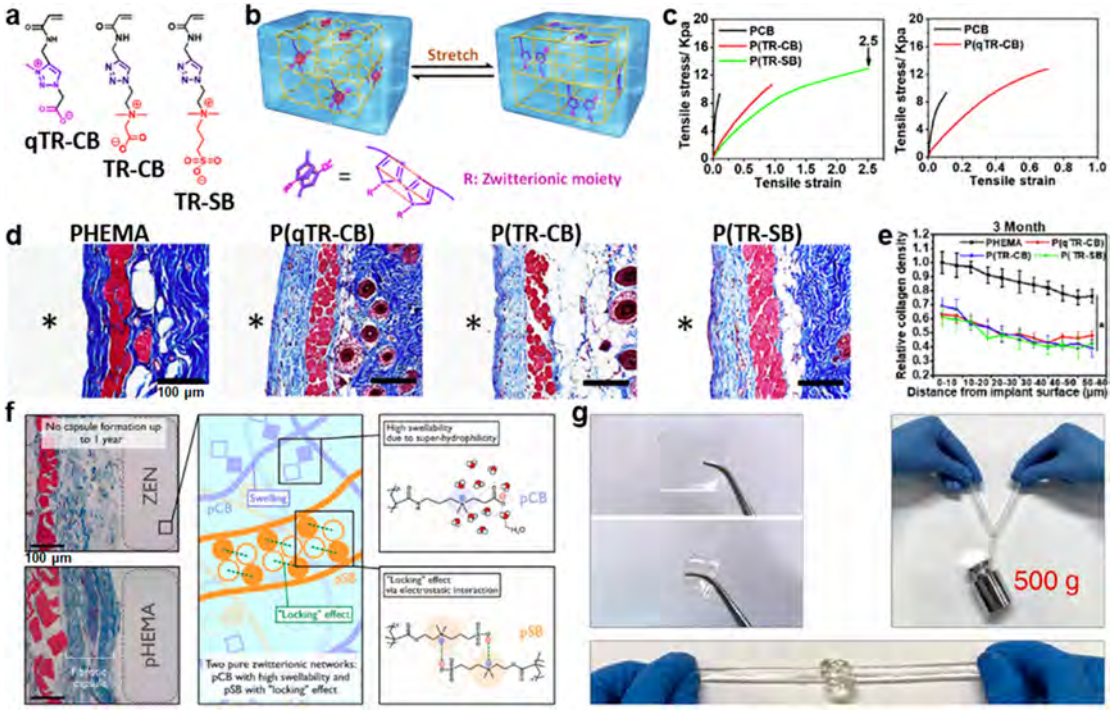

Figure 20. Mechanically robust and anti-FBR (a–e) triazole zwitterionic (TR-ZW) and (f, g) zwitterionic-elastomeric-networked (ZEN) hydrogels. (a) Molecular structure of TR-ZW monomers. (b) Schematic illustration of energy-dissipating $\pi-\pi$ interaction to improve mechanical strength. (c) Tensile stress–strain curves of TR-ZW hydrogels. (d) Masson's trichrome staining images of PHEMA and TR-ZW hydrogels after subcutaneously implanted into immunocompetent mice for 3 months. Blue staining: collagen deposition surrounding implants. Asterisks (*): implant location. (e) Collagen density quantification surrounding implants. Adapted with permission from ref 187. Copyright 2020 Elsevier. (f) (right) Schematic illustration of pCB/pSB ZEN hydrogel based on "swelling" and "locking" mechanism and (left) Masson's trichrome staining images of PHEMA and ZEN hydrogels after subcutaneous implantation in mice for 1 year. (g) Photographs of ZEN hydrogels and their elastomeric behavior and mechanical robustness. Adapted with permission from ref 158. Copyright 2021 The American Association for the Advancement of Science.

the hydrogel to make it purely zwitterionic. Three months after implantation, collagen density around the PCB hydrogel was relatively uniform and diffuse (30–40%), indicating that the surrounding substance was a normal extracellular matrix rather than the FBR-induced capsule (Figure 19a,b). In sharp contrast, PHEMA hydrogel induced an extremely high collagen density (>90%) close to the PHEMA/tissue interface, suggesting the formation of a dense collagenous foreign body capsule (Figure 19a,b). These results demonstrated that PCB hydrogels could effectively resist FBR and avoid capsule formation for at least 3 months. In addition, PCB hydrogels facilitated angiogenesis in the surrounding tissue, beneficial to the mass transport between the host and the implants. Finally, PCB hydrogels were found to induce more anti-inflammatory macrophages and fewer pro-inflammatory macrophages in the surrounding tissue than PHEMA hydrogel (Figure 19c,d), facilitating the neovascularization and tissue remodeling. In addition to PCB, charge balanced alginate/polyethylenimine (PEI) polyampholyte hydrogel was also reported to effectively decrease the macrophage infiltration to the implant surface *in vivo* and to prevent capsule formation for at least 3 months in mice.[226]

Implantable devices require proper mechanical strength, but zwitterionic hydrogels are usually weak and fragile. A strong zwitterionic hydrogel maintaining an anti-FBR property is highly desired. Liu et al. designed a series of triazole zwitterionic (TR-ZW) monomers, including quaternized triazole carboxybetaine acrylamide (qTR-CB), triazole carboxybetaine acrylamide (TR-CB), and triazole sulfobetaine acrylamide (TR-SB) (Figure 20a).[187] These TR-ZW monomers were cross-linked by CBAAX cross-linker to form TR-ZW hydrogels via UV-induced radical polymerization, named p(qTR-CB), p(TR-CB), and p(TR-SB) hydrogel, respectively. In virtue of the introduction of triazole moieties, energy-dissipating $\pi-\pi$ interaction could be formed to enhance the mechanical robustness significantly (Figure 20b). Relative to pure PCB hydrogel (~10% of the tensile strain), p(qTR-CB) (~71%), p(TR-CB) (~96%), and p(TR-SB) hydrogels (~250%) presented higher tensile strain (Figure 20c). Meanwhile, after 3 months of subcutaneous implantation in immunocompetent mice, all TR-ZW hydrogels showed significantly lower fibrous capsule formation and higher blood vessel formation than PHEMA hydrogel (Figure 20d,e).[187] Apart from introducing additional functional moiety into the zwitterionic monomers, a double-network strategy based on pure zwitterions was also used to strengthen the mechanical property without compromising the FBR resistance ability. Dong et al. reported a "swelling" and "locking" mechanism to build a robust zwitterionic-elastomeric-networked (ZEN) hydrogel (Figure 20f).[158] In the ZEN hydrogel, the PCB network as the minor component was tightly cross-linked to provide elasticity and the PSB network was loosely cross-linked to provide viscosity via its strong inter- and intramolecular electrostatic interactions. This uniform structure makes ZEN hydrogel an elastomeric hydrogel with an exceptional fracture stress of 22.3 MPa (Figure 20g). Importantly, ZEN hydrogels retained superior anti-FBR properties as they prevented foreign body capsule formation

https://doi.org/10.1021/acs.chemrev.2c00344
Chem. Rev. 2022, 122, 17073–17154

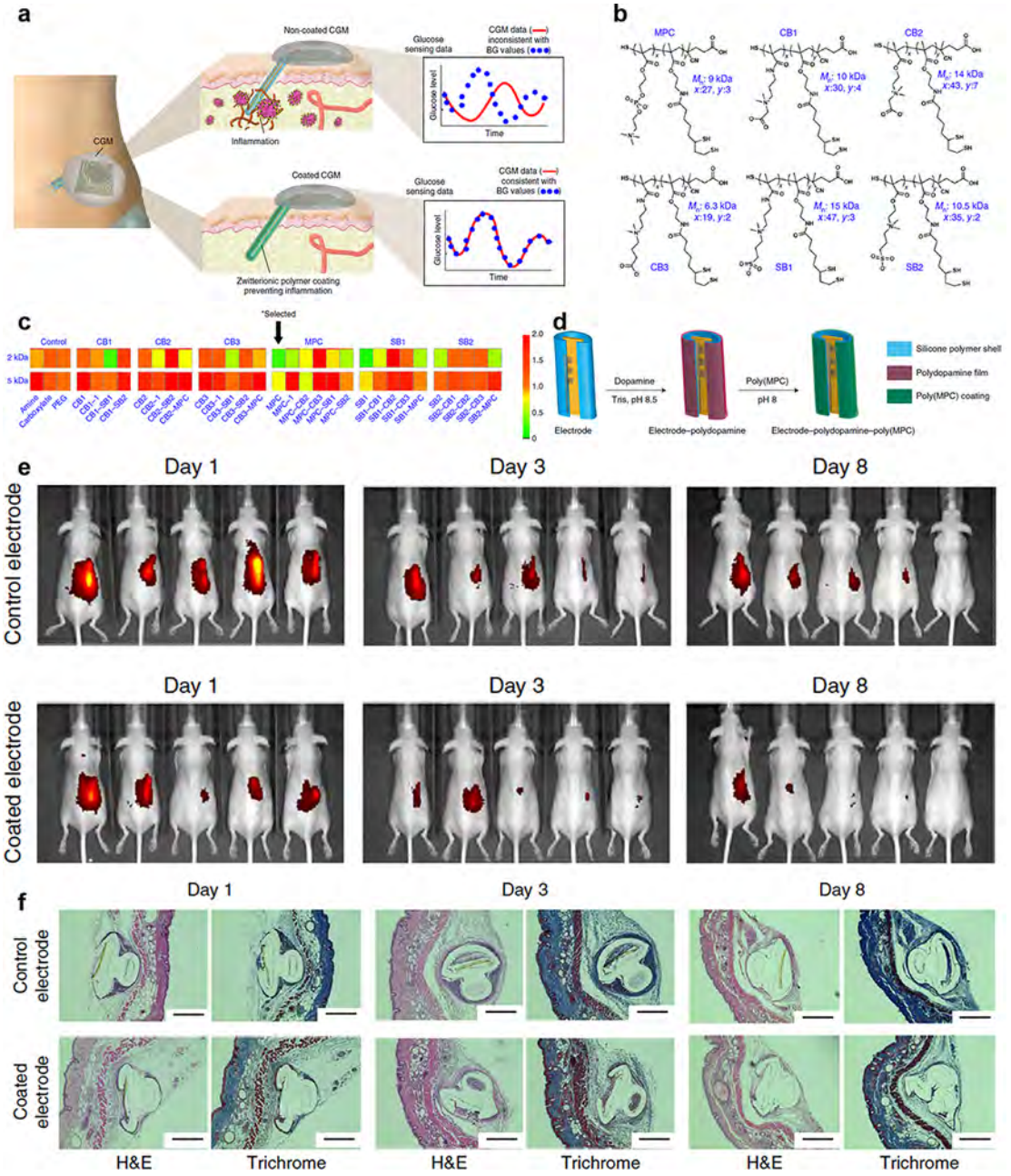

Figure 21. Zwitterionic coating for CGMs. (a) Schematic illustration of zwitterionic polymer coated and uncoated CGMs and their *in vivo* performances. (b) Chemical structures of zwitterionic copolymers. (c) Inflammation profile of tested zwitterionic polymers. Four-arm PEG polymers (2 or 5 kDa) are used as cross-linkers. (d) Schematic illustration of dopamine-mediated coating method. (e) Inflammation monitoring of (top) uncoated versus (bottom) coated CGMs after 1, 3, and 8 days postinsertion. (f) Histological images of retrieved tissues with (top) uncoated and (bottom) coated CGMs. Adapted with permission from ref 310. Copyright 2018 Springer Nature.

for at least 1 year in the C57BL/6 mice model (Figure 20f, left).[158]

4.2.3. Implantable Glucose Sensors. Diabetes mellitus threats the health of hundreds of millions of people worldwide, and many people with diabetes mellitus are still undiagnosed. The characteristics of diabetes mellitus are high blood glucose (BG) concentration and disordered BG regulation. The nonbiological artificial pancreas, also known as closed-loop glucose control, is an emerging approach to treating patients with diabetes, especially with type 1 diabetes, whose insulin-producing pancreatic β-cells are permanently destroyed.[19,335] The nonbiological artificial pancreas contains an insulin pump, a continuous glucose monitor (CGM), and a control algorithm. Among them, the sophisticated and implantable CGM is the core device designed for real-time glycemic tracking aiming to provide feedback to control insulin delivery. However, CGMs encounter FBR including inflammatory events and fibrosis after implantation. Considering that the lifespan of FDA-approved CGMs is less than 10 days, fibrosis is not the major challenge for current CGMs, although it may pose additional problems for long-term usage of CGMs in the future because fibrotic capsules can hamper the mass transfer. Indeed, all state-of-the-art CGMs address the issues of significant short-term noise, which is induced by the early inflammation response of FBR, resulting in very frequent

https://doi.org/10.1021/acs.chemrev.2c00344
Chem. Rev. 2022, 122, 17073−17154

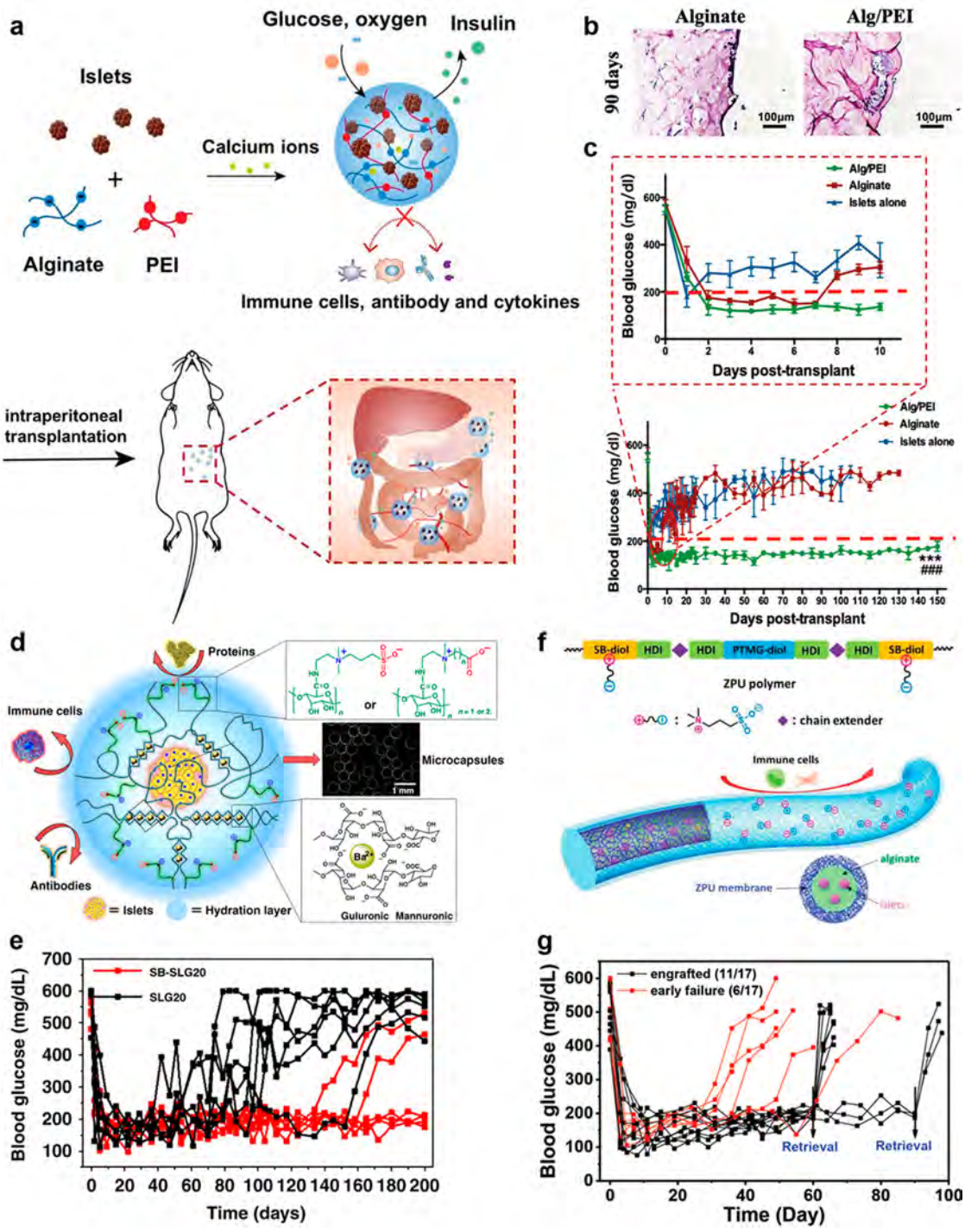

Figure 22. Zwitterionic materials used to protect islets. (a) Schematic illustration of charge balanced alginate/PEI hydrogel microsphere for islet encapsulation and (b) its anti-FBR and (c) blood glucose control performances. Adapted with permission from ref 19. Copyright 2019 John Wiley and Sons. (d) SB- or CB-modified alginate for islet encapsulation and (e) its blood glucose control performance. Adapted with permission from ref 333. Copyright 2019 Springer Nature. (f) Schematic illustration of the islet-encapsulated ZPU tube and (g) its blood glucose control performance. Adapted with permission from ref 334. Copyright 2021 John Wiley and Sons.

recalibration via the painful and wearisome constant finger-prick method.

Zwitterionic materials can be used to resolve this short-term noise issue. Xie et al. evaluated the performance of a series of zwitterionic polymers as the anti-inflammation coatings for the electrode of the CGM (Figure 21).[310] Zwitterionic polymers including PMPC, PCB, PSB, and their combinations were synthesized, and PMPC induced the lowest inflammation signal among all materials (Figure 21b,c). Then, PMPC was coated onto the electrodes of Medtronic CGMs through a dopamine-mediated coating method. After implantation into mice and evaluation by fluorescent whole-body imaging of inflammation-associated protease activity on days 1, 3, and 8, the PMPC-coated CGMs exhibited reduced inflammation profiles compared with the control. Histological examination also confirmed that the coated CGMs reduced the fibrotic

https://doi.org/10.1021/acs.chemrev.2c00344
Chem. Rev. 2022, 122, 17073−17154

tissue overgrowth from day 1 to day 8 compared with the uncoated CGMs. Gene-expression analysis also showed that the PMPC-coated CGMs elicited completely inhibited or even suppressed (less than background) levels of numerous inflammation markers. As a result, the coated CGMs eliminated the short-term signal noise and accurately tracked BG levels without the requirement of recalibration. In contrast, pristine CGMs started to generate significant noise even on day 1 postimplantation.

4.2.4. Islet Encapsulation and Implantation. Another promising treatment for type 1 diabetes patients is the transplantation of islets or β-cells; however, the transplanted cells face immune rejection from the host, thus requiring the long-term use of immunosuppressants. Encapsulating the xenogenous islets within an immune isolating material that resists FBR is a potential way to protect them from the immune attack. Alginate is a commonly used material for islet encapsulation, but it faces great challenges from the induced FBR. The charge balanced alginate/PEI hydrogel was tested for islet encapsulation and implantation (Figure 22a).[19] The results showed that the encapsulated islets could efficiently evade FBR for at least 90 days after intraperitoneal implantation in immunocompetent type 1 diabetic mice (Figure 22b), achieving rapid (within 2 days) and long-term (for at least 150 days) blood glucose correction (Figure 22c). In another approach, Liu et al. modified alginate with a series of zwitterionic SB or CB moieties (Figure 22d).[333] SB/CB-alginate microcapsules were then fabricated via the electrospraying technique and were found to reproducibly mitigate FBR in mice, dogs, and pigs. With the encapsulated islets, SB modified alginate microcapsules maintained long-term glycemic control (~200 days) in type 1 diabetes mice (Figure 22e).

Compared with hydrogel microspheres, retrievable devices are of particular interest due to the ease of removal after the device failure. When the SB-alginate hydrogel is used as the coating for an encapsulation device made of nylon-6 nanofibers, the device supports long-term rat islet cell engraftment, correcting diabetes in C57BL6/J mice for up to 399 days.[336] The same group further developed a retrievable device made from SB modified zwitterionic polyurethanes (ZPUs), which contained polyurethane backbone ensuring mechanical robustness and SB side chains for nonfouling ability (Figure 22f).[334] After intraperitoneal implantation in mice for 6 months, the ZPU device induced significantly lower FBR than the pure polyurethane control device. A ZPU device loaded with rat islets corrected diabetes in mice for ~3 months (Figure 22g). Furthermore, the ZPU device showed scalability and retrievability in pigs and dogs.

4.2.5. Anti-FBR Zwitterionic Materials for Implantable Neutral Electrode. Implantable neuroprosthetic devices that can electrically stimulate neurons and track neural activities have shown promising potential in replacing or restoring lost motor functions of paralyzed patients and treating neurological disorders. However, the implantation of neuroprosthetic devices encounters brain FBR, which can lead to acute and chronic microglia activation, neuronal loss and silencing, glial scarring, persistent leakage of the blood–brain barrier (BBB), and demyelination, resulting in device failure.[311] After implantation, nonspecific protein adsorption initiates the adhesion and activation of microglia and macrophages on the implant surface, followed by a cascade of inflammatory responses. Finally, a scar mainly composed of microglia, activated astrocytes, and fibroblasts is formed, posing a signal transmission barrier between the implant and nearby neurons. In virtue of the ultralow fouling and anti-FBR properties, zwitterionic materials can be used to reduce brain inflammation and improve the performance of implantable neuroprosthetic devices. Golabchi et al. modified the silicone surface of neural electrode devices with PSB via two different methods.[311] One is the utilization of PSB with a terminal catechol group, and the other is the codeposition of PSB and polydopamine (PDA). The PSB–PDA codeposition method was demonstrated to form a stable and potent nonfouling coating for neural probes. PSB–PDA coated probes were implanted into the mouse brain for 1 week, and the coating significantly reduced inflammatory cell recruitment and activation. Moreover, the activation of astrocytes and microglia/macrophages was depressed, and the BBB integrity was improved.

4.3. Lubricated Surfaces

Lubrication is needed for many biomedical devices, e.g., orthopedic implants, to maintain their functions. Zwitterionic surfaces have been found to be effective to reduce interfacial frictions. It is believed that the hydration shell around zwitterionic materials enables friction reduction through hydration lubrication. The hydration shell is firmly attached to the zwitterionic moieties to avoid being squeezed out under high pressure, yet it possesses high mobility to ensure rapid water molecule exchange.[337]

4.3.1. Hydration Lubrication of Zwitterionic Surfaces. Charged moieties, such as zwitterions, attract abundant water molecules to form a hydration layer. This layer performs strong repulsion against van der Waals attraction when two surfaces get close to each other within the range of nanometers, resulting in surface lubrication in their contacting interface. The hydration lubrication layer is strongly held by the charged moieties, leading to reduced Born energy, and considerable energy is required to remove it.[337] It should be noticed that this layer is in dynamic status rather than static. In a thin film with a thickness of 1.0 ± 0.3 nm, most of the water molecules are bound around the charged moieties, yet these bound water molecules still exhibit fluid behavior.[338] As a result, the lubrication layer is very stable yet flexible, so it can withstand huge pressure without being squeezed out and retain fluidity even under high shear, guaranteeing surface lubrication in biomedical use.

Zwitterionic moieties are capable of tenaciously attracting water molecules; thus they can generate a hydration layer to resist dehydration and sustain high pressure, leading to stable surface lubrication.[136,339−344] In 2004, Kawaguchi and coworkers first reported the usage of PMPC coating to reduce friction in artificial joints.[135] Subsequently, Jiang and coworkers studied nanoscale friction between two PC-SAM surfaces using MD simulations, showing that the hydration of surfaces plays a key role in water-based lubrication systems.[345] In addition, the friction coefficient exhibited a strong correlation with the number of hydration water molecules. The study also found that a high concentration of ions in the solution could result in higher friction due to disruption of the hydration layer around the zwitterionic surfaces. Ions with shorter Debye lengths had a greater disturbance in the hydration layer. Finally, the friction coefficients were directly proportional to both the shear velocity and the surface separation distance under nanoscale confinement. Later, the effects of monovalent ions in the Hofmeister series on the

https://doi.org/10.1021/acs.chemrev.2c00344
Chem. Rev. 2022, 122, 17073−17154

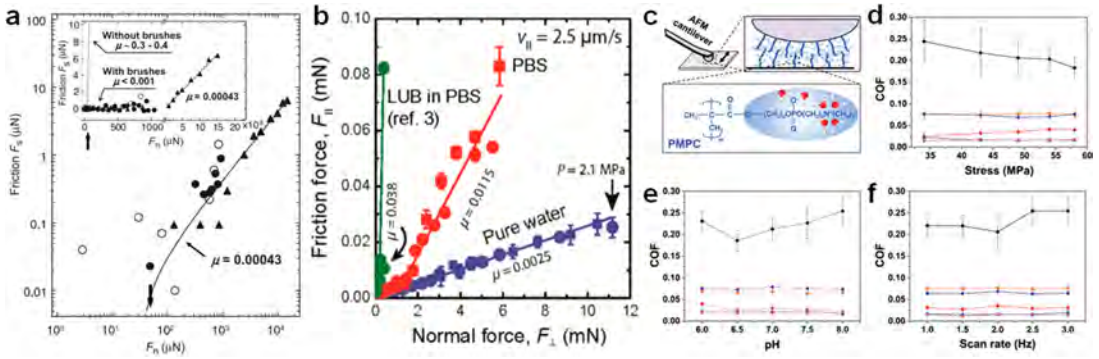

Figure 23. (a) Friction F_s versus load F_n between PMPC brush coated surfaces. The coefficient of friction μ reached a minimum value of 0.00043. Adapted with permission from ref 136. Copyright 2009 The American Association for the Advancement of Science. (b) Coefficient of friction μ on MPC-containing polymer-modified mica sheets in pure water and PBS. Adapted from ref 339. Copyright 2014 American Chemical Society. (c) Schematic illustration showing the lubrication test setup with the tribopair between PMPC-grafted SiO_2 wafer and PMPC-grafted PS microsphere. (d–f) Lubrication performance of SiO_2 wafer contacted with PS microsphere with COF values obtained under different values of stress, pH, and scan rate. Black diamond, bare SiO_2 and aminated PS; orange square, bare SiO_2 and PMPC-grafted PS; navy left-pointing triangle, PMPC-grafted SiO_2 and aminated PS; red circle, blue up triangle, and magenta down triangle, PMPC-grafted SiO_2 and PMPC-grafted PS with concentrations of 0.05, 0.10, and 0.15 M in the polymerization process, respectively. Adapted with permission from ref 344. Copyright 2019 John Wiley and Sons.

friction of zwitterionic surfaces were studied by the same group with carboxybetaine self-assembled monolayers (CB-SAMs).[346] A strong correlation was found between the order of ions in the Hofmeister series and the friction of the CB-SAM surfaces. Experimentally, Chen et al. grafted PMPC chains on a mica model surface, which dramatically decreased the coefficient of friction (COF) from 0.33 to an ultralow value of 0.00043 under high pressure of 7.5 MPa (Figure 23a).[136] This value was even lower than that of the natural joints, a COF of <0.002 under a pressure of 5 MPa. Banquy et al. synthesized an MPC-containing bottle-brush polymer inspired by the mammalian synovial fluid protein lubricin.[339] The polymer-adsorbed mica sheets exhibited a COF of 0.0025 in water and a slightly increased COF of 0.0115 in PBS buffer under a pressure of 2.1 MPa (Figure 23b),[339] lower than that of lubricin in PBS (COF = 0.038).[340] The higher COF in PBS than in water is ascribed to the polymer conformational change. The unperturbed height of the polymer was found to be 33 nm in pure water but only 15 nm in PBS. Further studies demonstrated that in the presence of multivalent ions zwitterionic brushes performed significantly better than polyelectrolyte brushes.[343] Wang et al. grafted the PMPC brush layer on a silica sheet (PMPC–SiO_2) and polystyrene microsphere (PMPC–PS) and investigated the lubrication behavior between the PMPC–SiO_2 and PMPC–PS (Figure 23c–f). Attributed to the tenacious hydration layer and rapid water movement, the coating displayed durable lubrication with stable low COFs under wide ranges of stress (34–58.15 MPa), pH (6.0–8.0), and scan rate (1–3 Hz).[344]

4.3.2. Zwitterionic Polymer Coating for Orthopedic Implants. Due to its outstanding performance, MPC coating has been applied at interfaces of orthopedic implants to improve lubricity and reduce wear.[135,347−353] Moro et al. covalently grafted PMPC on a polyethylene (PE) artificial joint and thoroughly compared the lubrication properties of pristine PE and PMPC–PE.[135] The water affinity of PMPC–PE was significantly improved as its water contact angle decreased to less than 20°. In friction tests, the COF of the PE joint surface reduced to 1/7 of the original value after coating, and the friction torque of PMPC-modified PE was 80–90% lower than that of the pristine PE. Importantly, after 3×10^6 cycles of gravity loading via a hip-joint simulator, the wear amount of PMPC–PE was 40 times lower than that of the pristine PE. The study also compared the biological responses of PMPC-coated and noncoated PS particles at a size of 500 nm, simulating the clinically failed prostheses. Both *in vitro* and *in vivo* results demonstrated that the MPC-coated PS particles were inert and did not induce osteoclastic bone resorption. Subsequently, the PMPC-coated artificial joints were approved by the regulatory agencies in Japan and the United States.[142] For example, a PMPC-coated artificial hip joint system, named Aquala from KYOCERA Co. Ltd., Japan, has been implanted in over 52 000 patients from November 2011 to January 2019.[142] Despite the outstanding performance demonstrated on the simulators *in vitro*, recent studies on retrieved Aquala hip joints from short-term total hip arthroplasty suggested that PMPC grafts on polyethylene did not offer additional protection from oxidation and can delaminate prematurely after short-term *in vivo* exposure.[354] Further studies are needed to investigate the mechanism behind this, and an improved coating strategy may be required to overcome this issue.

4.3.3. Lubrication between Hydrogels. Hydrogels hold the potential to be used as cartilage substitutes. Zwitterionic moieties are introduced into various hydrogel systems to reduce their interfacial friction. For example, MPC was copolymerized with gelatin methacrylate and acrylamide to fabricate a composite hydrogel as a scaffold for articular cartilage defects.[355] The lubrication property was found to be highly dependent on the MPC content. Under the test conditions of 0.5 N load and 2 Hz frequency, the addition of 30% MPC reduced the COF value from 0.052 to 0.011, while increasing the MPC content to 50% did not further improve the lubrication. For many applications such as cartilage replacement, both low friction and high mechanical strength are required for the hydrogel system. Zwitterionic polymers were explored as a component to fabricate strong and lubricant double-network (DN) hydrogels.[356−358] It should be noted that the lubrication performance of SB is more sensitive to ions than that of PC due to its salt-responsive solution behavior.[357] In pure water, the incorporation of MPC into an SBMA hydrogel effectively reduced its friction at the interface.[359]

In a biological system, the articular cartilage remains well lubricated over a lifetime of sliding and wear by exposing phosphatidylcholine lipids at their nonfluid boundary layers.

https://doi.org/10.1021/acs.chemrev.2c00344
Chem. Rev. 2022, 122, 17073−17154

The highly hydrated PC head groups reduce friction via the hydration lubrication mechanism, while the lipids are well maintained through cellular replenishment after frictional wear occurs. Lin et al. showed a simple biomimetic lubricated hydrogel system by incorporating trace amounts of PC lipids in a bulk hydrogel (Figure 24).[360] The lipids were sequestered in

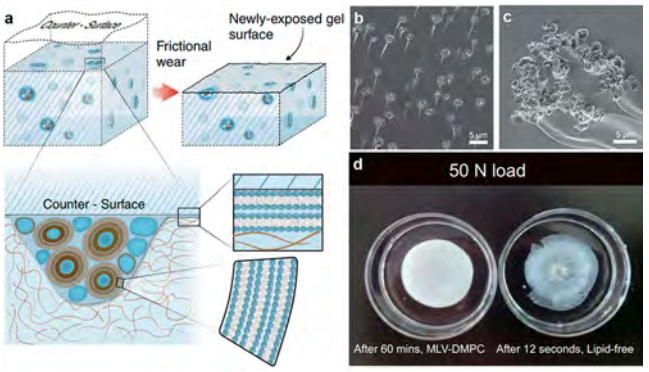

Figure 24. Surface lubrication performance of zwitterionic hybrid hydrogels. (a) Hydration lubrication of lipid-incorporating hydrogel. Cryo-SEM images of (b) DMPC-HEMA and (c) HSPC-HEMA hydrogels. (d) Optical images of hydrogels after 50 N load on the steel sphere. Adapted with permission from ref 360. Copyright 2020 The American Association for the Advancement of Science.

clusters within the bulk hydrogels and formed boundary layers of lipids on the surfaces. The addition of the lipids reduced 80−99.3% in friction and wear relative to the lipid-free hydrogel over a wide range of conditions, and the effect was observed even after the hydrogels were dried and rehydrated. Importantly, the lubrication effect was well maintained after frictional wear as the surface boundary layer can be continuously replenished.

4.4. Antibacterial Coatings

Humankind has been suffering from biofilm-related infections for all of history. For example, it has been revealed by the National Institutes of Health that approximately 65% of microbial infections and 80% of chronic infections are related to biofilms, including urinary tract infection, dental plaque formation, and catheter infection.[361,362] Therefore, it is necessary to focus on preventing biofilm formation, and understanding the biofilm development process and mechanisms is a prerequisite.

4.4.1. Biofilm Formation. Biofilms are composed of clusters of microorganisms, surrounded by the extracellular matrix (ECM). The ECM is very complex and includes extracellular polysaccharides, proteins, lipids, and nucleic acids.[363] The ECM protects microorganisms and helps them to stick to and grow on nearly all natural and synthetic materials. The formation of biofilm generally starts from organic molecule adsorption, forming a "conditioning film" at the surfaces (Figure 25).[364] When microbial cells get closer to the surface, nonspecific attraction and specific recognition play key roles in cell adhesion. Protein adsorption increases the overall surface area and leaves nano- and microstructures on surfaces.[365] Microbial cells can use their strong and flexible flagella and/or fimbriae to wrap around the hummocks and explore hollows on the surfaces, thereby performing tight anchoring.[366] In addition, microbes can also get attached via nonspecific physicochemical forces, including electrostatic

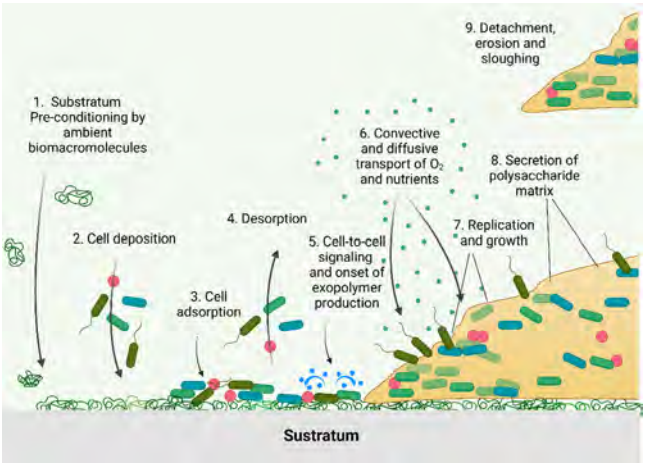

Figure 25. Biofilm formation process.[364] Created with BioRender.com.

interactions, hydrophobic interactions, and van der Waals interactions.[367] Electrostatic attraction originates from the positively and negatively charged moieties on protein and material surfaces. Protein adsorption locally charges the surfaces; thus, microbes possessing opposite charges can be attracted. Hydrophobic interactions have a greater influence on the initial adhesion.[368] Some proteins can help hydrophobize the surface by exposing nonpolar groups to the surrounding environment when they are adsorbed, which facilitates the microbe's anchoring.

4.4.2. Repelling Bacteria. According to the mechanism mentioned above, protein adsorption plays a crucial role in biofilm formation. Therefore, a primary antibacterial strategy is using a nonfouling surface to repel protein adsorption and bacterial adhesion. Zwitterionic polymers based on natural zwitterions have demonstrated superior nonfouling properties, thus achieving various remarkable performances in antibacterial applications.

PC- and SB-based zwitterionic materials have been proven to repel microbial cells. Kang et al. demonstrated that MPC-based copolymer reduced over 80% of *Streptococcus mutans* attachment compared with unmodified hydroxyapatite in 24 h of culture.[369] PSBMA effectively resisted biofilm formation of *Pseudomonas aeruginosa* in a nutrient-rich medium under flow conditions for 3 days.[370,371] Smith et al. showed PSBMA coating reduced 96% of microbial adhesion from *E. coli* and *S. aureus* on both internal and external catheter surfaces after 24 h of incubation.[22] Diaz Blanco et al. demonstrated that PSBMA reduced biofilm of *P. aeruginosa* and *S. aureus* by 80 and 90% for 7 days on urinary catheters, respectively.[372] However, it still showed the colonization of *P. aeruginosa* over time. Kwon et al. developed a poly(sulfobetaine-*co*-tyramine) copolymer that reduced the adhesion of *S. aureus* by 90% for 18 h.[373] Peng et al. reported a zwitterionic sulfobetaine/active ester block copolymer, PSBMA-*b*-PNHSMA, which could resist biofilm formation of *S. aureus* for 21 days.[266]

CB-based zwitterionic materials can also resist bacterial adhesion and biofilm formation. In 2009, for the first time, Cheng et al. showed that PCBMA grafted surface could prevent biofilms for up to 10 days with less than 6% bacteria accumulation compared with unmodified glass at room temperature.[374] Wang et al. reported the undetectable attachment of *S. aureus* on PCB-modified polyurethane (PU)

https://doi.org/10.1021/acs.chemrev.2c00344
Chem. Rev. 2022, 122, 17073−17154

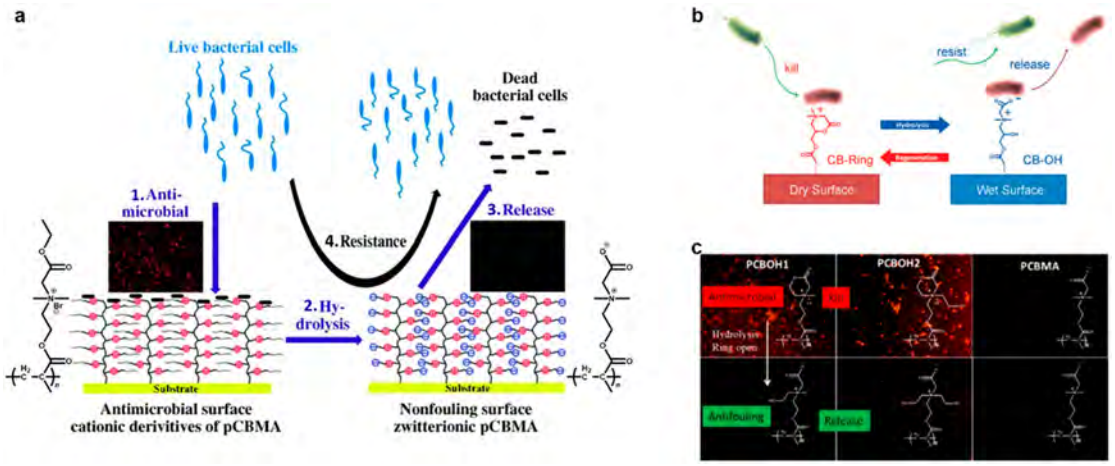

Figure 26. Zwitterionic polymers with "kill-and-release" functions. (a) PCB ester that switches from a cationic antibacterial form to a nonfouling PCB surface upon hydrolysis. Adapted with permission from ref 191. Copyright 2008 John Wiley and Sons. (b) The polymer coating that reversibly switches between CB-ring to kill bacteria under dry conditions and CB-OH to release and resist bacteria under wet conditions. Reproduced with permission from ref 182. Copyright 2011 John Wiley and Sons. (c) Bacteria killing and release of PCBOH1 and PCBOH2. (left) CBOH1 and (middle) CBOH2 can switch between the zwitterionic form and the cationic form. Adapted with permission from ref 185. Copyright 2014 John Wiley and Sons.

surface for 1 h.[197] In 2017, Cao and co-workers developed a durable and ultrarobust nonfouling zwitterionic PCBAA (DURA-Z) coating, which highly resisted the biofilm of *E. coli* and *S. aureus* and achieved "zero" biofilm formation for up to 30 days.[375] In addition to surface coatings, Wang et al. integrated zwitterionic moieties via the chain extenders in PU, achieving "zero" biofilm formation of *P. aeruginosa* for 14 days on the PU surface.[376] To further improve the long-term antibiofilm and mechanical properties of the zwitterionic polymer, they further improved the PU formulation. The material showed critical nonfouling properties that resulted in undetectable levels of bacterial attachment and undetectable biofilm formation after 6 months of constant exposure to *P. aeruginosa* and *S. epidermidis* in a nutrient-rich medium.[377] This study validated the widely used but unproven hypothesis that nonfouling materials can completely avoid biofilm formation. Due to their merits of bacterial resistance, zwitterionic materials have been explored as antimicrobial coatings for many medical devices and implants, including catheters, contact lenses, teeth, etc.[22,378−380]

4.4.3. "Kill and Release". Traditional antibacterial surfaces use agents or materials that can kill microorganisms or inhibit their growth, such as quaternary ammonium modified materials. However, one major challenge for such approach is that dead cells deactivate the surface. For successful antimicrobial surfaces, it is important to not only kill microbes but also release them afterward. On the other side, the usage of nonfouling coatings alone might introduce pathogenic microbes into the patient during implantation operations and catheter insertions, which results in the failure of implanted devices. The integrated antimicrobial/nonfouling surface copolymerized by the zwitterionic nonfouling blocks with antimicrobial agents can address this long-standing challenge.[381−385] For example, Yan et al. used surface-initiated photoiniferter-mediated polymerization (SI-PIMP) to create diblock copolymer brushes consisting of a cationic inner block and a zwitterionic outer block. Under dry conditions, the cationic block killed the attached *S. aureus* and *E. coli*, while the zwitterionic block repelled both strains from adhering to the surface.[381] Ma et al. developed rechargeable biocidal poly(vinyl alcohol-*co*-ethylene) films (SBMA@HAFfilms), which were modified with PSBMA and *N*-halamine (HAF). The chlorinated HAF could rapidly kill attached bacteria, and SBMA enabled the surface to repel and release bacteria. After use, the material could be recharged by chlorination of the HAF. These SBMA@HAFfilms achieved 6 logs of reduction of *E. coli* and *L. innocua* in 15 min and released 95% of *E. coli* and *L. innocua*.[382]

Benefiting from the functionalizable carboxyl group, the "kill-and-release" mechanism can be realized on PCB-derived surfaces without copolymerization with other components. Cheng et al. originally reported the usage of PCB esters as antimicrobial coatings (Figure 26a).[191] The PCB ester is positively charged that effectively kills bacteria attached on the surface, while it converts to zwitterionic PCB upon hydrolysis to release the dead bacteria. Once hydrolyzed, the surface permanently becomes zwitterionic and loses the bactericidal activity. Later on, Cao et al. showed an improved strategy that enabled the reversible switching between bactericidal and repelling states by adding a hydroxyl group to the CB structure (CB-OH).[182] Esterification of CB-OH occurred in acidic media, forming a cationic inner six-membered ring which effectively killed bacteria (Figure 26b). The ring can then be easily hydrolyzed back to zwitterionic CB-OH in neutral or basic solutions, which released the dead bacteria. On the basis of a similar mechanism, Cheng and co-workers further developed a series of materials that can reversibly switch between bactericidal and nonfouling states upon pH stimuli (Figure 26c).[185,186,386]

In addition to pH stimuli, an electroswitchable zwitterionic material was also reported for switchable antimicrobial/nonfouling properties.[387] In this study, an electroactive nonfouling polymer, poly(sulfobetaine-3,4-ethylenedioxythiophene) (PSBEDOT) was directly electropolymerized on metallic and ceramic surfaces, including gold, stainless steel, and indium tin oxide, in an aqueous solution. PSBEDOT could be oxidized electrochemically to the cationic state as well as be reduced back to the zwitterionic state. At its oxidized cationic state, the PSBEDOT surface caught and killed the attached *E. coli K12* cells. After the surface was reduced to the zwitterionic

https://doi.org/10.1021/acs.chemrev.2c00344
Chem. Rev. 2022, 122, 17073−17154

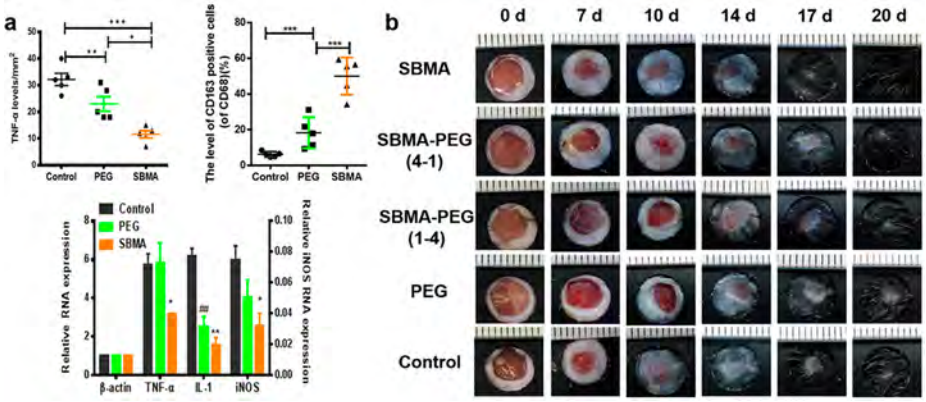

Figure 27. Comparison of PSBMA and PEG hydrogel wound dressings. (a) Levels of pro-inflammatory and anti-inflammatory factors. (top, left) TNF-α and (top, right) CD-163 levels. (bottom) mRNA levels of TNF-a, IL-1β, and iNOS. (b) Wound closure of mice at different time points treated with PEG, PSB, and hybrid PSB−PEG hydrogels. Adapted with permission from ref 395. Copyright 2018 Elsevier.

state, PSBEDOT released the killed microbes and exhibited excellent nonfouling properties to resist protein adsorption, mammalian cell attachment, and bacterial adhesion.

Although the cationic coatings can effectively kill bacterial cells attached to surfaces, they have limited antimicrobial capacity against the planktonic bacterial cells. To solve this issue, Cheng et al. integrated a negatively charged mild antimicrobial agent, salicylate, into a CB ester hydrogel as the counterion.[388] Through hydrolysis or ion exchange, the hydrogel sustainedly released salicylate to kill the planktonic bacteria. Meanwhile, it exposed a zwitterionic nonfouling surface to resist bacterial adhesion after hydrolysis. In a following study, the researchers conjugated the antibacterial salicylate anion to the carboxyl group of PCB as a leaving group.[389] The material maintained the zwitterionic state before, during, and after salicylate release, preventing bacterial surface adhesion and bulk proliferation simultaneously.

4.5. Wound Dressings

Over the past decades, traditional dressings such as cotton gauze and bandages have been widely used to manage wounds. The primary functions of these dressings are to adsorb wound exudates and keep the wound dry. However, they tend to adhere to the desiccated wound and easily damage the newly generated tissue upon removal. With the rise and development of the moist wound healing concept, dressings are expected to support wound healing in addition to wound protection. An ideal wound dressing should possess several necessary characteristics, such as maintaining the optimum moisture, allowing the diffusion of oxygen, relieving the patient's pain, preventing bacterial infections, and promoting wound healing.[390,391] From this perspective, superhydrophilic zwitterionic materials are superior candidates.

Zwitterionic hydrogels have been found to promote wound healing. In a study, Huang et al. synthesized poly(sulfobetaine acrylamide) (PSBAA) hydrogels incorporated with nanoclay as dressings to treat diabetic chronic wounds.[392] The diabetic wound treated with PSBAA hydrogel exhibited re-epithelialization and new connective tissue generation after 12 days, faster than the commercial hydrofiber wound dressing, AQUACELs. The nonfouling property made PSBAA hydrogel easily removable from the wound surface, whereas removal of the commercial dressing typically damaged the newly generated tissues. Zwitterionic PCB hydrogels have been evaluated as the dressings in a third-degree burn treatment by Zhu et al.[393] With a higher water content and better biocompatibility, PCB hydrogels also induced a faster wound healing process than the commercial DuoDerm. To enhance the antimicrobial activity, bactericidal compounds can also be integrated into the zwitterionic hydrogel dressings.[394]

PEG has long been used for wound regeneration applications. To explore and reveal the differences between zwitterionic polymers and PEG materials, Wu et al. evaluated PSB hydrogels in a full-thickness skin defect mice model in comparison with PEG hydrogels.[395] Results demonstrated that the zwitterionic PSB hydrogels could increase the secretion of growth factors and motivate the macrophage polarization from M1 to M2, as demonstrated by the upregulation of anti-inflammatory factors (CD-163) and the downregulation of pro-inflammatory factors (TNF-α, IL-1β, and iNOS) (Figure 27a). As a result, they showed an improved *in vivo* wound healing performance compared with PEG hydrogels (Figure 27b).

Zwitterionic moieties can also be applied to modify various wound dressing materials. Qiu et al. used CB and SB to modify dextran hydrogels to fabricate wound dressing with merits from both components.[396] The zwitterionic groups resisted adhesions from tissue and bacteria, while dextran scavenged free hydroxyl radicals. Moreover, this hydrogel was stretchable to adapt to the wound, benefiting from the self-healing properties. Venault et al. used a postmodification method that converted poly(styrene-*r*-4-vinylpyridine) into a zwitterionic copolymer and blended it with poly(vinylidene fluoride) (PVDF) to make electrospun nanofiber membranes as dressings for diabetic wounds.[397] The zwitterionic moieties promoted the binding of water molecules and endowed the dressing with faster removal of exudates from the wound bed, thus favoring the healing process. Meanwhile, the membrane dressing efficiently resisted adhesions from biological substances, including proteins (>75% reduction), bacteria (>80% reduction), and blood cells (>95% reduction).

Smart wound dressings are emerging to provide readable signals regarding wound status, such as healing phases, bacterial density, oxygen content, pH, and temperature.[24] For example, pH is an essential parameter as it is related to many physiological processes such as wound infection, angiogenesis, and protease activity. Chronic wounds are hard to heal and are generally under alkaline conditions, while acute wounds with acidic conditions heal more efficiently. Zwitter-

https://doi.org/10.1021/acs.chemrev.2c00344
Chem. Rev. 2022, 122, 17073−17154

ionic hydrogels can be used as the substrate to fabricate smart wound dressings.[24,398] Based on enzymatic reactions, Zhu et al. designed a multifunctional zwitterionic dressing as a wound sensor to monitor the pH and glucose levels in diabetic wounds simultaneously.[24] The combination of glucose oxidase (Gox) and horseradish peroxidase (HRP) was used as the glucose indicator, and phenol red was selected as the pH dye. The fluorescence and color intensity of the dressing can be recorded by smartphones and calculated to qualify the glucose concentrations and pH values in the wound environment. Owing to the superhydrophilic and nonfouling properties of PCB hydrogel, both the activity and stability of enzymes were improved in wound exudate compared with free enzymes.

4.6. Nanocarriers for Drug Delivery

Nanoparticles (NPs) have emerged as a powerful tool for drug delivery. The *in vivo* fate and performance of these vehicles are strongly influenced by the protein corona and opsonization. Due to the strong hydration and nonfouling properties, zwitterionic materials can protect these vehicles from undesired interactions with the biological body, thus significantly improving the drug delivery performance and therapeutic effect.

4.6.1. Protein Corona and Opsonization. When injected in a biological milieu, a nanoparticle may rapidly adsorb proteins forming a protein corona. The protein corona changes the interfacial composition of a particle, giving it a new biological identity that determines the physiological response.[35] The major influence of protein corona on NPs is the undesired and rapid elimination by phagocytosis of the mononuclear phagocytic system (MPS), also known as the reticuloendothelial system (RES). This process is initiated by "opsonization" (Figure 28a), meaning the adsorption of

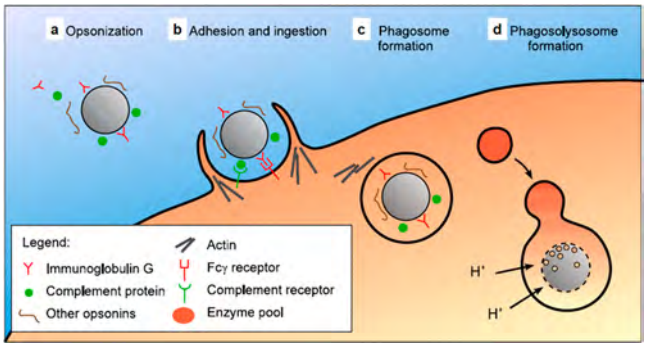

Figure 28. Opsonization and phagocytosis. Reproduced with permission from ref 400. Copyright 2009 Springer Nature.

opsonins, including immunoglobulins, fibrinogen, complement proteins, laminin, fibronectin, etc. The opsonized NPs will be rapidly recognized by mononuclear phagocytes through specific interactions between opsonins and specific cell receptors.[399] For instance, macrophages can interact with fibrinogen, immunoglobulins, and complement proteins in the corona on NPs through their integrin receptor, Fc receptor, and complement receptor, respectively (Figure 28b).[5] The recognition can accelerate a signaling cascade to assemble actin, resulting in the extension of cell membrane surface (Figure 28b). Subsequently, "phagosome" is formed to engulf and internalize the NPs (Figure 28c). After a battery of fusion and fission evens, the phagosome becomes a "phagolysosome" which owns an acid environment and plenty of enzymes, such as cathepsins and esterases, attempting to digest the foreign NPs (Figure 28d).[400] As a result, this elimination process leads to a significantly shortened blood circulation time, severely impeded bioavailability, and undesired biodistribution.[5,6] In addition, the protein corona may cover the targeting ligands of NPs, severely hampering their targeting ability.[34] Moreover, the protein corona might also lead to NP instability, causing agglomeration or structural damage.[6,401]

Resistance to opsonization is crucial for nanomedicine. A prerequisite is to understand the mechanism of protein corona formation. As is well-known, hydrophobic−hydrophobic interaction and electrostatic attraction are the two major driving forces for protein adsorption on macroscopic surfaces. This trend translates well to the protein corona formation on the surface of NPs. Therefore, the surface nature of NPs is the major factor influencing the constitution of the protein corona, which in turn strongly determines the effect on biological components.[35] Similar to bulk surfaces, NPs are usually coated with hydrophilic polymers, such as PEG[402] and zwitterionic polymers,[403] to resist nonspecific protein adsorption and increase stability.

4.6.2. Merits Brought by Zwitterionic Moieties. *4.6.2.1. Reduced Opsonization, Inhibited Cell Uptake, and Prolonged Circulation.* With superior nonfouling properties, zwitterionic materials endow nanocarriers with intriguing stability against the disturbance of blood proteins. As discussed in previous sections, zwitterionic small molecular ligands have been successfully applied to stabilize inorganic or metallic nanoparticles in the biological milieu.[109,110] For polymeric drug carriers, zwitterionic polymers have been shown to stabilize micelles, liposomes, and hydrogel nanoparticles in plasma and serum.[404−406] For instance, Cao et al. studied the stability of a nanoparticle self-assembled from PLGA−PCB block copolymers.[404] The obtained PLGA−PCB NPs were shown to be stable without significant change in size in 100% serum for over 5 days. In contrast, unmodified PLGA NPs immediately encountered severe aggregation after immersion in serum. Lu et al. conjugated PCB with a molecular weight of 5 kDa to 1,2-distearoyl-*sn*-glycero-3-phosphoethanolamine (DSPE) lipid, forming a "sharp polarity contrast" polymer (DSPE−PCB 5K).[407] The docetaxel-loaded micelles assembled from DSPE−PCB 5K (docetaxel/DSPE−PCB 5K) presented excellent stability in 100% FBS for over 72 h.

Avoiding nonspecific interactions helps the nanoparticles evade cellular uptake and immune clearance. Cheng et al. showed that nanogels made from PCB were not internalized by vascular endothelial cells without surface conjugation of targeting ligands.[405] Zhang et al. demonstrated that these nanogels could even avoid cellular uptake by macrophages.[189] Similar effects were also reported for other zwitterionic micelles and zwitterionic polymer modified organic and inorganic NPs.[220,408−410]

The enhanced blood stability and inhibited cellular clearance result in superior pharmacokinetics of various zwitterionic drug vehicles.[209,407,411−420] For example, the PCB-modified liposome showed long circulation behavior in an earlier study, with a half-life similar to or longer than that of the classic PEG-modified liposome.[416] In another study, the docetaxel/DSPE−PCB 5K micelles exhibited longer blood circulation than those of other formulations, including docetaxel/DSPE−PEG 5K, docetaxel/polysorbate 80, and Taxotere.[407] The elimination half-life of docetaxel/DSPE−PCB 5K was calculated to be 5.9 h, leading to a favored biodistribution. Zhang et al.

https://doi.org/10.1021/acs.chemrev.2c00344
Chem. Rev. 2022, 122, 17073−17154

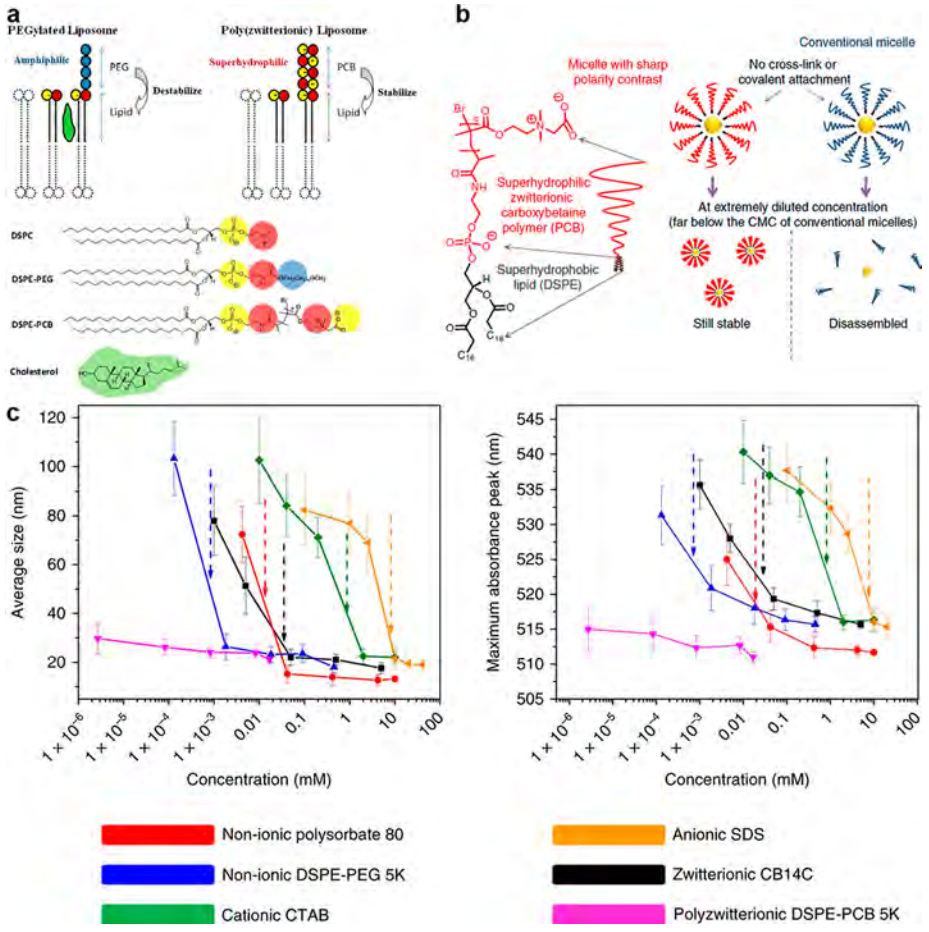

Figure 29. (a) Schematic illustration of components of liposome made from PCB or PEG conjugated lipids. Reproduced from ref 416. Copyright 2012 American Chemical Society. (b) Structure of DSPE−PCB 5K micelles. (c) Diluting−concentrating method to probe cmc's for DSPE−PCB 5K and other micelles. Known cmc values for micelles are indicated by dashed arrows. Reproduced with permission from ref 407. Copyright 2018 Springer Nature.

systematically studied the *in vivo* circulation behavior of a series of PCB nanogels with different cross-linking densities.[421] The results showed that, at a size of around 120 nm, softer nanogels with lower cross-linking densities tend to have longer circulation half-lives. When calculated with the use of a one-compartment model, the nanogels with cross-linking densities of less than 2% exhibited half-lives of around 20 h. Softer nanogels also showed less splenic accumulation.

4.6.2.2. Enhanced Stability and Ultralow cmc. Apart from the instability caused by protein corona, the stability of self-assembled polymeric NPs against aggregation and dissociation is another critical factor for successful drug delivery. These NPs need to remain stable during manufacture and storage. Due to its extreme polarity, zwitterionic polymer blocks exhibit sharp contrast to hydrophobic blocks in a copolymer, contributing to the stability of self-assembled NPs.[404,407,416,422] For instance, the self-assembled PLGA−PCB NPs were colloidally stable for at least 5 days, they and can maintain their size and distribution even after repeated high-speed centrifugation and resuspension.[404] In contrast, PLGA NPs aggregated after centrifugation. Moreover, the PLGA−PCB NPs could be freeze-dried without any protective additives for long-term storage. The particle size and polydispersity index of lyophilized PLGA−PCB NPs could be completely recovered via easy resuspension, greatly facilitating the manufacture and storage. The stabilizing effect was also seen in PCB-modified liposomes.[416] Classic liposomal formulation utilizes PEGylation and cholesterol to stabilize the formed vesicles. Cao et al. showed that the PCB-modified liposomes could well retain their structure with high colloidal stability without the addition of cholesterol or any other stabilizers (Figure 29a).[416]

Self-assembled micelles disassemble into free amphiphilic polymers when diluted below the critical micelle concentration (cmc). When injected into the blood flow, the concentration of drug-loaded micelles may quickly drop below the cmc. As a result, the nanocarriers disassemble and the encapsulated drugs are released before reaching the target, significantly reducing their efficacy. To address this problem, Lu et al. designed the "sharp polarity contrast" micelle system, DSPE−PCB 5K, which maintained a superhydrophobic lipid domain and a superhydrophilic zwitterionic polymer domain (Figure 29b).[407] Due to the drastically sharp polarity contrast between the two domains, DSPE−PCB 5K micelles showed an ultralow cmc below the detection limit of 2.7×10^{-6} mM (Figure 29c), at least 3 orders of magnitude lower than the cmc values of commonly seen micelles (usually $>10^{-3}$ mM). As a result, DSPE−PCB 5K micelles retained their capacity to hold drug cargos in extremely diluted conditions. When applied *in vivo*, the ultrastability of these zwitterionic micelles may significantly boost the therapeutic effects by simply retaining their structure intact in the challenging biological environments.[407]

https://doi.org/10.1021/acs.chemrev.2c00344
Chem. Rev. 2022, 122, 17073−17154

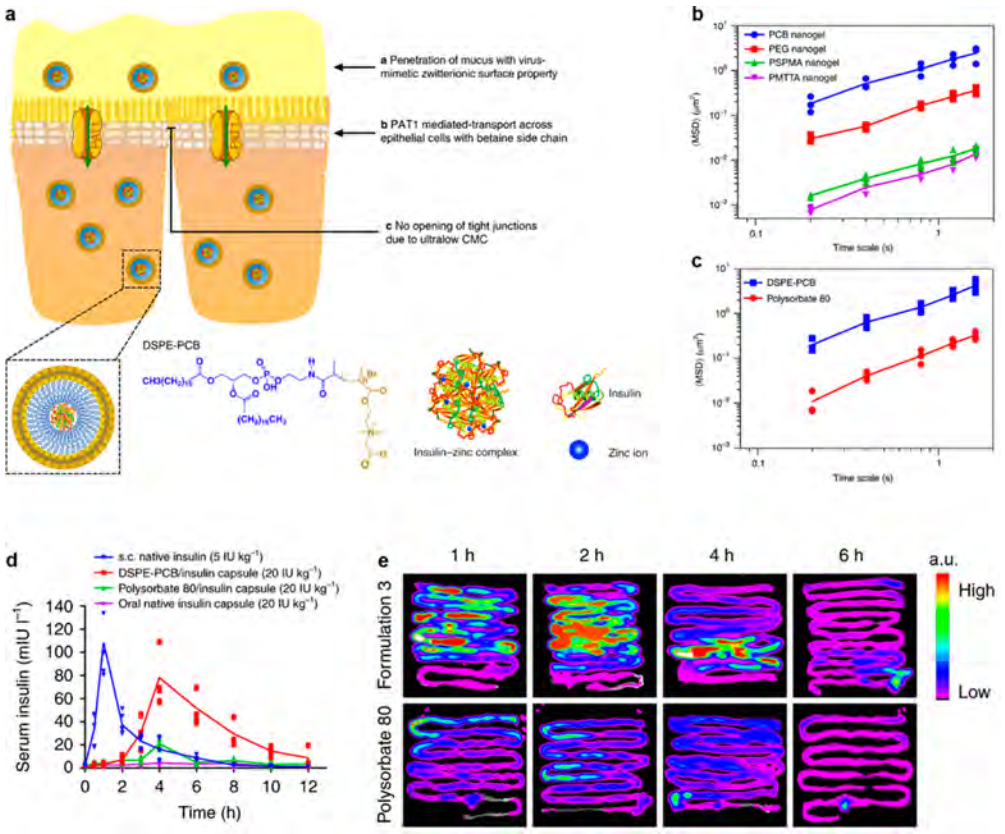

Figure 30. Zwitterionic nanocarriers penetrating intestinal mucus and epithelial cell layer. (a) Schematic illustration of DSPE−PCB micelles for intestinal barrier penetration and insulin delivery. (b, c) Transport of (b) nanogels and (c) micelles in reconstituted porcine stomach mucus. Neutral nonionic PEG, anionic poly(3-sulfopropyl methacrylate potassium salt) (PSPMA) and cationic poly((2-(methacryloyloxy) ethyl) trimethylammonium chloride) (PMTTA) nanogels are used as controls. (d) Bioavailability of DSPE−PCB/insulin, Polysorbate 80/insulin, and native insulin capsules. (e) *Ex vivo* fluorescent imaging of absorption sites of orally delivered insulin at different time points. Adapted with permission from ref 425. Copyright 2020 Springer Nature.

4.6.2.3. Improved Penetration of Mucus and Epithelial Cell Layer. Mucus and epithelial cell layer are two protective layers to prevent the entrance of foreign substances into the body. However, they are also two major barriers to systemic drug delivery via oral and pulmonary routes, leading to low bioavailability and poor therapeutic performance. Therefore, the ability to penetrate the mucus and epithelial cell layer is highly desired for the design of drug delivery vehicles. Mucus is a viscous, elastic, and sticky layer consisting of highly cross-linked mucins (major proteins in mucus), which can efficiently trap foreign particles or pathogens and rapidly clear them.[423] In nature, capsid virus can diffuse unhindered through mucus and readily infect mucosal epithelia. Analysis showed that capsid virus possesses an oppositely charged but net-neutral surface without any hydrophobic patches,[424] demonstrating typical zwitterionic characteristics. By learning from nature, zwitterionic materials are used to enhance the mucus penetration of drug delivery vehicles, taking advantage of the nonfouling property and strong resistance to mucus tracking (Figure 30a).[425−431] In a representative study of zwitterionic nanocarriers for oral drug delivery, Han et al. incubated PCB nanogel in reconstituted porcine stomach mucus and tracked the diffusion trajectory.[425] It was found that PCB nanogel diffused much faster than all other nanogels made from PEG, cationic polymers, and anionic polymers. The ensemble-averaged geometric mean square displacement (MSD) of zwitterionic nanogel was ∼6.7 times, ∼100 times, and >100 times higher than those of PEG, anionic nanogels, and cationic nanogels (Figure 30b). Similarly, zwitterionic DSPE−PCB micelles also exhibited superior mucus penetration, diffusing ∼12 times faster in mucus than Polysorbate 80 micelles (Figure 30c).[425]

The epithelial cell layer constitutes another major barrier. The common strategy to enhance penetration is to open tight junctions of the intestinal endothelial surface via absorption enhancers, such as ionic liquid and surfactants.[432,433] However, damage to the tight junctions can elicit a series of side effects, such as bacterial infection, autoimmune disease, and inflammatory bowel diseases.[434] Therefore, a strategy that enables penetration without opening the tight junctions is preferred. Han et al. showed that zwitterionic DSPE−PCB micelles are able to pass through the intestinal epithelial layer without the need to open the tight junction.[425] The transportation was mediated by proton-assisted amino acid transporter 1 (PAT1), a transporter present in the intestinal epithelial cell layer that can transport betaine and betaine derivatives (Figure 30a).[425] Importantly, repeated dosing (twice daily for 14 days) of DSPE−PCB micelles in mice did not lead to any damage to the small intestine tissue, nor any notable inflammation. A prototype oral insulin formulation was fabricated by encapsulating insulin-loaded DSPE−PCB micelles within an enteric-coated capsule. After administration to diabetic rats via oral gavage, the DSPE−PCB/insulin capsule achieved a remarkable bioavailability of ∼42.6% due to

https://doi.org/10.1021/acs.chemrev.2c00344
Chem. Rev. 2022, 122, 17073−17154

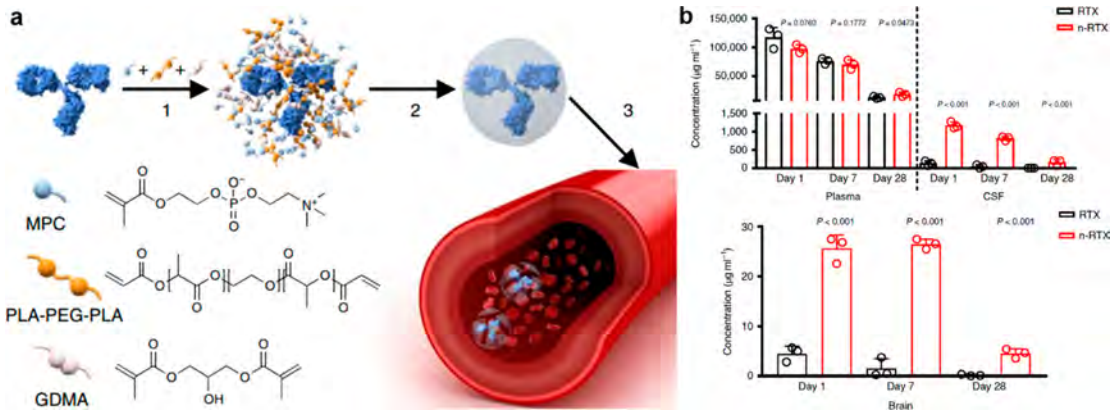

Figure 31. CNS delivery of antibody using PMPC nanogels. (a) Schematic illustration of synthesis and release of RTX nanocapsules. (b) RTX concentration in (top) plasma and cerebrospinal fluid (CSF) and (bottom) brain tissue after injection of 20 mg kg^{-1} native RTX or n-RTX into B6 mice (n = 3) via the retro-orbital vein. Adapted with permission from ref 437. Copyright 2019 Springer Nature.

its ability to penetrate the mucus and intestinal epithelial barriers, whereas the bioavailabilities of the Polysorbate 80/insulin capsule and the free insulin capsule were 8.35 and 0%, respectively (Figure 30d). The *ex vivo* fluorescent imaging study also confirmed that the intestinal retention and absorption of DSPE−PCB/insulin were significantly enhanced compared with Polysorbate 80/insulin (Figure 30e).[425]

4.6.2.4. Penetration through the Blood−Brain Barrier. For the treatment of central nervous system (CNS) diseases, such as brain tumors, Alzheimer's disease, and Parkinson's disease, a critical obstacle that limits the drug delivery performance is the blood−brain barrier (BBB). The BBB is a highly selective membrane barrier between the central nervous system and the circulating blood, which protects the brain from blood-borne substances. Successful delivery of the drug into the central nervous system requires the vehicles to penetrate the BBB. Recently, PMPC-based nanoparticles were reported to penetrate the BBB, benefiting from its structural similarity to choline and acetylcholine, two natural molecules that can actively pass through the BBB via choline transporters (ChT) and nicotinic acetylcholine receptors (nAChRs) overexpressed on the barrier.[435−438]

PMPC has been explored in the designing of delivery systems for protein therapeutics for the treatment of CNS diseases.[436−438] For instance, a PMPC-based nanogel was reported to encapsulate and deliver rituximab (RTX), an FDA-approved anticancer antibody, for the treatment of primary and relapsed CNS lymphoma.[437] The nanogel (n-RTX) was made by *in situ* polymerization of MPC monomers with hydrolyzable cross-linkers in the presence of the antibodies (Figure 31a). *In vivo* tests using B6 mice showed that a single intravenous injection of n-RTX improved the RTX levels in the CNS (Figure 31b, top) and brain tissue (Figure 31b, bottom) by 8−10-fold compared with those of the naked RTX. Conjugation of the nanogel with CXCL13, a specific ligand for CXCR5-expressing lymphoma cells, prevented metastases in a non-Hodgkin lymphoma (NHL) murine xenograft model and eliminated lymphoma in a mouse model with xenografted humanized bone marrow−liver−thymus.[437]

Apart from ChT and nAChRs, betaine/γ-aminobutyric acid (GABA) transporters (BGT1) are also expressed at the BBB and mediate betaine transport.[439] A more recent study showed that cylindrical polymer brushes (CPBs) made from PCB and fluorinated segments could efficiently pass the BBB via the BGT1 pathway.[440] Compared with CPBs made from PEG, PCB rapidly accumulated in the brains after intravenous injection. The mechanism investigation using BGT1-positive cells and BGT1 substrates confirmed that BGT1 promoted the cellular uptake of CB-bearing CPBs. Interestingly, fluorination further enhanced the BBB-crossing property of CB-bearing CPBs through the increase of hydrophobicity and decrease of surface energy. Benefiting from the BBB-crossing property, the fluorinated CB-bearing CPBs delivered 0.5% ID g^{-1} doxorubicin (DOX) into the brain of healthy ICR mice after tail-vein injection for 72 h.

4.6.3. Stealth Surface and Enhanced Cellular Uptake. In most scenarios drugs need to be delivered into living cells. However, the stealth surface made from zwitterionic materials usually reduces uptake of the nanocarriers by the targeted cells. An ideal drug nanocarrier should not only have a stealth surface for prolonged circulation but also possess enhanced cellular internalization in its targeted cells. Many strategies are employed in the designing of stealth particles with enhanced cellular uptake.[441] Here, we show several examples related to zwitterionic materials.

4.6.3.1. Conjugation with Active Targeting Ligands. Conjugating drug carriers with targeting ligands is a simple but effective way applied in many systems. The surface decoration of ligands induces receptor-mediated internalization of their targeted cells. Certain types of zwitterionic materials can be directly conjugated with specific ligands, thus achieving a combination between active targeting and ultralow-fouling background. An example is PCB-based nanocarriers bearing abundant functional carboxyl groups that can be conjugated with amine-containing targeting ligands.[31,189,418,442,443] Zhang et al. demonstrated that PCB-based NPs could be conjugated with RGD peptide via EDC/NHS chemistry for improved specific cellular uptake by HUVEC.[189,444] Other examples are zwitterionic amino acid derived polymers and poly(EK) peptides, which both have abundant carboxyl groups and amino groups for bioconjugation. In this case, both carboxyl- and amine-reactive compounds can be used, greatly expanding the range of ligand choices. For instance, folic acid was conjugated to nanogels made from pOrnAA by Li et al., to enable its specific internalization by cancer cells (Figure 32a).[445] The conjugated folic acid could specifically interact with folate receptors on cancer cells, resulting in its selective uptake by carcinoma cells with overexpressed folate receptor

https://doi.org/10.1021/acs.chemrev.2c00344
Chem. Rev. 2022, 122, 17073−17154

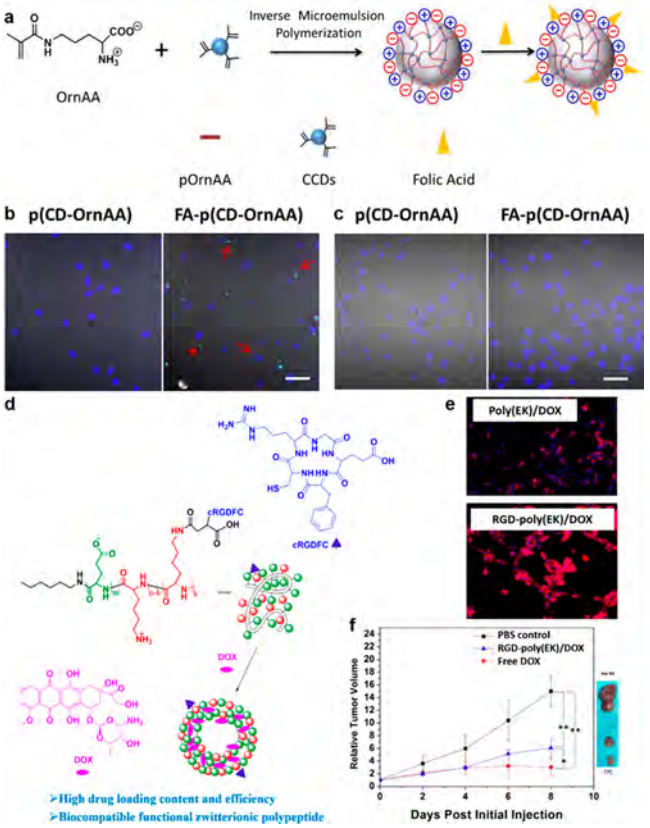

Figure 32. Ligand conjugation of amino acid derived or poly(EK) nanocarriers. (a) Zwitterionic p(CD-OrnAA) nanogels conjugated with folic acid for targeting SKOV3 ovarian carcinoma cells. (b) SKOV3 carcinoma cells and (c) NIH/3T3 normal cells after incubation with p(CD-OrnAA) and FA-p(CD-OrnAA). Adapted with permission from ref 445. Copyright 2016 Elsevier. (d) DOX-loaded poly(EK) vesicle conjugated with c(RGDFC) for targeting Uppsala 87 malignant glioma cells. (e) *In vitro* U87 cellular uptake and (f) *in vivo* tumor growth inhibition of the nanocarriers. Adapted from ref 446. Copyright 2019 American Chemical Society.

(Figure 32b), but not normal tissue cells (Figure 32c). Similarly, the primary amine group of lysine residues in poly(EK) could also be easily conjugated. Lin et al. showed that cyclo(Arg-Gly-Asp-D-Phe-Cys) (c(RGDFC)) decorated poly(EK) nanoparticles effectively targeted U87 cells (Uppsala 87 malignant glioma) both *in vitro* and *in vivo* (Figure 32b).[446]

4.6.3.2. Charge Switchable Nanoparticles. Cationic nanoparticles are well internalized by cells due to their strong interactions with the negatively charged cell surface. An alternative strategy to integrate stealthy surfaces with enhanced cellular internalization is the design of charge switchable vehicles. These vehicles maintain zwitterionic in circulation but switch to positive when reaching their targets. Through the sophisticated design of their chemical structures, these carriers can respond to a variety of stimuli, including pH, hypoxia, enzyme, etc.

The microenvironment of the tumor site is mildly acidic (pH ~6.8), which is distinct from the normal physiological environment (pH ~7.4). Utilizing this difference, pH-responsive zwitterionic nanocarriers were developed for their enhanced cellular uptake.[415,447−452] The simplest way to manipulate the surface charge of these nanocarriers is through the controlling of the protonation and deprotonation processes of the carboxyl and amino groups. Wang et al. reported a charge switchable nanodrug vehicle that self-assembled from a zwitterionic copolymer bearing side groups of hydrazine, carboxybetaine, sulfo group, and doxorubicin (DOX). Under physiological pH, the assembled nanoparticles were zwitterionic and showed strong resistance to proteins and cells.[448] Once the pH dropped below 6.8, the surface charge quickly switched to positive due to the protonation of carboxyl, hydrazine, and primary amine groups, resulting in significantly enhanced cancer cellular uptake. Another classic approach to realize pH-induced charge switching is the introduction of acid hydrolyzable bonds. Pioneering work was reported by Wang and co-workers, where 2,3-dimethylmaleamidic amide was used as the acid-sensitive group.[449] A primary amine group on a polymer can be easily amidated by reacting with 2,3-dimethylmaleic anhydride, resulting in a negatively charged pendant group, while the 2,3-dimethylmaleamidic amide can be easily hydrolyzed back to a primary amine when the pH drops below 6.8. The nanoparticle with a zwitterionic mixed-charge surface built by 2,3-dimethylmaleamidic amide exhibited a long circulation time in blood. When it accumulated at the tumor site, the amide bond quickly broke in the acidic microenvironment, making the nanoparticles become positive and internalized by tumor cells.

Apart from pH differences in the tumor microenvironment, enzymatic cleavage was also explored as a mechanism to achieve charge switching. For example, γ-glutamyl transpeptidase (GGT) is an enzyme that is overexpressed on the membranes of tumor cells and which hydrolyzes γ-glutamylamides with a structure-dependent activity. Zhou et al. designed a γ-glutamylamide-based zwitterionic polymer−camptothecin (CPT) drug conjugate, PBEAGA−CPT, of which the γ-glutamylamide can be cleaved by GGT, leaving a positively charged primary amine (Figure 33a,b).[412] The drug conjugate self-assembled into zwitterionic nanoparticles with long circulation times. Once passing through the blood vessels into the tumor interstitium, the γ-glutamyl moieties could be enzymatically cleaved by GGT on cell membranes, making the nanoparticles cationic. The cationic surface facilitated tumor filtration of the conjugates through caveolae-mediated endocytosis and transcytosis (Figure 33c,d). As a result, the conjugates could eradicate large established subcutaneous HepG2 tumors with clinically relevant sizes (~500 mm^3) (Figure 33e) and could significantly increase the survival rate of mice with orthotopic pancreatic tumors. Glutathione is a natural substrate for GGT. Conjugation of glutathione onto the surfaces was also reported to introduce GGT-mediated charge switching activity to the nanocarriers (Figure 33f,g).[453]

It is worth noting that, in addition to making the zwitterions charge switchable, these materials can also be combined with other functional components to construct various stimuli-responsive drug delivery vehicles, such as disulfide bonds (in response to chemical reduction)[189,413] and azobenzene moieties (in response to hypoxia).[414,454,455]

4.6.3.3. Membrane Fusion of Zwitterionic Copolymers. As a mimic of the cell membranes, PMPC-based amphiphilic block copolymers exhibit unique cell membrane penetrating properties.[456] Most nanoparticles are known to enter cells via endocytosis (Figure 34, left), which has been intensively studied and applied in drug delivery systems. However, when nanocarriers enter cells via endocytosis, they are trapped in endosomes, making it difficult to release the drugs into the cytoplasm. Although the cationic nanomaterials can enter cells

https://doi.org/10.1021/acs.chemrev.2c00344
Chem. Rev. 2022, 122, 17073−17154

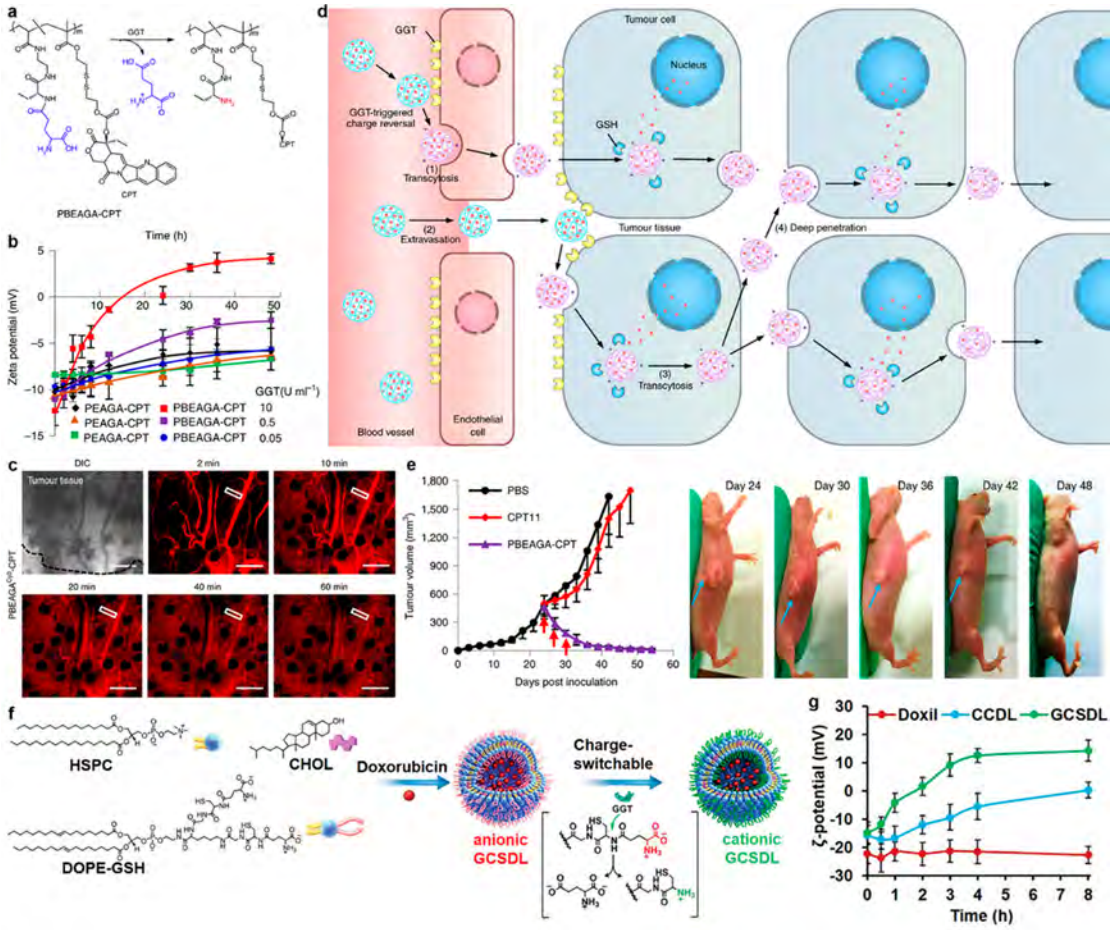

Figure 33. GGT-responsive charge switchable zwitterionic NPs. (a) Structures of γ-glutamylamide-based drug conjugate, PBEAGA−CPT, and its charge switching catalyzed by GGT. (b) ζ potential change of PBEAGA−CPT in the presence of GGT. (c) Confocal microscopy of time-dependent tumor filtration of PBEAGA−CPT in HepG2 tumors after injection. The NPs are labeled with Cy5 (red). (d) Illustration of cationization-initiated transcytosis-mediated active tumor penetration of PBEAGA−CPT. (e) Antitumor activity of PBEAGA−CPT against large solid tumors. The treatment was initiated when the tumor volume reached ∼500 mm^3 on day 24 after HepG2 cell inoculation. Adapted with permission from ref 412. Copyright 2019 Springer Nature. (f) Schematic representation of glutathione-based liposomal nanocarrier, GCSDL, and its GGT-triggered charge switching. (g) ζ potential change of GCSDL in the presence of GGT. Adapted with permission from ref 453. Copyright 2020 John Wiley and Sons.

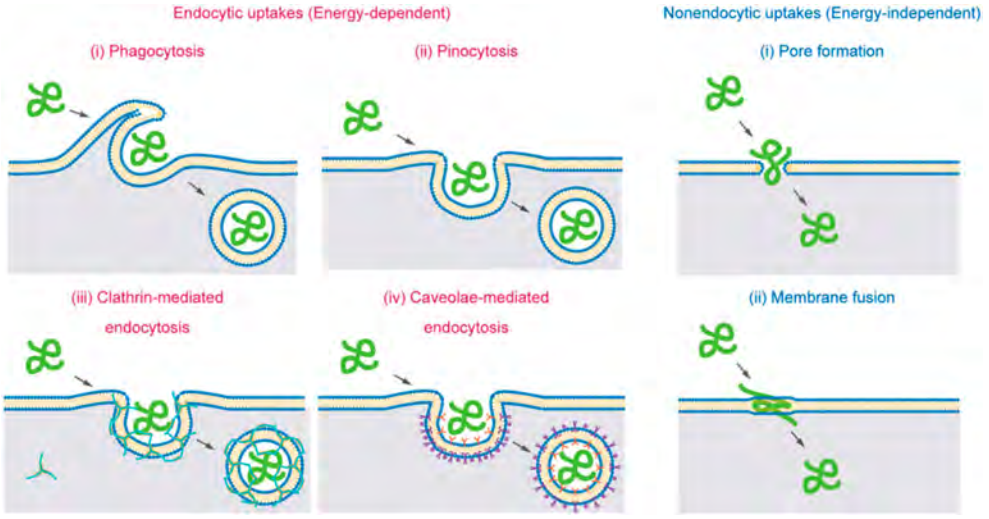

Figure 34. Types of translocation of nanocarriers across the plasma membrane. Energy-dependent endocytic uptake: phagocytosis, pinocytosis, clathrin-mediated endocytosis, and caveolae-mediated endocytosis. Energy-independent nonendocytic uptake: pore formation and membrane fusion. Reproduced with permission from ref 456. Copyright 2020 Royal Society of Chemistry.

https://doi.org/10.1021/acs.chemrev.2c00344
Chem. Rev. 2022, 122, 17073−17154

by making transient holes in the anionic membrane (Figure 34, right i), pore formation is usually associated with cytotoxicity.[457] Different from endocytic and pore formation uptakes, amphiphilic MPC copolymers can penetrate a cell via nonendocytic permeated methods without disturbing its membrane system.[458,459] This phenomenon was discovered by chance when Ishihara and co-workers studied MPC nanoassemblies for drug delivery applications.[457] It was found that an amphiphilic random copolymer (PMB30W) composed of 30% MPC and 70% hydrophobic *n*-butyl methacrylate (BMA) exhibited rapid cell penetration without overt bilayer disruption, and it could passively diffuse in both directions across the cell membrane, even in a cold environment where cell metabolism halted. By contrast, the PMPC homopolymer was not able to be internalized by the cells. Further mechanistic studies showed that the cell penetration of PMB30W copolymer might go through membrane fusion (Figure 34, right ii): the hydrophobic BMA segments attached to the core of phospholipid bilayer, followed by a conformational change of the copolymer to form a reversed micelle-like structure, resulting in the insertion of the copolymer into the cell membrane bilayer. Finally, the copolymer returned to its original confirmation and escaped from the phospholipid bilayer.[460,461] The nonendocytic cell penetrating behavior of PMPC copolymer makes it an interesting candidate for drug delivery. It is not clear yet whether such a property is PMPC-specific or general to other zwitterionic polymers.

The nonendocytic cell penetrating behavior of PMPC copolymer makes it an interesting candidate for drug carriers. Konno et al. first demonstrated that the PMB30W could form a polymeric lipid nanosphere (PLN) in water through hydrophobic interaction.[462] After intravenous injection into the bloodstream of mice, PMB30W solution induced no adverse effect. Importantly, this PMB30W PLN could load hydrophobic paclitaxel (PTX), an antineoplastic drug, to form a water-soluble and biocompatible drug formulation (PTX-PMB30W). Following this pioneering study, Wada et al. demonstrated that PTX-PMB30W showed similar antitumor efficacy compared with the commercial formulation of PTX, i.e., PTX dissolved in polyoxyethylated castor oil (CO) (PTX-CO), after intraperitoneal injection of 50 mg/kg PTX in nude mice with MX-1 tumors.[463] When the amount of PTX was increased to 200 mg/kg, the PTX-PMB30W administration did not harm the animal, while the PTX-CO administration caused animal death. The subcutaneous injection of PTX-PMB30W into rat did not change the skin state, while that of PTX-CO caused skin ulceration. Soma et al. investigated the therapeutic efficacy of PTX-PMB30W for peritoneal dissemination of gastric cancer.[464] Results showed that, compared with conventional PTX dissolved in Cremophor EL (PTX-Cre), PTX-PMB30W significantly decreased the metastatic nodule number and tumor volume and prolonged the survival time. Apart from loading within the PMB30W PLN through noncovalent interactions, drugs can also be covalently connected to PMB30W. Hatano et al. developed an insulin-conjugated PMPC copolymer, named insulin−PMBS, consisting of 30% MPC, 60% BMA, and 10% succinimidyloxycarbonyl tetra(ethylene glycol) monomethacrylate (PENHS), that was conjugated with insulin (Figure 35a, left).[465] They built a model epithelial barrier *in vitro* using the Madin−Darby canine kidney (MDCK) cells cultured in Transwell to evaluate the permeability of insulin−PMBS (Figure 35a, right). Results

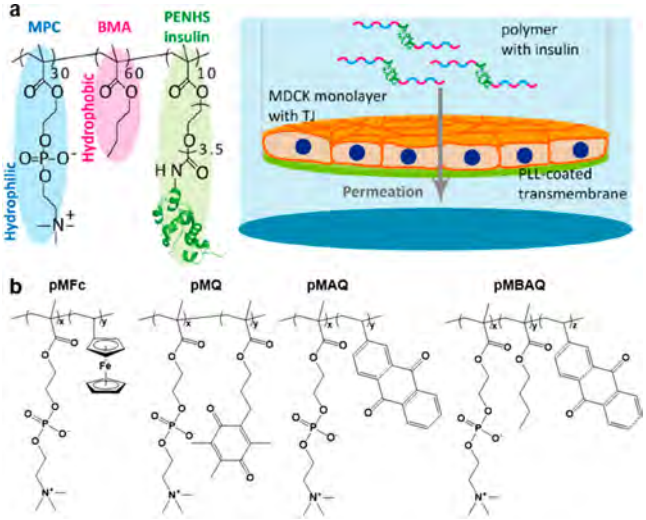

Figure 35. Drug delivery systems based on amphiphilic PMPC copolymer. (a) Chemical structure of insulin−PMBS and its penetration through epithelial barriers. Adapted with permission from ref 465. Copyright 2021 Elsevier. (b) Chemical structures of copolymers composed of MPC units with ferrocene, quinone, and anthraquinone. Adapted from ref 466. Copyright 2021 American Chemical Society.

showed that insulin−PMBS achieved energy-independent transepithelial permeation. Kaneko et al. directly copolymerized MPC with hydrophobic and redox-active units, including ferrocene, quinone, and anthraquinone, to develop amphiphilic PMPC copolymers with cell-penetrating property and anticancer activity (Figure 35b).[466]

4.6.3.4. Weak Interaction with the Cell Membrane. PMPC-modified nanoparticles have been found to have faster and higher cellular uptake than PEG-modified nanoparticles.[467−470] An explanation of this unusual phenomenon is that the MPC molecule has specific interactions with cell membranes due to its structural similarity with the phospholipids. These nanoparticles are not internalized via the membrane fusion mechanism aforementioned, as they possess solid metallic cores or were located in endosomes after internalization.[468,470] Jackson et al. compared the cell uptake and delivery efficiency of siRNA−polymer complexes that are capped by PMPC and PEG shells.[471] The PMPC-based polyplexes showed a 2−3-fold higher tumor cell uptake than that of the PEG-based counterparts, due to the MPC-mediated association with cell membranes.

Similar effects were also reported for poly(2-(*N*-oxide-*N*,*N*-diethylamino)ethyl methacrylate) (OPDEA). Chen et al. prepared an anticancer drug−polymer conjugate using OPDEA and 7-ethyl-10-hydroxycamptothecin (SN38) (Figure 36a).[209] OPDEA showed zwitterionic characteristics and strong resistance to the adsorption of blood proteins. Pharmacokinetic studies showed that the assembled nanoparticles of OPDEA were faster in distribution and slower in later clearance than the PEG-based conjugates. Interestingly, OPDEA drug conjugates reversibly bond to red blood cells (RBCs), thus "hitchhiking" on RBCs to have a longer circulation time (Figure 36b). The association was mediated by the reversible binding between the *N*-oxide-trimethylamine moiety with phosphatidylcholine (PC) or phosphatidylethanolamine (PE) ionic moieties of the phospholipids (Figure 36c). *In vitro* study further confirmed that the OPDEA-based

https://doi.org/10.1021/acs.chemrev.2c00344
Chem. Rev. 2022, 122, 17073−17154

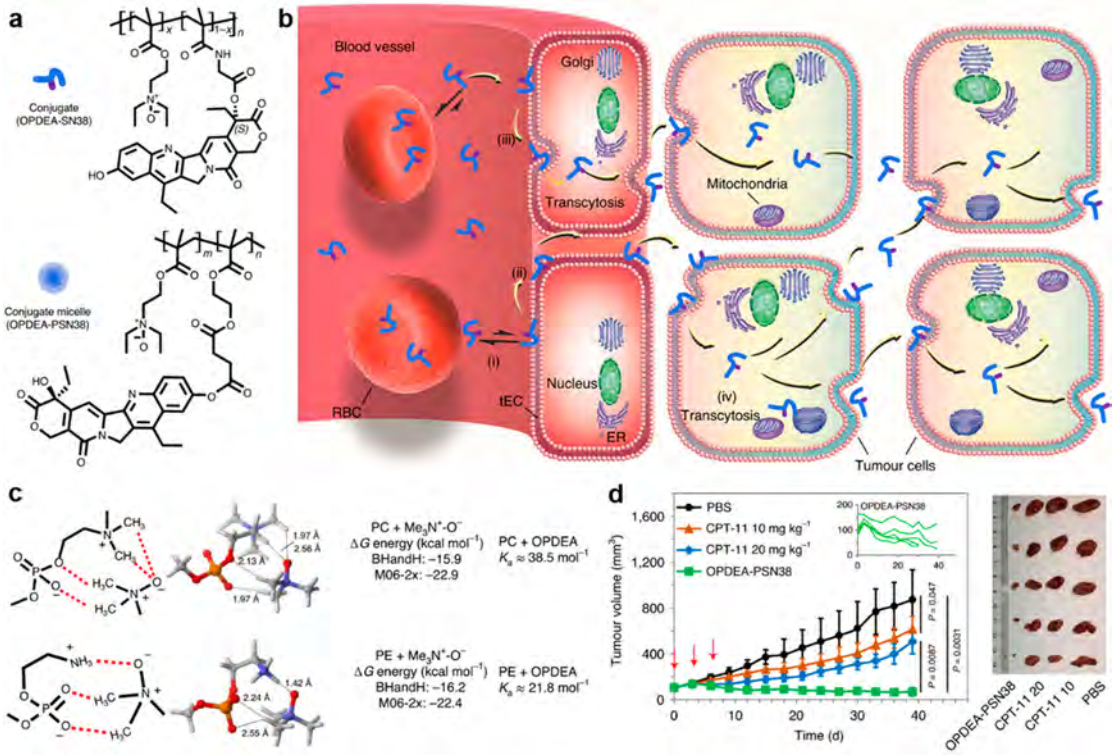

Figure 36. OPDEA-based nanocarriers. (a) Structures of OPDEA-based random copolymeric conjugate (OPDEA−SN38) and amphiphilic block copolymeric micelle (OPDEA−PSN38). (b) Schematic illustration of "hitchhiking" on RBCs and tumor penetration. Cell membrane binding property of OPDEA triggers cellular uptake for intracellular drug release and transcytosis-based active tumor penetration, thus facilitating the drug delivery process in large tumors. (c) Interaction between *N*-oxide-trimethylamine moiety with PC or PE ionic moieties and corresponding binding constants (K_a). (d) Antitumor activity of OPDEA−PSN38 micelles against a liver cancer patient derived xenograft model. Adapted with permission from ref 209. Copyright 2021 Springer Nature.

particles continuously translocated from RBCs to endothelial cells for endocytosis and subsequent transcytosis (Figure 36b). In consequence, they could eradicate large tumors and patient-derived tumor xenografts in mice (Figure 36d). Owing to the strong resistance to proteins and weak interaction with phospholipids, OPDEA provides useful characteristics for efficient drug delivery by integrating both stealthy and cellular uptake properties.

4.7. Protein Protection and Conjugation

Protein therapeutics exhibit extraordinary specificity and efficacy in the treatment of many diseases, and they have achieved great success in clinics over the past several decades. However, further development of these macromolecular drugs is hindered by their poor stability, inadequate pharmacokinetics, and high immunogenicity.[28] The current "gold standard" in the pharmaceutical industry to tackle these problems is "PEGylation". In addition, the surface coverage of protein epitopes also reduces both immunogenicity and antigenicity. Up to the present, approximately 15 PEGylated protein drugs have been approved by the FDA, and more are in the pipeline.[472]

Despite the success, recent clinical reports and many preclinical studies suggested that PEG conjugated protein therapeutics may induce anti-PEG antibodies in patients.[14] Furthermore, preexisting anti-PEG antibodies were found to be widespread in healthy populations.[473,474] The emergence of anti-PEG antibodies poses serious concerns for the further development of PEGylated drugs, as they may cause accelerated blood clearance and adverse reactions. Zwitterionic molecules are developed as natural osmolytes in many organisms including human cells. In virtue of their strong hydration capacity and low immunogenicity, zwitterionic polymers are considered as potential PEG alternatives for the preservation and conjugation of protein therapeutics.

4.7.1. Zwitterionic Polymer Enhances Protein Stability. Proteins are fragile molecules that can be easily destabilized by a number of environmental factors. Conditions such as heat, agitation, lyophilization, and UV exposure can lead to protein unfolding, aggregation, or loss of biological activity. Thus, a potent excipient to maintain the stability of therapeutic proteins during storage and transportation is critical for their clinical use. In an attempt to develop a biodegradable additive to protect the protein from environmental stressors, Pelegri-O'Day et al. synthesized a polycaprolactone (PCL) with pendant vinyl groups that could be easily substituted by thiol−ene click reactions.[475] Relevant side chains with known protein preservation abilities, such as trehalose, lactose, glucose, OEG, and zwitterionic CB were installed, and their protein protection efficacies were compared. With the use of granulocyte colony-stimulating factor (G-CSF) as the model protein, stabilities against storage and heat stressors were tested. It was found that polymers containing zwitterionic CB side chains were the most effective at maintaining G-CSF activity under both refrigerator and heating conditions.[475]

Surface conjugation of polymers is another approach to increase stability for proteins. The first report of protein conjugation with a zwitterionic polymer was published by the Ishihara group about two decades ago, which showed that the

https://doi.org/10.1021/acs.chemrev.2c00344
Chem. Rev. 2022, 122, 17073−17154

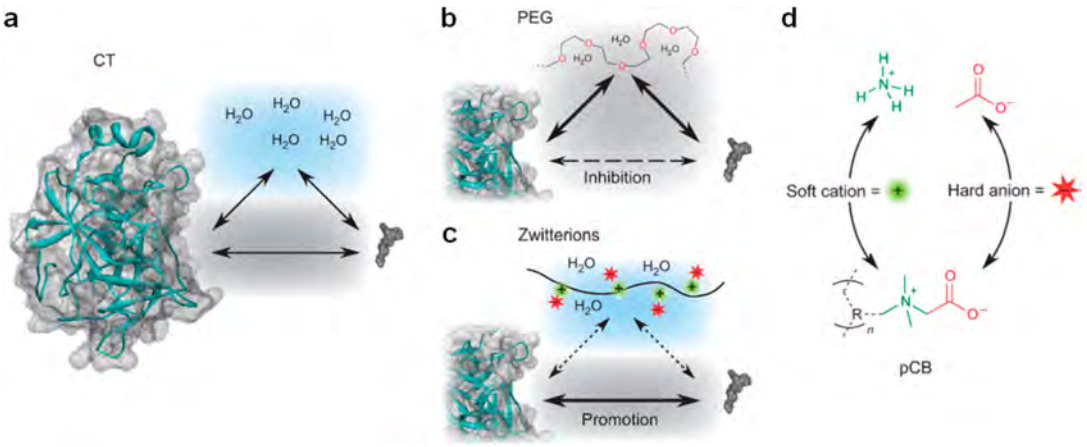

Figure 37. Mechanism of the influence of PEG and PCB polymers on protein binding affinity. (a) Interaction between enzyme and substrate in the absence of polymer. (b) Inhibited protein binding affinity by amphiphilic and sterically hindered PEG. (c) Increased binding affinity by superhydrophilic PCB which can enhance hydrophobic−hydrophobic interactions between binding sites in the enzyme and substrate. (d) Structure of PCB composed of soft cations (quaternary amines) and hard anions (carboxyl groups) which are protein-stabilizing ions found in the Hofmeister series. Reproduced with permission from ref 16. Copyright 2011 Springer Nature.

conjugated PMPC polymers enhanced the stability of papain.[476] Following this work, the same group demonstrated that the conjugation of PMPC preserved protein conformation during heat-quenched stress.[477] A study of PMPC copolymer conjugation suggested that the ability to keep secondary and tertiary structures of proteins highly depended on the hydrophilicity of the polymer.[478] One major drawback of PEGylated therapeutic proteins is that the conjugation of PEG diminishes the protein binding affinity, thereby reducing the overall bioactivity. To circumvent this problem, Keefe et al. conjugated PCB to a model enzyme chymotrypsin to test its protein stabilizing effect.[16] In this study, PCB exhibited a more robust ability than PEG to protect the conjugated enzyme against environmental stressors, benefiting from its superhydrophilicity. Surprisingly, PEG conjugation decreased the enzyme binding affinity to a peptide substrate, while conjugation to PCB with a similar hydrodynamic size increased the binding affinity. Hydrophobic−hydrophobic interactions are significant for proteins to bind to their targets (Figure 37a). The conjugated amphiphilic PEG imposes steric hindrances as well as competitive interactions with the substrate and binding site, resulting in reduced binding affinity (Figure 37b). On the contrary, superhydrophilic PCB chains draw water molecules away from the hydrophobic regions of the protein and substrates, thus facilitating the interaction between catalytic sites in the enzyme and the substrate (Figure 37c). In addition, the ion pairs of PCB are composed of quaternary amines and carboxyl groups. They are considered as soft cations and hard anions in the Hofmeister series, which are known for the protective effects on protein stability and activity (Figure 37d).[16]

4.7.2. *In Vivo* Performance of Zwitterionic Polymer−Protein Bioconjugates. The encouraging results on protein stability enhancement motivate subsequent *in vivo* studies of polyzwitterion−protein bioconjugates. Lewis et al. conjugated a bis-thiol specific derivative of PMPC to interferon-R2a (IFN) after reduction of the disulfide bonds in IFN.[479] PMPC with a hydrodynamic volume similar to that of 20 kDa PEG was used in this study, and the pharmacokinetic results showed slower absorption and longer elimination half-life than those of 20 kDa PEG−IFN after subcutaneous injections in mice. Liu et al. reported the immunological evaluation of PCB bioconjugates.[480] Uricase from *Candida* sp. served as the model drug. In a model of healthy rats, PCB conjugated uricase showed longer circulation half-lives than the PEGylated samples, and no accelerated blood clearance was observed for PCB conjugates following three intravenous injections. ELISA was applied to detect antibodies against both polymer and protein in animal blood, and PCB conjugated uricase presented significantly fewer antidrug antibodies than the PEGylated control. The lower immunogenicity of PCB than that of PEG as a protein modifier was further confirmed by a head-to-head comparative study (Figure 38).[481] PEG is known to be a hapten that generally does not elicit an immune response by itself.[482] The immunogenicity of the bioconjugate strongly depends on the immunogenicity of the conjugated protein.[14] As shown in Figure 38b, five proteins with different immunogenicities, including murine serum albumin (MSA), bovine serum albumin (BSA), ovalbumin (OVA), β-glucosidase, and keyhole limpet hemocyanin (KLH) were conjugated with PEG or PCB and tested for their ability to induce antipolymer antibodies in mice. The results showed that anti-PEG responses significantly increased with more immunogenic protein carriers, while PCB remained nonimmunogenic throughout the study.[481]

All the above results make polyzwitterions competitive candidates in substituting PEG for the design of polymer−protein conjugates. Tsao et al. conjugated a large PCB polymer with a molecular weight of 66 kDa to the terminal cysteine residue of glucagon-like peptide-1 (GLP-1), aiming to extend its blood circulation half-life without sacrificing too much activity.[483] GLP-1 is a peptide drug used in the treatment of type 2 diabetes mellitus (T2DM). Previously, a site-specific mono-PEGylated GLP-1 with a molecular weight of 50 kDa only retained 0.03% relative potency of the unconjugated peptide.[484] By contrast, GLP-1−PCB showed 98.8% of the relative potency and exerted activity up to 6 days after a single subcutaneous injection in a mouse study. Similar activity preservation and circulation enhancement effects were also reported for PCB conjugated interferon α-2a (IFN-α2a)[27] as well as insulin.[485] Site-specific conjugation is desired for many monopolymer conjugated protein drugs. Bhattacharjee et al. reported a site-specific conjugation approach by modifying the

https://doi.org/10.1021/acs.chemrev.2c00344
Chem. Rev. 2022, 122, 17073−17154

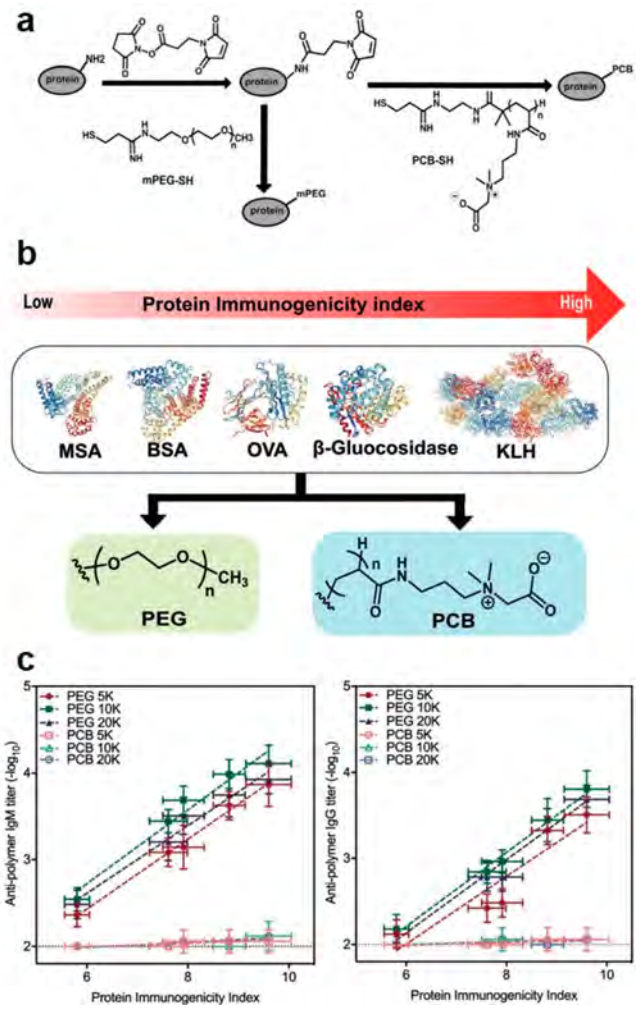

Figure 38. Head-to-head comparison of immunogenicities of PEG and PCB conjugated proteins. (a) Chemistry used to prepare the bioconjugates. (b) Proteins and polymers used in this study. (c) Antipolymer antibody titers induced by the bioconjugates in mice. Adapted with permission from ref 481. Copyright 2018 John Wiley and Sons.

N-terminal of myoglobin with an initiator, followed by *in situ* ATRP to grow PCB polymer from the protein molecule.[486] Pharmacokinetic tests in mice demonstrated that PCB conjugated myoglobin had a significantly longer half-life (17 h) than a protein conjugate of poly(oligo(ethylene glycol) methacrylate) (POEGMA) (13 h).[486] Similarly, Hu et al. developed a site-specific conjugation approach by enzymatically attaching an ATRP initiator onto a genetically modified C-terminal of IFN.[487] The *in vitro* antiproliferative bioactivity of the PMPC conjugate was 8.7-fold higher than that of PEGylated interferon α (PEGASYS). In a murine cancer model, the PMPC conjugate significantly outperformed interferon α or PEGASYS in terms of therapeutic efficacy.[487]

In addition to maintaining activity and prolonging blood circulation, PCB conjugation has also been shown to facilitate pulmonary[488] or lymphatic[489] delivery of protein drugs. Unlike direct intravenous injection, macromolecular drugs administered via these routes face additional challenges from physiological barriers and immunogenic risks. Surface conjugation of zwitterionic PCB polymers helps the underlying protein cargo elude immune cell uptake in mucus or lymph, dramatically increasing the bioavailability by enabling efficient transportation across those barriers. Recently, a new type of zwitterionic polymer (ZPS) with "built-in" immunomodulatory function was reported by Jiang and co-workers.[490] By mimicking phosphoserine, an immune-signaling molecule in nature, the specific interaction of ZPS with phosphatidylserine receptors enabled it to induce immune tolerogenic effects, while the zwitterionic nature of ZPS allows it to exhibit nonfouling properties like MPC. Conjugation of the ZPS to model proteins successfully prolonged their circulation with an inhibited antidrug response. Notably, the first polyzwitterion–protein bioconjugate that entered a clinical trial was KSI-301, which was a polymer conjugated anti-VEGF antibody developed by Kodiak Sciences.[491] A high molecular weight (~800 kDa) branched PMPC was site-specifically conjugated to an anti-VEGF antibody, aiming to improve its bioavailability for intravitreal injections. The conjugation of the large hydrated polyzwitterion delayed drug clearance and reduced dosing frequency to every 3–6 months. Phase I and II trials

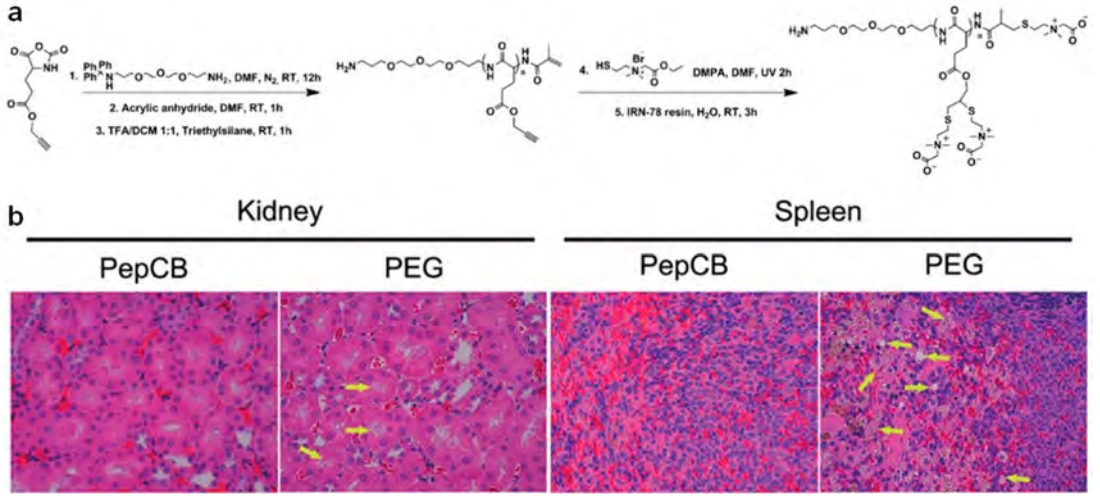

Figure 39. Synthesis and toxicity evaluation of PepCB. (a) Structure and synthesis of the polypeptide with CB side groups. (b) Tissue sections of rat organs after long-term dosage. Representative cytoplasmic vacuoles in tissues are indicated by arrows. Reproduced with permission from ref 494. Copyright 2018 John Wiley and Sons.

https://doi.org/10.1021/acs.chemrev.2c00344
Chem. Rev. 2022, 122, 17073–17154

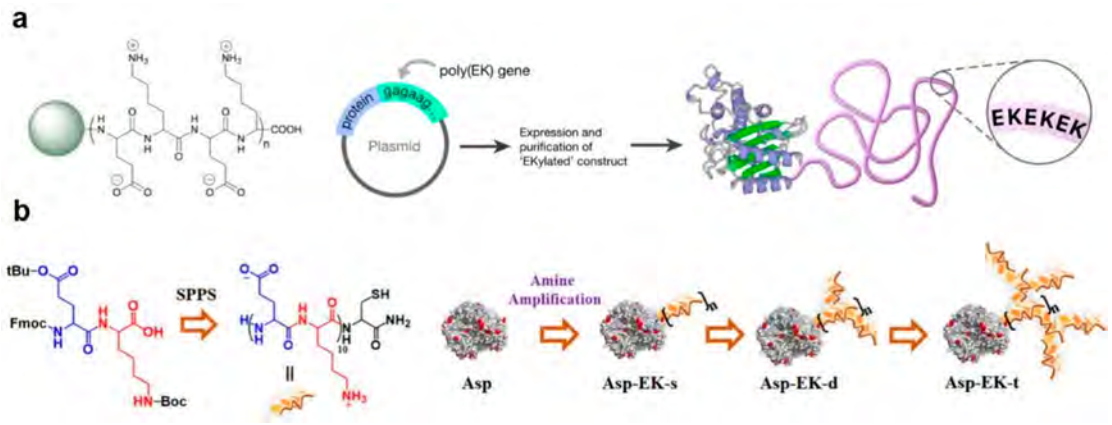

Figure 40. Protein ekylation. (a) Fusion of a poly(EK) tail to the terminus of a protein. Adapted from ref 238. Copyright 2015 American Chemical Society. (b) Multilayer EK cloak conjugated to a protein surface via a synthetic approach. Adapted with permission from ref 29. Copyright 2020 John Wiley and Sons.

demonstrated its excellent safety and efficacy in treating three phenotypically variable retinal diseases (wet age-related macular degeneration, diabetic macular edema, and retinal vein occlusion).[492]

The treatment of chronic diseases requires long-term use of therapeutics. However, the accumulation of nonbiodegradable polymers in organs poses safety concerns over their long-term pharmaceutical applications. Taking PEG as an example, nonclinical toxicology studies showed that 5 out of 12 approved PEGylated drugs would cause cellular vacuolation in a series of organs and tissues post high dosage or long-term administrations.[493] To address the safety concerns, Zhang et al. synthesized a zwitterionic polypeptide, named PepCB, as the PEG alternative for protein conjugation.[494] The polypeptide was made via *N*-carboxyanhydride (NCA) ring-opening polymerization followed by thiol−yne click chemistry (Figure 39a). The final product was composed of a biodegradable polyglutamate backbone, zwitterionic CB side chains, and a functionalizable primary amine end group. To maximize the hydration capacity of the polypeptide, thiol−yne type click reaction was used to install two CB moieties onto each of the repeating units. A toxicological study was performed by intravenous administration of the polymers into rats at a very high dosage of 200 mg kg^{-1} $week^{-1}$ for 3 months (Figure 39b). Neither tissue histological changes in the liver, kidney, or spleen nor abnormal behavior, sickness, or death were observed throughout the study. PepCB conjugated uricase also showed significantly improved pharmacokinetic and immunological performances compared with the PEGylated controls.

4.7.3. Protein Ekylation. Protein conjugation with the zwitterionic polypeptide, i.e., poly(EK), is of particular interest, as poly(EK) is composed of only natural amino acids. Conjugated poly(EK) has perfect structural homogeneity with the protein itself and eliminates any concerns of biocompatibility. Liu et al. reported the first attempt to directly fuse poly(EK) to the C-terminus of a model protein, *β*-lactamase, via genetic engineering.[238] Recombinant expression allowed for one-step production of the site-specific bioconjugates without the need for secondary chemical conjugation steps (Figure 40a). Attachment of EK tails of 10 and 30 kDa in length significantly improved the thermal stability of the enzymes.[238] Banskota et al. tested the *in vivo* performance of a series of disordered polypeptide motifs with the formula of $(VPX_1X_2G)_n$, where X_1 and X_2 are cationic and anionic amino acids, respectively.[495] Among all different pairs of residues (KE, RE, KD, and RD), KE had the best pharmacokinetic parameters after both intravenous and subcutaneous administration. The best performing peptide sequence $(VPKEG)_n$ was then genetically fused to GLP-1, and the conjugate demonstrated superior therapeutical efficacy in a mouse model of type 2 diabetes.[495] The Jiang group further attempted to incorporate structure-disrupting amino acids such as proline (P), serine (S), and glycine (G) into the expressed poly(EK) tails to avoid secondary structure formation when the poly(EK) chain is long. Eight EK-containing motif-based peptides were linked to keyhole limpet hemocyanin (KLH) and compared for their immunogenicity.[496] The results showed that EKS and EKG induced higher immunogenicity, while the other motifs, especially those containing P, exhibited lower immunogenicity. Simulation studies revealed that peptides with higher immunogenicity also exhibited regions of charge imbalance. In the following study, EKP conjugated growth colony-stimulating factor (GCSF) showed similar receptor binding ability but better thermal stability compared to unmodified GCSF, indicating its potential for protein drug conjugations.[497]

Like all recombinant fusions, genetic expression of zwitterionic peptides is restricted to the N- or C-termini of peptides and proteins. For proteins with high immunogenicity, one or two fused polymers are apparently inadequate to shield all surface epitopes. Yuan et al. reported a synthetic approach to cloak protein surfaces with a high density of poly(EK)s.[29] First, a short EK peptide with the sequence of $(EK)_{10}C$ was synthesized via Fmoc solid phase peptide synthesis using an EK dimer, Fmoc-Glu(tBu)-Lys(Boc)-OH, as the building block. After converting the K residues on protein surfaces to maleimide groups by a maleimide-NHS bifunctional cross-linker, the EK peptide was then conjugated onto protein surfaces via its terminal cysteine residue. As shown in Figure 40b, the attachment of short EK peptides provided more lysine residues as anchor points, which enabled multilayer branched conjugations. Asparaginase with a triple-layer EK cloak showed enhanced blood circulation with minimal immune responses in mice.

4.7.4. Zwitterionic Nanogel Protein Encapsulation. Besides the immunogenicities/antigenicities of polymers and proteins, polymer conjugation density on a protein surface also

https://doi.org/10.1021/acs.chemrev.2c00344
Chem. Rev. 2022, 122, 17073−17154

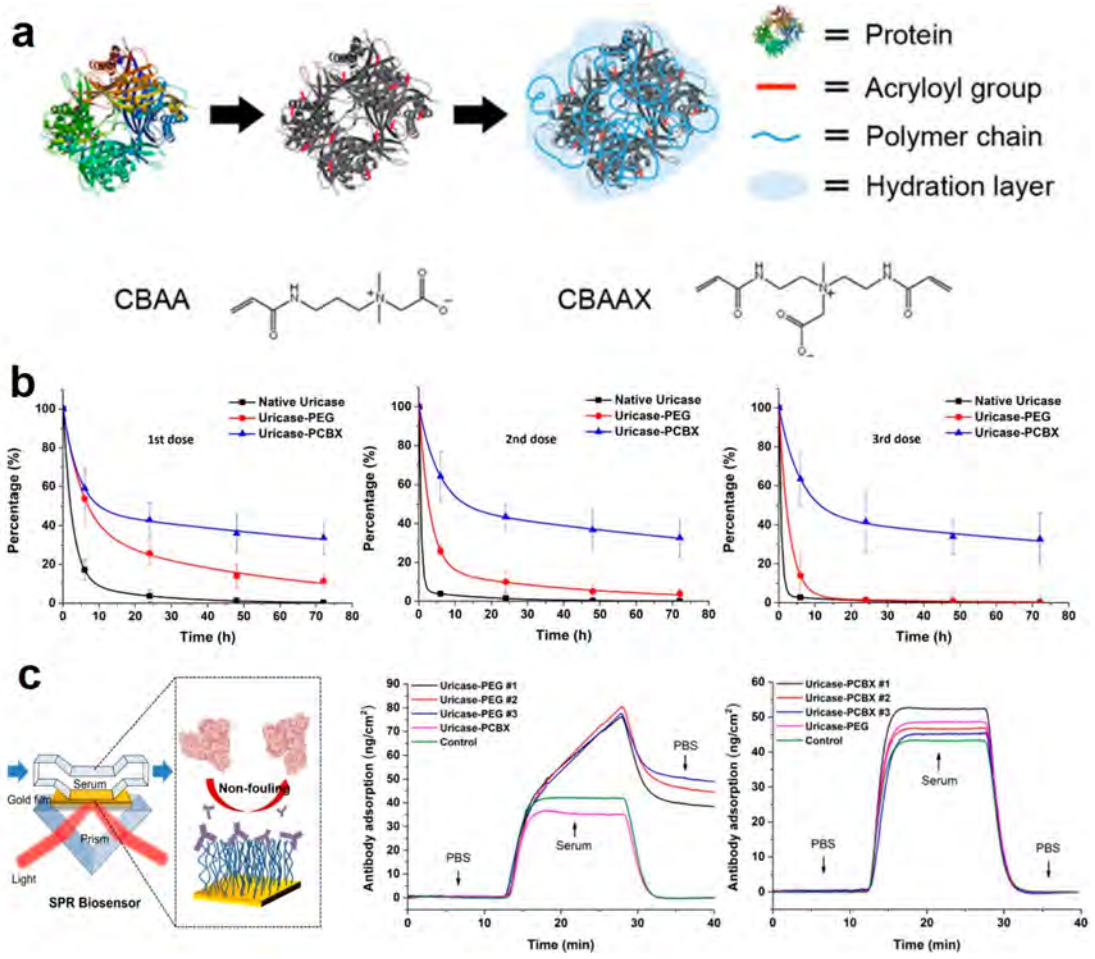

Figure 41. Zwitterionic nanogel encapsulation prolongs protein circulation time and eliminates immunogenicity. (a) Scheme of the encapsulation process. (b) Blood circulation curve after three injections. (c) SPR detection of antipolymer antibodies. Adapted with permission from ref 28. Copyright 2015 National Academy of Sciences.

plays a key role in determining the overall immunogenicity of the polymer−protein conjugate.[482] For classic protein bioconjugates, a high surface coverage is often difficult to achieve, due to the limited number of surface functional groups or as a trade-off to preserve protein activity. To reach complete concealment of all danger signals from the protein surface, Zhang et al. proposed a zwitterionic nanogel encapsulation strategy (Figure 41).[28] Surface conjugation of a cross-linked polymer hydrogel layer could completely mask the epitopes on the protein surface, making the modified protein "invisible" to the immune system. The conjugation process was done by protein acylation and subsequent *in situ* radical polymerization of CB monomers and cross-linkers (Figure 41a). An enzymatic activity test of the encapsulated uricase showed that the cross-linked PCB layer did not affect free diffusion of the enzyme substrates, while the enzyme exhibited exceptional stability under heat stressors. These nanogels had a superlong *in vivo* circulation half-life in rats, with no accelerated blood clearance (Figure 41b). Neither anti-PCB nor antiuricase antibody was observed when the animal blood was examined by both ELISA and SPR, suggesting the complete inhibition of drug immunogenicity (Figure 41c). Following the same concept, uricase loaded PCB nanogels made via the classic micro-emulsion approach showed satisfactory therapeutic efficacy in an animal model of gout.[498] Similar to PCB nanogels, a PMPC-based system was also demonstrated to extend protein circulation time and reduce immunogenicity effectively.[499,500]

As a platform technology, the nanogel encapsulation approach can be applied to design various enzyme-based therapeutics. Zhang et al. used PCB nanogels to construct nanoscavengers against the threats from organophosphate (OP) nerve agents, by encapsulation of butyrylcholinesterase (BchE)[501] or organophosphorus hydrolase (OPH).[502] OPs are used as chemical weapons and pesticides which kill hundreds of thousands of people each year. OPH was found to be a promising agent to prophylactically protect people from OP intoxication; however, the translation was hindered by its extremely poor pharmacokinetics and high immunogenicity. These two key issues were successfully addressed by PCB nanogel encapsulation.[502] When the efficacy was evaluated, a single prophylactic administration of the nanoscavenger effectively prevented lethality after multiple sarin exposures over a 1 week period in a guinea pig model. It should be noted that the nanogel encapsulation strategy is a promising way to modify enzymatic therapeutics, whose therapeutical targets are small molecules that can diffuse across the gel layer. For proteins functioning by binding to large molecules, e.g., antibodies, hormones, and cytokines, a releasing mechanism is needed as the hydrogel layer would significantly hinder protein bindings.

https://doi.org/10.1021/acs.chemrev.2c00344
Chem. Rev. 2022, 122, 17073−17154

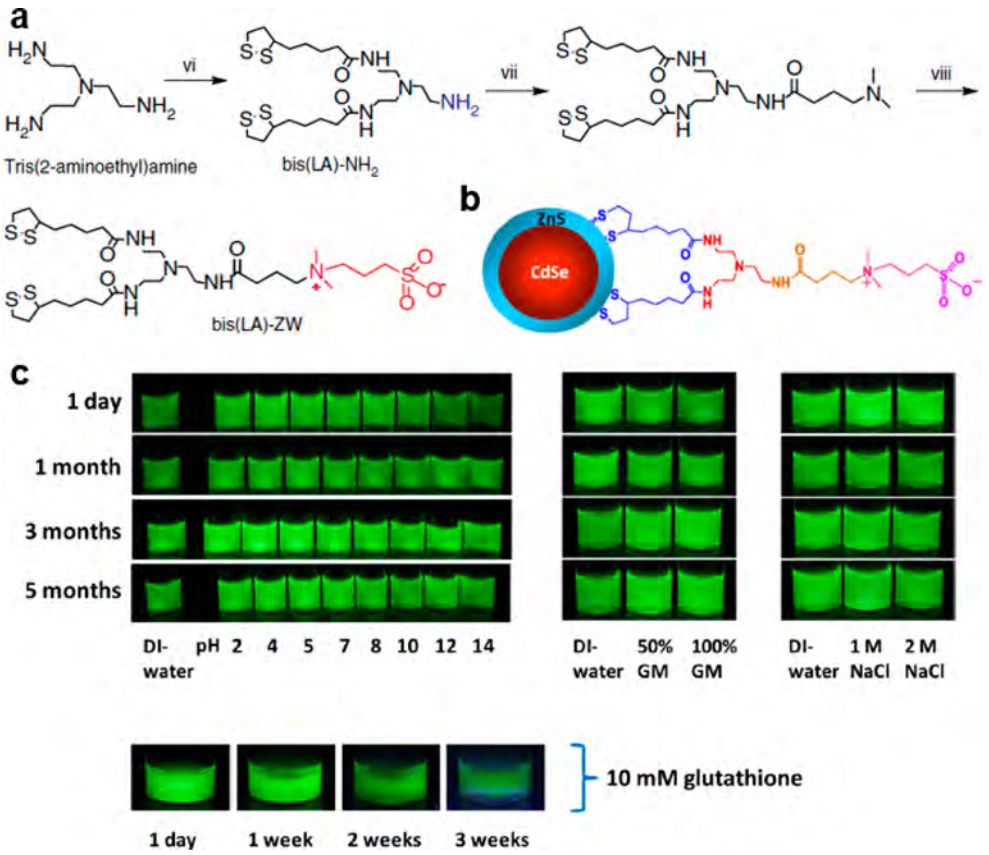

Figure 42. Bis(LA)-ZW coated QDs and their stability. (a) Synthesis of bis(LA)-ZW. Adapted with permission from ref 108. Copyright 2015 Springer Nature. (b) Structure of bis(LA)-ZW coated QDs. (c) Stability of bis(LA)-ZW coated QDs in various conditions. DI-water, deionized water; GM, RPMI growth media. Adapted from ref 511. Copyright 2013 American Chemical Society.

4.8. Nanodiagnostics

The detection of diseases is crucial for their prevention and treatment. Various imaging technologies have been deeply developed and used in the clinic, including magnetic resonance imaging (MRI), computed tomography (CT) imaging, and optical imaging. The emergence of nanomaterials can boost the performance of current imaging modalities, thus evolving the field of "nanodiagnostics".[503] Until now, a variety of nanomaterials have been explored to improve the imaging sensitivity and/or accuracy, including magnetic nanoparticles (MNPs) for ^{1}H MRI, fluorinated substances for ^{19}F MRI, gold NPs (GNPs) or tantalum oxide NPs for CT imaging, and quantum dots (QDs) or near-infrared (NIR) fluorophores for optical imaging. However, their imaging enhancement performance is significantly influenced by the undesired *in vivo* behaviors induced by protein corona formation, such as instability, capture by MPS, short blood circulation, poor biodistribution, low renal clearance, etc. In addition, certain types of these NPs own water insolubility or are a toxicity risk. Due to the resistance to protein corona formation, zwitterionic materials have been widely explored to overcome these issues.

4.8.1. Improved Stability and Enhanced Performance. As discussed in previous sections, nanoparticles are challenged by a protein corona in the biological milieu.[504] In addition, most NPs are hydrophobic with poor water dispersibility. For example, the as-synthesized semiconductor nanocrystal QDs cannot survive in the biological milieu due to the presence of hydrophobic ligands, including trioctylphosphine oxide (TOPO), trioctylphosphine (TOP), phosphonic acid, and alkylamines.[505] Therefore, improving hydrophilicity and protein resistance are crucial for their successful biomedical applications.

Due to the superhydrophilicity and nonfouling properties, zwitterions can impart excellent water dispersity and protein corona resistance to these hydrophobic NPs, thus significantly improving their physiological stability.[506−508] For example, Rouhana et al. developed water-dispersible and aggregation-resistant GNPs using zwitterionic SB to exchange citrate as the ligands.[509] The SB-coated GNPs showed dramatically improved colloidal stability without aggregation in high concentration salt (3 M), positively/negatively charged electrolyte and protein solutions.[509] Zhou et al. coated gadolinium-embedded iron oxide (GdIO) MNPs with zwitterionic dopamine sulfonate (ZDS), maintaining their size after incubation in 20% FBS for 4 h.[510] To obtain long-term stability, Zhan et al. designed a lipoic acid (LA) connected SB ligand and coated QDs via a photoligation strategy (Figure 42a,b).[108,511] The coated QDs showed excellent long-term physiological stability in cell growth media (for at least 5 months) and in 10 mM glutathione solutions (for 2 weeks) (Figure 42c). Notably, these coated QDs could be stored at 4 °C for over 1.5 years.

Learning from the fouling phenomenon of a macroscopic surface, the hydration of small ligands may not be sufficient to maintain their stability in complex biological environments. Zwitterionic polymers are used to modify or encapsulate these nanoparticles to tackle this issue.[189,444,512,513] As an example, Zhang et al. synthesized a PCBMA polymer terminated with

https://doi.org/10.1021/acs.chemrev.2c00344
Chem. Rev. 2022, 122, 17073−17154

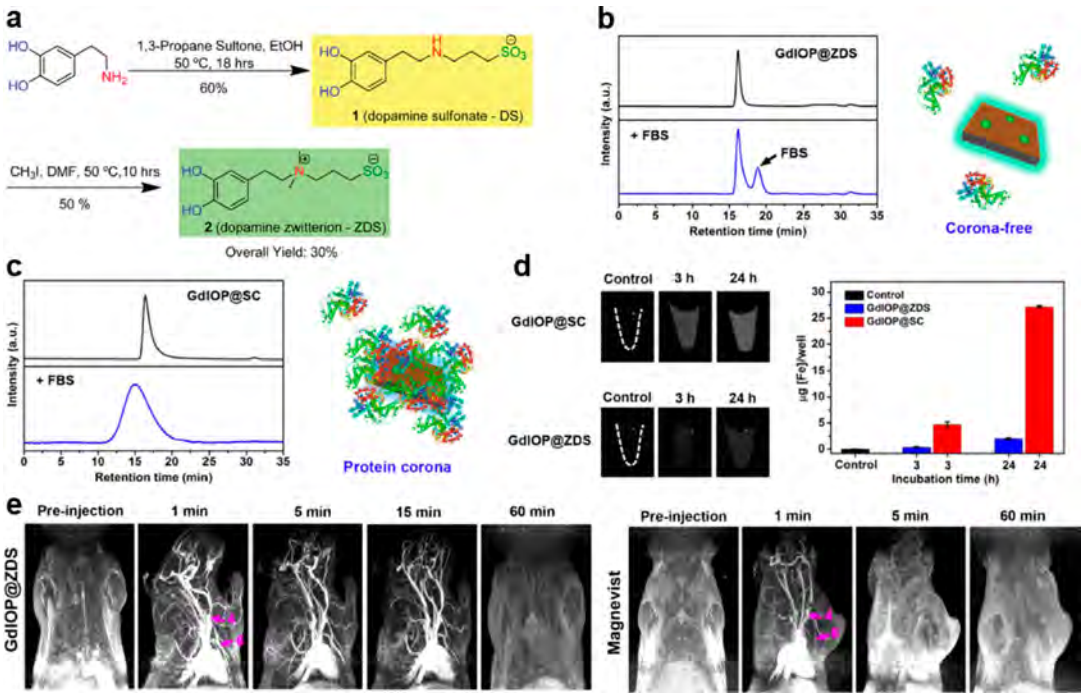

Figure 43. GdIOP@ZDS and its nonfouling and MRI performance. (a) Synthesis of ZDS. Adapted from ref 526. Copyright 2012 American Chemical Society. (b) Corona-free properties of GdIOP@ZDS measured by high performance liquid chromatography−gel filtration chromatography (HPLC−GFC). (c) Protein corona formation on GdIOP@SC measured by HPLC−GFC. (d) Cellular uptake tests of GdIOP@ZDS and GdIOP@SC. (e) MRA performance of GdIOP@ZDS and Magnevist. Adapted from ref 518. Copyright 2015 American Chemical Society.

two 3,4-dihydroxyphenyl-L-alanine (DOPA) groups ($DOPA_2$-PCBMA).[444] The polymer can be easily coated onto Fe_3O_4 MNPs via its DOPA anchoring groups. The polymer-coated MNPs maintained their stability for 6 months in PBS and 10% NaCl and for 24 h in 100% serum. Feng et al. designed a fluorinated zwitterionic nanogel ($PCBF_3$), which used the polymer itself as the ^{19}F MRI agent.[512] Stability tests showed that the $PCBF_3$ nanogels maintained their signal-to-noise ratio (SNR) unchanged after incubation in whole blood, heart, liver, spleen, lung, and kidney homogenates for 48 h.

Protein corona induces immune clearance and an undesired *in vivo* behavior of NPs, including high accumulation in the liver, spleen, and lymph nodes, resulting in low accumulation and poor imaging performance at the targeted sites. Zwitterionic materials, including small ligands[507,514,515] and polymers,[189,421,444,516] can be applied to help these diagnostic NPs against nonspecific protein adsorption and immune cell uptake. For instance, a short EK peptide with a sequence of KEKEKE-PPPPC-Am, composed of a stealthy E/K portion and an anchoring segment of four prolines (P) and one cysteine (C), was reported to modify GNPs.[516] The peptide-capped GNPs exhibited minimized nonspecific uptake by nonphagocytic cells and phagocytic macrophages. The encouraging results motivated subsequent studies of zwitterionic diagnostic NPs for various imaging applications, such as MRI for cancers,[515,517] blood pool, and blood vessels;[514,518,519] CT imaging for tumors,[520−522] lymph node, and blood;[522] and optical imaging for tumors,[523] cells,[524] and direct monitoring of specific interactions *in vivo*.[505]

The adoption of zwitterionic materials significantly enhances the performance of diagnostic NPs in terms of imaging sensitivity/accuracy and acquisition window. For example, the zwitterion dopamine ligand has been used to modify an iron oxide nanoplate with buried Gd_2O_3 clusters (GdIOP@ZDS) (Figure 43a,b).[518] Compared with the sodium citrate modified control group, the zwitterionic coating significantly reduced protein corona formation and cellular uptake by SMCC-7721 cells (Figure 43b−d). When tested *in vivo* by intravenous injection, the control group was rapidly recognized and captured by immune cells, resulting in fast accumulation in the liver. Attributed to the stealthy properties, GdIOP@ZDS circulated rapidly and unimpeded in blood vessels, and it immediately formed a strong MRI contrast of vascular nets and maintained a long acquisition time window of up to 15 min (Figure 43e, left). The detailed structure of the vessels could be clearly distinguished, achieving a highly efficient magnetic resonance angiograph (MRA) with superior resolution. In contrast, the commercial contrast agent Magnevist (Gd-DTPA) showed a vascular imaging with low resolution and short acquisition windows of <5 min (Figure 43e, right). Further functionalizing these NPs with targeting ligands or stimuli responsiveness on the nonfouling background could enhance their accumulation at specific sites for diagnosis.[517,525]

For imaging at the subcellular level, rapid Brownian diffusion is required for the NPs to explore unhindered the cytoplasmic environment and find their intracellular targets. Zwitterionic coatings eliminate the nonspecific interactions, thus achieving improved subcellular imaging and tracking.[508,527−529] For example, to investigate the intracellular behaviors of zwitterionic QDs, Debayle et al. designed a series of SB-vinylimidazole block copolymers to modify QDs via the anchoring of the poly(vinylimidazole) segment.[529] It was found that SB-QDs could prevent the formation of the protein corona. Electroporation or microinjection methods were used to make SB-QDs' internalization by HeLa cells, and their behaviors in intracellular environments were observed. Results showed that

https://doi.org/10.1021/acs.chemrev.2c00344
Chem. Rev. 2022, 122, 17073−17154

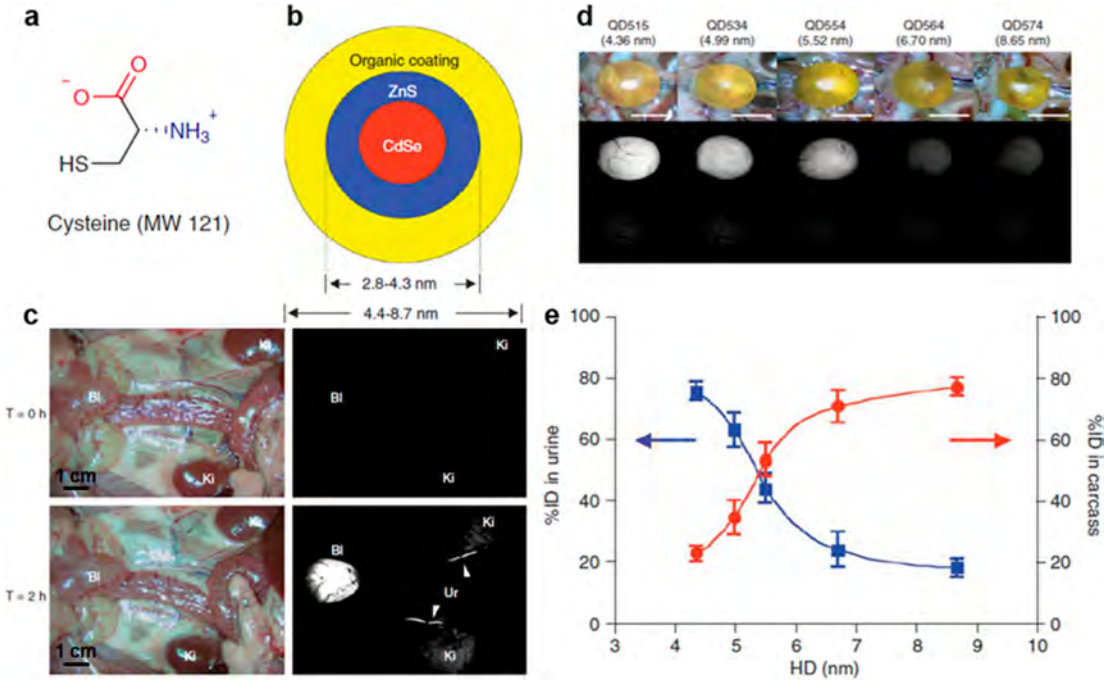

Figure 44. Zwitterionic cysteine coated QDs and their renal clearance performance. (a) Chemical structure of zwitterionic cysteine. Adapted with permission from ref 525. Copyright 2009 Springer Nature. (b) Chemical composition of cysteine coated QDs. (c) *In vivo* color video (left) and fluorescence images (right) of intravenously injected QD515 into rats. Ki, kidney; Ur, ureter; Bl, bladder. (d) Surgically exposed CD-1 mouse bladders after intravenous injection of QD515, QD534, QD554, QD564, or QD574 for 4 h. (top) Color video of the bladder after injection. (middle) Fluorescence images of the bladder after injection. (bottom) Control bladder without injection of Cys-QDs. (e) (blue curve) Renal clearance and (red curve) carcass retention of ^{99m}Tc-labeled QDs-Cys with different hydrodynamic diameters after intravenous injection into CD-1 mice for 4 h. Adapted with permission from ref 111. Copyright 2007 Springer Nature.

SB-QDs possessed an unhindered cytoplasmic Brownian motion. By conjugation of the SB-QDs with biotin, these NPs could rapidly find and image intracellular targets after microinjection into the cytoplasm of transfected HeLa cells.

4.8.2. Improved Renal Clearance. Toxicity concern is a major issue for clinical translation of nanodiagnostics. Fast renal clearance is important for diagnostic NPs to reduce the risk. Particle size is the determinant for efficient renal clearance as only small particles can pass the filtration barrier. However, opsonization and associated aggregation result in significantly increased particle size and hinder their fast clearance. Modifying the NPs with zwitterionic surfaces could maintain their size unchanged in blood circulation, allowing them to be effectively cleared via renal filtration. Liu et al. found that cysteine can form a compact zwitterionic layer on the surface of QDs, which effectively maintained the particle size in fetal bovine serum (Figure 44a, b).[109] A series of Cys-QDs with small diameters (4.36 nm, QD515; 4.99 nm, QD534; 5.52 nm, QD554; 6.70 nm, QD564; 8.65 nm, QD574) were prepared and used to detect the size threshold for renal clearance. After intravenous injection into rats, QD515 could pass through the glomerular filtration of the kidney, then be transported into the bladder along the bilateral ureters (Figure 44c), and finally be excreted outside the body. At 4 h post injection, QD515 showed a dominant signal in the bladder (Figure 44d) and a low accumulation (~4.5% injected dose) in the liver. In contrast, QD574 exhibited a low signal in the bladder (Figure 44d) and a high accumulation in the liver (~26.5% injected dose). After building a relationship between the hydrodynamic diameter, total body retention, and renal clearance, the authors concluded that the threshold value for renal clearance was 5.5 nm (defined as 50% point for total body clearance) (Figure 44e).[111,527]

4.9. Biosensors and Wearable Devices

4.9.1. Biosensors. *In vitro* detection of analytes in complex biological milieu such as body fluids remains crucial for diagnosis and biomedical studies. The biosensors used for such purposes are challenged by biofouling issues: nonspecific adsorption of biomolecules causes overwhelming background noise, and the adsorbed foulants may block the binding sites of biosensors, altogether leading to false positive signals and specificity loss.[530,531] In addition to biofouling issues, inflammation and associated foreign body reaction further impede the applications for implanted biosensors.[532,533]

Zwitterionic polymers have long been used to reduce biofouling on many types of biosensors, including SPR sensors,[188,534−536] surface-enhanced Raman spectroscopy (SERS) sensors,[531,537] enzymatic glucose sensors,[310,538−540] microelectrodes,[541,542] paper sensors,[543,544] etc. As discussed in previous sections, SPR sensors have been used to study the biofouling and nonfouling behaviors of zwitterionic coatings. PCB coatings were reported to reduce the nonspecific protein adsorption to a level of <0.3 ng cm^{-2} from 100% blood plasma or serum, which is below the detection limit of these sensors.[46] As an optical technique capable of measuring molecular interactions in real time, SPR sensors are widely applied in the studying of interactions between biomolecules and can be used for label-free analyte detections.[534] To build an SPR sensing platform with high sensitivity in real-world complex media, Jiang and co-workers grafted PCBAA-2 polymer brushes on a chip surface via SI-ATRP.[535] The zwitterionic PCB coating forms an ultralow fouling background to eliminate unwanted

https://doi.org/10.1021/acs.chemrev.2c00344
Chem. Rev. 2022, 122, 17073−17154

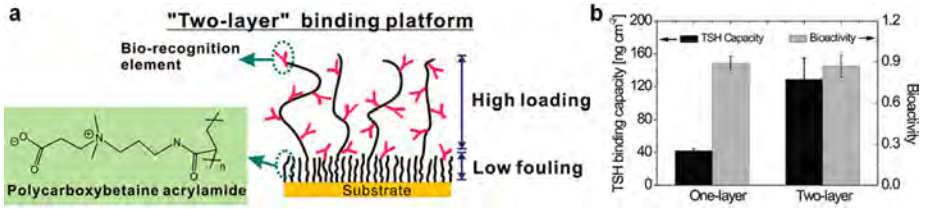

Figure 45. (a) Illustration of dual-functional hierarchical PCB coating. (b) TSH binding capacity and bioactivity of single layer and hierarchical PCB coatings. Adapted from ref 545. Copyright 2012 American Chemical Society.

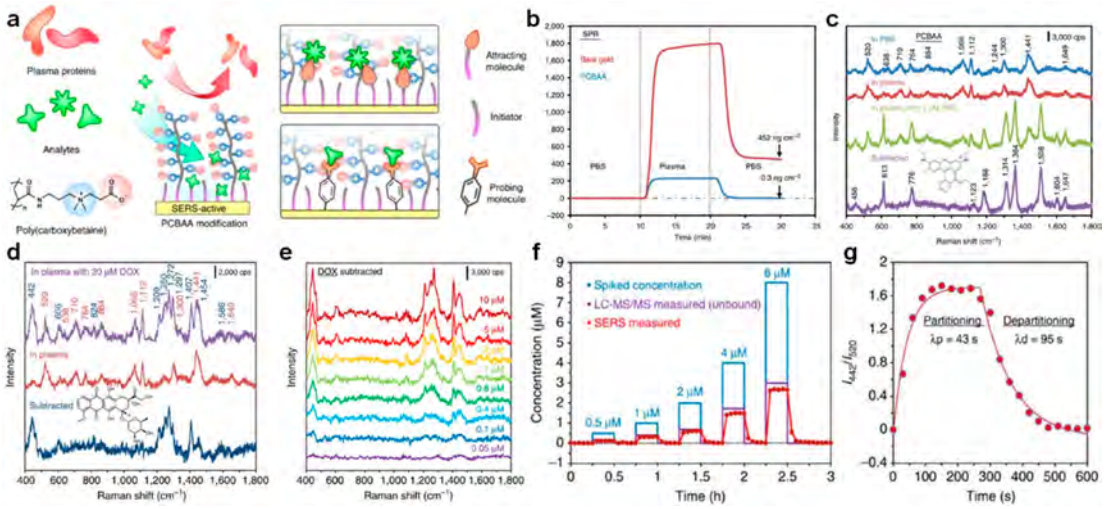

Figure 46. Hierarchical zwitterionic coating on SERS sensors. (a) Illustration of two-layer hierarchical coating. (b) Nonspecific protein adsorption resistance of the coating. (c) R6G detection after plasma exposure. (d) SERS spectra of DOX-spiked plasma, plasma, and the subtracted spectrum. (e) Subtracted SERS spectra of DOX in plasma ultrafiltrate control at different concentrations. (f) The DOX concentration measured by SERS is lower than the spiked concentration. (g) Partitioning and departitioning of DOX in plasma on the coated sensor. Reproduced with permission from ref 531. Copyright 2016 Springer Nature.

nonspecific interactions, while the carboxyl group of CB-2 can be functionalized with antibodies to provide the desired specificity. After antibody conjugation, the functionalized surface had a very low nonspecific protein adsorption (<3 ng/cm^2 for undiluted blood plasma). With the use of a cancer biomarker activated leukocyte cell adhesion molecule (ALCAM) as the model analyte, the PCB coated sensor reached a detection limit of 10 ng cm^{-2}, 10 times lower than that of the sensors coated with oligo(ethylene glycol) terminated SAMs. The coating procedure can also be done via a graft-to approach,[530] whereas the resulting detection limit was higher due to reduced packing density of the coated polymers.

High antibody loading is desired for SPR sensors to reach a high signal/noise ratio. However, the highly dense two-dimensional (2D) polymer nonfouling coatings elicit the limitation of a low ligand-loading capacity on the surface. The Jiang group proposed a hierarchical architecture of surface grafted zwitterionic polymer brushes to simultaneously realize ultralow fouling and high protein loading.[188,545] As shown in Figure 45a, a two-layer three-dimensional (3D) PCB coating can be prepared by either SI-ATRP or SI-PIMP. The first layer was grown in a controlled manner to reach a high packing density to eliminate surface fouling, while the second layer was kept loose by "termination" or "regeneration" of the living capped species to provide space for antibody functionalization. The antibody loading compacity and analyte binding on the hierarchical structure increased 2−3 times compared with those of the one-layer system (Figure 45b). These two methods were further optimized in detail in later studies.[545,546]

SERS is an ultrasensitive analytical technique with molecular specificity, making it a promising method for the detection of low-abundance biomolecules. Because of the near-field effect, SERS-based biosensing in complex media is impeded by nonspecific protein adsorptions, and it is challenging to modify SERS-active substrates using conventional nonfouling materials without introducing interference from their SERS signals.[531,537] Sun et al. reported a mixed-SAM approach for sensitive, specific, and accurate detection of fructose in protein solutions using SERS.[537] The mixed SAM was composed of a zwitterionic thiol, *N*,*N*-dimethyl-cysteamine-carboxybetaine (CBT), and a fructose probe, 4-mercaptophenylboronic acid (4-MPBA). With a surface composition of 94% CBT, the SAM demonstrated a very low BSA adsorption (~3 ng cm^{-2}). Quantification of fructose over clinically relevant concentrations (0.01−1 mM) was achieved. The detection sensitivity and accuracy were maintained for the measurements in 1 mg/mL BSA solutions. To further extend the application of SERS in real-time monitoring of drugs in blood, the same group developed a hierarchical structure consisting of two layers.[531] The first functional SAM layer attracted analytes with weak affinity and amplified signals from analytes with small Raman activity. The second PCB layer reduced the nonspecific protein adsorption on the sensor from 452 to 0.3 ng cm^{-2} in human plasma (Figure 46). With the use of rhodamine 6G (R6G) as the model analyte, the bare sensor failed to detect in the

https://doi.org/10.1021/acs.chemrev.2c00344
Chem. Rev. 2022, 122, 17073−17154

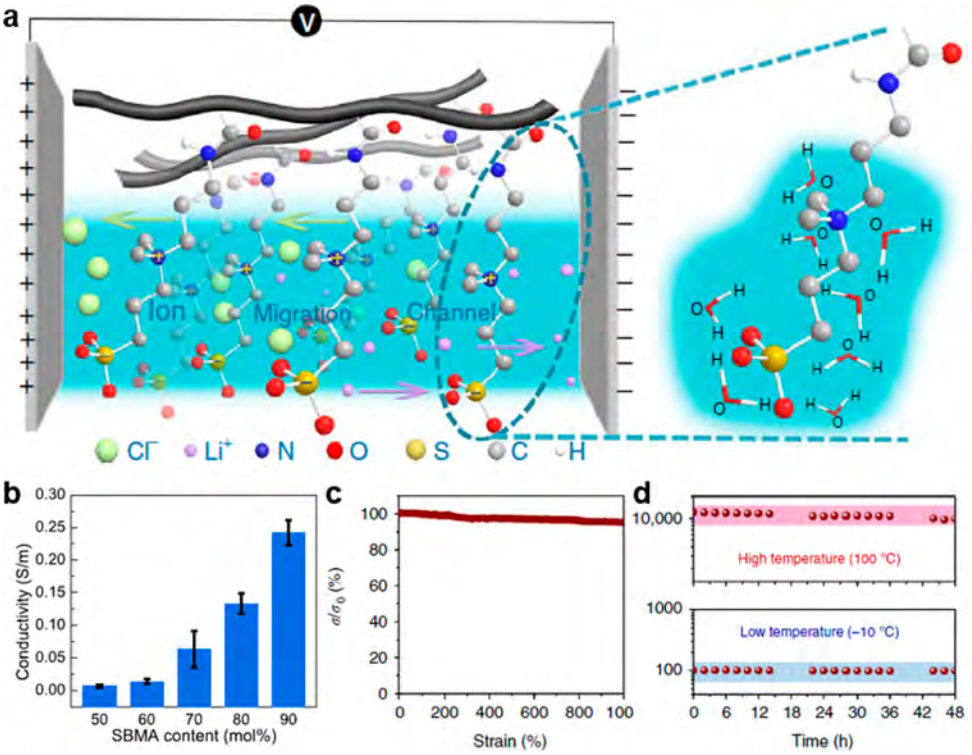

Figure 47. Ionic conductivity performance of zwitterionic materials. (a) Schematic illustration of ion migration channel in a zwitterionic gel. Adapted with permission from ref 548. Copyright 2016 Springer Nature. (b) Relationship between ionic conductivity and zwitterion content in zwitterionic skins. Adapted from ref 170. Copyright 2019 American Chemical Society. (c, d) Stable ionic conductivity of zwitterionic skins against (c) large deformation and (d) high/low temperature. Adapted with permission from ref 551. Copyright 2019 Springer Nature.

plasma due to severe protein fouling, while the sensing of the PCB coated substrate was not affected by media. The SERS signal relied on the partitioning effect of analytes into the SAM layer. It is worth noting that the coated SERS sensors could effectively monitor the concentrations of pharmacologically active doxorubicin that does not bond to blood proteins. With incorporated attracting or reporting reporters, the coated substrates were able to monitor concentration changes of drugs (tricyclic antidepressant amitriptyline hydrochloride, antiseizure medications carbamazepine and phenytoin) that are unable to petition into the SAM, or even molecules with low or no SERS signal (such as fructose).

For implantable biosensors that continuously monitor analytes *in vivo*, the situation is even more complicated. Undesirable interactions between the surface of the implanted probe and the biological medium have been proven to be the major barrier to the development of reliable implantable sensors. These interactions include not only protein adsorption but also more complicated reactions such as thrombus, inflammation, and foreign body reaction. CGMs can autonomously track fluctuations in blood glucose over time toward tight glycemic control in patients with diabetes mellitus. Yang et al. reported a PCB hydrogel coating method that enabled the sensor to monitor glucose response rapidly and accurately in undiluted human blood serum.[538] The hydrogel coating effectively prevented the nonspecific protein adsorptions from media but allowed free diffusion of glucose molecules in the polymer network. High linearity and sensitivity in the glucose detection range from 4 to 20 mM were obtained in PBS and in 10%, 50%, and even 100% human blood serum. Moreover, the sensor showed stable detection after exposure to 100% blood serum for 12 days. Hu et al. coated enzyme-based glucose biosensors with PSBMA via electrochemically mediated ATRP.[539] The PSB coated sensors remained stable after 15 days in undiluted bovine serum at 37 °C, with only 7% drift of the sensitivity. For enhanced conductivity and stability, Wu et al. reported a zwitterionic poly(sulfobetaine-3,4-ethylenedioxythiophene) (PSBEDOT)-based glucose biosensor, which was made by electropolymerization of SBMA-tailed EDOT monomers in the presence of glucose oxidase (GOx) on a platinum electrode.[540] PSBEDOT-GOx presented only 8.4% of protein adsorption from undiluted human plasma compared with that on the PEDOT-GOx biosensor without zwitterionic SBMA modifications. Upon 21 days of storage in dry or wet conditions, PSBEDOT-GOx maintained almost 100% of its current signal, while only <38% and <35% signals were preserved for PEDOT-GOx. The PSBEDOT-GOx sensor exhibited stable glucose detection with a signal decline of <10% after storage in human plasma for 14 days. In contrast, the PEDOT-GOx biosensor lost over 50% signal within a 7 day storage. More importantly, zwitterionic polymer coatings not only increase stability but also promote detection performance after implantation *in vivo* by inhibition of interferences from inflammations and foreign body reaction, which has been discussed in detail in section 4.2.3. In addition to glucose sensors, zwitterionic phosphorylcholine modified EDOT film and sulfobetaine modified polydopamine coatings were all shown to improve the biocompatibility and sensitivity of microelectrodes for the detection of neurochemicals in the central nervous system.[541,542] The zwitterionic coatings effectively reduced protein adsorption on the electrode as well as acute neuroinflammatory response during *in vivo* sensing.

https://doi.org/10.1021/acs.chemrev.2c00344
Chem. Rev. 2022, 122, 17073−17154

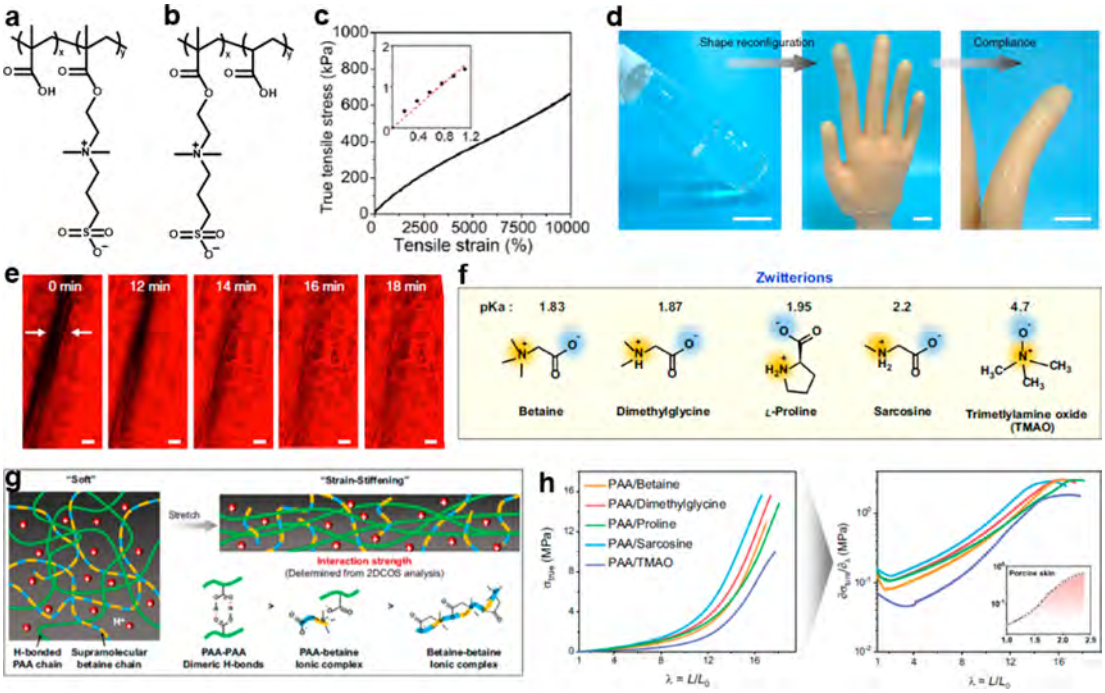

Figure 48. Zwitterionic skins constructed by polyzwitterion and small molecular zwitterion, and their mechanical performances. (a, b) Chemical structures of (a) p(SBMA-*co*-MAA) skin[553] and (b) p(SBMA-*co*-AA) skin.[552] (c) Ultrastretchability of p(SBMA-*co*-MAA) skin.[553] (d) Reconfiguration ability and (e) autonomous self-healability of p(SBMA-*co*-AA) skin. Scale bars: (d) 2 cm and (e) 20 μm.[552] Adapted from ref 553. Copyright 2018 American Chemical Society. Adapted with permission from ref 552. Copyright 2018 Springer Nature. (f) Small molecular zwitterions for the construction of zwitterionic skins. (g) Schematic illustration of strain-stiffening and the interaction strength order among the three main interacting pairs in PAA/betaine skin. (h) The strain-stiffening properties of PAA/betaine, PAA/dimethylglycine, PAA/proline, PAA/sarcosine, and PAA/TMAO. Adapted with permission from ref 555. Copyright 2021 Springer Nature.

4.9.2. Zwitterionic Wearable Devices. Wearable devices noninvasively provide continuous and real-time information for human health monitoring/diagnosis and human−machine interactions.[547] Due to the robust hydration induced by ionic solvation, zwitterionic materials can develop an ion migration channel along with the highly hydrated polyzwitterion skeleton under an external electric field.[548] In this channel, the cationic and anionic counterions can be easily separated, thus boosting ion transport efficiency and ensuring superior ionic conductivity (Figure 47a).[548,549] This property enables zwitterionic materials to attract increasing attention in the applications of wearable devices.

4.9.2.1. Zwitterions Enhance Ionic Conductivity and Stability. Hydrogel-based ionic skins are a type of biomimetic skin-like materials with various sensation functions, which require high ionic conductivity. Zwitterions can be used to enhance the ionic conductivity, taking advantage of the ion migration channel (Figure 47a). For example, Diao et al. designed a double-network hydrogel composed of PVA and poly(AM-*co*-SBMA).[550] Hydrogels without SBMA possessed relatively low ionic conductivity (0.33 S m^{-1}). The ionic conductivity increased to 2.89 S m^{-1} with the addition of 5% SBMA, and it further reached a maximum value of 7.49 S m^{-1} when 15% SBMA was added. Similarly, Wang et al. presented a zwitterionic nanocomposite hydrogel constructed from SBMA, HEMA, and Laponite XLG.[170] When the SBMA molar ratio increased from 50 to 90%, the conductivity increased from 0.0066 to 0.24 S m^{-1} (Figure 47b).

Apart from enhancing ionic conductivity, zwitterions can also improve the stability of ionic conductivity or the durability of an electrical signal. An example is an ionic conductor (PSBMA/PAA/IL) made from a tertiary system of PSBMA, PAA, and ionic liquid (IL), i.e., 1-ethyl-3-methylimidazolium ethyl sulfate.[551] Due to the ion−dipole interactions, ionic synergy was realized between PSBMA and the IL, thus forming a conductive nanochannel that could avoid aggregates or leakage of the IL electrolytes. As a result, this ionic conductor exhibited highly stable ionic conductivity under ambient conditions for 24 h and even during large deformation (Figure 47c). Furthermore, the conductivity of the PSBMA/PAA/IL ionic conductor could maintain good stability for 48 h under 100 or −10 °C (Figure 47d). To enhance the durability of an electrical signal, Lei et al. reported a supramolecular polyelectrolyte hydrogel prepared by the facile random copolymerization of SBMA and acrylic acid (AA).[552] Even after dehydration in the air with 60% relative humidity at 25 °C for 20 days, the p(SBMA-*co*-AA) xerogel still possessed a conductivity of 2 × 10^{-5} S cm^{-1}. As a result, the ionic skin fabricated by this p(SBMA-*co*-AA) hydrogel could maintain long-term stable signals for 20 days.

4.9.2.2. Zwitterionic Skins with Multiple Sensory Abilities and a Wide Spectrum of Mechanical Performances. Natural skins can sense multiple stimuli and exhibit a wide spectrum of mechanical performances. It is favorable for the ionic skins to match the sensory and mechanical performances with those of the natural skins. Taking the advantage of ionic conductivity, various zwitterionic gels have been explored for ionic skins, including p(SBMA-*co*-AA) hydrogel,[552] p(SBMA-*co*-methacrylic acid (MAA)) hydrogel,[553] PSBMA/PAA/IL ion gel,[551] silk fibroin/PSBMA/Ca^{2+} hydrogel,[554] small molecular zwitterions/PAA hydrogel,[555] etc. These zwitterionic gels were fabricated as parallel plate capacitor/ionic resistor type skins

https://doi.org/10.1021/acs.chemrev.2c00344
Chem. Rev. 2022, 122, 17073−17154

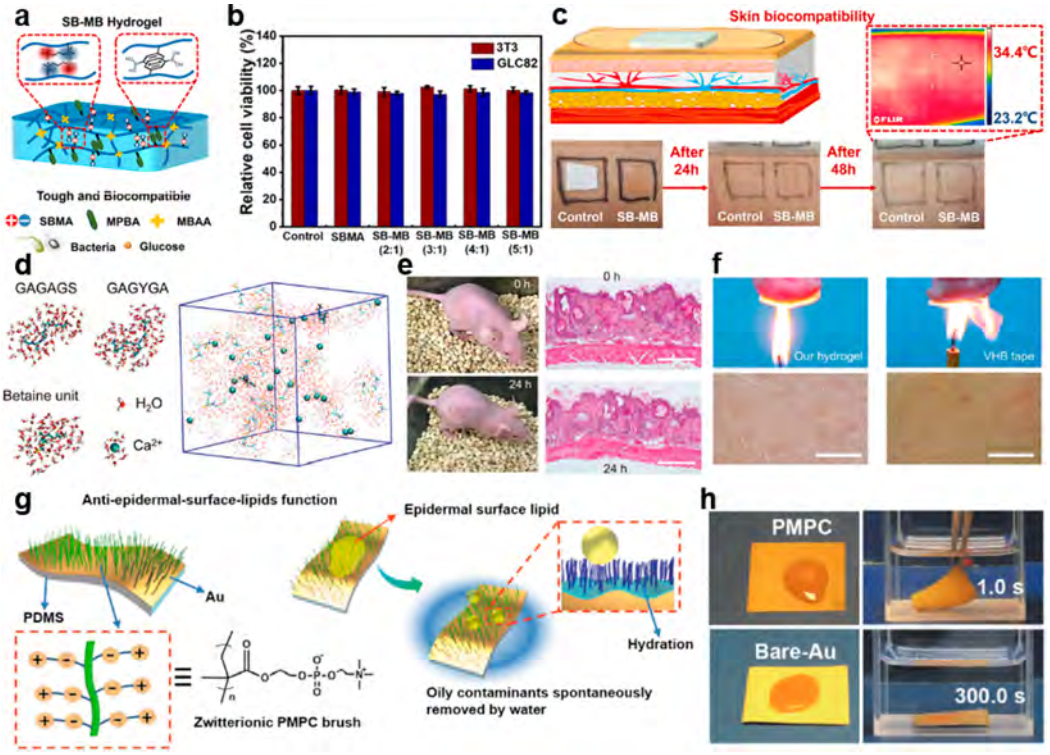

Figure 49. Zwitterionic skins with biocompatibility, bioprotectivity, and nonfouling properties. (a) Schematic illustration of the SB-MB skin. (b) Cytocompatibility and (c) skin biocompatibility of the SB-MB skin. Adapted with permission from ref 556. Copyright 2021 Elsevier. (d) Simulated molecular conformations in the silk fibroin/PSBMA/Ca^{2+} skin. (e) Photographs and corresponding histological images of a nude mouse before (top) and after wearing the silk fibroin/PSBMA/Ca^{2+} skin for 24 h (bottom). (f) Bioprotective effect of the silk fibroin/PSBMA/Ca^{2+} skin against burn injuries. Adapted with permission from ref 554. Copyright 2020 John Wiley and Sons. (g) Schematic illustration of PMPC brush modified Au/PDMS electrode with antilipid functions. (h) Canola oil (dyed) polluted (top) PMPC-Au/PDMS and (bottom) bare Au/PDMS electrodes before and after dipping into water. Oil was easily removed from the PMPC surface after dipping into water for 1 s. In contrast, oil remained on the Au surface after dipping into water for 300 s. Adapted with permission from ref 557. Copyright 2020 John Wiley and Sons.

that could achieve diverse sensations toward various stimuli, including mechanostimuli (stretch, compression, bending, etc.), temperature, humidity, and even liquid types.[551−555]

Along with the multiple sensory abilities, a wide spectrum of mechanical performances, such as stretchability, elasticity, self-healability, and even strain stiffening, can also be achieved in the same zwitterionic skins, enabling the recreation of sophisticated intelligence found in natural skins. Such broad mechanical properties can be ascribed to the zwitterion associated dynamic networks, which are usually combined with the hydrogen-bonded networks, such as PAA and poly(methacrylic acid) (PMAA). For example, the ionic skins built with PSBMA and PAA (or PMAA) showed diverse mechanical properties, including flexible reconfiguration ability, robust elasticity, ultrastretchability (>10000% strain), and autonomous self-healability (Figure 48a−e).[551−553] Another strategy is the utilization of small molecular zwitterions to build the entropy-driven supramolecular zwitterionic networks in the ionic skins. This strategy can achieve the strain-stiffening property, a J-shaped stress−strain mechanoresponse that is a key defense of natural skin to prevent injury. Zhang et al. designed a series of highly elastic, self-healable, and strain-stiffening ionic skins by introducing five types of small molecular zwitterions, including betaine, dimethylglycine, L-proline, sarcosine, and trimethylamine oxide (TMAO), into hydrogen-bonded PAA networks (Figure 48f).[555] In the original state, the zwitterionic supramolecular chains formed by weakly complexed zwitterions could combine with the random-coil PAA chains to cause softness. In the stretched state, the fragile zwitterion chains rapidly fragmented, causing a stiffened network dominated by extended hydrogen-bonded PAA chains (Figure 48g,h).

4.9.2.3. Biocompatibility, Bioprotectivity, and Nonfouling Property of the Zwitterionic Skins. Zwitterionic skins possess biocompatibility to ensure safe wear. For example, Guo et al. designed an ionic skin based on SBMA and aromatic (3-methacrylamidophenyl) boronic acid (MPBA) motifs, named SB-MB (Figure 49a). The zwitterionic SBMA endowed this biosensor with excellent cytocompatibility with cell viability close to 100% (Figure 49b).[556] Moreover, the SB-MB induced no irradiation and inflammation after being adhered to human skins for 24 and 48 h, indicating excellent skin biocompatibility (Figure 49c). Similarly, Lei et al. developed a zwitterionic skin through dynamical cross-linking of bioextracted silk fibroin, PSBMA, and biomineral calcium ions, named silk fibroin/PSBMA/Ca^{2+} (Figure 49d).[554] It showed little influence on cell proliferation after incubation with mouse embryonic fibroblast (MEF) and human mammary epithelial acini (MCF-10A) cells for 24 or 48 h, indicating good biocompatibility. In contrast, the polyacrylamide skin showed significantly lower cell viability. After wearing by a nude mouse for 24 h, both digital photos and histological images demonstrated that the silk fibroin/PSBMA/Ca^{2+} could avoid the animal skin dehydration which might be induced by common ionic skins with high salt concentrations (Figure 49e).

https://doi.org/10.1021/acs.chemrev.2c00344
Chem. Rev. 2022, 122, 17073−17154

Like the natural skins, zwitterionic skins can also provide a protective barrier for the wearer. A common bioprotectivity of zwitterionic skins is the prevention of bacterial contamination. For example, the SB-MB reported by Guo et al. showed obvious resistance to the adhesion of *E. coli* and *S. aureus*.[556] Interestingly, the p(SBMA-*co*-MAA) and silk fibroin/PSBMA/Ca^{2+} skins even could kill bacteria and fungi, including *E. coli* and *Candida albicans*.[553,554] Another bioprotective effect of zwitterionic skins is to avoid burn injuries. Due to the high hydration property, zwitterionic skins can show low thermal diffusivity and conductivity, thus preventing accidental burns. For example, when one side of the silk fibroin/PSBMA/Ca^{2+} skin was heated to 126.8 °C, the other side only showed a temperature increase of 3.6 °C, protecting the porcine skin from fire burn (Figure 49f).[554]

Nonfouling properties are needed for skin-like materials to prevent pollutant-induced unstable signals. For example, the human sebaceous gland and keratinocytes secrete oil and grease, which can pollute the skin-like devices adhered to human skin and lead to signal degradation. Zwitterionic materials can impart nonfouling properties to skin-like materials, thus solving this problem. He et al. grafted nonfouling PMPC brushes to the Au/PDMS on-skin electrodes (Figure 49g).[557] The superhydrophilic zwitterionic brushes allowed the lipid-polluted electrode surface to be cleaned by simple water rinsing (Figure 49g,h), thus maintaining stable skin-electrode impedance and good signal-to-noise ratio when electrocardiography (ECG) and electromyography (EMG) signals were recorded. In addition, the nonfouling property of zwitterionic materials also benefits the sensitivity of the hydrogel-based skin sensor, which can achieve multiple sensing performance.[398]

4.10. Ophthalmological Applications

4.10.1. Contact Lens. The contact lens is a widely used vision correction device in direct contact with eyes. Silicone and PHEMA-based hydrogels are the most commonly used materials for contact lens due to their suitable mechanical strength, optical transparency, and oxygen permeability. However, the vulnerability of these materials to protein adsorption from tear film can negatively affect the lens visibility, comfort, and wear lifetime, and even cause bacterial contamination or inflammatory responses.[558] Superhydrophilic zwitterionic materials have been used to improve the performance of contact lenses. Taking the most widely used PMPC as an example, many studies have been conducted to coat PMPC onto the surfaces of silicone contact lenses to make them durable and comfortable. These methods include in-mold coating,[559] SI-ATRP technique,[558] benzophenone initiated polymerization,[560,561] electrostatic adsorption and cross-linking,[562−564] etc. These PMPC coatings could effectively improve surface hydrophilicity, lubricity, and nonfouling performance without compromising the mechanical strength and oxygen permeability of the silicone contact lens.

It is worth noting that a PMPC-containing contact lens (Proclear, Omafilcon A) was produced by Biocompatibles and is now commercially available from CooperVision. Proclear is a cross-linked hydrogel polymerized from HEMA and MPC monomers. It showed low adhesion of corneal epithelium eukaryotic cells[565] and reduced biofilm formation by *S. epidermidis* or *P. aeruginosa* compared with silicone hydrogel lens (PureVision, Balafilcon A) and PHEMA hydrogel lens (AcuVue, Etafilcon A).[566] In addition, due to the strong hydrophilicity of PMPC, Proclear ameliorates on-eye dehydration and has been approved by the FDA to help sufferers with dry-eye syndrome.[142,561] Apart from copolymerization, PMPC was also explored as an interpenetration network (IPN) to enforce the performance of silicone hydrogels as contact lenses.[567] Compared with the hydrogels copolymerized from MPC and silicone, the hydrogels fabricated with IPN structure showed better performances in terms of mechanical, optical, and oxygen diffusive properties, suggesting their potential for contact lens application.

Considering the superhydrophilicity and biocompatibility, it would be interesting to make the contact lens from pure PMPC components. However, the PMPC hydrogels made from conventional cross-linkers suffer from uncontrolled swelling behavior and weak mechanical strength.[568] Ishihara and co-workers reported a phosphocholine-based cross-linker, named 2-(methacryloyloxy)ethyl-[*N*-(2-methacryloyloxy)-ethyl]phosphorylcholine (MMPC), which can control the hydrogel swelling when polymerized with MPC monomers in aqueous solutions.[569] They found that PMPC hydrogel cross-linked with 3 mol % MMPC showed an equilibrium water content (EWC) similar to the cornea (82%), and its tensile fracture stress was ∼170% higher than that of the PMPC hydrogel cross-linked with methylenebis(acrylamide).[561] Furthermore, the oxygen permeability of the PMPC hydrogel was 3-fold higher than that of PHEMA hydrogel. The protein adsorption on MMPC cross-linked PMPC hydrogel decreased 96 and 60% compared with the commercial disposable contact lens (1 DAY ACUVUE, etafilcon A) and MPC-containing HEMA-based contact lens (Proclear, Omafilcon A), respectively.

Apart from MPC, other zwitterions have also been explored in contact lens applications. Xu et al. prepared a silicone hydrogel contact lens via photopolymerization from silicone-containing monomer and glycidyl methacrylate (GMA) and then grafted the amino acid serine to the surface.[570] After *in vivo* wearing in rabbit eyes for 12 h, zwitterionic serine grafted contact lens exhibited excellent protein resistance. In addition, after wearing for 4 weeks, it showed no irritation and damage to the rabbit eyeballs according to histopathological images.[570] Similarly, contact lenses coated or copolymerized with PCB and PSB all showed improved performance compared with traditional contact lenses made from silicone and PHEMA.[378,571,572]

4.10.2. Intraocular Lens and Artificial Vitreous Body. The intraocular lens (IOL) is a commonly used ophthalmological device for treating cataracts. However, the IOL surface is susceptible to protein adsorption and residual lens epithelial cell adhesion, which is likely to cause posterior capsular hyperplasia, thus resulting in posterior capsular opacification (PCO) and even sight loss. Zwitterionic materials can be applied to retard posterior capsular hyperplasia. For example, Han et al. fabricated a zwitterionic PMPC brush layer on the IOL surface via RAFT polymerization.[573] This PMPC coating effectively reduced the lens epithelial cell adhesion due to the strong hydration. After implantation in rabbit eyes for 1, 3, 7, and 30 days, slit lamp images revealed that acute anterior chamber inflammation did not occur. Through histological examination, PMPC-modified IOL did not change the typical morphology of ocular tissue and did not induce posterior capsular hyperplasia, thus inhibiting PCO formation. By contrast, PCO occurred on the unmodified IOL after implantation for 30 days.[573]

https://doi.org/10.1021/acs.chemrev.2c00344
Chem. Rev. 2022, 122, 17073−17154

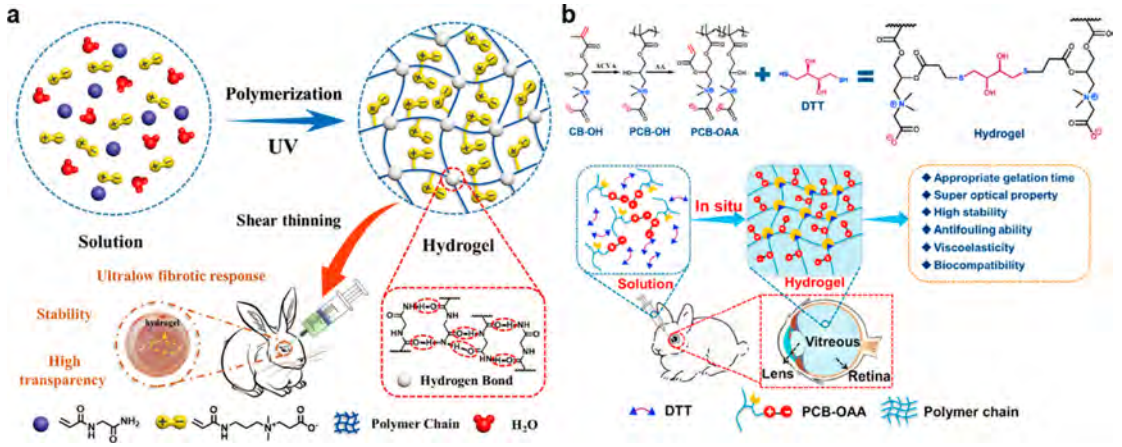

Figure 50. Zwitterionic artificial vitreous body. (a) Schematic illustration of zwitterionic PNAGA−PCBAA binary copolymer hydrogel and its injection into rabbit eyes as a vitreous substitute. Reproduced with permission from ref 331. Copyright 2018 John Wiley and Sons. (b) Schematic illustration of zwitterionic PCB-OAA polymer and PCB-OAA-DTT hydrogel and the coinjection of PCB-OAA and DTT into rabbit eyes to form a vitreous substitute *in situ*. Adapted with permission from ref 574. Copyright 2021 Elsevier.

The artificial vitreous body is an implantable substitute for the damaged vitreous body to execute normal functions, including mechanical support to ocular tissues, maintenance of a clear light path, and transportation of oxygen and nutrients. They are clinically desired to treat the blindness caused by the dysfunctional vitreous body. Zwitterionic hydrogels have been used to fabricate artificial vitreous bodies that can prevent FBR after implantation. For example, Wang et al. designed a binary copolymer of *N*-acryloyl glycinamide (NAGA) and zwitterionic CBAA.[331] The copolymer could be physically cross-linked into a zwitterionic supramolecular hydrogel via the dual amide hydrogen bonding between NAGA segments (Figure 50a). The formed hydrogel could be injected into rabbit eyes and used as an appealing vitreous substitute (Figure 50a). After subcutaneous implantation into mice for 1 month, the PNAGA−PCBAA hydrogel showed an enormously reduced inflammatory response and fibrotic response compared with pure PNAGA hydrogel, indicating that the introduced PCBAA segment imparted excellent FBR alleviating properties to the entire hydrogel. In addition, PNAGA−PCBAA hydrogel possessed body temperature extrudability/self-healability and suitable modulus, light transmittance, and refractive index similar to the human normal vitreous body. These results encouraged the authors to explore PNAGA−PCBAA hydrogel as an artificial vitreous body. After injection into rabbit eyes for 16 weeks, PNAGA−PCBAA hydrogel functioned well as an artificial vitreous body. It was stable without any adverse effects to the eye soft tissues according to the B-scan ultrasound test, funduscopic examination, electroretinogram measurement, and histopathologic examination.[331] The same group also tested an *in situ* forming zwitterionic hydrogel based on thiol−ene Michael addition for vitreous substitute application (Figure 50b).[574] The PCB hydrogel precursors could be rapidly cross-linked by the coinjected dithiothreitol in the vitreous cavity of the rabbit eyes. A 6 months post injection, the hydrogel remained stable and elicited no inflammatory response, fibrosis, or complications including increased intraocular pressure (IOP) and cataract formation.

4.11. Cell Culture Scaffold

In contrast to culture cells in 2D monolayers, hydrogel-encapsulated 3D culture is closely mimicking extracellular matrix (ECM) as well as tissue physiology *in vivo*. The 3D cell culture can avoid the forced apicobasal polarity in cells to prevent their excessive spreading and migration.[575,576] Thereinto, zwitterionic hydrogels have presented significant advantages, including their hydrophilicity and resistance to nonspecific protein adsorption, resulting in prolonged cell longevity and sustained stem cell multipotency. Jiang and co-workers demonstrated the superior cytocompatibility of CBMA monomers compared with other commonly used monomers for the preparation of hydrogels, such as HEMA and PEGMA.[577] Living NIH-3T3 cells were directly encapsulated into PCBMA hydrogels via free radical polymerization *in situ* and achieved 80% of cell viability after 28 days of culture, almost 2 times longer than that into PHEMA and PEGMA hydrogels. Subsequently, Lin et al. and Chien et al. used peptide-modified zwitterionic hydrogels to culture NIH-3T3, MG63, HepG2, and bovine aortic endothelial cells, in order to enhance the biochemical signals for cell attachment and growth to better mimic ECM.[578,579] Because the facile and mild hydrogel formation is highly desirable in cell encapsulation, strategies based on "click" reactions of end-modified zwitterionic polymers or self-healing microgels were developed. These methods could rapidly encapsulate different types of cells, including HEK-293T, NIH3T3, and even human mesenchymal stem cells (hMSCs), and maintain their cell viability for at least 14 days, presenting a potential application for injectable therapy.[25,580,581]

Maintenance of cellular multipotency is critical for stem cell based therapies but a huge challenge for *in vitro* culture. Notably, zwitterionic scaffolds were found to restrict the differentiation of stem cells cultured *in vitro* effectively. Villa-Diaz et al. investigated several kinds of synthetic polymer coating on culture dishes for human embryonic stem cell (hESC) growth.[582] It was found that zwitterionic PSBMA coatings could sustain the long-term growth, self-differentiation, and specific gene and protein expressions of hESCs after 25-fold cell propagation, compared with only doubling of cell proliferation on PEGMA and PHEMA coatings. Later, Bai et al. showed that PCB hydrogel encapsulated hMSCs retained their stem cell phenotype and multipotency, which was independent of differentiation-promoting media, cytoskeletal-manipulation agents, and stiffness of the hydrogel matrix (Figure 51a).[583] The authors

https://doi.org/10.1021/acs.chemrev.2c00344
Chem. Rev. 2022, 122, 17073−17154

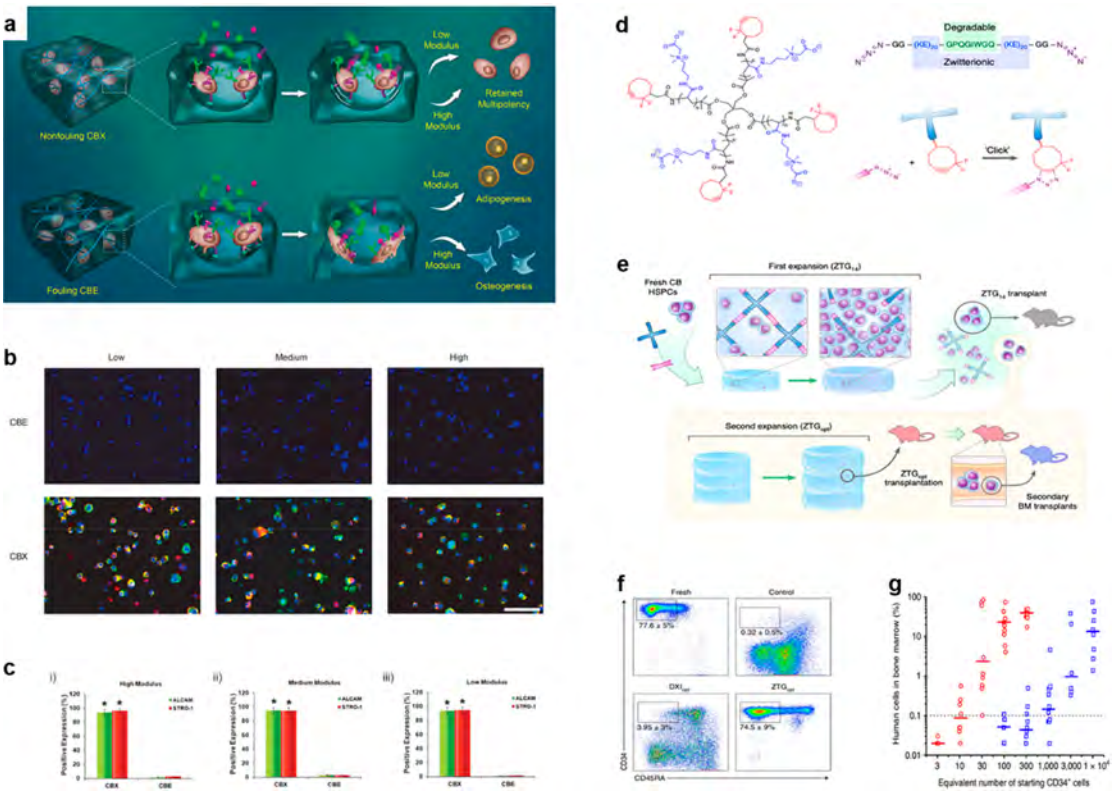

Figure 51. Zwitterionic scaffolds for stem cell culture. (a) Schematic illustration of the behavior and fate choice of hMSCs in CBX (CBAA cross-linked by a zwitterionic cross-linker, carboxybetaine dimethacrylate (CBDMA)) or CBE (CBAA cross-linked by a hydrophobic cross-linker, EGDMA) hydrogels. cRGD moieties are denoted as cyan hemispheres, and differentiation factors are denoted as colored particles. (b) Detection of undifferentiated hMSCs by immunofluorescence staining by visualization of the undifferentiated-cell markers ALCAM (green) and STRO-1 (red; nuclei, blue) in CBX hydrogels and CBE hydrogels. Scale bar: 50 mm. (c) Percentage of cells expressing either ALCAM or STRO-1 when encapsulated in CBX and CBE hydrogels with different moduli (high, i; medium, ii; low, iii), after incubation for 21 days in bipotential differentiation media. Adapted with permission from ref 583. Copyright 2014 John Wiley and Sons. (d) Biodegradable zwitterionic hydrogels (ZTG) were formed from star-shaped PCBAA and polypeptide cross-linkers containing alternating KE sequences and a metalloproteinase-degradable motif through Huisgen cycloaddition. (e) Schematic of ZTG culture procedure and experimental outline for promoting the expansion of $CD34^+$ CB progenitor cells. (f) Representative fluorescence-activated cell sorting (FACS) profiles of fresh HSPCs and cells cultured in control (TCPS), DXIopt, and ZTG opt conditions, showing CD34 and lineage marker expression. (g) Percentage of human $CD45^+$ cells in bone marrow at weeks 24−30 after mice were injected with either (blue) fresh $CD34^+$ CB derived HSPCs or (red) the ZTG_{opt}-expanded progeny of equivalent starting HSPC populations. Each marker represents an individual mouse ($n \geq 5$ mice per group). Adapted with permission from ref 586. Copyright 2019 Springer Nature.

revealed that the extreme nonfouling property of the superhydrophilic zwitterionic hydrogel system was the key to sustaining the multipotency of hMSCs, as the cells differentiated significantly when a small number of hydrophobic cross-linkers were used in the zwitterionic hydrogels (Figure 51b,c). Subsequently, the authors also designed a photoresponsible PCB hydrogel platform to trigger and suspend stem cell differentiation reversibly.[584] Dong et al. also found that the stemness of brown adipose derived stem cells can be well maintained when expending them in a zwitterionic starch-based hydrogel.[585] In 2019, Jiang and co-workers developed a zwitterionic hydrogel based culture system (ZTG) based on the orthogonal "click" cross-linking of a four-armed PCB polymer and a polypeptide cross-linker consisting of poly(EK) and a metalloproteinase-cleavable sequence (Figure 51d).[586] Cord blood and bone-marrow-derived human hematopoietic stem and progenitor cells (HSPCs) were expended in the ZTG culture system, leading to a 73-fold increase in long-term HSPC frequency, which significantly outperformed other culture systems (Figure 51e,f). After transplantation in immunocompromised mice, the expended cells enabled the hematopoietic reconstitution for at least 24 weeks *in vivo* (Figure 51g). Mechanism studies showed that the 3D zwitterionic hydrogel culture might inhibit the production of excessive reactive oxygen species (ROS) via suppression of O_2-related metabolism pathways, leading to the mitigated HSPC differentiation and promoted self-renewal during culture.

4.12. Industrial Applications

4.12.1. Marine/Aquaculture Antifouling Coatings. Marine biofouling is a challenging issue to be resolved in the ocean industry. In the maritime industry, the biofouling-induced extra load can increase the roughness of ships, leading to reduced navigational speed and increased fuel consumption as well as operation cost. In the aquaculture industry, biofouling on equipment leads to the reduction of dissolved oxygen and competition for limited food and space, resulting in poor water quality, increased risk of diseases, and death of the aquatic organisms. Moreover, marine biofouling can cause biocorrosion on ships, offshore drilling platforms, levees, aquaculture nets, cages, etc., resulting in the degradation and invalidation of equipment. Owing to their nonfouling properties and biocompatibility, zwitterionic materials are promising

https://doi.org/10.1021/acs.chemrev.2c00344
Chem. Rev. 2022, 122, 17073−17154

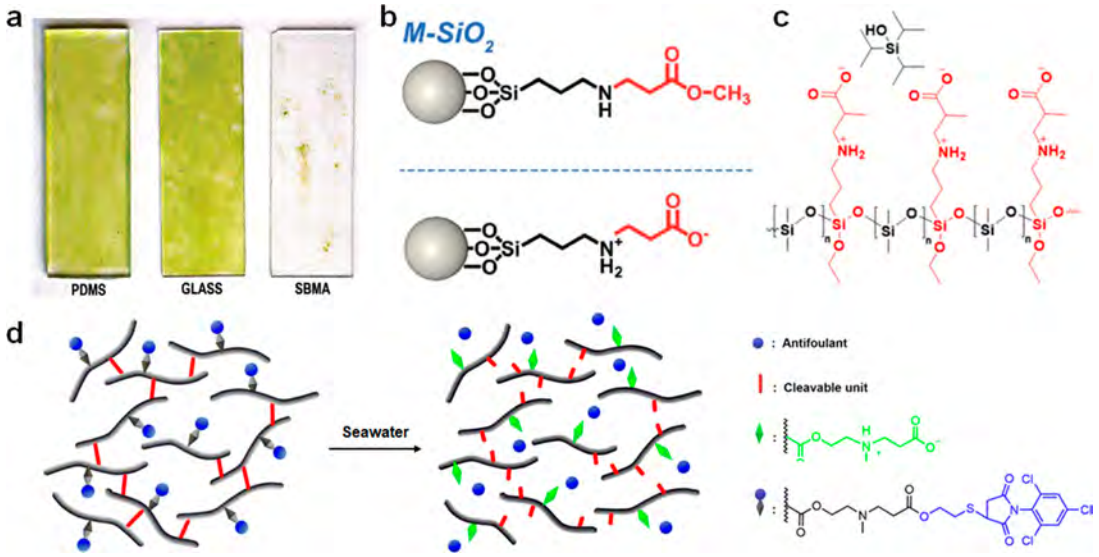

Figure 52. Zwitterionic materials in marine antifouling applications. (a) Green marine alga (*Ulva*) settlement on the surfaces of PDMS, glass, and PSBMA-grafted glass slides. Adapted from ref 610. Copyright 2009 American Chemical Society. Hydrolysis and zwitterionic group generation on (b) M-SiO_2[608] and (c) TMAP.[609] Adapted with permission from ref 608. Copyright 2020 Royal Society of Chemistry. Adapted with permission from ref 609. Copyright 2021 Elsevier. (d) Hydrolysis and release of attacking TCPM segments. TCPM segments can perform bacterial killing, and the residual zwitterionic segments can perform biofouling repellence. Adapted from ref 614. Copyright 2021 American Chemical Society.

candidates to prevent biofouling as well as avoid impact on the marine ecological environment.

4.12.1.1. Marine Biofouling. Minutes after being immersed in seawater, the surfaces of marine equipment will adsorb biomolecules, followed by colonization of bacteria, diatoms, and protozoa, resulting in biofilm formation.[587] In marine biofilms, heterotrophic bacteria, cyanobacteria, archaea, and unicellular eukaryotes are the main inhabitants with relatively low densities of sarcodines, ciliates, and fungi.[588] The hierarchical structure and dynamics of biofilms are usually dependent on the species composition, microbial activity, and environmental conditions. Their major adverse impacts on marine equipment include weight increment, friction increase, and biological corrosion.[37] Among various biofoulers, mussels have the most serious impact on the gained weight of marine equipment. For instance, panels were submerged in the sea at a depth of 5 m off the Portuguese west coast. After 12 month of fouling, severe mussel growth on the panels led to a significant increase of fresh weight (~24 kg m^{-2}).[589] In addition, biofoulers (e.g., kelp) increase the surface roughness and friction drag of ships, inducing the reduction of mobility or even damage of sensitive machine units. Moreover, biological corrosion is induced by microbial metabolites and accelerated by macrofouling organisms. Macrofoulers such as barnacles can adhere to or even perforate the ship hull via metabolites.[590]

Marine biofouling accumulation is generally considered to be a plague in the aquaculture industry. Because of the exposure of both cultured infrastructures and species to the biofoulants, there are commonly significant impacts on aquaculture production.[591] The culturing infrastructure invariably consists of pillars, cages, nets, buoys, and ropes, which provide the landing surfaces for biofouling.[591] In addition, the diverse fouling organisms lead to the physical damage and mechanical interference of cultured species, as well as competition for limited food and space. Biofouling organisms have impacts on the aquaculture of various species. For example, in shellfish aquaculture, the shells can provide the ideal and accessible surfaces for epibiotic biofouling to grow. In oyster culture, epibiotic biofouling accumulation hinders the water current and nutrient exchange between the culturing oyster and outside, resulting in food depletion.[592] Worse still, some endolithic organisms attach to the shell surface to subsequently penetrate and excavate the shell. They can induce cavities, blisters, and tunnels inside the nacreous layer, further leading to shell fragility and thickness loss.[593] In fish aquaculture, biofouling growth causes the occlusion of fishing nets, thus reducing water exchange and decreasing the dissolved oxygen level, which has a negative impact on fish growth and respiration to further induce their death.[594] The restriction of water exchange also hinders the removal of excess feed and waste to decrease water quality. Moreover, these biofouling taxa can increase the stress level and lower the immunity of the fish against various diseases, owing to the reservoirs for pathogenic microorganisms.

4.12.1.2. Maritime Antifouling. Zwitterionic functionalized surfaces have been reported to enable effective repellence of marine micro- and macro-biofoulers, such as bacteria,[595,596] diatoms,[597−600] alga,[601−603] barnacle,[604−606] and mussel.[607−609] For instance, Zhang et al. modified glass slides for a PSBMA brush coating via the ATRP method. Their results showed that the alga adhesion on the modified surface was 92% lower than that on the pristine glass, attributable to the neutral charge of PSBMA in seawater (pH ~8.2). In addition, 66% of the adherent alga could be removed by 63 kPa of impact pressure, compared with only 16.8% of alga removal on PDMS (Figure 52a). PSBMA coating also exhibited significant resistance to diatom settlement, corresponding to an 85% reduction compared with the settlement on the pristine glass.[610] Most of the invertebrate colonization of submerged equipment surfaces is by macrofoulers, such as barnacles and mussel. Aldred et al. respectively developed PCBMAp and PSBMA-coated glass slides and demonstrated that no settlement of barnacle was observed on either coating after 72 h of coculture.[611] In order to be applied in industry, it has been attempted to incorporate zwitterionic groups with commonly used coating materials such as PDMS. But it is a

https://doi.org/10.1021/acs.chemrev.2c00344
Chem. Rev. 2022, 122, 17073−17154

challenge owing to the noncompatibility between zwitterionic and silicone-based materials. In 2020, Tan et al. prepared hydrolyzable CB-ester ligands on SiO_2 particles that were embedded in PDMS coatings. Zwitterionic groups could be generated via *in situ* hydrolysis to display a reduction of 41.1% for mussel adhesion after 14 days of exposure (Figure 52b).[608] One year later, Wang et al. synthesized a precursor, triisopropylsilyl 2-methyl-3-((3-(triethoxysilyl)propyl) amino) propanoate (TMAP), bearing a triisopropylsilyl group and a triethoxysilyl group on the CB ligand. The triethoxysilyl units could be polymerized with hydroxyl-terminated PDMS to obtain a homogeneous coating, and the triisopropylsilyl groups could be hydrolyzed into zwitterionic groups via self-catalytic effects (Figure 52c).[609] As a result, the coating containing 50% TMAP exhibited maximum decreases of bacteria and diatom adhesion (72 and 72.1%, respectively). After 2 days of cultivation, no mussel settlement could be observed on this coating, indicating its outstanding nonfouling performance.

Apart from passive nonfouling, biocidal active ingredients have been incorporated into zwitterionic coatings to enhance their fouling-resistant performance. Zhang et al. employed Bi_5O_7I with zwitterionic fluorinated polymer to perform the synergistic effects of hydration and photocatalysis. On the one hand, the zwitterionic polymer was hydrated to form a shielding layer to resist bacteria and alga attachment. On the other hand, light irradiation excited Bi_5O_7I generated the reactive oxygen species including $^{\bullet}OH$ and $^{\bullet}O_2^-$, leading to the damage of DNA and proteins in bacteria and alga to death.[612,613] In 2021, Dai et al. developed a kill−resist−renew coating for biofouling repellency. The authors synthesized a zwitterionic CB-ester bearing an *N*-(2,4,6-trichlorophenyl) maleimide (TCPM) group, and the attacking TCPM segments could kill microbial cells and then be hydrolyzed to release. The residual zwitterionic segments were superhydrophilic to resist the attachment of various biofoulants (Figure 52d). This kill−resist−renew coating exhibited a recyclable usage in marine antifouling.[614]

4.12.1.3. Aquaculture Antifouling. Zwitterionic materials can prevent biofouling in the aquaculture industry without biotoxicity, owing to their superior biocompatibility. For instance, Mohan et al. designed a SiO_2-incorporated mixed charge hydrogel layer on polyaniline (PE) aquaculture cage nets. The anionic sulfonic acid and cationic quaternary ammonium groups could act as pseudozwitterionic interfaces to resist biofoulers, while the ceramic oxide SiO_2 was considered to possess antibacterial capacities. After a 2 month field exposure, the biofouling was decreased by ∼41% on this hydrogel layer compared with that on the pristine PE cage nets; upon a 6 month field exposure, there were no hard-shell organisms observed on the hydrogel-coated cage nets.[615] Pu et al. modified an effective but hemolytic antimicrobial agent (POSS-*g*-PDMA) with zwitterionic PSB to improve its biocompatibility. The obtained POSS-*g*-(PDMA-*co*-PSB) polymer presented hemocompatibility, bactericidal activity, and nontoxicity to zebrafish embryos, indicating its potential to prevent bacterial infection in the aquaculture industry.[616]

4.12.2. Membrane Separation. Membrane separation is a sustainable strategy owing to its energy conservation, cost-effectiveness, mild operating conditions, etc.[617,618] However, contamination of membranes sharply decreases their performance and longevity.[619] Membranes can be impacted by four major pollutants: organic fouling, inorganic fouling, colloidal fouling, and biofouling.[620] Compared with other pollutants, biofouling presents the most difficulty to deal with due to self-replication. Most sterilization methods without 100% efficiency will leave residue living cells to induce microorganism reproduction and further biofouling.[621] In the membrane filtration system, biofouling can change the pore size distribution and porosity of membranes to reduce the flow flux or throughput. During the filtration process, convective transport and concentration polarization can offer an extra driving force for biofouling deposition, leaving a steady supply of nutrients for biofilm growth.[622] Once biofouling occurs, the pressure drop within the membrane module is prominently increased, leading to a reduced effective driving force, energy waste, and even device destruction.[623,624] Membrane-based separation covers multiple fields, including healthcare, food production, water processing, etc.[625] Due to the requirement of nonfouling property, zwitterionic material modified membranes have been recently developed, and they significantly improve the durability for separation.[626−631]

4.12.2.1. Bioseparation. In microbiological fermentation, membrane separation is useful in primary purification for product concentration and impurity removal. Nonfouling zwitterionic materials can improve the bioseparation efficiency and selectivity of membranes. For example, Sun et al. immobilized zwitterionic PSB−DOPA polymer on the PVDF membrane, and its hydrophilicity was significantly improved. The modified membrane achieved the highest water uptake and lowest protein adsorption among all samples and improved the separation performance with a BSA rejection of ∼93.8% as well as the recycling property with a flux recovery ratio of ∼96.9%.[632] Thereinto, the selective separation of proteins is a challenge and can be dependent on their inconstant isoelectric point, surface charge, and special binding sites.[633] Liu et al. synthesized zwitterionic chitosan through Schiff base formation and subsequent sulfonation reaction.[634] Then, the zwitterionic chitosan was linked with PVA through tetraethyl orthosilicate to prepare the ultrafiltration membranes for BSA/LYZ separation. The solution permeation flux was gradually increased with the content of zwitterionic chitosan, while the protein transmission was affected by the pH owing to the electrostatic repulsion. Therefore, dependent on regulating the zwitterionic chitosan content and the pH, the membrane could exhibit different retention performances toward various proteins, achieving a high selectivity in protein separation.

4.12.2.2. Desalination and Water Purification. Membranes, in particular reverse osmosis (RO) membranes, have taken the dominant role in the seawater desalination and water purification industry. Zwitterionic modifications have been applied to these membranes to enhance their water permeability and antideposition properties.[635−640] Gleason and co-workers developed a scalable method to deposit sulfobetaine-based ultrathin antifouling coatings onto various substrates using an all-dry-initiated chemical vapor deposition (iCVD) technique followed by a diffusion-limited vapor-phase reaction.[641] In the modification process, poly[2-(dimethylamino)ethyl methacrylate-*co*-ethylene glycol dimethacrylate] (PDE) thin films were first synthesized via initiated chemical vapor deposition (iCVD) and then reacted with 1,3-propane sultone to obtain the zwitterionic structure. The coated RO membranes showed strong resistance against biofoulings, with impaired salt rejection and slightly compromised permeate flux.[631] To further improve the resistance of RO membranes to the chlorine used in water pretreatment, they replaced the acrylate-based coating with pyridine-based

https://doi.org/10.1021/acs.chemrev.2c00344
Chem. Rev. 2022, 122, 17073−17154

zwitterionic moieties.[642] This new coating structure provided a path toward solving the desalination industry's bottleneck of the susceptibility of RO membranes to oxidative damage by chlorine. Benefiting from the synergy between surface chemistry and chlorination, with concentrations as low as the regulated chlorine residue in drinking water, the long-term fouling resistance of the zwitterionic coating was enhanced by 9.4-fold after 12 h. Subsequently, the same coating system was shown to be effective for the purification of highly contaminated high-salinity shale gas produced water.[643]

4.12.2.3. Oil/Water Separation. The separation of oil/water mixtures remains challenging, especially for the purification of seawater after crude oil leakage. Attributed to their superhydrophilicity, zwitterion modified surfaces demonstrate strong underwater superoleophobicity.[644] Utilizing that property, different techniques have been developed to functionalize membranes with zwitterionic moieties to improve their oil/water selectivity as well as nonfouling performance.[644−653] As a typical example, He et al. showed that a PMPC-coated steel mesh had a strong underwater superoleophobicity (oil contact angle >165°).[644] Apart from the efficient separation of oil from oil/water mixtures, the zwitterionic membrane showed a self-cleaning ability that resulted in no oil residue adherent on the mesh during separation processing. More importantly, the coated mesh can lift oil out from the oil/water mixture without prewetting even in a dry state, mainly owing to the complete displacement of oily foulant by water. Therefore, this PMPC-coated mesh was perfectly suitable for oil spill remediation since the separation device would preferentially contact the floating oil. On the contrary, oil contamination on conventional hydrophilic oil−water separation membranes would permanently induce the loss of oil−water separation function. In addition to simple oil/water mixtures, zwitterionic polymer modified membranes were shown to effectively separate oil under various challenging conditions, including surfactant-stabilized oil-in-water emulsions.[562]

4.12.3. Antifreezing Coatings and Hydrogels. With the recent reports of antifreezing capability, zwitterionic materials have been utilized for novel anti-icing coatings and antifreezing hydrogel-based skins. Yuan et al. developed a zwitterionic PSBMA-based copolymer for highly efficient antifogging and anti-icing coating (freezing delay time of more than 2 min), due to a self-lubricating aqueous layer generated by non-freezable bound water on the surface.[654,655] Liang et al. and Ma et al. revealed that the zwitterionic polymer bushes contained more nonfreezable bound water than typical polyelectrolytes, leading to lower ice adhesion strength for anti-icing.[119,656] Zhang et al. designed the zwitterionic mussel-inspired chimeric protein to be a facile anchoring coating, which can achieve antifogging, anti-icing, and self-cleaning peformances.[657]

In the hot field of flexible skin-like sensors, the conductivity and flexibility of ionic skins are commonly significantly decreased at the freezing temperature, which promotes the more recent research of antifreezing skin-like materials based on zwitterionic hydrogels. Sui et al. designed a zwitterionic osmoprotectant-based conductive hydrogel, which presented a high conductivity (2.7 S m^{-1}) even under −40 °C.[658] Zhang et al. also demonstrated the antifreezing capability of more zwitterionic molecules including betaine, dimethylglycine, L-proline, sarcosine, and trimethylamine oxide used in skin-like materials.[555] Recently, Liu et al. further improved the conductivity (12.6 S m^{-1}) of materials based on zwitterionic polymeric hydrogels at −40 °C.[121] Sui et al. developed a zwitterionic skin that enabled the resistance to freeze for 30 days at −80 °C and self-regeneration by spontaneously harvesting water molecules from surrounding environments under −40 °C.[659] Subsequently, Zheng et al. designed a general zwitterionic cross-link to develop intrinsic freezing-resistant hydrogels and revealed that the cross-linking hydrophilicity induced strong water-network bindings to prevent ice crystal formation from free water molecules in hydrogels.[122]

4.12.4. Fresh Water Collection. Zwitterionic materials possess high water affinity, which is beneficial for steam nucleation in moisture harvesting and bulk water pumping in solar evaporation. Patterns of hydrophilic/hydrophobic surfaces made from zwitterionic materials are effective for fog harvesting. For example, Wen et al. developed a hierarchical array composed of hydrophilic CBMA-grafted needles and hydrophobic sheet.[660] The hydrophilic needles provided numerous water affinity sites for fog condensation, enabling an order of magnitude higher nucleation density than hydrophobic surfaces, resulting in a harvesting rate of 1066 mg cm^{-2} h^{-1}.[661] Moreover, hydrophilic zwitterionic channels were conducted on the hydrophobic substrates, endowing this device with controllable water transport.

The excellent fouling repellence of zwitterionic materials is essential in long-term usage for solar evaporation devices in complex conditions, such as the ocean. The Zhang group designed a superhydrophilic but self-floatable hybrid hydrogel evaporator that was composed of zwitterionic PSB and a hollow glass microsphere.[662] The resultant evaporator reached an evaporation rate as high as 1.35 kg m^{-2} h^{-2}. Owing to the zwitterionic components, this hydrogel could be fully hydrated to process a continuous water supply and resist multi-contamination including protein adsorption, bacterial adhesion, crude oil pollution, and salt accumulation, to guarantee its long-term performance. In another work, the same group employed PCB as an nonfouling coating to protect the evaporator from various foulants, achieving a higher evaporation rate of 2.2 kg m^{-2} h^{-1}.[663]

5. SUMMARY AND OUTLOOK

A fundamental understanding of nonfouling mechanisms at the molecular level leads to the generalization of the concept of nonfouling zwitterionic materials and enables the development of a new class of nonfouling zwitterionic materials beyond the early pioneering work of "cell membrane mimic" PMPC by Kazuhiko Ishihara and of PEG-alternative materials by George Whitesides. From the historical perspective, PMPC was first developed to mimic cell membranes and later developed into a number of commercial products. Although PMPC is zwitterionic in nature, its nonfouling mechanism is mainly linked to "cell membrane mimic". PSB and PCB were also studied in the early days as hydrophilic coatings to reduce nonspecific adsorption on hydrophobic surfaces.[664,665] While all hydrophilic surfaces generally have lower protein adsorption than hydrophobic surfaces, ultralow protein adsorption of <5 ng/cm^2 is the key to the prevention of blood clotting for blood-contacting devices. There were potentially several reasons why truly ultralow fouling surfaces were not realized or discovered in the early days. The first was a significant lack of a fundamental understanding of nonfouling mechanisms such as the critical role of hydration. For example, it was a puzzle why PMPC and PEG resist nonspecific protein adsorption quite well although their molecular structures are

https://doi.org/10.1021/acs.chemrev.2c00344
Chem. Rev. 2022, 122, 17073−17154

totally different, and why mannitol and sorbitol have very different behaviors against nonspecific protein adsorption although their structures are quite similar. The second was a lack of an effective method to create nonfouling coatings with high surface packing densities such as ATRP or RAFT. For example, PSB coatings were often achieved with random copolymers. While protein adsorption on these coatings was not as low as expected, people often considered that PSB was not as effective as PEG or PMPC as a nonfouling material. In many cases, fouling actually came from the hydrophobic component of the copolymer, not from its SB component. The third is the lack of a sensitive method to quantify nonspecific protein adsorptions from complex media such as undiluted blood plasma or serum such as SPR biosensors. The application of SPR biosensors to evaluating nonfouling surfaces enables quantitative and accurate measurements of nonspecific adsorption down to 0.3 ng/cm^2 from complex media. With minimized charge and dipole, and free of hydrophobic interactions, it has been shown that hydration plays a key role in achieving nonfouling properties. When hydration is sufficient, flexibility is not required to achieve nonfouling properties but is helpful. ATRP and RAFT were employed to create nonfouling coatings with the highest packing densities possible, while SPR biosensors were employed to measure nonspecific protein adsorption quantitatively even from complex media such as undiluted blood plasma and serum on nonfouling surfaces with high sensitivity.

There are two common ways to achieve high hydration. While hydrophilic and neutral materials such as PEG achieve hydration via hydrogen bonding, zwitterionic materials bind water molecules strongly via electrostatically induced hydration. In general, zwitterionic materials have much higher hydration than their hydrophilic and neutral counterparts. Among zwitterionic materials, as the hydration similarity of ions determines the ion−ion associations, CB has a high-charge-density anionic group and a low-charge-density cationic group; thus, it does not self-aggregate and uses all sites to bind water molecules to maximize hydration. As a result, PCB polymers have the strongest hydration, the fewest self-associations, and the least interactions with proteins where many carboxylic groups and primary amine groups dominate protein surfaces.

When two opposite charges are on the same monomer, we generally refer to the material as "zwitterionic". When two opposite charges are on different monomers, we then refer to the material as "mixed-charge" or "pseudo-zwitterionic". Zwitterionic materials can be in the form of a polymer or a peptide. One advantage of a zwitterionic peptide is that it can be produced from cells and can be fused to a protein directly in cells via genetic engineering although both polymers and peptides can be chemically conjugated to a protein. PCB polymers are derived from naturally occurring zwitterions such as glycine betaine, while EK polypeptides mimic the protein surfaces. Among zwitterionic materials, PCB polymers are particularly unique. Besides their excellent nonfouling properties, they are unique in two more aspects. One aspect is that PCB is dual functional, i.e., nonfouling and functionalizable. One can directly attach ligands to PCB polymers via NHS/EDC chemistry for biosensors and targeted drug delivery applications. The other aspect is that the positively and negatively charged sites can be readily hidden by using tertiary amine and hydrolyzable groups, respectively. This property is particularly useful for applications such as antimicrobial materials, gene delivery carriers, and coating-free nonfouling elastomers where charge switching is required. Zwitterionic materials have been used extensively in all three forms, i.e., surface coatings, bulk materials particularly hydrogels, and nanoparticles as summarized below.

For surface coatings, to achieve nonfouling properties, excellent nonfouling materials alone are not sufficient. High surface packing density on surfaces is another key factor. Conventional "nonfouling" materials and surfaces are evaluated for their nonfouling properties with single protein solutions or 10% diluted blood serum, which is not challenging enough and will often fail in more complex media in real-world applications. Instead, these surfaces should be challenged at least with 100% undiluted blood plasma or serum. Even for those surfaces passing these tests, they may still induce capsule formation after long-term implantation, antibody generation in blood when conjugated with immunogenetic biological moieties, and biofilm formation. Studies should be further conducted to evaluate the performance of these materials in these even more challenging conditions for real-world biomedical applications. For hydrogels, if a zwitterionic monomer and a zwitterionic cross-linker are used to prepare hydrogels, these hydrogels can achieve the maximum nonfouling properties and can be free from nonspecific interactions. This is particularly important as these hydrogels can serve as the ground state free of nonspecific interactions to study the effects of external perturbations by varying chemical, biological, and mechanical cues on cells. By taking advantage of the unique features of different zwitterionic materials, double- and triple-network pure zwitterionic elastomers are achieved with both excellent nonfouling and mechanical properties. For nanoparticles, zwitterionic micelles with sharp-contrast polarity were shown to be much more stable than their PEG counterparts. Zwitterionic liposomes without cholesterols are as stable as those PEG counterparts with 39% cholesterol required for particle stabilization. Zwitterionic polymers or peptide-modified proteins do not induce antibodies against zwitterionic polymers or peptides even when they are conjugated to highly immunogenetic proteins. PEGylated proteins induce anti-PEG antibodies, which increase exponentially with the immunogenicity of proteins being conjugated.

To move forward, there are several areas to consider. The first is to provide further fundamental understanding. As of now, nonfouling mechanisms are attributed to "water-like" materials with high hydration, resulting in free interactions. These mechanisms only reflect how to avoid materials from interacting with cells, i.e., mainly reduce the innate immunity in the initial stage of interactions. This does not say anything about adaptive immunity once nanoparticles, even a trace amount, are taken into, say, antigen-present cells (APCs). How these materials are processed and presented by APCs and subsequent interactions with T and B cells are critical to the understanding of material immunogenicity. This is particularly important as PEG used in COVID-19 vaccines is susceptibly associated with allergic reactions. These are well beyond our current nonfouling mechanisms based on hydration. While we have achieved many excellent capabilities with zwitterionic materials for applications, we still do not fully understand their mechanisms of action at the molecular or cellular level. Thus, it is important to study how nanoparticles interact with the immune systems, how implants interact with the surrounding tissues, and how culture media interact with stem cells beyond hydration. Immunology and cellular and molecular biology

https://doi.org/10.1021/acs.chemrev.2c00344
Chem. Rev. 2022, 122, 17073−17154

tools are very useful in these studies. The ideal outcome is the development of new materials which cannot be or are hard to be detected by the immune surveillance system.

The second is to design better materials than what are known so far. While one will continue to adopt biomimetic approaches and learn from nature for the design of new materials, the combined molecular modeling and machine-learning approach is very powerful in designing better materials, particularly polypeptides, for which conformations play a critical role in their nonfouling properties. It has been demonstrated that proteins have rich E and K compositions on their outer surfaces, and polypeptides containing E and K have excellent nonfouling properties. However, for a long E and K peptide, particularly with amino acids other than E and K added, its conformation becomes critical for its properties. When a polypeptide containing E and K is conjugated or fused to a protein, the conformation of this polypeptide will determine its effects on the stability and activity of the protein being conjugated or fused. In addition, it will be helpful to create a database of nonfouling zwitterionic materials. With the database, machine learning provides a means of screening novel materials with excellent performance and discovering new materials. These approaches allow us to examine other parameters, such as conformations, than the chemical compositions we have focused on so far.

The third is to go deeper and broader for applications. Zwitterionic materials have been demonstrated to achieve anticoagulant-free coatings for 36 h when tested in a 36 h veno−venous sheep extracorporeal life support model, capsule-free implants in the C57BL/6 mice model for at least 1 year, expanded culture of HSPCs without differentiation, antibody-free protein conjugates after multiple injections, and long-lasting marine coatings. PMPC has been adopted in multiple commercial products, while PSB-coated catheters have received FDA approval. What is needed next is to move these new zwitterionic materials into products. Many applications can benefit greatly from zwitterionic materials such as existing PEG-based lipid nanoparticles (LNPs) for mRNA delivery. These efforts can be accelerated through technology transfer and commercialization toward the development of FDA-approved projects. One concern regarding these materials is their chemical stabilities, as they are all ester- and amide-based materials which might be vulnerable to hydrolysis. Currently, there is still a lack of systemic studies of the chemical stabilities of these materials, although the stability of acrylate or acrylamide as a backbone does not seem to be a major concern under physiological conditions. To move forward toward products for clinical applications, the stabilities and metabolisms of zwitterionic materials should be studied further.

The fourth is to bring functionality into zwitterionic materials. There are many zwitterions in nature—each has its unique functions, while the zwitterionic nature is common to all to keep them from being interacted with by charged species. Similarly, nonfouling properties are shared by all zwitterionic materials, although some may work better than others so that they will not be recognized by the immune system. Ideally, each zwitterionic material should have its unique built-in functions. This is similar to proteins which are zwitterionic. Each protein in blood has its unique functions, but all of them share one common feature of zwitterionic materials, i.e., maintaining certain blood circulation.

Collectively, an important challenge in many applications is the prevention of unwanted nonspecific biomolecular attachment on surfaces, which compromises the performance of many medical devices, drug delivery carriers, consumer products, and engineering products. Nonfouling materials are needed for almost all biomedical and engineering applications involving complex media. Over the past 45 years, PEG-based materials have been a gold standard and are almost exclusively used as nonfouling materials. Zwitterionic materials have offered fresh ideas and potentially provided more effective and safer solutions than PEG-based materials. Although several new zwitterionic materials and many of their excellent properties have been reported, we believe that research on zwitterionic materials is just the beginning. There is still a lot to learn from nature for the design of many more nonfouling zwitterionic materials with built-in biological functions, and there are many applications that can benefit from these zwitterionic materials. The success of zwitterionic materials further emphasizes the importance of fundamental and interdisciplinary research from molecular principles to product development.

AUTHOR INFORMATION

Corresponding Authors

Shaoyi Jiang − *Meinig School of Biomedical Engineering, Cornell University, Ithaca, New York 14853, United States;* orcid.org/0000-0001-9863-6899; Email: sj19@cornell.edu

Lei Zhang − *Department of Biochemical Engineering, Frontier Science Center for Synthetic Biology and Key Laboratory of Systems Bioengineering (MOE), School of Chemical Engineering and Technology, Tianjin University, Tianjin 300350, China;* orcid.org/0000-0003-3638-6219; Email: lei_zhang@tju.edu.cn

Peng Zhang − *MOE Key Laboratory of Macromolecule Synthesis and Functionalization, Department of Polymer Science and Engineering, Zhejiang University, Hangzhou 310027, China;* orcid.org/0000-0002-5409-7480; Email: zhangp7@zju.edu.cn

Authors

Qingsi Li − *Department of Biochemical Engineering, Frontier Science Center for Synthetic Biology and Key Laboratory of Systems Bioengineering (MOE), School of Chemical Engineering and Technology, Tianjin University, Tianjin 300350, China*

Chiyu Wen − *Department of Biochemical Engineering, Frontier Science Center for Synthetic Biology and Key Laboratory of Systems Bioengineering (MOE), School of Chemical Engineering and Technology, Tianjin University, Tianjin 300350, China*

Jing Yang − *Department of Biochemical Engineering, Frontier Science Center for Synthetic Biology and Key Laboratory of Systems Bioengineering (MOE), School of Chemical Engineering and Technology, Tianjin University, Tianjin 300350, China;* orcid.org/0000-0002-2829-3947

Xianchi Zhou − *MOE Key Laboratory of Macromolecule Synthesis and Functionalization, Department of Polymer Science and Engineering, Zhejiang University, Hangzhou 310027, China*

Yingnan Zhu − *Institute of Drug Discovery and Development, School of Pharmaceutical Sciences, Center for Drug Safety*

https://doi.org/10.1021/acs.chemrev.2c00344
Chem. Rev. 2022, 122, 17073−17154

Evaluation and Research, Zhengzhou University, Zhengzhou 450001, China

Jie Zheng − *Department of Chemical, Biomolecular, and Corrosion Engineering, The University of Akron, Akron, Ohio 44325, United States;* orcid.org/0000-0003-1547-3612

Gang Cheng − *Department of Chemical Engineering, The University of Illinois at Chicago, Chicago, Illinois 60607, United States;* orcid.org/0000-0002-7170-8968

Jie Bai − *College of Chemical Engineering, Inner Mongolia University of Technology, Hohhot, Inner Mongolia 010051, China;* orcid.org/0000-0002-7662-8238

Tong Xu − *College of Chemical Engineering, Inner Mongolia University of Technology, Hohhot, Inner Mongolia 010051, China*

Jian Ji − *MOE Key Laboratory of Macromolecule Synthesis and Functionalization, Department of Polymer Science and Engineering, Zhejiang University, Hangzhou 310027, China;* orcid.org/0000-0001-9870-4038

Complete contact information is available at: https://pubs.acs.org/10.1021/acs.chemrev.2c00344

Author Contributions

○Q.L., C.W., J.Y., and X.Z. contributed equally to this paper.

Notes

The authors declare the following competing financial interest(s): S. Jiang is a co-founder of ZWI Therapeutics, Taproot Medical, and Imperion.

Biographies

Qingsi Li received his M.S. degree in 2017 and his Ph.D. degree in 2021, both from the School of Chemical Engineering and Technology at Tianjin University (China) under the supervision of Prof. Lei Zhang. In 2021 he joined the Lei Zhang team at Tianjin University, where he is currently a research assistant. His scientific interests include the development of zwitterionic materials, porous materials, and encapsulation materials for biomedical applications.

Chiyu Wen received her bachelor's degree (2017) and Ph.D. degree (2022) in biochemical engineering from Tianjin University (China) under the supervision of Prof. Lei Zhang. Her research interests are focused on the fundamental study of zwitterionic materials and their applications in biomedical usage and fresh water production.

Jing Yang received her Ph.D. degree in Biochemical Engineering in 2018 from Tianjin University (China) under the supervision of Prof. Lei Zhang and has serves as an assistant professor for 3 years. In 2021, she became an associate professor in Lei Zhang's lab at Tianjin University. Her research activity is currently focused on biomimetic antifreeze materials applied in cryopreservation, anti-icing coatings, and freezing-tolerant electronic/ionic skins.

Xianchi Zhou received his bachelor's degree in polymer science and engineering from Beijing University of Chemical Technology (BUCT) in 2020. He is currently a Ph.D. candidate under the guidance of Prof. Peng Zhang in the Department of Polymer Science and Engineering, Zhejiang University. His research interests include nonfouling and anti-foreign-body-response biomaterials and their biomedical applications.

Yingnan Zhu received her Ph.D. degree in 2020 from the School of Chemical Engineering and Technology, Tianjin University, under the supervision of Prof. Lei Zhang. In 2020 she joined Zhengzhou University, where she is currently a professor at the Institute of Drug Discovery and Development, School of Pharmaceutical Sciences, Center for Drug Safety Evaluation and Research. Her research interests are mainly focused on antifouling and antimicrobial biomaterials, wound dressing, and cell transplantation.

Jie Zheng is a full professor and chair of Chemical, Biomolecular, and Corrosion Engineering at The University of Akron. He received his B.S. and M.S. degrees in chemical engineering in 1995 and in 1999 from Zhejiang University and his Ph.D. degree in chemical engineering from the University of Washington with Prof. Shaoyi Jiang in 2005. He is a recipient of an NSF Career Award, a 3M Nontenured Faculty Award, and an Anton Award from National Resource for Biomedical Supercomputing. He has published >260 journal papers in biofunctional and biomimetic soft materials for engineering and biomedical applications, with a total citation of >16 900 times and an *h*-index of 67.

Gang Cheng is an associate professor of Chemical Engineering at The University of Illinois at Chicago. Dr. Cheng received his bachelor's degree in biochemical engineering from the Beijing University of Chemical Technology. He completed his master's degree in microbial engineering at the University of Minnesota Twin Cities in 2005. Then he moved to the University of Washington, Seattle, and obtained his doctoral degree in chemical engineering with Prof. Shaoyi Jiang in 2009. In August 2009, Dr. Cheng started his independent academic career as an assistant professor at The University of Akron. In 2016, Dr. Cheng joined the Department of Chemical Engineering at The University of Illinois at Chicago. His research interest is developing novel polymeric materials for biomedical applications, including gene/drug delivery, biosensing, and antimicrobial coatings. In 2015, He received the prestigious NSF Faculty Early Career Award.

Jie Bai is a professor and dean of the Department of Chemical Engineering, Inner Mongolia University. He received his Ph.D. from Jilin University. Since 2008 he has been directing his research group on the design and synthesis of nanosized materials.

Tong Xu is an assistant professor in the Department of Chemical Engineering, Inner Mongolia University. He received his Ph.D. from Tianjin University in 2019 under the direction of Prof. Lei Zhang. His current research interests focus on the superwettability materials applied in biomaterials, catalysis, and water treatment.

Jian Ji received his Ph.D. degree in polymer science from Zhejiang University in 1997. He became a full professor in the Department of Polymer Science and Engineering, Zhejiang University, in 2004. Since 2017, he has served as the director of the Institute of Biomedical Macromolecules at Zhejiang University. He is currently an associate editor for *Journal of Materials Chemistry B*, *Materials Advances*, and *Discover Materials*; an editorial board member for *Biointerphases*, *Research*, and *Journal of Biomaterials Science, Polymer Edition*; an advisory board member for *Biomaterials Science*; a fellow of the Royal Society of Chemistry; and a commission member of the International Union of Materials Research Societies (IUMRS). His research focuses on the interfacial materiobiology of biomedical implants, tissue engineering, and nanomedicine.

Shaoyi Jiang joined the Meinig School of Biomedical Engineering at Cornell University as the Robert S. Langer '70 Family and Friends Professor in June 2020. Before Cornell, he was the Boeing-Roundhill Professor of Engineering in the Department of Chemical Engineering and an adjunct professor of Bioengineering at the University of Washington, Seattle. He received his Ph.D. degree in chemical engineering from Cornell University in 1993. He was a postdoctoral fellow at the University of California, Berkeley, between 1993 and 1994 and a research fellow at the California Institute of Technology between 1994 and 1996, both in chemistry. He is currently an executive editor for *Langmuir*, an associate editor for *Science Advances*,

a fellow of the American Institute of Chemical Engineers (AIChE), and a fellow of the American Institute for Medical and Biological Engineering (AIMBE). He received the Braskem Award for Excellence in Materials Engineering and Science, AIChE (2017). His research focuses on biomaterials, drug delivery, vaccines/immunotherapies, and regenerative/precision medicine, particularly the molecular understanding, design, and development of zwitterionic materials for biomedical and engineering applications.

Lei Zhang is a professor in the Department of Biochemical Engineering, School of Chemical Engineering and Technology, Tianjin University. He received his Ph.D. in chemical engineering from the University of Washington with Prof. Shaoyi Jiang and then worked as a senior fellow in the Department of Bioengineering at the University of Washington. His research interests are synthetic biology, biomaterials, antimicrobial applications, and cryobiology.

Peng Zhang obtained his bachelor's and master's degrees in materials science from Tianjin University with Prof. Wenguang Liu in 2009 and 2012, respectively. In 2018, he received his Ph.D. degree in chemical engineering from the University of Washington, Seattle, under the supervision of Prof. Shaoyi Jiang. From 2018 to 2020, he was a postdoctoral associate in the laboratory of Prof. Daniel Anderson and Prof. Robert Langer at the Koch Institute for Integrative Cancer Research, Massachusetts Institute of Technology. In 2020, he joined the Department of Polymer Science and Engineering at Zhejiang University as a ZJU100 Professor. His research focuses on biomaterials, immunoengineering, biointerfaces, and protein/peptide based therapeutics.

ACKNOWLEDGMENTS

This work was financially supported by the National Key Research and Development Program of China (2020YFE0204400 to P.Z., 2021YFC2100800 to L.Z.), the National Natural Science Foundation of China (22208240 to Q.L., 22175152 to P.Z., 52103188 to P.Z., 21621004 to L.Z., 21961132005 to L.Z., 22078238 to L.Z.), the Joint Funds of the Zhejiang Provincial Natural Science Foundation of China and Huadong Medicine (LHDMZ22H300011 to P.Z.), the Fundamental Research Funds for the Central Universities (226-2022-00146 to P.Z.), and the Open Funding Project of the National Key Laboratory of Biochemical Engineering (to L.Z.). We also acknowledge the start-up support from Cornell University, including the Robert S. Langer Professorship (to S.J), and the Cornell NEXT Nano Initiative (to S.J), and financial support from the Office of Naval Research (N00014-20-1-2731 to S.J), the National Science Foundation (DMR 2002940 and CBET 2103295 to S.J, and 1806138 and 2107619 to J.Z.) and the ACS Petroleum Research Fund (65277-ND7 to J.Z.).

REFERENCES

(1) Zhang, P.; Ratner, B. D.; Hoffman, A. S.; Jiang, S. 1.4.3a - Nonfouling Surfaces. In *Biomaterials Science*, 4th ed.; Academic Press: 2020; pp 507−513.
(2) Flemming, H. C.; Wingender, J.; Szewzyk, U.; Steinberg, P.; Rice, S. A.; Kjelleberg, S. Biofilms: An Emergent Form of Bacterial Life. *Nat. Rev. Microbiol.* **2016**, *14*, 563−575.
(3) Arciola, C. R.; Campoccia, D.; Montanaro, L. Implant Infections: Adhesion, Biofilm Formation and Immune Evasion. *Nat. Rev. Microbiol.* **2018**, *16*, 397−409.
(4) Frutiger, A.; Tanno, A.; Hwu, S.; Tiefenauer, R. F.; Vörös, J.; Nakatsuka, N. Nonspecific Binding—Fundamental Concepts and Consequences for Biosensing Applications. *Chem. Rev.* **2021**, *121*, 8095−8160.
(5) Cai, R.; Chen, C. The Crown and the Scepter: Roles of the Protein Corona in Nanomedicine. *Adv. Mater.* **2019**, *31*, 1805740.
(6) Rosenblum, D.; Joshi, N.; Tao, W.; Karp, J. M.; Peer, D. Progress and Challenges towards Targeted Delivery of Cancer Therapeutics. *Nat. Commun.* **2018**, *9*, 1410.
(7) Wilhelm, S.; Tavares, A. J.; Dai, Q.; Ohta, S.; Audet, J.; Dvorak, H. F.; Chan, W. C. W. Analysis of Nanoparticle Delivery to Tumours. *Nat. Rev. Mater.* **2016**, *1*, 16014.
(8) Zhang, L.; Cao, Z. Q.; Bai, T.; Carr, L.; Ella-Menye, J. R.; Irvin, C.; Ratner, B. D.; Jiang, S. Zwitterionic Hydrogels Implanted in Mice Resist the Foreign-Body Reaction. *Nat. Biotechnol.* **2013**, *31*, 553−556.
(9) Tsai, W.-B.; Grunkemeier, J. M.; Horbett, T. A. Human Plasma Fibrinogen Adsorption and Platelet Adhesion to Polystyrene. *J. Biomed. Mater. Res.* **1999**, *44*, 130−139.
(10) Chen, S.; Zheng, J.; Li, L.; Jiang, S. Strong Resistance of Phosphorylcholine Self-Assembled Monolayers to Protein Adsorption: Insights into Nonfouling Properties of Zwitterionic Materials. *J. Am. Chem. Soc.* **2005**, *127*, 14473−14478.
(11) Chen, S.; Yu, F.; Yu, Q.; He, Y.; Jiang, S. Strong Resistance of a Thin Crystalline Layer of Balanced Charged Groups to Protein Adsorption. *Langmuir* **2006**, *22*, 8186−8191.
(12) Lynn, A. D.; Kyriakides, T. R.; Bryant, S. J. Characterization of the in Vitro Macrophage Response and in Vivo Host Response to Poly(Ethylene Glycol)-Based Hydrogels. *J. Biomed. Mater. Res.* **2010**, *93A*, 941−953.
(13) Kane, R. S.; Deschatelets, P.; Whitesides, G. M. Kosmotropes Form the Basis of Protein-Resistant Surfaces. *Langmuir* **2003**, *19*, 2388−2391.
(14) Zhang, P.; Sun, F.; Liu, S. J.; Jiang, S. Y. Anti-PEG Antibodies in the Clinic: Current Issues and Beyond PEGylation. *J. Controlled Release* **2016**, *244*, 184−193.
(15) Shao, Q.; Jiang, S. Y. Molecular Understanding and Design of Zwitterionic Materials. *Adv. Mater.* **2015**, *27*, 15−26.
(16) Keefe, A. J.; Jiang, S. Poly(zwitterionic)protein Conjugates Offer Increased Stability without Sacrificing Binding Affinity or Bioactivity. *Nat. Chem.* **2012**, *4*, 59−63.
(17) Cao, B.; Tang, Q.; Cheng, G. Recent Advances of Zwitterionic Carboxybetaine Materials and Their Derivatives. *J. Biomater. Sci., Polym. Ed.* **2014**, *25*, 1502−1513.
(18) Zhang, Z.; Chao, T.; Chen, S.; Jiang, S. Superlow Fouling Sulfobetaine and Carboxybetaine Polymers on Glass Slides. *Langmuir* **2006**, *22*, 10072−10077.
(19) Zhang, J. M.; Zhu, Y. N.; Song, J. Y.; Xu, T.; Yang, J.; Du, Y.; Zhang, L. Rapid and Long-Term Glycemic Regulation with a Balanced Charged Immune-Evasive Hydrogel in T1dm Mice. *Adv. Funct. Mater.* **2019**, *29*, 1900140.
(20) Shi, Q.; Su, Y.; Chen, W.; Peng, J.; Nie, L.; Zhang, L.; Jiang, Z. Grafting Short-Chain Amino Acids onto Membrane Surfaces to Resist Protein Fouling. *J. Membr. Sci.* **2011**, *366*, 398−404.
(21) Blackman, L. D.; Gunatillake, P. A.; Cass, P.; Locock, K. E. S. An Introduction to Zwitterionic Polymer Behavior and Applications in Solution and at Surfaces. *Chem. Soc. Rev.* **2019**, *48*, 757−770.
(22) Smith, R. S.; Zhang, Z.; Bouchard, M.; Li, J.; Lapp, H. S.; Brotske, G. R.; Lucchino, D. L.; Weaver, D.; Roth, L. A.; Coury, A.; et al. Vascular Catheters with a Nonleaching Poly-Sulfobetaine Surface Modification Reduce Thrombus Formation and Microbial Attachment. *Sci. Transl. Med.* **2012**, *4*, 153ra132.
(23) Yang, W.; Bai, T.; Carr, L. R.; Keefe, A. J.; Xu, J.; Xue, H.; Irvin, C. A.; Chen, S.; Wang, J.; Jiang, S. The Effect of Lightly Crosslinked Poly(Carboxybetaine) Hydrogel Coating on the Performance of Sensors in Whole Blood. *Biomaterials* **2012**, *33*, 7945−7951.
(24) Zhu, Y. N.; Zhang, J. M.; Song, J. Y.; Yang, J.; Du, Z.; Zhao, W. Q.; Guo, H. S.; Wen, C. Y.; Li, Q. S.; Sui, X. J.; et al. A Multifunctional Pro-Healing Zwitterionic Hydrogel for Simultaneous Optical Monitoring of pH and Glucose in Diabetic Wound Treatment. *Adv. Funct. Mater.* **2020**, *30*, 1905493.
(25) Sinclair, A.; O'Kelly, M. B.; Bai, T.; Hung, H.-C.; Jain, P.; Jiang, S. Self-Healing Zwitterionic Microgels as a Versatile Platform for

https://doi.org/10.1021/acs.chemrev.2c00344
Chem. Rev. 2022, 122, 17073−17154

Malleable Cell Constructs and Injectable Therapies. *Adv. Mater.* **2018**, *30*, 1803087.
(26) Li, B.; Xie, J.; Yuan, Z.; Jain, P.; Lin, X.; Wu, K.; Jiang, S. Mitigation of Inflammatory Immune Responses with Hydrophilic Nanoparticles. *Angew. Chem., Int. Ed.* **2018**, *57*, 4527−4531.
(27) Han, Y.; Yuan, Z.; Zhang, P.; Jiang, S. Zwitterlation Mitigates Protein Bioactivity Loss in Vitro over PEGylation. *Chem. Sci.* **2018**, *9*, 8561−8566.
(28) Zhang, P.; Sun, F.; Tsao, C.; Liu, S.; Jain, P.; Sinclair, A.; Hung, H.-C.; Bai, T.; Wu, K.; Jiang, S. Zwitterionic Gel Encapsulation Promotes Protein Stability, Enhances Pharmacokinetics, and Reduces Immunogenicity. *Proc. Natl. Acad. Sci. U. S. A.* **2015**, *112*, 12046−12051.
(29) Yuan, Z.; Li, B.; Niu, L.; Tang, C.; McMullen, P.; Jain, P.; He, Y.; Jiang, S. Zwitterionic Peptide Cloak Mimics Protein Surfaces for Protein Protection. *Angew. Chem., Int. Ed.* **2020**, *59*, 22378−22381.
(30) Chen, S.; Li, L.; Zhao, C.; Zheng, J. Surface Hydration: Principles and Applications toward Low-Fouling/Nonfouling Biomaterials. *Polymer* **2010**, *51*, 5283−5293.
(31) Jiang, S. Y.; Cao, Z. Q. Ultralow-Fouling, Functionalizable, and Hydrolyzable Zwitterionic Materials and Their Derivatives for Biological Applications. *Adv. Mater.* **2010**, *22*, 920−932.
(32) Erfani, A.; Seaberg, J.; Aichele, C. P.; Ramsey, J. D. Interactions between Biomolecules and Zwitterionic Moieties: A Review. *Biomacromolecules* **2020**, *21*, 2557−2573.
(33) Li, Q.; Yang, J.; Cai, N. N.; Zhang, J. R. N.; Xu, T.; Zhao, W. A.; Guo, H. S.; Zhu, Y. N.; Zhang, L. Hemocompatible Hemoadsorbent for Effective Removal of Protein-Bound Toxin in Serum. *J. Colloid Interface Sci.* **2019**, *555*, 145−156.
(34) Salvati, A.; Pitek, A. S.; Monopoli, M. P.; Prapainop, K.; Bombelli, F. B.; Hristov, D. R.; Kelly, P. M.; Åberg, C.; Mahon, E.; Dawson, K. A. Transferrin-Functionalized Nanoparticles Lose Their Targeting Capabilities When a Biomolecule Corona Adsorbs on the Surface. *Nat. Nanotechnol.* **2013**, *8*, 137−143.
(35) Mahmoudi, M.; Bertrand, N.; Zope, H.; Farokhzad, O. C. Emerging Understanding of the Protein Corona at the Nano-Bio Interfaces. *Nano Today* **2016**, *11*, 817−832.
(36) Mollahosseini, A.; Abdelrasoul, A.; Shoker, A. Latest Advances in Zwitterionic Structures Modified Dialysis Membranes. *Mater. Today Chem.* **2020**, *15*, 100227.
(37) Lejars, M.; Margaillan, A.; Bressy, C. Fouling Release Coatings: A Nontoxic Alternative to Biocidal Antifouling Coatings. *Chem. Rev.* **2012**, *112*, 4347−4390.
(38) Arnebrant, T.; Wahlgren, M. C. Protein Surfactant Interactions at Solid Surfaces. In *Proteins at Interfaces II: Fundamentals and Applications*; Horbett, T. A., Brash, J. L., Eds.; ACS Symposium Series 602; American Chemical Society: 1995; pp 239−254..
(39) Agashe, M.; Raut, V.; Stuart, S. J.; Latour, R. A. Molecular Simulation to Characterize the Adsorption Behavior of a Fibrinogen Gamma-Chain Fragment. *Langmuir* **2005**, *21*, 1103−1117.
(40) Horbett, T. A.; Latour, R. A. 2.1.2 - Adsorbed Proteins on Biomaterials. In *Biomaterials Science*, 4th ed.; Academic Press: 2020; 645−660.
(41) Wei, Q.; Becherer, T.; Angioletti-Uberti, S.; Dzubiella, J.; Wischke, C.; Neffe, A. T.; Lendlein, A.; Ballauff, M.; Haag, R. Protein Interactions with Polymer Coatings and Biomaterials. *Angew. Chem., Int. Ed.* **2014**, *53*, 8004−8031.
(42) Jeyachandran, Y. L.; Mielczarski, E.; Rai, B.; Mielczarski, J. A. Quantitative and Qualitative Evaluation of Adsorption/Desorption of Bovine Serum Albumin on Hydrophilic and Hydrophobic Surfaces. *Langmuir* **2009**, *25*, 11614−11620.
(43) Hoffman, A. S. Non-Fouling Surface Technologies. *J. Biomater. Sci., Polym. Ed.* **1999**, *10*, 1011−1014.
(44) Horbett, T. A. Principles Underlying the Role of Adsorbed Plasma Proteins in Blood Interactions with Foreign Materials. *Cardiovasc. Pathol.* **1993**, *2*, 137−148.
(45) Latour, R. A. The Langmuir Isotherm: A Commonly Applied but Misleading Approach for the Analysis of Protein Adsorption Behavior. *J. Biomed. Mater. Res. Part A* **2015**, *103*, 949−958.
(46) Ladd, J.; Zhang, Z.; Chen, S.; Hower, J. C.; Jiang, S. Zwitterionic Polymers Exhibiting High Resistance to Nonspecific Protein Adsorption from Human Serum and Plasma. *Biomacromolecules* **2008**, *9*, 1357−1361.
(47) Quan, X. B.; Liu, J.; Zhou, J. Multiscale Modeling and Simulations of Protein Adsorption: Progresses and Perspectives. *Curr. Opin. Colloid Interface Sci.* **2019**, *41*, 74−85.
(48) Sivaraman, B.; Latour, R. A. The Relationship between Platelet Adhesion on Surfaces and the Structure Versus the Amount of Adsorbed Fibrinogen. *Biomaterials* **2010**, *31*, 832−839.
(49) Ostuni, E.; Chapman, R. G.; Holmlin, R. E.; Takayama, S.; Whitesides, G. M. A Survey of Structure-Property Relationships of Surfaces That Resist the Adsorption of Protein. *Langmuir* **2001**, *17*, 5605−5620.
(50) Choi, W.; Park, S.; Kwon, J.-S.; Jang, E.-Y.; Kim, J.-Y.; Heo, J.; Hwang, Y.; Kim, B.-S.; Moon, J.-H.; Jung, S.; et al. Reverse Actuation of Polyelectrolyte Effect for in Vivo Antifouling. *ACS Nano* **2021**, *15*, 6811−6828.
(51) Azzaroni, O.; Brown, A. A.; Huck, W. T. S. UCST Wetting Transitions of Polyzwitterionic Brushes Driven by Self-Association. *Angew. Chem., Int. Ed.* **2006**, *45*, 1770−1774.
(52) Morisaku, T.; Watanabe, J.; Konno, T.; Takai, M.; Ishihara, K. Hydration of Phosphorylcholine Groups Attached to Highly Swollen Polymer Hydrogels Studied by Thermal Analysis. *Polymer* **2008**, *49*, 4652−4657.
(53) Mukai, M.; Ihara, D.; Chu, C.-W.; Cheng, C.-H.; Takahara, A. Synthesis and Hydration Behavior of a Hydrolysis-Resistant Quasi-Choline Phosphate Zwitterionic Polymer. *Biomacromolecules* **2020**, *21*, 2125−2131.
(54) Tada, S.; Inaba, C.; Mizukami, K.; Fujishita, S.; Gemmei-Ide, M.; Kitano, H.; Mochizuki, A.; Tanaka, M.; Matsunaga, T. Anti-Biofouling Properties of Polymers with a Carboxybetaine Moiety. *Macromol. Biosci.* **2009**, *9*, 63−70.
(55) Kitano, H.; Mori, T.; Takeuchi, Y.; Tada, S.; Gemmei-Ide, M.; Yokoyama, Y.; Tanaka, M. Structure of Water Incorporated in Sulfobetaine Polymer Films as Studied by ATR-FTIR. *Macromol. Biosci.* **2005**, *5*, 314−321.
(56) Kitano, H.; Nagaoka, K.; Tada, S.; Gemmei-Ide, M.; Tanaka, M. Structure of Water Incorporated in Amphoteric Polymer Thin Films as Revealed by FT-IR Spectroscopy. *Macromol. Biosci.* **2008**, *8*, 77−85.
(57) Leng, C.; Sun, S.; Zhang, K.; Jiang, S.; Chen, Z. Molecular Level Studies on Interfacial Hydration of Zwitterionic and Other Antifouling Polymers in Situ. *Acta Biomater.* **2016**, *40*, 6−15.
(58) Kitano, H.; Sudo, K.; Ichikawa, K.; Ide, M.; Ishihara, K. Raman Spectroscopic Study on the Structure of Water in Aqueous Polyelectrolyte Solutions. *J. Phys. Chem. B* **2000**, *104*, 11425−11429.
(59) Kitano, H.; Imai, M.; Sudo, K.; Ide, M. Hydrogen-Bonded Network Structure of Water in Aqueous Solution of Sulfobetaine Polymers. *J. Phys. Chem. B* **2002**, *106*, 11391−11396.
(60) Kitano, H.; Imai, M.; Mori, T.; Gemmei-Ide, M.; Yokoyama, Y.; Ishihara, K. Structure of Water in the Vicinity of Phospholipid Analogue Copolymers as Studied by Vibrational Spectroscopy. *Langmuir* **2003**, *19*, 10260−10266.
(61) Kitano, H.; Tada, S.; Mori, T.; Takaha, K.; Gemmei-Ide, M.; Tanaka, M.; Fukuda, M.; Yokoyama, Y. Correlation between the Structure of Water in the Vicinity of Carboxybetaine Polymers and Their Blood-Compatibility. *Langmuir* **2005**, *21*, 11932−11940.
(62) Leng, C.; Hung, H.-C.; Sieggreen, O. A.; Li, Y.; Jiang, S.; Chen, Z. Probing the Surface Hydration of Nonfouling Zwitterionic and Poly(Ethylene Glycol) Materials with Isotopic Dilution Spectroscopy. *J. Phys. Chem. C* **2015**, *119*, 8775−8780.
(63) Leng, C.; Hung, H.-C.; Sun, S.; Wang, D.; Li, Y.; Jiang, S.; Chen, Z. Probing the Surface Hydration of Nonfouling Zwitterionic and PEG Materials in Contact with Proteins. *ACS Appl. Mater. Interfaces* **2015**, *7*, 16881−16888.
(64) Zhang, Y.; Liu, Y.; Ren, B.; Zhang, D.; Xie, S.; Chang, Y.; Yang, J.; Wu, J.; Xu, L.; Zheng, J. Fundamentals and Applications of

https://doi.org/10.1021/acs.chemrev.2c00344
Chem. Rev. 2022, 122, 17073−17154

Zwitterionic Antifouling Polymers. *J. Phys. D: Appl. Phys.* **2019**, *52*, 403001.
(65) Shao, Q.; He, Y.; White, A. D.; Jiang, S. Difference in Hydration between Carboxybetaine and Sulfobetaine. *J. Phys. Chem. B* **2010**, *114*, 16625−16631.
(66) Shao, Q.; He, Y.; Jiang, S. Molecular Dynamics Simulation Study of Ion Interactions with Zwitterions. *J. Phys. Chem. B* **2011**, *115*, 8358−8363.
(67) Shao, Q.; Jiang, S. Influence of Charged Groups on the Properties of Zwitterionic Moieties: A Molecular Simulation Study. *J. Phys. Chem. B* **2014**, *118*, 7630−7637.
(68) Shao, Q.; He, Y.; White, A. D.; Jiang, S. Different Effects of Zwitterion and Ethylene Glycol on Proteins. *J. Chem. Phys.* **2012**, *136*, 225101.
(69) Du, H.; Qian, X. The Hydration Properties of Carboxybetaine Zwitterion Brushes. *J. Comput. Chem.* **2016**, *37*, 877−885.
(70) Zheng, J.; He, Y.; Chen, S.; Li, L.; Bernards, M. T.; Jiang, S. Molecular Simulation Studies of the Structure of Phosphorylcholine Self-Assembled Monolayers. *J. Chem. Phys.* **2006**, *125*, 174714.
(71) Nagumo, R.; Ito, T.; Akamatsu, K.; Miura, R.; Suzuki, A.; Tsuboi, H.; Hatakeyama, N.; Takaba, H.; Miyamoto, A. Molecular Dynamics Simulations for Microscopic Behavior of Water Molecules in the Vicinity of Zwitterionic Self-Assembled Monolayers. *Polym. J.* **2012**, *44*, 1149−1153.
(72) Cheung, D. L.; Lau, K. H. A. Atomistic Study of Zwitterionic Peptoid Antifouling Brushes. *Langmuir* **2019**, *35*, 1483−1494.
(73) Penna, M.; Ley, K. J.; Belessiotis-Richards, A.; MacLaughlin, S.; Winkler, D. A.; Yarovsky, I. Hydration and Dynamics of Ligands Determine the Antifouling Capacity of Functionalized Surfaces. *J. Phys. Chem. C* **2019**, *123*, 30360−30372.
(74) Unsworth, L. D.; Sheardown, H.; Brash, J. L. Protein-Resistant Poly(Ethylene Oxide)-Grafted Surfaces: Chain Density-Dependent Multiple Mechanisms of Action. *Langmuir* **2008**, *24*, 1924−1929.
(75) Abraham, S.; So, A.; Unsworth, L. D. Poly(Carboxybetaine Methacrylamide)-Modified Nanoparticles: A Model System for Studying the Effect of Chain Chemistry on Film Properties, Adsorbed Protein Conformation, and Clot Formation Kinetics. *Biomacromolecules* **2011**, *12*, 3567−3580.
(76) He, Y.; Hower, J.; Chen, S.; Bernards, M. T.; Chang, Y.; Jiang, S. Molecular Simulation Studies of Protein Interactions with Zwitterionic Phosphorylcholine Self-Assembled Monolayers in the Presence of Water. *Langmuir* **2008**, *24*, 10358−10364.
(77) Liu, Z.-Y.; Jiang, Q.; Jin, Z.; Sun, Z.; Ma, W.; Wang, Y. Understanding the Antifouling Mechanism of Zwitterionic Monomer-Grafted Polyvinylidene Difluoride Membranes: A Comparative Experimental and Molecular Dynamics Simulation Study. *ACS Appl. Mater. Interfaces* **2019**, *11*, 14408−14417.
(78) Xiang, Y.; Xu, R.-G.; Leng, Y. Molecular Simulations of the Hydration Behavior of a Zwitterion Brush Array and Its Antifouling Property in an Aqueous Environment. *Langmuir* **2018**, *34*, 2245−2257.
(79) Nagumo, R.; Akamatsu, K.; Miura, R.; Suzuki, A.; Tsuboi, H.; Hatakeyama, N.; Takaba, H.; Miyamoto, A. Assessment of the Antifouling Properties of Polyzwitterions from Free Energy Calculations by Molecular Dynamics Simulations. *Ind. Eng. Chem. Res.* **2012**, *51*, 4458−4462.
(80) Liu, Y.; Zhang, D.; Ren, B.; Gong, X.; Xu, L.; Feng, Z.-Q.; Chang, Y.; He, Y.; Zheng, J. Molecular Simulations and Understanding of Antifouling Zwitterionic Polymer Brushes. *J. Mater. Chem. B* **2020**, *8*, 3814−3828.
(81) Xiang, Y.; Xu, R.-G.; Leng, Y. Molecular Dynamics Simulations of a Poly(Ethylene Glycol)-Grafted Polyamide Membrane and Its Interaction with a Calcium Alginate Gel. *Langmuir* **2016**, *32*, 4424−4433.
(82) Ekins, S.; Puhl, A. C.; Zorn, K. M.; Lane, T. R.; Russo, D. P.; Klein, J. J.; Hickey, A. J.; Clark, A. M. Exploiting Machine Learning for End-to-End Drug Discovery and Development. *Nat. Mater.* **2019**, *18*, 435−441.
(83) Vamathevan, J.; Clark, D.; Czodrowski, P.; Dunham, I.; Ferran, E.; Lee, G.; Li, B.; Madabhushi, A.; Shah, P.; Spitzer, M.; et al. Applications of Machine Learning in Drug Discovery and Development. *Nat. Rev. Drug Discovery* **2019**, *18*, 463−477.
(84) Kavakiotis, I.; Tsave, O.; Salifoglou, A.; Maglaveras, N.; Vlahavas, I.; Chouvarda, I. Machine Learning and Data Mining Methods in Diabetes Research. *Comput. Struct. Biotechnol. J.* **2017**, *15*, 104−116.
(85) Sendek, A. D.; Cheon, G.; Pasta, M.; Reed, E. J. Quantifying the Search for Solid Li-Ion Electrolyte Materials by Anion: A Data-Driven Perspective. *J. Phys. Chem. C* **2020**, *124*, 8067−8079.
(86) Fujimura, K.; Seko, A.; Koyama, Y.; Kuwabara, A.; Kishida, I.; Shitara, K.; Fisher, C. A. J.; Moriwake, H.; Tanaka, I. Accelerated Materials Design of Lithium Superionic Conductors Based on First-Principles Calculations and Machine Learning Algorithms. *Adv. Energy Mater.* **2013**, *3*, 980−985.
(87) Kitchin, J. R. Machine Learning in Catalysis. *Nat. Catal.* **2018**, *1*, 230−232.
(88) Sun, B.; Fernandez, M.; Barnard, A. S. Machine Learning for Silver Nanoparticle Electron Transfer Property Prediction. *J. Chem. Inf. Model.* **2017**, *57*, 2413−2423.
(89) Kunkel, C.; Schober, C.; Margraf, J. T.; Reuter, K.; Oberhofer, H. Finding the Right Bricks for Molecular Legos: A Data Mining Approach to Organic Semiconductor Design. *Chem. Mater.* **2019**, *31*, 969−978.
(90) Khakifirooz, M.; Chien, C. F.; Chen, Y.-J. Bayesian Inference for Mining Semiconductor Manufacturing Big Data for Yield Enhancement and Smart Production to Empower Industry 4.0. *Appl. Soft Comput.* **2018**, *68*, 990−999.
(91) Muratov, E. N.; Bajorath, J.; Sheridan, R. P.; Tetko, I. V.; Filimonov, D.; Poroikov, V.; Oprea, T. I.; Baskin, I. I.; Varnek, A.; Roitberg, A.; et al. Qsar without Borders. *Chem. Soc. Rev.* **2020**, *49*, 3525−3564.
(92) Almeida, J. R.; Moreira, J.; Pereira, D.; Pereira, S.; Antunes, J.; Palmeira, A.; Vasconcelos, V.; Pinto, M.; Correia-da-Silva, M.; Cidade, H. Potential of Synthetic Chalcone Derivatives to Prevent Marine Biofouling. *Sci. Total Environ.* **2018**, *643*, 98−106.
(93) Feng, K.; Li, X.; Yu, L. Synthesis, Antibacterial Activity, and Application in the Antifouling Marine Coatings of Novel Acylamino Compounds Containing Gramine Groups. *Prog. Org. Coat.* **2018**, *118*, 141−147.
(94) Rasulev, B.; Jabeen, F.; Stafslien, S.; Chisholm, B. J.; Bahr, J.; Ossowski, M.; Boudjouk, P. Polymer Coating Materials and Their Fouling Release Activity: A Cheminformatics Approach to Predict Properties. *ACS Appl. Mater. Interfaces* **2017**, *9*, 1781−1792.
(95) Le, T. C.; Penna, M.; Winkler, D. A.; Yarovsky, I. Quantitative Design Rules for Protein-Resistant Surface Coatings Using Machine Learning. *Sci. Rep.* **2019**, *9*, 265.
(96) Kwaria, R. J.; Mondarte, E. A. Q.; Tahara, H.; Chang, R.; Hayashi, T. Data-Driven Prediction of Protein Adsorption on Self-Assembled Monolayers toward Material Screening and Design. *ACS Biomater. Sci. Eng.* **2020**, *6*, 4949−4956.
(97) Liu, Y.; Zhang, D.; Tang, Y.; Zhang, Y.; Chang, Y.; Zheng, J. Machine Learning-Enabled Design and Prediction of Protein Resistance on Self-Assembled Monolayers and Beyond. *ACS Appl. Mater. Interfaces* **2021**, *13*, 11306−11319.
(98) Liu, Y.; Zhang, D.; Tang, Y.; Zhang, Y.; Gong, X.; Xie, S.; Zheng, J. Machine Learning-Enabled Repurposing and Design of Antifouling Polymer Brushes. *Chem. Eng. J.* **2021**, *420*, 129872.
(99) Morriss-Andrews, A.; Shea, J.-E. Simulations of Protein Aggregation: Insights from Atomistic and Coarse-Grained Models. *J. Phys. Chem. Lett.* **2014**, *5*, 1899−1908.
(100) Derreumaux, P.; Mousseau, N. Coarse-Grained Protein Molecular Dynamics Simulations. *J. Chem. Phys.* **2007**, *126*, 025101.
(101) Sterpone, F.; Melchionna, S.; Tuffery, P.; Pasquali, S.; Mousseau, N.; Cragnolini, T.; Chebaro, Y.; St-Pierre, J.-F.; Kalimeri, M.; Barducci, A.; et al. The OPEP Protein Model: From Single Molecules, Amyloid Formation, Crowding and Hydrodynamics to DNA/RNA Systems. *Chem. Soc. Rev.* **2014**, *43*, 4871−4893.

(102) Monticelli, L.; Kandasamy, S. K.; Periole, X.; Larson, R. G.; Tieleman, D. P.; Marrink, S.-J. The Martini Coarse-Grained Force Field: Extension to Proteins. *J. Chem. Theory Comput.* **2008**, *4*, 819−834.
(103) Mrksich, M.; Sigal, G. B.; Whitesides, G. M. Surface Plasmon Resonance Permits in Situ Measurement of Protein Adsorption on Self-Assembled Monolayers of Alkanethiolates on Gold. *Langmuir* **1995**, *11*, 4383−4385.
(104) Holmlin, R. E.; Chen, X. X.; Chapman, R. G.; Takayama, S.; Whitesides, G. M. Zwitterionic SAMs That Resist Nonspecific Adsorption of Protein from Aqueous Buffer. *Langmuir* **2001**, *17*, 2841−2850.
(105) Chang Chung, Y.; Hong Chiu, Y.; Wei Wu, Y.; Tai Tao, Y. Self-Assembled Biomimetic Monolayers Using Phospholipid-Containing Disulfides. *Biomaterials* **2005**, *26*, 2313−2324.
(106) Tegoulia, V. A.; Rao, W.; Kalambur, A. T.; Rabolt, J. F.; Cooper, S. L. Surface Properties, Fibrinogen Adsorption, and Cellular Interactions of a Novel Phosphorylcholine-Containing Self-Assembled Monolayer on Gold. *Langmuir* **2001**, *17*, 4396−4404.
(107) Garcia, K. P.; Zarschler, K.; Barbaro, L.; Barreto, J. A.; O'Malley, W.; Spiccia, L.; Stephan, H.; Graham, B. Zwitterionic-Coated "Stealth" Nanoparticles for Biomedical Applications: Recent Advances in Countering Biomolecular Corona Formation and Uptake by the Mononuclear Phagocyte System. *Small* **2014**, *10*, 2516−2529.
(108) Zhan, N.; Palui, G.; Mattoussi, H. Preparation of Compact Biocompatible Quantum Dots Using Multicoordinating Molecular-Scale Ligands Based on a Zwitterionic Hydrophilic Motif and Lipoic Acid Anchors. *Nat. Protoc.* **2015**, *10*, 859−874.
(109) Liu, W.; Choi, H. S.; Zimmer, J. P.; Tanaka, E.; Frangioni, J. V.; Bawendi, M. Compact Cysteine-Coated Cdse(Zncds) Quantum Dots for in Vivo Applications. *J. Am. Chem. Soc.* **2007**, *129*, 14530−14531.
(110) Murthy, A. K.; Stover, R. J.; Hardin, W. G.; Schramm, R.; Nie, G. D.; Gourisankar, S.; Truskett, T. M.; Sokolov, K. V.; Johnston, K. P. Charged Gold Nanoparticles with Essentially Zero Serum Protein Adsorption in Undiluted Fetal Bovine Serum. *J. Am. Chem. Soc.* **2013**, *135*, 7799−7802.
(111) Soo Choi, H.; Liu, W.; Misra, P.; Tanaka, E.; Zimmer, J. P.; Itty Ipe, B.; Bawendi, M. G.; Frangioni, J. V. Renal Clearance of Quantum Dots. *Nat. Biotechnol.* **2007**, *25*, 1165−1170.
(112) Choi, H. S.; Ashitate, Y.; Lee, J. H.; Kim, S. H.; Matsui, A.; Insin, N.; Bawendi, M. G.; Semmler-Behnke, M.; Frangioni, J. V.; Tsuda, A. Rapid Translocation of Nanoparticles from the Lung Airspaces to the Body. *Nat. Biotechnol.* **2010**, *28*, 1300−1303.
(113) Ostuni, E.; Chapman, R. G.; Liang, M. N.; Meluleni, G.; Pier, G.; Ingber, D. E.; Whitesides, G. M. Self-Assembled Monolayers That Resist the Adsorption of Proteins and the Adhesion of Bacterial and Mammalian Cells. *Langmuir* **2001**, *17*, 6336−6343.
(114) Zhang, Z.; Zhang, M.; Chen, S.; Horbett, T. A.; Ratner, B. D.; Jiang, S. Blood Compatibility of Surfaces with Superlow Protein Adsorption. *Biomaterials* **2008**, *29*, 4285−4291.
(115) Cheng, G.; Zhang, Z.; Chen, S.; Bryers, J. D.; Jiang, S. Inhibition of Bacterial Adhesion and Biofilm Formation on Zwitterionic Surfaces. *Biomaterials* **2007**, *28*, 4192−4199.
(116) Yang, J.; Cai, N.; Zhai, H.; Zhang, J.; Zhu, Y.; Zhang, L. Natural Zwitterionic Betaine Enables Cells to Survive Ultrarapid Cryopreservation. *Sci. Rep.* **2016**, *6*, 37458.
(117) Yang, J.; Pan, C.; Zhang, J.; Sui, X.; Zhu, Y.; Wen, C.; Zhang, L. Exploring the Potential of Biocompatible Osmoprotectants as Highly Efficient Cryoprotectants. *ACS Appl. Mater. Interfaces* **2017**, *9*, 42516−42524.
(118) Zhai, H.; Yang, J.; Zhang, J.; Pan, C.; Cai, N.; Zhu, Y.; Zhang, L. Natural Zwitterionic L-Carnitine as Efficient Cryoprotectant for Solvent-Free Cell Cryopreservation. *Biochem. Biophys. Res. Commun.* **2017**, *489*, 76−82.
(119) Ma, M.-Q.; Zhang, C.; Chen, T.-T.; Yang, J.; Wang, J.-J.; Ji, J.; Xu, Z.-K. Bioinspired Polydopamine/Polyzwitterion Coatings for Underwater Anti-Oil and -Freezing Surfaces. *Langmuir* **2019**, *35*, 1895−1901.
(120) Yang, J.; Sui, X.; Li, Q.; Zhao, W.; Zhang, J.; Zhu, Y.; Chen, P.; Zhang, L. In Situ Encapsulation of Postcryopreserved Cells Using Alginate Polymer and Zwitterionic Betaine. *ACS Biomater. Sci. Eng.* **2019**, *5*, 2621−2630.
(121) Yang, J.; Xu, Z.; Wang, J.; Gai, L.; Ji, X.; Jiang, H.; Liu, L. Antifreezing Zwitterionic Hydrogel Electrolyte with High Conductivity of 12.6 mS cm^{-1} at −40 °C through Hydrated Lithium Ion Hopping Migration. *Adv. Funct. Mater.* **2021**, *31*, 2009438.
(122) Zhang, D.; Liu, Y.; Liu, Y.; Peng, Y.; Tang, Y.; Xiong, L.; Gong, X.; Zheng, J. A General Crosslinker Strategy to Realize Intrinsic Frozen Resistance of Hydrogels. *Adv. Mater.* **2021**, *33*, 2104006.
(123) Sastry, S. Ins and Outs of Ice Nucleation. *Nature* **2005**, *438*, 746−747.
(124) Yang, J.; Sui, X.; Wen, C.; Pan, C.; Zhu, Y.; Zhang, J.; Zhang, L. A Hemocompatible Cryoprotectant Inspired by Freezing-Tolerant Plants. *Colloids Surf., B* **2019**, *176*, 106−114.
(125) Yang, J.; Liu, M.; Zhang, T.; Ma, J.; Ma, Y.; Tian, S.; Li, R.; Han, Y.; Zhang, L. Cell-Friendly Regulation of Ice Crystals by Antifreeze Organism-Inspired Materials. *AlChE J.* **2022**, *68*, No. e17822.
(126) Liu, M.; Zhang, X.; Guo, H.; Zhu, Y.; Wen, C.; Sui, X.; Yang, J.; Zhang, L. Dimethyl Sulfoxide-Free Cryopreservation of Chondrocytes Based on Zwitterionic Molecule and Polymers. *Biomacromolecules* **2019**, *20*, 3980−3988.
(127) Kadoma, Y.; Nakabayashi, N.; Masuhara, E.; Yamauchi, J. Synthesis and Hemolysis Test of Polymer Containing Phosphorylcholine Groups. *Kobunshi Ronbunshu* **1978**, *35*, 423−427.
(128) Umeda, T.; Nakaya, T.; Imoto, M. Polymeric Phospholipid Analogues, 14. The Convenient Preparation of a Vinyl Monomer Containing a Phospholipid Analogue. *Makromol. Chem., Rapid Commun.* **1982**, *3*, 457−459.
(129) Ishihara, K.; Ueda, T.; Nakabayashi, N. Preparation of Phospholipid Polymers and Their Properties as Polymer Hydrogel Membranes. *Polym. J.* **1990**, *22*, 355−360.
(130) Iwasaki, Y.; Ishihara, K. Cell Membrane-Inspired Phospholipid Polymers for Developing Medical Devices with Excellent Biointerfaces. *Sci. Technol. Adv. Mater.* **2012**, *13*, 064101.
(131) Ishihara, K.; Ziats, N. P.; Tierney, B. P.; Nakabayashi, N.; Anderson, J. M. Protein Adsorption from Human Plasma Is Reduced on Phospholipid Polymers. *J. Biomed. Mater. Res.* **1991**, *25*, 1397−1407.
(132) Ishihara, K.; Oshida, H.; Endo, Y.; Ueda, T.; Watanabe, A.; Nakabayashi, N. Hemocompatibility of Human Whole Blood on Polymers with a Phospholipid Polar Group and Its Mechanism. *J. Biomed. Mater. Res.* **1992**, *26*, 1543−1552.
(133) Ishihara, K.; Tsuji, T.; Kurosaki, T.; Nakabayashi, N. Hemocompatibility on Graft Copolymers Composed of Poly(2-Methacryloyloxyethyl Phosphorylcholine) Side Chain and Poly(N-Butyl Methacrylate) Backbone. *J. Biomed. Mater. Res.* **1994**, *28*, 225−232.
(134) Ishihara, K.; Nomura, H.; Mihara, T.; Kurita, K.; Iwasaki, Y.; Nakabayashi, N. Why Do Phospholipid Polymers Reduce Protein Adsorption? *J. Biomed. Mater. Res.* **1998**, *39*, 323−330.
(135) Moro, T.; Takatori, Y.; Ishihara, K.; Konno, T.; Takigawa, Y.; Matsushita, T.; Chung, U.-i.; Nakamura, K.; Kawaguchi, H. Surface Grafting of Artificial Joints with a Biocompatible Polymer for Preventing Periprosthetic Osteolysis. *Nat. Mater.* **2004**, *3*, 829−836.
(136) Chen, M.; Briscoe, W. H.; Armes, S. P.; Klein, J. Lubrication at Physiological Pressures by Polyzwitterionic Brushes. *Science* **2009**, *323*, 1698−1701.
(137) Lobb, E. J.; Ma, I.; Billingham, N. C.; Armes, S. P.; Lewis, A. L. Facile Synthesis of Well-Defined, Biocompatible Phosphorylcholine-Based Methacrylate Copolymers via Atom Transfer Radical Polymerization at 20 °C. *J. Am. Chem. Soc.* **2001**, *123*, 7913−7914.
(138) Feng, W.; Brash, J. L.; Zhu, S. Non-Biofouling Materials Prepared by Atom Transfer Radical Polymerization Grafting of 2-Methacryloloxyethyl Phosphorylcholine: Separate Effects of Graft Density and Chain Length on Protein Repulsion. *Biomaterials* **2006**, *27*, 847−855.

https://doi.org/10.1021/acs.chemrev.2c00344
Chem. Rev. 2022, 122, 17073−17154

(139) Feng, W.; Zhu, S.; Ishihara, K.; Brash, J. L. Adsorption of Fibrinogen and Lysozyme on Silicon Grafted with Poly(2-Methacryloyloxyethyl Phosphorylcholine) via Surface-Initiated Atom Transfer Radical Polymerization. *Langmuir* **2005**, *21*, 5980−5987.
(140) Goda, T.; Ishihara, K.; Miyahara, Y. Critical Update on 2-Methacryloyloxyethyl Phosphorylcholine (MPC) Polymer Science. *J. Appl. Polym. Sci.* **2015**, *132*, 41766.
(141) Ishihara, K. Blood-Compatible Surfaces with Phosphorylcholine-Based Polymers for Cardiovascular Medical Devices. *Langmuir* **2019**, *35*, 1778−1787.
(142) Ishihara, K. Revolutionary Advances in 2-Methacryloyloxyethyl Phosphorylcholine Polymers as Biomaterials. *J. Biomed. Mater. Res. Part A* **2019**, *107*, 933−943.
(143) Hart, R.; Timmerman, D. New Polyampholytes: The Polysulfobetaines. *J. Polym. Sci.* **1958**, *28*, 638−640.
(144) Zhang, Z.; Chen, S.; Chang, Y.; Jiang, S. Surface Grafted Sulfobetaine Polymers via Atom Transfer Radical Polymerization as Superlow Fouling Coatings. *J. Phys. Chem. B* **2006**, *110*, 10799−10804.
(145) Zhang, Z.; Vaisocherová, H.; Cheng, G.; Yang, W.; Xue, H.; Jiang, S. Nonfouling Behavior of Polycarboxybetaine-Grafted Surfaces: Structural and Environmental Effects. *Biomacromolecules* **2008**, *9*, 2686−2692.
(146) Bredas, J. L.; Chance, R. R.; Silbey, R. Head-Head Interactions in Zwitterionic Associating Polymers. *Macromolecules* **1988**, *21*, 1633−1639.
(147) Cheng, N.; Brown, A. A.; Azzaroni, O.; Huck, W. T. S. Thickness-Dependent Properties of Polyzwitterionic Brushes. *Macromolecules* **2008**, *41*, 6317−6321.
(148) Schulz, D. N.; Peiffer, D. G.; Agarwal, P. K.; Larabee, J.; Kaladas, J. J.; Soni, L.; Handwerker, B.; Garner, R. T. Phase Behaviour and Solution Properties of Sulphobetaine Polymers. *Polymer* **1986**, *27*, 1734−1742.
(149) Xiao, S.; Ren, B.; Huang, L.; Shen, M.; Zhang, Y.; Zhong, M.; Yang, J.; Zheng, J. Salt-Responsive Zwitterionic Polymer Brushes with Anti-Polyelectrolyte Property. *Curr. Opin. Chem. Eng.* **2018**, *19*, 86−93.
(150) Lowe, A. B.; McCormick, C. L. Synthesis and Solution Properties of Zwitterionic Polymers. *Chem. Rev.* **2002**, *102*, 4177−4190.
(151) Niskanen, J.; Tenhu, H. How to Manipulate the Upper Critical Solution Temperature (UCST)? *Polym. Chem.* **2017**, *8*, 220−232.
(152) Li, X. H.; Tang, C. J.; Liu, D.; Yuan, Z. F.; Hung, H. C.; Luozhong, S.; Gu, W. C.; Wu, K.; Jiang, S. Y. High-Strength and Nonfouling Zwitterionic Triple-Network Hydrogel in Saline Environments. *Adv. Mater.* **2021**, *33*, 2102479.
(153) Hildebrand, V.; Laschewsky, A.; Päch, M.; Müller-Buschbaum, P.; Papadakis, C. M. Effect of the Zwitterion Structure on the Thermo-Responsive Behaviour of Poly(Sulfobetaine Methacrylates). *Polym. Chem.* **2017**, *8*, 310−322.
(154) Wang, N.; Seymour, B. T.; Lewoczko, E. M.; Kent, E. W.; Chen, M.-L.; Wang, J.-H.; Zhao, B. Zwitterionic Poly(sulfobetaine methacrylate)s in Water: From Upper Critical Solution Temperature (UCST) to Lower Critical Solution Temperature (LCST) with Increasing Length of One Alkyl Substituent on the Nitrogen Atom. *Polym. Chem.* **2018**, *9*, 5257−5261.
(155) Willcock, H.; Lu, A.; Hansell, C. F.; Chapman, E.; Collins, I. R.; O'Reilly, R. K. One-Pot Synthesis of Responsive Sulfobetaine Nanoparticles by RAFT Polymerisation: The Effect of Branching on the UCST Cloud Point. *Polym. Chem.* **2014**, *5*, 1023−1030.
(156) Chen, L.; Honma, Y.; Mizutani, T.; Liaw, D. J.; Gong, J. P.; Osada, Y. Effects of Polyelectrolyte Complexation on the UCST of Zwitterionic Polymer. *Polymer* **2000**, *41*, 141−147.
(157) Ye, L.; Zhang, Y.; Wang, Q.; Zhou, X.; Yang, B.; Ji, F.; Dong, D.; Gao, L.; Cui, Y.; Yao, F. Physical Cross-Linking Starch-Based Zwitterionic Hydrogel Exhibiting Excellent Biocompatibility, Protein Resistance, and Biodegradability. *ACS Appl. Mater. Interfaces* **2016**, *8*, 15710−15723.
(158) Dong, D.; Tsao, C.; Hung, H.-C.; Yao, F.; Tang, C.; Niu, L.; Ma, J.; MacArthur, J.; Sinclair, A.; Wu, K.; et al. High-Strength and Fibrous Capsule-Resistant Zwitterionic Elastomers. *Sci. Adv.* **2021**, *7*, No. eabc5442.
(159) Zeng, R.; Xu, S.; Cheng, J.; Cai, Z.; Pi, P.; Wen, X. Thermoresponsive/Low-Fouling Zwitterionic Hydrogel for Controlled Drug Release. *J. Appl. Polym. Sci.* **2014**, *131*, 39816.
(160) Erfani, A.; Flynn, N. H.; Aichele, C. P.; Ramsey, J. D. Encapsulation and Delivery of Protein from within Poly(Sulfobetaine) Hydrogel Beads. *J. Appl. Polym. Sci.* **2020**, *137*, 49550.
(161) Sun, Z.; Li, Y.; Zheng, S. Y.; Mao, S.; He, X.; Wang, X.; Yang, J. Zwitterionic Nanocapsules with Salt- and Thermo-Responsiveness for Controlled Encapsulation and Release. *ACS Appl. Mater. Interfaces* **2021**, *13*, 47090−47099.
(162) Liu, H.; Xiong, C.; Tao, Z.; Fan, Y.; Tang, X.; Yang, H. Zwitterionic Copolymer-Based and Hydrogen Bonding-Strengthened Self-Healing Hydrogel. *RSC Adv.* **2015**, *5*, 33083−33088.
(163) Shi, Y.; Zhang, Y.; Jia, L.; Zhang, Q.; Xu, X. Stretchable and Self-Healing Integrated All-Gel-State Supercapacitors Enabled by a Notch-Insensitive Supramolecular Hydrogel Electrolyte. *ACS Appl. Mater. Interfaces* **2018**, *10*, 36028−36036.
(164) D'Angelo, A. J.; Panzer, M. J. Design of Stretchable and Self-Healing Gel Electrolytes via Fully Zwitterionic Polymer Networks in Solvate Ionic Liquids for Li-Based Batteries. *Chem. Mater.* **2019**, *31*, 2913−2922.
(165) Homayun, B.; Lin, X. T.; Choi, H. J. Challenges and Recent Progress in Oral Drug Delivery Systems for Biopharmaceuticals. *Pharmaceutics* **2019**, *11*, 129.
(166) Banerjee, S. L.; Samanta, S.; Sarkar, S.; Singha, N. K. A Self-Healable and Antifouling Hydrogel Based on PDMS Centered ABA Tri-Block Copolymer Polymersomes: A Potential Material for Therapeutic Contact Lenses. *J. Mater. Chem. B* **2020**, *8*, 226−243.
(167) Dahlke, J.; Kimmig, J.; Abend, M.; Zechel, S.; Vitz, J.; Schubert, U. S.; Hager, M. D. Quantification of the Scratch-Healing Efficiency for Novel Zwitterionic Polymers. *NPG Asia Mater.* **2020**, *12*, 13.
(168) Lin, Y.; Hu, H.; Yi, P.; Sun, S.; Li, Y.; Liu, X.; Li, G. Zwitterionic Hydrogels Formed via Quadruple Hydrogen-Bonds with Ultra-Fast Room-Temperature Self-Healing Ability. *Mater. Lett.* **2020**, *269*, 127665.
(169) Sun, Y.; Lu, S.; Li, Q.; Ren, Y.; Ding, Y.; Wu, H.; He, X.; Shang, Y. High Strength Zwitterionic Nano-Micelle Hydrogels with Superior Self-Healing, Adhesive and Ion Conductive Properties. *Eur. Polym. J.* **2020**, *133*, 109761.
(170) Wang, L.; Gao, G.; Zhou, Y.; Xu, T.; Chen, J.; Wang, R.; Zhang, R.; Fu, J. Tough, Adhesive, Self-Healable, and Transparent Ionically Conductive Zwitterionic Nanocomposite Hydrogels as Skin Strain Sensors. *ACS Appl. Mater. Interfaces* **2019**, *11*, 3506−3515.
(171) Pei, X. J.; Zhang, H.; Zhou, Y.; Zhou, L. J.; Fu, J. Stretchable, Self-Healing and Tissue-Adhesive Zwitterionic Hydrogels as Strain Sensors for Wireless Monitoring of Organ Motions. *Mater. Horiz.* **2020**, *7*, 1872−1882.
(172) Wang, Z.; Fei, G.; Xia, H.; Zuilhof, H. Dual Water-Healable Zwitterionic Polymer Coatings for Anti-Biofouling Surfaces. *J. Mater. Chem. B* **2018**, *6*, 6930−6935.
(173) He, B.; Du, Y.; Wang, B.; Zhao, X.; Liu, S.; Ye, Q.; Zhou, F. Self-Healing Polydimethylsiloxane Antifouling Coatings Based on Zwitterionic Polyethylenimine-Functionalized Gallium Nanodroplets. *Chem. Eng. J.* **2022**, *427*, 131019.
(174) Liang, B.; Zhong, Z.; Jia, E.; Zhang, G.; Su, Z. Transparent and Scratch-Resistant Antifogging Coatings with Rapid Self-Healing Capability. *ACS Appl. Mater. Interfaces* **2019**, *11*, 30300−30307.
(175) Wang, Z.; van Andel, E.; Pujari, S. P.; Feng, H.; Dijksman, J. A.; Smulders, M. M. J.; Zuilhof, H. Water-Repairable Zwitterionic Polymer Coatings for Anti-Biofouling Surfaces. *J. Mater. Chem. B* **2017**, *5*, 6728−6733.
(176) Chen, S.; Mo, F.; Yang, Y.; Stadler, F. J.; Chen, S.; Yang, H.; Ge, Z. Development of Zwitterionic Polyurethanes with Multi-Shape

https://doi.org/10.1021/acs.chemrev.2c00344
Chem. Rev. 2022, 122, 17073−17154

Memory Effects and Self-Healing Properties. *J. Mater. Chem. A* **2015**, *3*, 2924−2933.
(177) Kang, J.; Kim, J.; Choi, K.; Hong, P. H.; Park, H. J.; Kim, K.; Kim, Y. K.; Moon, G.; Jeon, H.; Lee, S.; et al. A Water-Triggered Highly Self-Healable Elastomer with Enhanced Mechanical Properties Achieved Using Localized Zwitterionic Assemblies. *Chem. Eng. J.* **2021**, *420*, 127636.
(178) Ladenheim, H.; Morawetz, H. A New Type of Polyampholyte: Poly(4-Vinyl Pyridine Betaine). *J. Polym. Sci.* **1957**, *26*, 251−254.
(179) Weers, J. G.; Rathman, J. F.; Axe, F. U.; Crichlow, C. A.; Foland, L. D.; Scheuing, D. R.; Wiersema, R. J.; Zielske, A. G. Effect of the Intramolecular Charge Separation Distance on the Solution Properties of Betaines and Sulfobetaines. *Langmuir* **1991**, *7*, 854−867.
(180) Vaisocherová, H.; Zhang, Z.; Yang, W.; Cao, Z.; Cheng, G.; Taylor, A. D.; Piliarik, M.; Homola, J.; Jiang, S. Functionalizable Surface Platform with Reduced Nonspecific Protein Adsorption from Full Blood Plasma—Material Selection and Protein Immobilization Optimization. *Biosens. Bioelectron.* **2009**, *24*, 1924−1930.
(181) Cao, Z.; Brault, N.; Xue, H.; Keefe, A.; Jiang, S. Manipulating Sticky and Non-Sticky Properties in a Single Material. *Angew. Chem., Int. Ed.* **2011**, *50*, 6102−6104.
(182) Cao, Z.; Mi, L.; Mendiola, J.; Ella-Menye, J.-R.; Zhang, L.; Xue, H.; Jiang, S. Reversibly Switching the Function of a Surface between Attacking and Defending against Bacteria. *Angew. Chem., Int. Ed.* **2012**, *51*, 2602−2605.
(183) Sundaram, H. S.; Ella-Menye, J.-R.; Brault, N. D.; Shao, Q.; Jiang, S. Reversibly Switchable Polymer with Cationic/Zwitterionic/Anionic Behavior through Synergistic Protonation and Deprotonation. *Chem. Sci.* **2014**, *5*, 200−205.
(184) Carr, L. R.; Xue, H.; Jiang, S. Functionalizable and Nonfouling Zwitterionic Carboxybetaine Hydrogels with a Carboxybetaine Dimethacrylate Crosslinker. *Biomaterials* **2011**, *32*, 961−968.
(185) Cao, B.; Tang, Q.; Li, L. L.; Humble, J.; Wu, H. Y.; Liu, L. Y.; Cheng, G. Switchable Antimicrobial and Antifouling Hydrogels with Enhanced Mechanical Properties. *Adv. Healthcare Mater.* **2013**, *2*, 1096−1102.
(186) Cao, B.; Li, L. L.; Tang, Q.; Cheng, G. The Impact of Structure on Elasticity, Switchability, Stability and Functionality of an All-in-One Carboxybetaine Elastomer. *Biomaterials* **2013**, *34*, 7592−7600.
(187) Liu, Q.; Chiu, A.; Wang, L.; An, D.; Li, W.; Chen, E. Y.; Zhang, Y.; Pardo, Y.; McDonough, S. P.; Liu, L.; et al. Developing Mechanically Robust, Triazole-Zwitterionic Hydrogels to Mitigate Foreign Body Response (FBR) for Islet Encapsulation. *Biomaterials* **2020**, *230*, 119640.
(188) Huang, C.-J.; Brault, N. D.; Li, Y.; Yu, Q.; Jiang, S. Controlled Hierarchical Architecture in Surface-Initiated Zwitterionic Polymer Brushes with Structurally Regulated Functionalities. *Adv. Mater.* **2012**, *24*, 1834−1837.
(189) Zhang, L.; Xue, H.; Cao, Z. Q.; Keefe, A.; Wang, J. N.; Jiang, S. Y. Multifunctional and Degradable Zwitterionic Nanogels for Targeted Delivery, Enhanced MR Imaging, Reduction-Sensitive Drug Release, and Renal Clearance. *Biomaterials* **2011**, *32*, 4604−4608.
(190) Zhang, Z.; Cheng, G.; Carr, L. R.; Vaisocherova, H.; Chen, S. F.; Jiang, S. Y. The Hydrolysis of Cationic Polycarboxybetaine Esters to Zwitterionic Polycarboxybetaines with Controlled Properties. *Biomaterials* **2008**, *29*, 4719−4725.
(191) Cheng, G.; Xue, H.; Zhang, Z.; Chen, S.; Jiang, S. A Switchable Biocompatible Polymer Surface with Self-Sterilizing and Nonfouling Capabilities. *Angew. Chem., Int. Ed.* **2008**, *47*, 8831−8834.
(192) Mi, L.; Xue, H.; Li, Y.; Jiang, S. A Thermoresponsive Antimicrobial Wound Dressing Hydrogel Based on a Cationic Betaine Ester. *Adv. Funct. Mater.* **2011**, *21*, 4028−4034.
(193) Ji, F.; Lin, W.; Wang, Z.; Wang, L.; Zhang, J.; Ma, G.; Chen, S. Development of Nonstick and Drug-Loaded Wound Dressing Based on the Hydrolytic Hydrophobic Poly(Carboxybetaine) Ester Analogue. *ACS Appl. Mater. Interfaces* **2013**, *5*, 10489−10494.
(194) Carr, L. R.; Jiang, S. Mediating High Levels of Gene Transfer without Cytotoxicity via Hydrolytic Cationic Ester Polymers. *Biomaterials* **2010**, *31*, 4186−4193.
(195) Zhang, L.; Sinclair, A.; Cao, Z.; Ella-Menye, J.-R.; Xu, X.; Carr, L. R.; Pun, S. H.; Jiang, S. Hydrolytic Cationic Ester Microparticles for Highly Efficient DNA Vaccine Delivery. *Small* **2013**, *9*, 3439−3444.
(196) Sinclair, A.; Bai, T.; Carr, L. R.; Ella-Menye, J.-R.; Zhang, L.; Jiang, S. Engineering Buffering and Hydrolytic or Photolabile Charge Shifting in a Polycarboxybetaine Ester Gene Delivery Platform. *Biomacromolecules* **2013**, *14*, 1587−1593.
(197) Wang, G.; Wang, L.; Lin, W.; Wang, Z.; Zhang, J.; Ji, F.; Ma, G.; Yuan, Z.; Chen, S. Development of Robust and Recoverable Ultralow-Fouling Coatings Based on Poly(Carboxybetaine) Ester Analogue. *ACS Appl. Mater. Interfaces* **2015**, *7*, 16938−16945.
(198) Hung, H. C.; Jain, P.; Zhang, P.; Sun, F.; Sinclair, A.; Bai, T.; Li, B.; Wu, K.; Tsao, C.; Liu, E. J.; et al. A Coating-Free Nonfouling Polymeric Elastomer. *Adv. Mater.* **2017**, *29*, 1700617.
(199) Ignatova, Z.; Gierasch, L. M. Inhibition of Protein Aggregation in Vitro and in Vivo by a Natural Osmoprotectant. *Proc. Natl. Acad. Sci. U. S. A.* **2006**, *103*, 13357−13361.
(200) Ma, H.; Zhao, Y.; Huang, W.; Zhang, L.; Wu, F.; Ye, J.; Chen, G.-Q. Rational Flux-Tuning of Halomonas Bluephagenesis for Co-Production of Bioplastic PHB and Ectoine. *Nat. Commun.* **2020**, *11*, 3313.
(201) Hahn, M. B.; Meyer, S.; Schroeter, M.-A.; Kunte, H.-J.; Solomun, T.; Sturm, H. DNA Protection by Ectoine from Ionizing Radiation: Molecular Mechanisms. *Phys. Chem. Chem. Phys.* **2017**, *19*, 25717−25722.
(202) Graf, R.; Anzali, S.; Buenger, J.; Pfluecker, F.; Driller, H. The Multifunctional Role of Ectoine as a Natural Cell Protectant. *Clin. Dermatol.* **2008**, *26*, 326−333.
(203) Bownik, A.; Stepniewska, Z. Ectoine as a Promising Protective Agent in Humans and Animals. *Arh. Hig. Rada. Toksikol.* **2016**, *67*, 260−265.
(204) Jain, P.; Hung, H.-C.; Lin, X.; Ma, J.; Zhang, P.; Sun, F.; Wu, K.; Jiang, S. Poly(ectoine) Hydrogels Resist Nonspecific Protein Adsorption. *Langmuir* **2017**, *33*, 11264−11269.
(205) Bruce, E. E.; van der Vegt, N. F. A. Molecular Scale Solvation in Complex Solutions. *J. Am. Chem. Soc.* **2019**, *141*, 12948−12956.
(206) Li, B.; Jain, P.; Ma, J.; Smith, J. K.; Yuan, Z.; Hung, H.-C.; He, Y.; Lin, X.; Wu, K.; Pfaendtner, J.; et al. Trimethylamine N-Oxide-Derived Zwitterionic Polymers: A New Class of Ultralow Fouling Bioinspired Materials. *Sci. Adv.* **2019**, *5*, No. eaaw9562.
(207) Huang, H.; Zhang, C.; Crisci, R.; Lu, T.; Hung, H.-C.; Sajib, M. S. J.; Sarker, P.; Ma, J.; Wei, T.; Jiang, S.; et al. Strong Surface Hydration and Salt Resistant Mechanism of a New Nonfouling Zwitterionic Polymer Based on Protein Stabilizer TMAO. *J. Am. Chem. Soc.* **2021**, *143*, 16786−16795.
(208) Ohto, T.; Backus, E. H. G.; Mizukami, W.; Hunger, J.; Bonn, M.; Nagata, Y. Unveiling the Amphiphilic Nature of TMAO by Vibrational Sum Frequency Generation Spectroscopy. *J. Phys. Chem. C* **2016**, *120*, 17435−17443.
(209) Chen, S.; Zhong, Y.; Fan, W.; Xiang, J.; Wang, G.; Zhou, Q.; Wang, J.; Geng, Y.; Sun, R.; Zhang, Z.; et al. Enhanced Tumour Penetration and Prolonged Circulation in Blood of Polyzwitterion-Drug Conjugates with Cell-Membrane Affinity. *Nat. Biomed. Eng.* **2021**, *5*, 1019−1037.
(210) Alswieleh, A. M.; Cheng, N.; Canton, I.; Ustbas, B.; Xue, X.; Ladmiral, V.; Xia, S.; Ducker, R. E.; El Zubir, O.; Cartron, M. L.; et al. Zwitterionic Poly(amino acid methacrylate) Brushes. *J. Am. Chem. Soc.* **2014**, *136*, 9404−9413.
(211) Liu, Q.; Singh, A.; Liu, L. Amino Acid-Based Zwitterionic Poly(serine methacrylate) as an Antifouling Material. *Biomacromolecules* **2013**, *14*, 226−231.
(212) Li, W.; Liu, Q.; Liu, L. Antifouling Gold Surfaces Grafted with Aspartic Acid and Glutamic Acid Based Zwitterionic Polymer Brushes. *Langmuir* **2014**, *30*, 12619−12626.

https://doi.org/10.1021/acs.chemrev.2c00344
Chem. Rev. 2022, 122, 17073−17154

(213) Li, W.; Liu, Q.; Liu, L. Amino Acid-Based Zwitterionic Polymers: Antifouling Properties and Low Cytotoxicity. *J. Biomater. Sci., Polym. Ed.* **2014**, *25*, 1730−1742.
(214) Liu, Q.; Li, W.; Singh, A.; Cheng, G.; Liu, L. Two Amino Acid-Based Superlow Fouling Polymers: Poly(lysine methacrylamide) and Poly(ornithine methacrylamide). *Acta Biomater.* **2014**, *10*, 2956−2964.
(215) Liu, Q.; Li, W.; Wang, H.; Newby, B.-m. Z.; Cheng, F.; Liu, L. Amino Acid-Based Zwitterionic Polymer Surfaces Highly Resist Long-Term Bacterial Adhesion. *Langmuir* **2016**, *32*, 7866−7874.
(216) Wang, H.; Wu, H.; Lee, C.-J.; Lei, X.; Zhe, J.; Xu, F.; Cheng, F.; Cheng, G. pH-Sensitive Poly(histidine methacrylamide). *Langmuir* **2016**, *32*, 6544−6550.
(217) Jhong, J.-F.; Sin, M.-C.; Kung, H.-H.; Chinnathambi, A.; Alharbi, S. A.; Chang, Y. Hemocompatibility of Pseudozwitterionic Polymer Brushes with a Systematic Well-Defined Charge-Bias Control. *J. Biomater. Sci., Polym. Ed.* **2014**, *25*, 1558−1572.
(218) Chang, Y.; Shu, S.-H.; Shih, Y.-J.; Chu, C.-W.; Ruaan, R.-C.; Chen, W.-Y. Hemocompatible Mixed-Charge Copolymer Brushes of Pseudozwitterionic Surfaces Resistant to Nonspecific Plasma Protein Fouling. *Langmuir* **2010**, *26*, 3522−3530.
(219) Venault, A.; Wei, T. C.; Shih, H. L.; Yeh, C. C.; Chinnathambi, A.; Alharbi, S. A.; Carretier, S.; Aimar, P.; Lai, J. Y.; Chang, Y. Antifouling Pseudo-Zwitterionic Poly(vinylidene fluoride) Membranes with Efficient Mixed-Charge Surface Grafting via Glow Dielectric Barrier Discharge Plasma-Induced Copolymerization. *J. Membr. Sci.* **2016**, *516*, 13−25.
(220) Encinas, N.; Angulo, M.; Astorga, C.; Colilla, M.; Izquierdo-Barba, I.; Vallet-Regí, M. Mixed-Charge Pseudo-Zwitterionic Mesoporous Silica Nanoparticles with Low-Fouling and Reduced Cell Uptake Properties. *Acta Biomater.* **2019**, *84*, 317−327.
(221) Wu, Y.; Raju, C.; Hou, Z.; Si, Z.; Xu, C.; Pranantyo, D.; Marimuthu, K.; De, P. P.; Ng, O. T.; Pethe, K.; et al. Mixed-Charge Pseudo-Zwitterionic Copolymer Brush as Broad Spectrum Anti-biofilm Coating. *Biomaterials* **2021**, *273*, 120794.
(222) Bernards, M.; He, Y. Polyampholyte Polymers as a Versatile Zwitterionic Biomaterial Platform. *J. Biomater. Sci., Polym. Ed.* **2014**, *25*, 1479−1488.
(223) Chen, S.; Jiang, S. An New Avenue to Nonfouling Materials. *Adv. Mater.* **2008**, *20*, 335−338.
(224) Bernards, M. T.; Cheng, G.; Zhang, Z.; Chen, S.; Jiang, S. Nonfouling Polymer Brushes via Surface-Initiated, Two-Component Atom Transfer Radical Polymerization. *Macromolecules* **2008**, *41*, 4216−4219.
(225) Wei, Y.; Hung, H.-C.; Sun, F.; Bai, T.; Zhang, P.; Nowinski, A. K.; Jiang, S. Achieving Low-Fouling Surfaces with Oppositely Charged Polysaccharides via LBL Assembly. *Acta Biomater.* **2016**, *40*, 16−22.
(226) Zhang, J.; Zhu, Y.; Song, J.; Yang, J.; Pan, C.; Xu, T.; Zhang, L. Novel Balanced Charged Alginate/PEI Polyelectrolyte Hydrogel That Resists Foreign-Body Reaction. *ACS Appl. Mater. Interfaces* **2018**, *10*, 6879−6886.
(227) Peng, X.; Zhao, L.; Du, G.; Wei, X.; Guo, J.; Wang, X.; Guo, G.; Pu, Q. Charge Tunable Zwitterionic Polyampholyte Layers Formed in Cyclic Olefin Copolymer Microchannels through Photochemical Graft Polymerization. *ACS Appl. Mater. Interfaces* **2013**, *5*, 1017−1023.
(228) Zhao, T.; Chen, K.; Gu, H. Investigations on the Interactions of Proteins with Polyampholyte-Coated Magnetite Nanoparticles. *J. Phys. Chem. B* **2013**, *117*, 14129−14135.
(229) Jhong, J.-F.; Venault, A.; Liu, L.; Zheng, J.; Chen, S.-H.; Higuchi, A.; Huang, J.; Chang, Y. Introducing Mixed-Charge Copolymers as Wound Dressing Biomaterials. *ACS Appl. Mater. Interfaces* **2014**, *6*, 9858−9870.
(230) Yang, Z.; Saeki, D.; Takagi, R.; Matsuyama, H. Improved Anti-Biofouling Performance of Polyamide Reverse Osmosis Membranes Modified with a Polyampholyte with Effective Carboxyl Anion and Quaternary Ammonium Cation Ratio. *J. Membr. Sci.* **2020**, *595*, 117529.
(231) Charaya, H.; Li, X.; Jen, N.; Chung, H.-J. Specific Ion Effects in Polyampholyte Hydrogels Dialyzed in Aqueous Electrolytic Solutions. *Langmuir* **2019**, *35*, 1526−1533.
(232) Sun, T. L.; Kurokawa, T.; Kuroda, S.; Ihsan, A. B.; Akasaki, T.; Sato, K.; Haque, M. A.; Nakajima, T.; Gong, J. P. Physical Hydrogels Composed of Polyampholytes Demonstrate High Toughness and Viscoelasticity. *Nat. Mater.* **2013**, *12*, 932−937.
(233) Chen, S.; Cao, Z.; Jiang, S. Ultra-Low Fouling Peptide Surfaces Derived from Natural Amino Acids. *Biomaterials* **2009**, *30*, 5892−5896.
(234) White, A. D.; Nowinski, A. K.; Huang, W.; Keefe, A. J.; Sun, F.; Jiang, S. Decoding Nonspecific Interactions from Nature. *Chem. Sci.* **2012**, *3*, 3488−3494.
(235) Daly, W. H.; Poché, D. The Preparation of *N*-Carboxyanhydrides of α-Amino Acids Using Bis(trichloromethyl)carbonate. *Tetrahedron Lett.* **1988**, *29*, 5859−5862.
(236) Chen, C.; Wang, Z.; Li, Z. Thermoresponsive Polypeptides from PEGylated Poly-L-Glutamates. *Biomacromolecules* **2011**, *12*, 2859−2863.
(237) Yang, Q.; Wang, L.; Lin, W.; Ma, G.; Yuan, J.; Chen, S. Development of Nonfouling Polypeptides with Uniform Alternating Charges by Polycondensation of the Covalently Bonded Dimer of Glutamic Acid and Lysine. *J. Mater. Chem. B* **2014**, *2*, 577−584.
(238) Liu, E. J.; Sinclair, A.; Keefe, A. J.; Nannenga, B. L.; Coyle, B. L.; Baneyx, F.; Jiang, S. Ekylation: Addition of an Alternating-Charge Peptide Stabilizes Proteins. *Biomacromolecules* **2015**, *16*, 3357−3361.
(239) Qi, H.; Zheng, W.; Zhou, X.; Zhang, C.; Zhang, L. A Mussel-Inspired Chimeric Protein as a Novel Facile Antifouling Coating. *Chem. Commun.* **2018**, *54*, 11328−11331.
(240) Erathodiyil, N.; Chan, H.-M.; Wu, H.; Ying, J. Y. Zwitterionic Polymers and Hydrogels for Antibiofouling Applications in Implantable Devices. *Mater. Today* **2020**, *38*, 84−98.
(241) Ren, X. K.; Feng, Y. K.; Guo, J. T.; Wang, H. X.; Li, Q.; Yang, J.; Hao, X. F.; Lv, J.; Ma, N.; Li, W. Z. Surface Modification and Endothelialization of Biomaterials as Potential Scaffolds for Vascular Tissue Engineering Applications. *Chem. Soc. Rev.* **2015**, *44*, 5680−5742.
(242) Himmelfarb, J.; Ikizler, T. A. Hemodialysis. *N. Engl. J. Med.* **2010**, *363*, 1833−1845.
(243) Rosenbaum, J. L.; Winsten, S.; Kramer, M. S.; Moros, J.; Raja, R. Resin Hemoperfusion in the Treatment of Drug Intoxication. *Clin. Toxicol.* **1972**, *136*, 263−266.
(244) Siemsen, A. W.; Dunea, G.; Mamdani, B. H.; Guruprakash, G. Charcoal Hemoperfusion for Chronic Renal Failure. *Nephron* **2004**, *22*, 386−390.
(245) Ukita, R.; Wu, K.; Lin, X.; Carleton, N. M.; Naito, N.; Lai, A.; Do-Nguyen, C. C.; Demarest, C. T.; Jiang, S.; Cook, K. E. Zwitterionic Poly-Carboxybetaine Coating Reduces Artificial Lung Thrombosis in Sheep and Rabbits. *Acta Biomater.* **2019**, *92*, 71−81.
(246) Naito, N.; Ukita, R.; Wilbs, J.; Wu, K.; Lin, X. J.; Carleton, N. M.; Roberts, K.; Jiang, S. Y.; Heinis, C.; Cook, K. E. Combination of Polycarboxybetaine Coating and Factor XII Inhibitor Reduces Clot Formation While Preserving Normal Tissue Coagulation During Extracorporeal Life Support. *Biomaterials* **2021**, *272*, 120778.
(247) Badv, M.; Bayat, F.; Weitz, J. I.; Didar, T. F. Single and Multi-Functional Coating Strategies for Enhancing the Biocompatibility and Tissue Integration of Blood-Contacting Medical Implants. *Biomaterials* **2020**, *258*, 120291.
(248) Murphy, D. A.; Hockings, L. E.; Andrews, R. K.; Aubron, C.; Gardiner, E. E.; Pellegrino, V. A.; Davis, A. K. Extracorporeal Membrane Oxygenation—Hemostatic Complications. *Transfus. Med. Rev.* **2015**, *29*, 90−101.
(249) Mallik, S.; Prasad, R.; Bhattacharya, A.; Sen, P. Synthesis of Phosphatidylserine and Its Stereoisomers: Their Role in Activation of Blood Coagulation. *ACS Med. Chem. Lett.* **2018**, *9*, 434−439.
(250) Kvolik, S.; Jukic, M.; Matijevic, M.; Marjanovic, K.; Glavas-Obrovac, L. An Overview of Coagulation Disorders in Cancer Patients. *Surg. Oncol.* **2010**, *19*, e33−e46.

https://doi.org/10.1021/acs.chemrev.2c00344
Chem. Rev. 2022, 122, 17073−17154

(251) Hanson, S. R.; Tucker, E. I.; Latour, R. A. 2.2.6 - Blood Coagulation and Blood-Material Interactions. In *Biomaterials Science*, 4th ed.; Academic Press: 2020; pp 801−812.
(252) Wilson, C. J.; Clegg, R. E.; Leavesley, D. I.; Pearcy, M. J. Mediation of Biomaterial-Cell Interactions by Adsorbed Proteins: A Review. *Tissue Eng.* **2005**, *11*, 1−18.
(253) Bültmann, A.; Li, Z.; Wagner, S.; Peluso, M.; Schönberger, T.; Weis, C.; Konrad, I.; Stellos, K.; Massberg, S.; Nieswandt, B.; et al. Impact of Glycoprotein VI and Platelet Adhesion on Atherosclerosis—a Possible Role of Fibronectin. *J. Mol. Cell. Cardiol.* **2010**, *49*, 532−542.
(254) Molino, D.; De Lucia, D.; Marotta, R.; Perna, A.; Lombardi, C.; Cirillo, M.; De Santo, N. G. In Uremia, Plasma Levels of Anti-Protein C and Anti-Protein S Antibodies Are Associated with Thrombosis. *Kidney Int.* **2005**, *68*, 1223−1229.
(255) Haines, N. M.; Rycus, P. T.; Zwischenberger, J. B.; Bartlett, R. H.; Ündar, A. Extracorporeal Life Support Registry Report 2008: Neonatal and Pediatric Cardiac Cases. *ASAIO J.* **2009**, *55*, 111−116.
(256) Raman, J.; Alimohamed, M.; Dobrilovic, N.; Lateef, O.; Aziz, S. A Comparison of Low and Standard Anti-Coagulation Regimens in Extracorporeal Membrane Oxygenation. *J. Heart Lung Transpl.* **2019**, *38*, 433−439.
(257) Benesch, J.; Svedhem, S.; Svensson, S. C. T.; Valiokas, R.; Liedberg, B.; Tengvall, P. Protein Adsorption to Oligo(Ethylene Glycol) Self-Assembled Monolayers: Experiments with Fibrinogen, Heparinized Plasma, and Serum. *J. Biomater. Sci., Polym. Ed.* **2001**, *12*, 581−597.
(258) Chang, Y.; Liao, S.-C.; Higuchi, A.; Ruaan, R.-C.; Chu, C.-W.; Chen, W.-Y. A Highly Stable Nonbiofouling Surface with Well-Packed Grafted Zwitterionic Polysulfobetaine for Plasma Protein Repulsion. *Langmuir* **2008**, *24*, 5453−5458.
(259) Hayward, J. A.; Chapman, D. Biomembrane Surfaces as Models for Polymer Design: The Potential for Haemocompatibility. *Biomaterials* **1984**, *5*, 135−142.
(260) Ueda, T.; Oshida, H.; Kurita, K.; Ishihara, K.; Nakabayashi, N. Preparation of 2-Methacryloyloxyethyl Phosphorylcholine Copolymers with Alkyl Methacrylates and Their Blood Compatibility. *Polym. J.* **1992**, *24*, 1259−1269.
(261) Ishihara, K.; Aragaki, R.; Ueda, T.; Watenabe, A.; Nakabayashi, N. Reduced Thrombogenicity of Polymers Having Phospholipid Polar Groups. *J. Biomed. Mater. Res.* **1990**, *24*, 1069−1077.
(262) Ye, S. H.; Johnson, C. A.; Woolley, J. R.; Murata, H.; Gamble, L. J.; Ishihara, K.; Wagner, W. R. Simple Surface Modification of a Titanium Alloy with Silanated Zwitterionic Phosphorylcholine or Sulfobetaine Modifiers to Reduce Thrombogenicity. *Colloids Surf., B* **2010**, *79*, 357−364.
(263) Kuo, W. H.; Wang, M. J.; Chien, H. W.; Wei, T. C.; Lee, C.; Tsai, W. B. Surface Modification with Poly(sulfobetaine methacrylate-*co*-acrylic acid) to Reduce Fibrinogen Adsorption, Platelet Adhesion, and Plasma Coagulation. *Biomacromolecules* **2011**, *12*, 4348−4356.
(264) Lin, X. J.; Wu, K.; Zhou, Q.; Jain, P.; Boit, M. O.; Li, B. W.; Hung, H. C.; Creason, S. A.; Himmelfarb, J.; Ratner, B. D.; et al. Photoreactive Carboxybetaine Copolymers Impart Biocompatibility and Inhibit Plasticizer Leaching on Polyvinyl Chloride. *ACS Appl. Mater. Interfaces* **2020**, *12*, 41026−41037.
(265) Lin, X.; Boit, M. O.; Wu, K.; Jain, P.; Liu, E. J.; Hsieh, Y. F.; Zhou, Q.; Li, B.; Hung, H. C.; Jiang, S. Zwitterionic Carboxybetaine Polymers Extend the Shelf-Life of Human Platelets. *Acta Biomater.* **2020**, *109*, 51−60.
(266) Peng, W.; Liu, P.; Zhang, X.; Peng, J.; Gu, Y.; Dong, X.; Ma, Z.; Liu, P.; Shen, J. Multi-Functional Zwitterionic Coating for Silicone-Based Biomedical Devices. *Chem. Eng. J.* **2020**, *398*, 125663.
(267) Chopra, V.; Anand, S.; Hickner, A.; Buist, M.; Rogers, M. A. M.; Saint, S.; Flanders, S. A. Risk of Venous Thromboembolism Associated with Peripherally Inserted Central Catheters: A Systematic Review and Meta-Analysis. *Lancet* **2013**, *382*, 311−325.
(268) Ishihara, K.; Fukumoto, K.; Iwasaki, Y.; Nakabayashi, N. Modification of Polysulfone with Phospholipid Polymer for Improvement of the Blood Compatibility. Part 1. Surface Characterization. *Biomaterials* **1999**, *20*, 1545−1551.
(269) Ishihara, K.; Fukumoto, K.; Iwasaki, Y.; Nakabayashi, N. Modification of Polysulfone with Phospholipid Polymer for Improvement of the Blood Compatibility. Part 2. Protein Adsorption and Platelet Adhesion. *Biomaterials* **1999**, *20*, 1553−1559.
(270) Hasegawa, T.; Iwasaki, Y.; Ishihara, K. Preparation of Blood-Compatible Hollow Fibers from a Polymer Alloy Composed of Polysulfone and 2-Methacryloyloxyethyl Phosphorylcholine Polymer. *J. Biomed. Mater. Res.* **2002**, *63*, 333−341.
(271) Iwasaki, Y.; Nakabayashi, N.; Ishihara, K. In Vitro and ex Vivo Blood Compatibility Study of 2-Methacryloyloxyethyl Phosphorylcholine (MPC) Copolymer-Coated Hemodialysis Hollow Fibers. *J. Artif. Organs* **2003**, *6*, 260−266.
(272) Ye, S. H.; Watanabe, J.; Takai, M.; Iwasaki, Y.; Ishihara, K. Design of Functional Hollow Fiber Membranes Modified with Phospholipid Polymers for Application in Total Hemopurification System. *Biomaterials* **2005**, *26*, 5032−5041.
(273) Ye, S. H.; Watanabe, J.; Iwasaki, Y.; Ishihara, K. Antifouling Blood Purification Membrane Composed of Cellulose Acetate and Phospholipid Polymer. *Biomaterials* **2003**, *24*, 4143−4152.
(274) An, Z. H.; Dai, F. Y.; Wei, C. J.; Zhao, Y. P.; Chen, L. Polydopamine/Cysteine Surface Modified Hemocompatible Poly(vinylidene fluoride) Hollow Fiber Membranes for Hemodialysis. *J. Biomed. Mater. Res., Part B* **2018**, *106*, 2869−2877.
(275) Liu, Y.; Li, G. L.; Han, Q.; Lin, H. B.; Li, Q.; Deng, G.; Liu, F. Construction of Electro-Neutral Surface on Dialysis Membrane for Improved Toxin Clearance and Anti-Coagulation/Inflammation through Saltwater Fish Inspired Trimethylamine N-Oxide (TMAO). *J. Membr. Sci.* **2022**, *641*, 119900.
(276) Cai, N. N.; Li, Q. S.; Zhang, J. M.; Xu, T.; Zhao, W. Q.; Yang, J.; Zhang, L. Antifouling Zwitterionic Hydrogel Coating Improves Hemocompatibility of Activated Carbon Hemoadsorbent. *J. Colloid Interface Sci.* **2017**, *503*, 168−177.
(277) Li, Q. S.; Guo, H. S.; Yang, J.; Zhao, W.; Zhu, Y.; Sui, X.; Xu, T.; Zhang, J.; Zhang, L. MOF-Based Antibiofouling Hemoadsorbent for Highly Efficient Removal of Protein-Bound Bilirubin. *Langmuir* **2020**, *36*, 8753−8763.
(278) Iwasaki, Y.; Uchiyama, S.; Kurita, K.; Morimoto, N.; Nakabayashi, N. A Nonthrombogenic Gas-Permeable Membrane Composed of a Phospholipid Polymer Skin Film Adhered to a Polyethylene Porous Membrane. *Biomaterials* **2002**, *23*, 3421−3427.
(279) Myers, G. J.; Johnstone, D. R.; Swyer, W. J.; McTeer, S.; Maxwell, S. L.; Squires, C.; Ditmore, S. N.; Power, C. V.; Mitchell, L. B.; Ditmore, J. E.; et al. Evaluation of Mimesys Phosphorylcholine (PC)-Coated Oxygenators During Cardiopulmonary Bypass in Adults. *J. Extra-Corpor. Technol.* **2003**, *35*, 6−12.
(280) Wang, Y.-B.; Gong, M.; Yang, S.; Nakashima, K.; Gong, Y.-K. Hemocompatibility and Film Stability Improvement of Crosslinkable MPC Copolymer Coated Polypropylene Hollow Fiber Membrane. *J. Membr. Sci.* **2014**, *452*, 29−36.
(281) Wang, Y.-B.; Shi, K.-H.; Jiang, H.-L.; Gong, Y.-K. Significantly Reduced Adsorption and Activation of Blood Components in a Membrane Oxygenator System Coated with Crosslinkable Zwitterionic Copolymer. *Acta Biomater.* **2016**, *40*, 153−161.
(282) Ishihara, K.; Iwasaki, Y.; Nojiri, C. Phospholipid Polymer Biomaterials for Making Ventricular Assist Devices. *J. Congest. Heart Fail. Circ. Support* **2001**, *1*, 265−270.
(283) Kihara, S.; Yamazaki, K.; Litwak, K. N.; Litwak, P.; Kameneva, M. V.; Ushiyama, H.; Tokuno, T.; Borzelleca, D. C.; Umezu, M.; Tomioka, J.; et al. In Vivo Evaluation of a MPC Polymer Coated Continuous Flow Left Ventricular Assist System. *Artif. Organs* **2003**, *27*, 188−192.
(284) Snyder, T. A.; Tsukui, H.; Kihara, S.; Akimoto, T.; Litwak, K. N.; Kameneva, M. V.; Yamazaki, K.; Wagner, W. R. Preclinical Biocompatibility Assessment of the Evaheart Ventricular Assist Device: Coating Comparison and Platelet Activation. *J. Biomed. Mater. Res. Part A* **2007**, *81A*, 85−92.

https://doi.org/10.1021/acs.chemrev.2c00344
Chem. Rev. 2022, 122, 17073−17154

(285) Campbell, E. J.; O'Byrne, V.; Stratford, P. W.; Quirk, I.; Vick, T. A.; Wiles, M. C.; Yianni, Y. P. Biocompatible Surfaces Using Methacryloylphosphorylcholine Laurylmethacrylate Copolymer. *ASAIO J.* **1994**, *40*, M853−M857.
(286) Whelan, D. M.; van der Giessen, W. J.; Krabbendam, S. C.; van Vliet, E. A.; Verdouw, P. D.; Serruys, P. W.; van Beusekom, H. M. M. Biocompatibility of Phosphorylcholine Coated Stents in Normal Porcine Coronary Arteries. *Heart* **2000**, *83*, 338−345.
(287) Murphy, E. F.; Lu, J. R.; Lewis, A. L.; Brewer, J.; Russell, J.; Stratford, P. Characterization of Protein Adsorption at the Phosphorylcholine Incorporated Polymer-Water Interface. *Macromolecules* **2000**, *33*, 4545−4554.
(288) Lewis, A. L.; Cumming, Z. L.; Goreish, H. H.; Kirkwood, L. C.; Tolhurst, L. A.; Stratford, P. W. Crosslinkable Coatings from Phosphorylcholine-Based Polymers. *Biomaterials* **2001**, *22*, 99−111.
(289) Grenadier, E.; Roguin, A.; Hertz, I.; Peled, B.; Boulos, M.; Nikolsky, E.; Amikam, S.; Kerner, A.; Cohen, S.; Beyar, R. Stenting Very Small Coronary Narrowings (< 2 mm) Using the Biocompatible Phosphorylcholine-Coated Coronary Stent. *Catheter. Cardiovasc. Interv.* **2002**, *55*, 303−308.
(290) Lewis, A. L.; Tolhurst, L. A.; Stratford, P. W. Analysis of a Phosphorylcholine-Based Polymer Coating on a Coronary Stent Pre- and Post-Implantation. *Biomaterials* **2002**, *23*, 1697−1706.
(291) Lewis, A. L.; Furze, J. D.; Small, S.; Robertson, J. D.; Higgins, B. J.; Taylor, S.; Ricci, D. R. Long-Term Stability of a Coronary Stent Coating Post-Implantation. *J. Biomed. Mater. Res.* **2002**, *63*, 699−705.
(292) Shinozaki, N.; Yokoi, H.; Iwabuchi, M.; Nosaka, H.; Kadota, K.; Mitsudo, K.; Nobuyoshi, M. Initial and Follow-up Results of the Biodivysio Phosphorylicholine Coated Stent for Treatment of Coronary Artery Disease. *Circ. J.* **2005**, *69*, 295−300.
(293) Wang, X.; Chen, X.; Xing, L.; Mao, C.; Yu, H.; Shen, J. Blood Compatibility of a New Zwitterionic Bare Metal Stent with Hyperbranched Polymer Brushes. *J. Mater. Chem. B* **2013**, *1*, 5036−5044.
(294) Wang, X. B.; Miao, J. J.; Shao, X. B.; Mao, C.; Shen, J. Zwitterionic Hyperbranched Polyester Functionalized Cardiovascular Stent and Its Biocompatibility. *J. Colloid Interface Sci.* **2014**, *420*, 88−96.
(295) Chou, Y.-N.; Chang, Y.; Wen, T.-C. Applying Thermosettable Zwitterionic Copolymers as General Fouling-Resistant and Thermal-Tolerant Biomaterial Interfaces. *ACS Appl. Mater. Interfaces* **2015**, *7*, 10096−10107.
(296) Ye, S. H.; Chen, Y. Q.; Mao, Z. W.; Gu, X. Z.; Shankarraman, V.; Hong, Y.; Shanov, V.; Wagner, W. R. Biodegradable Zwitterionic Polymer Coatings for Magnesium Alloy Stents. *Langmuir* **2019**, *35*, 1421−1429.
(297) Wen, C.; Zhang, J.; Li, Y.; Zheng, W.; Liu, M.; Zhu, Y.; Sui, X.; Zhang, X.; Han, Q.; Lin, Y.; et al. A Zwitterionic Hydrogel Coated Titanium Surface with High-Efficiency Endothelial Cell Selectivity for Rapid Re-Endothelialization. *Biomater. Sci.* **2020**, *8*, 5441−5451.
(298) Chen, H.; Wang, X. B.; Zhou, Q.; Xu, P.; Liu, Y.; Wan, M. M.; Zhou, M.; Mao, C. Preparation of Vascular Endothelial Cadherin Loaded-Amphoteric Copolymer Decorated Coronary Stents for Anticoagulation and Endothelialization. *Langmuir* **2017**, *33*, 13430−13437.
(299) Zhu, T.; Gao, W.; Fang, D.; Liu, Z.; Wu, G.; Zhou, M.; Wan, M.; Mao, C. Bifunctional Polymer Brush-Grafted Coronary Stent for Anticoagulation and Endothelialization. *Mater. Sci. Eng., C* **2021**, *120*, 111725.
(300) Yoneyama, T.; Ishihara, K.; Nakabayashi, N.; Ito, M.; Mishima, Y. Short-Term in Vivo Evaluation of Small-Diameter Vascular Prosthesis Composed of Segmented Poly(etherurethane)/2-Methacryloyloxyethyl Phosphorylcholine Polymer Blend. *J. Biomed. Mater. Res.* **1998**, *43*, 15−20.
(301) Yoneyama, T.; Ito, M.; Sugihara, K.-i.; Ishihara, K.; Nakabayashi, N. Small Diameter Vascular Prosthesis with a Nonthrombogenic Phospholipid Polymer Surface: Preliminary Study of a New Concept for Functioning in the Absence of Pseudo- or Neointimaformation. *Artif. Organs* **2000**, *24*, 23−28.
(302) Yoneyama, T.; Sugihara, K.-i.; Ishihara, K.; Iwasaki, Y.; Nakabayashi, N. The Vascular Prosthesis without Pseudointima Prepared by Antithrombogenic Phospholipid Polymer. *Biomaterials* **2002**, *23*, 1455−1459.
(303) Fowler, P.; Dizon, G. V.; Tayo, L. L.; Caparanga, A. R.; Huang, J.; Zheng, J.; Aimar, P.; Chang, Y. Surface Zwitterionization of Expanded Poly(tetrafluoroethylene) via Dopamine-Assisted Consecutive Immersion Coating. *ACS Appl. Mater. Interfaces* **2020**, *12*, 41000−41010.
(304) Yao, M. M.; Sun, H.; Guo, Z. C.; Sun, X.; Yu, Q. Y.; Wu, X. J.; Yu, C. J.; Zhang, H. T.; Yao, F. L.; Li, J. J. A Starch-Based Zwitterionic Hydrogel Coating for Blood-Contacting Devices with Durability and Bio-Functionality. *Chem. Eng. J.* **2021**, *421*, 129702.
(305) Zheng, W. W.; Liu, M.; Qi, H. S.; Wen, C. Y.; Zhang, C.; Mi, J. L.; Zhou, X.; Zhang, L.; Fan, D. D. Mussel-Inspired Triblock Functional Protein Coating with Endothelial Cell Selectivity for Endothelialization. *J. Colloid Interface Sci.* **2020**, *576*, 68−78.
(306) Hong, Y.; Ye, S.-H.; Nieponice, A.; Soletti, L.; Vorp, D. A.; Wagner, W. R. A Small Diameter, Fibrous Vascular Conduit Generated from a Poly(ester urethane)urea and Phospholipid Polymer Blend. *Biomaterials* **2009**, *30*, 2457−2467.
(307) Yang, F.; Xu, L. P.; Kuang, D. J.; Ge, Y.; Guo, G. Y.; Wang, Y. B. Polyzwitterion-Crosslinked Hybrid Tissue with Antithrombogenicity, Endothelialization, Anticalcification Properties. *Chem. Eng. J.* **2021**, *410*, 128244.
(308) Guo, F.; Liu, Y.; Jiao, K.; Yang, R.; Hou, M.; Zhang, X. Artificial Heart Valves with Balanced Charged Networks Exhibiting Anti-Calcification Properties. *ACS Appl. Bio Mater.* **2020**, *3*, 838−847.
(309) Luo, Y.; Huang, S. Y.; Ma, L. Zwitterionic Hydrogel-Coated Heart Valves with Improved Endothelialization and Anti-Calcification Properties. *Mater. Sci. Eng., C* **2021**, *128*, 112329.
(310) Xie, X.; Doloff, J. C.; Yesilyurt, V.; Sadraei, A.; McGarrigle, J. J.; Omami, M.; Veiseh, O.; Farah, S.; Isa, D.; Ghani, S.; et al. Reduction of Measurement Noise in a Continuous Glucose Monitor by Coating the Sensor with a Zwitterionic Polymer. *Nat. Biomed. Eng.* **2018**, *2*, 894−906.
(311) Golabchi, A.; Wu, B.; Cao, B.; Bettinger, C. J.; Cui, X. T. Zwitterionic Polymer/Polydopamine Coating Reduce Acute Inflammatory Tissue Responses to Neural Implants. *Biomaterials* **2019**, *225*, 119519.
(312) Zhang, D. H.; Chen, Q.; Shi, C.; Chen, M. Z.; Ma, K. Q.; Wan, J. L.; Liu, R. H. Dealing with the Foreign-Body Response to Implanted Biomaterials: Strategies and Applications of New Materials. *Adv. Funct. Mater.* **2021**, *31*, 2007226.
(313) Veiseh, O.; Vegas, A. J. Domesticating the Foreign Body Response: Recent Advances and Applications. *Adv. Drug Delivery Rev.* **2019**, *144*, 148−161.
(314) Babensee, J. E. 2.2.2 - Inflammation, Wound Healing, the Foreign-Body Response, and Alternative Tissue Responses. In *Biomaterials Science*, 4th ed.; Academic Press: 2020; pp 737−746.
(315) Tsai, Y.-T.; Zhou, J.; Weng, H.; Tang, E. N.; Baker, D. W.; Tang, L. Optical Imaging of Fibrin Deposition to Elucidate Participation of Mast Cells in Foreign Body Responses. *Biomaterials* **2014**, *35*, 2089−2096.
(316) Sun, B. K.; Siprashvili, Z.; Khavari, P. A. Advances in Skin Grafting and Treatment of Cutaneous Wounds. *Science* **2014**, *346*, 941−945.
(317) Christo, S. N.; Diener, K. R.; Bachhuka, A.; Vasilev, K.; Hayball, J. D. Innate Immunity and Biomaterials at the Nexus: Friends or Foes. *BioMed. Res. Int.* **2015**, *2015*, 342304.
(318) Anderson, J. M.; Rodriguez, A.; Chang, D. T. Foreign Body Reaction to Biomaterials. *Semin. Immunol.* **2008**, *20*, 86−100.
(319) Kolaczkowska, E.; Kubes, P. Neutrophil Recruitment and Function in Health and Inflammation. *Nat. Rev. Immunol.* **2013**, *13*, 159−175.
(320) Brinkmann, V.; Reichard, U.; Goosmann, C.; Fauler, B.; Uhlemann, Y.; Weiss, D. S.; Weinrauch, Y.; Zychlinsky, A. Neutrophil Extracellular Traps Kill Bacteria. *Science* **2004**, *303*, 1532−1535.

https://doi.org/10.1021/acs.chemrev.2c00344
Chem. Rev. 2022, 122, 17073−17154

(321) Mariani, E.; Lisignoli, G.; Borzi, R. M.; Pulsatelli, L. Biomaterials: Foreign Bodies or Tuners for the Immune Response? *Int. J. Mol. Sci.* **2019**, *20*, 636.
(322) Selders, G. S.; Fetz, A. E.; Radic, M. Z.; Bowlin, G. L. An Overview of the Role of Neutrophils in Innate Immunity, Inflammation and Host-Biomaterial Integration. *Regener. Biomater.* **2017**, *4*, 55−68.
(323) Grainger, D. W. All Charged up About Implanted Biomaterials. *Nat. Biotechnol.* **2013**, *31*, 507−509.
(324) Kastellorizios, M.; Tipnis, N.; Burgess, D. J. Foreign Body Reaction to Subcutaneous Implants. In *Immune Responses to Biosurfaces*; Lambris, J., Ekdahl, K., Ricklin, D., Nilsson, B., Eds.; Advances in Experimental Medicine and Biology 865; Springer International Publishing: 2015; pp 93−108..
(325) Li, C. M.; Guo, C. C.; Fitzpatrick, V.; Ibrahim, A.; Zwierstra, M. J.; Hanna, P.; Lechtig, A.; Nazarian, A.; Lin, S. J.; Kaplan, D. L. Design of Biodegradable, Implantable Devices towards Clinical Translation. *Nat. Rev. Mater.* **2020**, *5*, 61−81.
(326) Vishwakarma, A.; Bhise, N. S.; Evangelista, M. B.; Rouwkema, J.; Dokmeci, M. R.; Ghaemmaghami, A. M.; Vrana, N. E.; Khademhosseini, A. Engineering Immunomodulatory Biomaterials to Tune the Inflammatory Response. *Trends Biotechnol.* **2016**, *34*, 470−482.
(327) Madden, L. R.; Mortisen, D. J.; Sussman, E. M.; Dupras, S. K.; Fugate, J. A.; Cuy, J. L.; Hauch, K. D.; Laflamme, M. A.; Murry, C. E.; Ratner, B. D. Proangiogenic Scaffolds as Functional Templates for Cardiac Tissue Engineering. *Proc. Natl. Acad. Sci. U. S. A.* **2010**, *107*, 15211−15216.
(328) Mosser, D. M.; Edwards, J. P. Exploring the Full Spectrum of Macrophage Activation. *Nat. Rev. Immunol.* **2008**, *8*, 958−969.
(329) Hetrick, E. M.; Prichard, H. L.; Klitzman, B.; Schoenfisch, M. H. Reduced Foreign Body Response at Nitric Oxide-Releasing Subcutaneous Implants. *Biomaterials* **2007**, *28*, 4571−4580.
(330) Yesilyurt, V.; Veiseh, O.; Doloff, J. C.; Li, J.; Bose, S.; Xie, X.; Bader, A. R.; Chen, M.; Webber, M. J.; Vegas, A. J.; et al. A Facile and Versatile Method to Endow Biomaterial Devices with Zwitterionic Surface Coatings. *Adv. Healthcare Mater.* **2017**, *6*, 1601091.
(331) Wang, H.; Wu, Y.; Cui, C.; Yang, J.; Liu, W. Antifouling Super Water Absorbent Supramolecular Polymer Hydrogel as an Artificial Vitreous Body. *Adv. Sci.* **2018**, *5*, 1800711.
(332) Chen, X.; Lin, Z.; Feng, Y.; Tan, H.; Xu, X.; Luo, J.; Li, J. Zwitterionic Pmcp-Modified Polycaprolactone Surface for Tissue Engineering: Antifouling, Cell Adhesion Promotion, and Osteogenic Differentiation Properties. *Small* **2019**, *15*, 1903784.
(333) Liu, Q.; Chiu, A.; Wang, L.-H.; An, D.; Zhong, M.; Smink, A. M.; de Haan, B. J.; de Vos, P.; Keane, K.; Vegge, A.; et al. Zwitterionically Modified Alginates Mitigate Cellular Overgrowth for Cell Encapsulation. *Nat. Commun.* **2019**, *10*, 5262.
(334) Liu, Q.; Wang, X.; Chiu, A.; Liu, W.; Fuchs, S.; Wang, B.; Wang, L.-H.; Flanders, J.; Zhang, Y.; Wang, K.; et al. A Zwitterionic Polyurethane Nanoporous Device with Low Foreign-Body Response for Islet Encapsulation. *Adv. Mater.* **2021**, *33*, 2102852.
(335) Bekiari, E.; Kitsios, K.; Thabit, H.; Tauschmann, M.; Athanasiadou, E.; Karagiannis, T.; Haidich, A. B.; Hovorka, R.; Tsapas, A. Artificial Pancreas Treatment for Outpatients with Type 1 Diabetes: Systematic Review and Meta-Analysis. *BMJ.* **2018**, *361*, k1310.
(336) Liu, W.; Flanders, J. A.; Wang, L.-H.; Liu, Q.; Bowers, D. T.; Wang, K.; Chiu, A.; Wang, X.; Ernst, A. U.; Shariati, K.; et al. A Safe, Fibrosis-Mitigating, and Scalable Encapsulation Device Supports Long-Term Function of Insulin-Producing Cells. *Small* **2022**, *18*, 2104899.
(337) Gaisinskaya, A.; Ma, L.; Silbert, G.; Sorkin, R.; Tairy, O.; Goldberg, R.; Kampf, N.; Klein, J. Hydration Lubrication: Exploring a New Paradigm. *Faraday Discuss.* **2012**, *156*, 217−233.
(338) Raviv, U.; Klein, J. Fluidity of Bound Hydration Layers. *Science* **2002**, *297*, 1540−1543.
(339) Banquy, X.; Burdyńska, J.; Lee, D. W.; Matyjaszewski, K.; Israelachvili, J. Bioinspired Bottle-Brush Polymer Exhibits Low Friction and Amontons-Like Behavior. *J. Am. Chem. Soc.* **2014**, *136*, 6199−6202.
(340) Zappone, B.; Ruths, M.; Greene, G. W.; Jay, G. D.; Israelachvili, J. N. Adsorption, Lubrication, and Wear of Lubricin on Model Surfaces: Polymer Brush-Like Behavior of a Glycoprotein. *Biophys. J.* **2007**, *92*, 1693−1708.
(341) Chen, M.; Briscoe, W. H.; Armes, S. P.; Cohen, H.; Klein, J. Polyzwitterionic Brushes: Extreme Lubrication by Design. *Eur. Polym. J.* **2011**, *47*, 511−523.
(342) Yang, J.; Chen, H.; Xiao, S.; Shen, M.; Chen, F.; Fan, P.; Zhong, M.; Zheng, J. Salt-Responsive Zwitterionic Polymer Brushes with Tunable Friction and Antifouling Properties. *Langmuir* **2015**, *31*, 9125−9133.
(343) Adibnia, V.; Olszewski, M.; De Crescenzo, G.; Matyjaszewski, K.; Banquy, X. Superlubricity of Zwitterionic Bottlebrush Polymers in the Presence of Multivalent Ions. *J. Am. Chem. Soc.* **2020**, *142*, 14843−14847.
(344) Wang, Y.; Sun, Y.; Gu, Y.; Zhang, H. Articular Cartilage-Inspired Surface Functionalization for Enhanced Lubrication. *Adv. Mater. Interfaces* **2019**, *6*, 1900180.
(345) He, Y.; Chen, S.; Hower, J. C.; Bernards, M. T.; Jiang, S. Molecular Simulation Studies of Nanoscale Friction between Phosphorylcholine Self-Assembled Monolayer Surfaces: Correlation between Surface Hydration and Friction. *J. Chem. Phys.* **2007**, *127*, 084708.
(346) He, Y.; Shao, Q.; Chen, S.; Jiang, S. Water Mobility: A Bridge between the Hofmeister Series of Ions and the Friction of Zwitterionic Surfaces in Aqueous Environments. *J. Phys. Chem. C* **2011**, *115*, 15525−15531.
(347) Kyomoto, M.; Moro, T.; Miyaji, F.; Hashimoto, M.; Kawaguchi, H.; Takatori, Y.; Nakamura, K.; Ishihara, K. Effect of 2-Methacryloyloxyethyl Phosphorylcholine Concentration on Photo-Induced Graft Polymerization of Polyethylene in Reducing the Wear of Orthopaedic Bearing Surface. *J. Biomed. Mater. Res. Part A* **2008**, *86A*, 439−447.
(348) Kyomoto, M.; Moro, T.; Saiga, K.; Hashimoto, M.; Ito, H.; Kawaguchi, H.; Takatori, Y.; Ishihara, K. Biomimetic Hydration Lubrication with Various Polyelectrolyte Layers on Cross-Linked Polyethylene Orthopedic Bearing Materials. *Biomaterials* **2012**, *33*, 4451−4459.
(349) Chen, H.; Sun, T.; Yan, Y.; Ji, X.; Sun, Y.; Zhao, X.; Qi, J.; Cui, W.; Deng, L.; Zhang, H. Cartilage Matrix-Inspired Biomimetic Superlubricated Nanospheres for Treatment of Osteoarthritis. *Biomaterials* **2020**, *242*, 119931.
(350) Osaheni, A. O.; Ash-Shakoor, A.; Gitsov, I.; Mather, P. T.; Blum, M. M. Synthesis and Characterization of Zwitterionic Polymer Brush Functionalized Hydrogels with Ionic Responsive Coefficient of Friction. *Langmuir* **2020**, *36*, 3932−3940.
(351) Yang, J.; Han, Y.; Lin, J.; Zhu, Y.; Wang, F.; Deng, L.; Zhang, H.; Xu, X.; Cui, W. Ball-Bearing-Inspired Polyampholyte-Modified Microspheres as Bio-Lubricants Attenuate Osteoarthritis. *Small* **2020**, *16*, 2004519.
(352) Wan, L.; Wang, Y.; Tan, X.; Sun, Y.; Luo, J.; Zhang, H. Biodegradable Lubricating Mesoporous Silica Nanoparticles for Osteoarthritis Therapy. *Friction* **2022**, *10*, 68−79.
(353) Wan, H.; Ren, K.; Kaper, H. J.; Sharma, P. K. Cartilage Lamina Splendens Inspired Nanostructured Coating for Biomaterial Lubrication. *J. Colloid Interface Sci.* **2021**, *594*, 435−445.
(354) Hosoi, T.; Hasegawa, M.; Tone, S.; Nakasone, S.; Kishida, N.; Marin, E.; Zhu, W.; Pezzotti, G.; Sudo, A. MPC-Grafted Highly Cross-Linked Polyethylene Liners Retrieved from Short-Term Total Hip Arthroplasty: Further Evidences for the Unsuitability of the MPC Method. *J. Biomed. Mater. Res., Part B* **2020**, *108*, 2857−2867.
(355) Zhang, K.; Yang, J.; Sun, Y.; Wang, Y.; Liang, J.; Luo, J.; Cui, W.; Deng, L.; Xu, X.; Wang, B.; et al. Gelatin-Based Composite Hydrogels with Biomimetic Lubrication and Sustained Drug Release. *Friction* **2022**, *10*, 232−246.

https://doi.org/10.1021/acs.chemrev.2c00344
Chem. Rev. 2022, 122, 17073−17154

(356) Bonyadi, S. Z.; Demott, C. J.; Grunlan, M. A.; Dunn, A. C. Cartilage-Like Tribological Performance of Charged Double Network Hydrogels. *J. Mech. Behav. Biomed. Mater.* **2021**, *114*, 104202.
(357) Xiao, S.; He, X.; Zhao, Z.; Huang, G.; Yan, Z.; He, Z.; Zhao, Z.; Chen, F.; Yang, J. Strong Anti-Polyelectrolyte Zwitterionic Hydrogels with Superior Self-Recovery, Tunable Surface Friction, Conductivity, and Antifreezing Properties. *Eur. Polym. J.* **2021**, *148*, 110350.
(358) Osaheni, A. O.; Finkelstein, E. B.; Mather, P. T.; Blum, M. M. Synthesis and Characterization of a Zwitterionic Hydrogel Blend with Low Coefficient of Friction. *Acta Biomater.* **2016**, *46*, 245−255.
(359) Wang, Z.; Li, J.; Liu, Y.; Luo, J. Synthesis and Characterizations of Zwitterionic Copolymer Hydrogels with Excellent Lubrication Behavior. *Tribol. Int.* **2020**, *143*, 106026.
(360) Lin, W.; Kluzek, M.; Iuster, N.; Shimoni, E.; Kampf, N.; Goldberg, R.; Klein, J. Cartilage-Inspired, Lipid-Based Boundary-Lubricated Hydrogels. *Science* **2020**, *370*, 335−338.
(361) Lewis, K. Riddle of Biofilm Resistance. *Antimicrob. Agents Chemother.* **2001**, *45*, 999−1007.
(362) Jamal, M.; Ahmad, W.; Andleeb, S.; Jalil, F.; Imran, M.; Nawaz, M. A.; Hussain, T.; Ali, M.; Rafiq, M.; Kamil, M. A. Bacterial Biofilm and Associated Infections. *J. Chin. Med. Assoc.* **2018**, *81*, 7−11.
(363) Karygianni, L.; Ren, Z.; Koo, H.; Thurnheer, T. Biofilm Matrixome: Extracellular Components in Structured Microbial Communities. *Trends Microbiol.* **2020**, *28*, 668−681.
(364) Bryers, J. D.; Ratner, B. D. Bioinspired Implant Materials Befuddle Bacteria. *ASM News* **2004**, *70*, 232−237.
(365) Palmer, J.; Flint, S.; Brooks, J. Bacterial Cell Attachment, the Beginning of a Biofilm. *J. Ind. Microbiol. Biotechnol.* **2007**, *34*, 577−588.
(366) Friedlander, R. S.; Vlamakis, H.; Kim, P.; Khan, M.; Kolter, R.; Aizenberg, J. Bacterial Flagella Explore Microscale Hummocks and Hollows to Increase Adhesion. *Proc. Natl. Acad. Sci. U. S. A.* **2013**, *110*, 5624−5629.
(367) Ren, Y.; Wang, C.; Chen, Z.; Allan, E.; van der Mei, H. C.; Busscher, H. J. Emergent Heterogeneous Microenvironments in Biofilms: Substratum Surface Heterogeneity and Bacterial Adhesion Force-Sensing. *FEMS Microbiol. Rev.* **2018**, *42*, 259−272.
(368) Carpentier, B.; Cerf, O. Biofilms and Their Consequences, with Particular Reference to Hygiene in the Food Industry. *J. Appl. Bacteriol.* **1993**, *75*, 499−511.
(369) Kang, S.; Lee, M.; Kang, M.; Noh, M.; Jeon, J.; Lee, Y.; Seo, J.-H. Development of Anti-Biofouling Interface on Hydroxyapatite Surface by Coating Zwitterionic MPC Polymer Containing Calcium-Binding Moieties to Prevent Oral Bacterial Adhesion. *Acta Biomater.* **2016**, *40*, 70−77.
(370) Li, G.; Xue, H.; Cheng, G.; Chen, S.; Zhang, F.; Jiang, S. Ultralow Fouling Zwitterionic Polymers Grafted from Surfaces Covered with an Initiator via an Adhesive Mussel Mimetic Linkage. *J. Phys. Chem. B* **2008**, *112*, 15269−15274.
(371) Li, G.; Cheng, G.; Xue, H.; Chen, S.; Zhang, F.; Jiang, S. Ultra Low Fouling Zwitterionic Polymers with a Biomimetic Adhesive Group. *Biomaterials* **2008**, *29*, 4592−4597.
(372) Diaz Blanco, C.; Ortner, A.; Dimitrov, R.; Navarro, A.; Mendoza, E.; Tzanov, T. Building an Antifouling Zwitterionic Coating on Urinary Catheters Using an Enzymatically Triggered Bottom-up Approach. *ACS Appl. Mater. Interfaces* **2014**, *6*, 11385−11393.
(373) Kwon, H. J.; Lee, Y.; Phuong, L. T.; Seon, G. M.; Kim, E.; Park, J. C.; Yoon, H.; Park, K. D. Zwitterionic Sulfobetaine Polymer-Immobilized Surface by Simple Tyrosinase-Mediated Grafting for Enhanced Antifouling Property. *Acta Biomater.* **2017**, *61*, 169−179.
(374) Cheng, G.; Li, G.; Xue, H.; Chen, S.; Bryers, J. D.; Jiang, S. Zwitterionic Carboxybetaine Polymer Surfaces and Their Resistance to Long-Term Biofilm Formation. *Biomaterials* **2009**, *30*, 5234−5240.
(375) Wang, W.; Lu, Y.; Zhu, H.; Cao, Z. Superdurable Coating Fabricated from a Double-Sided Tape with Long Term "Zero" Bacterial Adhesion. *Adv. Mater.* **2017**, *29*, 1606506.
(376) Wang, H.; Hu, Y.; Lynch, D.; Young, M.; Li, S.; Cong, H.; Xu, F.-J.; Cheng, G. Zwitterionic Polyurethanes with Tunable Surface and Bulk Properties. *ACS Appl. Mater. Interfaces* **2018**, *10*, 37609−37617.
(377) Wang, H. F.; Christiansen, D. E.; Mehraeen, S.; Cheng, G. Winning the Fight against Biofilms: The First Six-Month Study Showing No Biofilm Formation on Zwitterionic Polyurethanes. *Chem. Sci.* **2020**, *11*, 4709−4721.
(378) Liu, G.; Li, K.; Wang, H.; Ma, L.; Yu, L.; Nie, Y. Stable Fabrication of Zwitterionic Coating Based on Copper-Phenolic Networks on Contact Lens with Improved Surface Wettability and Broad-Spectrum Antimicrobial Activity. *ACS Appl. Mater. Interfaces* **2020**, *12*, 16125−16136.
(379) Venault, A.; Yang, H.-S.; Chiang, Y.-C.; Lee, B.-S.; Ruaan, R.-C.; Chang, Y. Bacterial Resistance Control on Mineral Surfaces of Hydroxyapatite and Human Teeth via Surface Charge-Driven Antifouling Coatings. *ACS Appl. Mater. Interfaces* **2014**, *6*, 3201−3210.
(380) Sun, F.; Hung, H.-C.; Yan, W.; Wu, K.; Shimchuk, A. A.; Gray, S. D.; He, W.; Huang, X.; Zhang, H. Inhibition of Oral Biofilm Formation by Zwitterionic Nonfouling Coating. *J. Biomed. Mater. Res., Part B* **2021**, *109*, 1418−1425.
(381) Yan, S.; Luan, S.; Shi, H.; Xu, X.; Zhang, J.; Yuan, S.; Yang, Y.; Yin, J. Hierarchical Polymer Brushes with Dominant Antibacterial Mechanisms Switching from Bactericidal to Bacteria Repellent. *Biomacromolecules* **2016**, *17*, 1696−1704.
(382) Ma, Y.; Li, J.; Si, Y.; Huang, K.; Nitin, N.; Sun, G. Rechargeable Antibacterial N-Halamine Films with Antifouling Function for Food Packaging Applications. *ACS Appl. Mater. Interfaces* **2019**, *11*, 17814−17822.
(383) He, Y.; Wan, X.; Xiao, K.; Lin, W.; Li, J.; Li, Z.; Luo, F.; Tan, H.; Li, J.; Fu, Q. Anti-Biofilm Surfaces from Mixed Dopamine-Modified Polymer Brushes: Synergistic Role of Cationic and Zwitterionic Chains to Resist Staphyloccocus Aureus. *Biomater. Sci.* **2019**, *7*, 5369−5382.
(384) Blackman, L. D.; Fros, M. K.; Welch, N. G.; Gengenbach, T. R.; Qu, Y.; Pasic, P.; Gunatillake, P. A.; Thissen, H.; Cass, P.; Locock, K. E. S. Dual Action Antimicrobial Surfaces: Alternating Photopatterns Maintain Contact-Killing Properties with Reduced Biofilm Formation. *Macromol. Mater. Eng.* **2020**, *305*, 2000371.
(385) Ma, Y.; Zhang, Z.; Nitin, N.; Sun, G. Integration of Photo-Induced Biocidal and Hydrophilic Antifouling Functions on Nanofibrous Membranes with Demonstrated Reduction of Biofilm Formation. *J. Colloid Interface Sci.* **2020**, *578*, 779−787.
(386) Lee, C. J.; Wu, H. Y.; Tang, Q.; Cao, B.; Wang, H. F.; Cong, H. B.; Zhe, J.; Xu, F. J.; Cheng, G. Structure-Function Relationships of a Tertiary Amine-Based Polycarboxybetaine. *Langmuir* **2015**, *31*, 9965−9972.
(387) Cao, B.; Lee, C.-J.; Zeng, Z.; Cheng, F.; Xu, F.; Cong, H.; Cheng, G. Electroactive Poly(sulfobetaine-3,4-ethylenedioxythiophene) (PSBEDOT) with Controllable Antifouling and Antimicrobial Properties. *Chem. Sci.* **2016**, *7*, 1976−1981.
(388) Cheng, G.; Xue, H.; Li, G. Z.; Jiang, S. Y. Integrated Antimicrobial and Nonfouling Hydrogels to Inhibit the Growth of Planktonic Bacterial Cells and Keep the Surface Clean. *Langmuir* **2010**, *26*, 10425−10428.
(389) Mi, L.; Jiang, S. Y. Synchronizing Nonfouling and Antimicrobial Properties in a Zwitterionic Hydrogel. *Biomaterials* **2012**, *33*, 8928−8933.
(390) Sun, G.; Zhang, X.; Shen, Y.; Sebastian, R.; Dickinson, L. E.; Fox-Talbot, K.; Reinblatt, M.; Steenbergen, C.; Harmon, J. W.; Gerecht, S. Dextran Hydrogel Scaffolds Enhance Angiogenic Responses and Promote Complete Skin Regeneration During Burn Wound Healing. *Proc. Natl. Acad. Sci. U. S. A.* **2011**, *108*, 20976−20981.
(391) Eming, S. A.; Wynn, T. A.; Martin, P. Inflammation and Metabolism in Tissue Repair and Regeneration. *Science* **2017**, *356*, 1026−1030.

(392) Huang, K. T.; Fang, Y. L.; Hsieh, P. S.; Li, C. C.; Dai, N. T.; Huang, C. J. Zwitterionic Nanocomposite Hydrogels as Effective Wound Dressings. *J. Mater. Chem. B* **2016**, *4*, 4206−4215.
(393) Zhu, Y.; Zhang, J.; Yang, J.; Pan, C.; Xu, T.; Zhang, L. Zwitterionic Hydrogels Promote Skin Wound Healing. *J. Mater. Chem. B* **2016**, *4*, 5105−5111.
(394) Zhu, Y.; Zhang, J.; Song, J.; Yang, J.; Xu, T.; Pan, C.; Zhang, L. One-Step Synthesis of an Antibacterial and Pro-Healing Wound Dressing That Can Treat Wound Infections. *J. Mater. Chem. B* **2017**, *5*, 8451−8458.
(395) Wu, J.; Xiao, Z.; Chen, A.; He, H.; He, C.; Shuai, X.; Li, X.; Chen, S.; Zhang, Y.; Ren, B.; et al. Sulfated Zwitterionic Poly(sulfobetaine methacrylate) Hydrogels Promote Complete Skin Regeneration. *Acta Biomater.* **2018**, *71*, 293−305.
(396) Qiu, X.; Zhang, J.; Cao, L.; Jiao, Q.; Zhou, J.; Yang, L.; Zhang, H.; Wei, Y. Antifouling Antioxidant Zwitterionic Dextran Hydrogels as Wound Dressing Materials with Excellent Healing Activities. *ACS Appl. Mater. Interfaces* **2021**, *13*, 7060−7069.
(397) Venault, A.; Lin, K. H.; Tang, S. H.; Dizon, G. V.; Hsu, C. H.; Maggay, I. V. B.; Chang, Y. Zwitterionic Electrospun PVDF Fibrous Membranes with a Well-Controlled Hydration for Diabetic Wound Recovery. *J. Membr. Sci.* **2020**, *598*, 117648.
(398) Guo, H.; Bai, M.; Zhu, Y.; Liu, X.; Tian, S.; Long, Y.; Ma, Y.; Wen, C.; Li, Q.; Yang, J.; et al. Pro-Healing Zwitterionic Skin Sensor Enables Multi-Indicator Distinction and Continuous Real-Time Monitoring. *Adv. Funct. Mater.* **2021**, *31*, 2106406.
(399) Behzadi, S.; Serpooshan, V.; Tao, W.; Hamaly, M. A.; Alkawareek, M. Y.; Dreaden, E. C.; Brown, D.; Alkilany, A. M.; Farokhzad, O. C.; Mahmoudi, M. Cellular Uptake of Nanoparticles: Journey inside the Cell. *Chem. Soc. Rev.* **2017**, *46*, 4218−4244.
(400) Hillaireau, H.; Couvreur, P. Nanocarriers' Entry into the Cell: Relevance to Drug Delivery. *Cell. Mol. Life Sci.* **2009**, *66*, 2873−2896.
(401) Caracciolo, G.; Palchetti, S.; Digiacomo, L.; Chiozzi, R. Z.; Capriotti, A. L.; Amenitsch, H.; Tentori, P. M.; Palmieri, V.; Papi, M.; Cardarelli, F.; et al. Human Biomolecular Corona of Liposomal Doxorubicin: The Overlooked Factor in Anticancer Drug Delivery. *ACS Appl. Mater. Interfaces* **2018**, *10*, 22951−22962.
(402) Li, N.; Wang, Z.; Zhang, L.; Nian, L.; Lei, L.; Yang, X.; Zhang, H.; Yu, A. Liquid-Phase Extraction Coupled with Metal-Organic Frameworks-Based Dispersive Solid Phase Extraction of Herbicides in Peanuts. *Talanta* **2014**, *128*, 345−353.
(403) Cao, Z.; Jiang, S. Super-Hydrophilic Zwitterionic Poly(carboxybetaine) and Amphiphilic Non-Ionic Poly(ethylene glycol) for Stealth Nanoparticles. *Nano Today* **2012**, *7*, 404−413.
(404) Cao, Z.; Yu, Q.; Xue, H.; Cheng, G.; Jiang, S. Nanoparticles for Drug Delivery Prepared from Amphiphilic PLGA Zwitterionic Block Copolymers with Sharp Contrast in Polarity between Two Blocks. *Angew. Chem., Int. Ed.* **2010**, *49*, 3771−3776.
(405) Cheng, G.; Mi, L.; Cao, Z.; Xue, H.; Yu, Q.; Carr, L.; Jiang, S. Functionalizable and Ultrastable Zwitterionic Nanogels. *Langmuir* **2010**, *26*, 6883−6886.
(406) Li, Y.; Cheng, Q.; Jiang, Q.; Huang, Y.; Liu, H.; Zhao, Y.; Cao, W.; Ma, G.; Dai, F.; Liang, X.; et al. Enhanced Endosomal/Lysosomal Escape by Distearoyl Phosphoethanolamine-Polycarboxybetaine Lipid for Systemic Delivery of Sirna. *J. Controlled Release* **2014**, *176*, 104−114.
(407) Lu, Y.; Yue, Z.; Xie, J.; Wang, W.; Zhu, H.; Zhang, E.; Cao, Z. Micelles with Ultralow Critical Micelle Concentration as Carriers for Drug Delivery. *Nat. Biomed. Eng.* **2018**, *2*, 318−325.
(408) Zhu, Y.; Sundaram, H. S.; Liu, S.; Zhang, L.; Xu, X.; Yu, Q.; Xu, J.; Jiang, S. A Robust Graft-to Strategy to Form Multifunctional and Stealth Zwitterionic Polymer-Coated Mesoporous Silica Nanoparticles. *Biomacromolecules* **2014**, *15*, 1845−1851.
(409) Ye, L.; Zhang, Y.; Yang, B.; Zhou, X.; Li, J.; Qin, Z.; Dong, D.; Cui, Y.; Yao, F. Zwitterionic-Modified Starch-Based Stealth Micelles for Prolonging Circulation Time and Reducing Macrophage Response. *ACS Appl. Mater. Interfaces* **2016**, *8*, 4385−4398.
(410) Lin, W.; Ma, G.; Ji, F.; Zhang, J.; Wang, L.; Sun, H.; Chen, S. Biocompatible Long-Circulating Star Carboxybetaine Polymers. *J. Mater. Chem. B* **2015**, *3*, 440−448.
(411) Wang, Z.; Ma, G.; Zhang, J.; Lin, W.; Ji, F.; Bernards, M. T.; Chen, S. Development of Zwitterionic Polymer-Based Doxorubicin Conjugates: Tuning the Surface Charge to Prolong the Circulation and Reduce Toxicity. *Langmuir* **2014**, *30*, 3764−3774.
(412) Zhou, Q.; Shao, S.; Wang, J.; Xu, C.; Xiang, J.; Piao, Y.; Zhou, Z.; Yu, Q.; Tang, J.; Liu, X.; et al. Enzyme-Activatable Polymer-Drug Conjugate Augments Tumour Penetration and Treatment Efficacy. *Nat. Nanotechnol.* **2019**, *14*, 799−809.
(413) Men, Y.; Peng, S.; Yang, P.; Jiang, Q.; Zhang, Y.; Shen, B.; Dong, P.; Pang, Z.; Yang, W. Biodegradable Zwitterionic Nanogels with Long Circulation for Antitumor Drug Delivery. *ACS Appl. Mater. Interfaces* **2018**, *10*, 23509−23521.
(414) Peng, S.; Ouyang, B.; Xin, Y.; Zhao, W.; Shen, S.; Zhan, M.; Lu, L. Hypoxia-Degradable and Long-Circulating Zwitterionic Phosphorylcholine-Based Nanogel for Enhanced Tumor Drug Delivery. *Acta Pharm. Sin. B* **2021**, *11*, 560−571.
(415) Liu, Z.; Chen, X.; Zhang, X.; Gooding, J. J.; Zhou, Y. Carbon-Quantum-Dots-Loaded Mesoporous Silica Nanocarriers with Ph-Switchable Zwitterionic Surface and Enzyme-Responsive Pore-Cap for Targeted Imaging and Drug Delivery to Tumor. *Adv. Healthcare Mater.* **2016**, *5*, 1401−1407.
(416) Cao, Z.; Zhang, L.; Jiang, S. Superhydrophilic Zwitterionic Polymers Stabilize Liposomes. *Langmuir* **2012**, *28*, 11625−11632.
(417) Wang, L. L.; Shi, C. Y.; Wang, X.; Guo, D. D.; Duncan, T. M.; Luo, J. T. Zwitterionic Janus Dendrimer with Distinct Functional Disparity for Enhanced Protein Delivery. *Biomaterials* **2019**, *215*, 119233.
(418) Lin, W.; Ma, G.; Kampf, N.; Yuan, Z.; Chen, S. Development of Long-Circulating Zwitterionic Cross-Linked Micelles for Active-Targeted Drug Delivery. *Biomacromolecules* **2016**, *17*, 2010−2018.
(419) Li, G.; Sun, B.; Zheng, S.; Xu, L.; Tao, W.; Zhao, D.; Yu, J.; Fu, S.; Zhang, X.; Zhang, H.; et al. Zwitterion-Driven Shape Program of Prodrug Nanoassemblies with High Stability, High Tumor Accumulation, and High Antitumor Activity. *Adv. Healthcare Mater.* **2021**, *10*, 2101407.
(420) Morimoto, N.; Wakamura, M.; Muramatsu, K.; Toita, S.; Nakayama, M.; Shoji, W.; Suzuki, M.; Winnik, F. M. Membrane Translocation and Organelle-Selective Delivery Steered by Polymeric Zwitterionic Nanospheres. *Biomacromolecules* **2016**, *17*, 1523−1535.
(421) Zhang, L.; Cao, Z. Q.; Li, Y. T.; Ella-Menye, J. R.; Bai, T.; Jiang, S. Y. Softer Zwitterionic Nanogels for Longer Circulation and Lower Splenic Accumulation. *ACS Nano* **2012**, *6*, 6681−6686.
(422) Zhao, G.; Sun, Y.; Dong, X. Zwitterionic Polymer Micelles with Dual Conjugation of Doxorubicin and Curcumin: Synergistically Enhanced Efficacy against Multidrug-Resistant Tumor Cells. *Langmuir* **2020**, *36*, 2383−2395.
(423) Ensign, L. M.; Schneider, C.; Suk, J. S.; Cone, R.; Hanes, J. Mucus Penetrating Nanoparticles: Biophysical Tool and Method of Drug and Gene Delivery. *Adv. Mater.* **2012**, *24*, 3887−3894.
(424) Cone, R. A. Barrier Properties of Mucus. *Adv. Drug Delivery Rev.* **2009**, *61*, 75−85.
(425) Han, X.; Lu, Y.; Xie, J.; Zhang, E.; Zhu, H.; Du, H.; Wang, K.; Song, B.; Yang, C.; Shi, Y.; et al. Zwitterionic Micelles Efficiently Deliver Oral Insulin without Opening Tight Junctions. *Nat. Nanotechnol.* **2020**, *15*, 605−614.
(426) Biosca, A.; Cabanach, P.; Abdulkarim, M.; Gumbleton, M.; Gómez-Canela, C.; Ramírez, M.; Bouzón-Arnáiz, I.; Avalos-Padilla, Y.; Borros, S.; Fernàndez-Busquets, X. Zwitterionic Self-Assembled Nanoparticles as Carriers for Plasmodium Targeting in Malaria Oral Treatment. *J. Controlled Release* **2021**, *331*, 364−375.
(427) Rao, R.; Liu, X. H.; Li, Y. H.; Tan, X.; Zhou, H.; Bai, X. C.; Yang, X. L.; Liu, W. Bioinspired Zwitterionic Polyphosphoester Modified Porous Silicon Nanoparticles for Efficient Oral Insulin Delivery. *Biomater. Sci.* **2021**, *9*, 685−699.
(428) Shan, W.; Zhu, X.; Tao, W.; Cui, Y.; Liu, M.; Wu, L.; Li, L.; Zheng, Y.; Huang, Y. Enhanced Oral Delivery of Protein Drugs Using

https://doi.org/10.1021/acs.chemrev.2c00344
Chem. Rev. 2022, 122, 17073−17154

Zwitterion-Functionalized Nanoparticles to Overcome Both the Diffusion and Absorption Barriers. *ACS Appl. Mater. Interfaces* **2016**, *8*, 25444−25453.
(429) Taipaleenmäki, E.; Brodszkij, E.; Städler, B. Mucopenetrating Zwitterionic Micelles. *ChemNanoMat* **2020**, *6*, 744−750.
(430) Gao, Y.; He, Y.; Zhang, H.; Zhang, Y.; Gao, T.; Wang, J.-H.; Wang, S. Zwitterion-Functionalized Mesoporous Silica Nanoparticles for Enhancing Oral Delivery of Protein Drugs by Overcoming Multiple Gastrointestinal Barriers. *J. Colloid Interface Sci.* **2021**, *582*, 364−375.
(431) Li, Y.; Ji, W.; Peng, H.; Zhao, R.; Zhang, T.; Lu, Z.; Yang, J.; Liu, R.; Zhang, X. Charge-Switchable Zwitterionic Polycarboxybetaine Particle as an Intestinal Permeation Enhancer for Efficient Oral Insulin Delivery. *Theranostics* **2021**, *11*, 4452−4466.
(432) Banerjee, A.; Ibsen, K.; Brown, T.; Chen, R. W.; Agatemor, C.; Mitragotri, S. Ionic Liquids for Oral Insulin Delivery. *Proc. Natl. Acad. Sci. U. S. A.* **2018**, *115*, 7296−7301.
(433) Maher, S.; Mrsny, R. J.; Brayden, D. J. Intestinal Permeation Enhancers for Oral Peptide Delivery. *Adv. Drug Delivery Rev.* **2016**, *106*, 277−319.
(434) McCartney, F.; Gleeson, J. P.; Brayden, D. J. Safety Concerns over the Use of Intestinal Permeation Enhancers: A Mini-Review. *Tissue Barriers* **2016**, *4*, No. e1176822.
(435) Wu, D.; Qin, M.; Xu, D.; Wang, L.; Liu, C.; Ren, J.; Zhou, G.; Chen, C.; Yang, F.; Li, Y.; et al. A Bioinspired Platform for Effective Delivery of Protein Therapeutics to the Central Nervous System. *Adv. Mater.* **2019**, *31*, 1807557.
(436) Han, L.; Liu, C.; Qi, H.; Zhou, J.; Wen, J.; Wu, D.; Xu, D.; Qin, M.; Ren, J.; Wang, Q.; et al. Systemic Delivery of Monoclonal Antibodies to the Central Nervous System for Brain Tumor Therapy. *Adv. Mater.* **2019**, *31*, 1805697.
(437) Wen, J.; Wu, D.; Qin, M.; Liu, C.; Wang, L.; Xu, D.; Vinters, H. V.; Liu, Y.; Kranz, E.; Guan, X.; et al. Sustained Delivery and Molecular Targeting of a Therapeutic Monoclonal Antibody to Metastases in the Central Nervous System of Mice. *Nat. Biomed. Eng.* **2019**, *3*, 706−716.
(438) Xu, D.; Wu, D.; Qin, M.; Nih, L. R.; Liu, C.; Cao, Z.; Ren, J.; Chen, X.; He, Z.; Yu, W.; et al. Efficient Delivery of Nerve Growth Factors to the Central Nervous System for Neural Regeneration. *Adv. Mater.* **2019**, *31*, 1900727.
(439) Zhou, Y.; Holmseth, S.; Hua, R.; Lehre, A. C.; Olofsson, A. M.; Poblete-Naredo, I.; Kempson, S. A.; Danbolt, N. C. The Betaine-GABA Transporter (BGT1, slc6a12) Is Predominantly Expressed in the Liver and at Lower Levels in the Kidneys and at the Brain Surface. *Am. J. Physiol. Ren. Physiol.* **2012**, *302*, F316−F328.
(440) Wang, R.; Yang, S.; Xiao, P.; Sun, Y.; Li, J.; Jiang, X.; Wu, W. Fluorination and Betaine Modification Augment the Blood-Brain Barrier-Crossing Ability of Cylindrical Polymer Brushes. *Angew. Chem., Int. Ed.* **2022**, *61*, No. e202201390.
(441) Jin, Q.; Deng, Y.; Chen, X.; Ji, J. Rational Design of Cancer Nanomedicine for Simultaneous Stealth Surface and Enhanced Cellular Uptake. *ACS Nano* **2019**, *13*, 954−977.
(442) Cabanach, P.; Pena-Francesch, A.; Sheehan, D.; Bozuyuk, U.; Yasa, O.; Borros, S.; Sitti, M. Zwitterionic 3D-Printed Non-Immunogenic Stealth Microrobots. *Adv. Mater.* **2020**, *32*, 2003013.
(443) Wang, X.; Sun, X.; Jiang, G.; Wang, R.; Hu, R.; Xi, X.; Zhou, Y.; Wang, S.; Wang, T. Synthesis of Biomimetic Hyperbranched Zwitterionic Polymers as Targeting Drug Delivery Carriers. *J. Appl. Polym. Sci.* **2013**, *128*, 3289−3294.
(444) Zhang, L.; Xue, H.; Gao, C. L.; Carr, L.; Wang, J. N.; Chu, B. C.; Jiang, S. Y. Imaging and Cell Targeting Characteristics of Magnetic Nanoparticles Modified by a Functionalizable Zwitterionic Polymer with Adhesive 3,4-Dihydroxyphenyl-L-Alanine Linkages. *Biomaterials* **2010**, *31*, 6582−6588.
(445) Li, W. C.; Liu, Q. S.; Zhang, P.; Liu, L. Y. Zwitterionic Nanogels Crosslinked by Fluorescent Carbon Dots for Targeted Drug Delivery and Simultaneous Bioimaging. *Acta Biomater.* **2016**, *40*, 254−262.
(446) Lin, W.; Ma, G.; Yuan, Z.; Qian, H.; Xu, L.; Sidransky, E.; Chen, S. Development of Zwitterionic Polypeptide Nanoformulation with High Doxorubicin Loading Content for Targeted Drug Delivery. *Langmuir* **2019**, *35*, 1273−1283.
(447) Pillai, P. P.; Huda, S.; Kowalczyk, B.; Grzybowski, B. A. Controlled pH Stability and Adjustable Cellular Uptake of Mixed-Charge Nanoparticles. *J. Am. Chem. Soc.* **2013**, *135*, 6392−6395.
(448) Wang, Z.; Ma, G. L.; Zhang, J.; Yuan, Z. F.; Wang, L. G.; Bernards, M.; Chen, S. F. Surface Protonation/Deprotonation Controlled Instant Affinity Switch of Nano Drug Vehicle (NDV) for pH Triggered Tumor Cell Targeting. *Biomaterials* **2015**, *62*, 116−127.
(449) Yuan, Y. Y.; Mao, C. Q.; Du, X. J.; Du, J. Z.; Wang, F.; Wang, J. Surface Charge Switchable Nanoparticles Based on Zwitterionic Polymer for Enhanced Drug Delivery to Tumor. *Adv. Mater.* **2012**, *24*, 5476−5480.
(450) Jin, R.; Liu, Z.; Bai, Y.; Zhou, Y.; Chen, X. Multiple-Responsive Mesoporous Silica Nanoparticles for Highly Accurate Drugs Delivery to Tumor Cells. *ACS Omega* **2018**, *3*, 4306−4315.
(451) Qin, Z.; Chen, T.; Teng, W.; Jin, Q.; Ji, J. Mixed-Charged Zwitterionic Polymeric Micelles for Tumor Acidic Environment Responsive Intracellular Drug Delivery. *Langmuir* **2019**, *35*, 1242−1248.
(452) Wang, S.; Zhang, F. W.; Yu, G. C.; Wang, Z. T.; Jacobson, O.; Ma, Y.; Tian, R.; Deng, H. Z.; Yang, W. J.; Chen, Z. Y.; et al. Zwitterionic-to-Cationic Charge Conversion Polyprodrug Nanomedicine for Enhanced Drug Delivery. *Theranostics* **2020**, *10*, 6629−6637.
(453) Wang, G.; Wu, B.; Li, Q.; Chen, S.; Jin, X.; Liu, Y.; Zhou, Z.; Shen, Y.; Huang, P. Active Transportation of Liposome Enhances Tumor Accumulation, Penetration, and Therapeutic Efficacy. *Small* **2020**, *16*, 2004172.
(454) She, D.; Huang, H.; Li, J.; Peng, S.; Wang, H.; Yu, X. Hypoxia-Degradable Zwitterionic Phosphorylcholine Drug Nanogel for Enhanced Drug Delivery to Glioblastoma. *Chem. Eng. J.* **2021**, *408*, 127359.
(455) Yin, T.; Chu, X.; Cheng, J.; Liang, J.; Zhou, J.; Huo, M. Hypoxia-Sensitive Zwitterionic Vehicle for Tumor-Specific Drug Delivery through Antifouling-Based Stable Biotransport Alongside PDT-Sensitized Controlled Release. *Biomacromolecules* **2021**, *22*, 2233−2247.
(456) Goda, T.; Miyahara, Y.; Ishihara, K. Phospholipid-Mimicking Cell-Penetrating Polymers: Principles and Applications. *J. Mater. Chem. B* **2020**, *8*, 7633−7641.
(457) Goda, T.; Goto, Y.; Ishihara, K. Cell-Penetrating Macromolecules: Direct Penetration of Amphipathic Phospholipid Polymers across Plasma Membrane of Living Cells. *Biomaterials* **2010**, *31*, 2380−2387.
(458) Copolovici, D. M.; Langel, K.; Eriste, E.; Langel, Ü. Cell-Penetrating Peptides: Design, Synthesis, and Applications. *ACS Nano* **2014**, *8*, 1972−1994.
(459) Guidotti, G.; Brambilla, L.; Rossi, D. Cell-Penetrating Peptides: From Basic Research to Clinics. *Trends Pharmacol. Sci.* **2017**, *38*, 406−424.
(460) Goda, T.; Imaizumi, Y.; Hatano, H.; Matsumoto, A.; Ishihara, K.; Miyahara, Y. Translocation Mechanisms of Cell-Penetrating Polymers Identified by Induced Proton Dynamics. *Langmuir* **2019**, *35*, 8167−8173.
(461) Imaizumi, Y.; Goda, T.; Schaffhauser, D. F.; Okada, J.-i.; Matsumoto, A.; Miyahara, Y. Proton-Sensing Transistor Systems for Detecting Ion Leakage from Plasma Membranes under Chemical Stimuli. *Acta Biomater.* **2017**, *50*, 502−509.
(462) Konno, T.; Watanabe, J.; Ishihara, K. Enhanced Solubility of Paclitaxel Using Water-Soluble and Biocompatible 2-Methacryloyloxyethyl Phosphorylcholine Polymers. *J. Biomed. Mater. Res. Part A* **2003**, *65A*, 209−214.
(463) Wada, M.; Jinno, H.; Ueda, M.; Ikeda, T.; Kitajima, M.; Konno, T.; Watanabe, J.; Ishihara, K. Efficacy of an MPC-BMA Co-

Polymer as a Nanotransporter for Paclitaxel. *Anticancer Res.* **2007**, *27*, 1431−1435.
(464) Soma, D.; Kitayama, J.; Konno, T.; Ishihara, K.; Yamada, J.; Kamei, T.; Ishigami, H.; Kaisaki, S.; Nagawa, H. Intraperitoneal Administration of Paclitaxel Solubilized with Poly(2-methacryloxyethyl phosphorylcholine-co *N*-butyl methacrylate) for Peritoneal Dissemination of Gastric Cancer. *Cancer Sci.* **2009**, *100*, 1979−1985.
(465) Hatano, H.; Meng, F.; Sakata, M.; Matsumoto, A.; Ishihara, K.; Miyahara, Y.; Goda, T. Transepithelial Delivery of Insulin Conjugated with Phospholipid-Mimicking Polymers via Biomembrane Fusion-Mediated Transcellular Pathways. *Acta Biomater.* **2022**, *140*, 674−685.
(466) Kaneko, M.; Ishikawa, M.; Nakanishi, S.; Ishihara, K. Anticancer Activity of Cell-Penetrating Redox Phospholipid Polymers. *ACS Macro Lett.* **2021**, *10*, 926−932.
(467) Wang, J.; Yuan, S.; Zhang, Y.; Wu, W.; Hu, Y.; Jiang, X. The Effects of Poly(zwitterions)s versus Poly(ethylene glycol) Surface Coatings on the Biodistribution of Protein Nanoparticles. *Biomater. Sci.* **2016**, *4*, 1351−1360.
(468) Zhou, W.; Shao, J.; Jin, Q.; Wei, Q.; Tang, J.; Ji, J. Zwitterionic Phosphorylcholine as a Better Ligand for Gold Nanorods Cell Uptake and Selective Photothermal Ablation of Cancer Cells. *Chem. Commun.* **2010**, *46*, 1479−1481.
(469) Chen, L.; Wang, H.; Zhang, Y.; Wang, Y.; Hu, Q.; Ji, J. Bioinspired Phosphorylcholine-Modified Polyplexes as an Effective Strategy for Selective Uptake and Transfection of Cancer Cells. *Colloids Surf., B* **2013**, *111*, 297−305.
(470) Tu, S.; Chen, Y.-W.; Qiu, Y.-B.; Zhu, K.; Luo, X.-L. Enhancement of Cellular Uptake and Antitumor Efficiencies of Micelles with Phosphorylcholine. *Macromol. Biosci.* **2011**, *11*, 1416−1425.
(471) Jackson, M. A.; Werfel, T. A.; Curvino, E. J.; Yu, F.; Kavanaugh, T. E.; Sarett, S. M.; Dockery, M. D.; Kilchrist, K. V.; Jackson, A. N.; Giorgio, T. D.; et al. Zwitterionic Nanocarrier Surface Chemistry Improves Sirna Tumor Delivery and Silencing Activity Relative to Polyethylene Glycol. *ACS Nano* **2017**, *11*, 5680−5696.
(472) Hou, Y.; Lu, H. Protein Pepylation: A New Paradigm of Protein-Polymer Conjugation. *Bioconjugate Chem.* **2019**, *30*, 1604−1616.
(473) Chen, B.-M.; Su, Y.-C.; Chang, C.-J.; Burnouf, P.-A.; Chuang, K.-H.; Chen, C.-H.; Cheng, T.-L.; Chen, Y.-T.; Wu, J.-Y.; Roffler, S. R. Measurement of Pre-Existing IgG and IgM Antibodies against Polyethylene Glycol in Healthy Individuals. *Anal. Chem.* **2016**, *88*, 10661−10666.
(474) Yang, Q.; Jacobs, T. M.; McCallen, J. D.; Moore, D. T.; Huckaby, J. T.; Edelstein, J. N.; Lai, S. K. Analysis of Pre-Existing IgG and IgM Antibodies against Polyethylene Glycol (PEG) in the General Population. *Anal. Chem.* **2016**, *88*, 11804−11812.
(475) Pelegri-O'Day, E. M.; Paluck, S. J.; Maynard, H. D. Substituted Polyesters by Thiol-Ene Modification: Rapid Diversification for Therapeutic Protein Stabilization. *J. Am. Chem. Soc.* **2017**, *139*, 1145−1154.
(476) Miyamoto, D.; Watanabe, J.; Ishihara, K. Effect of Water-Soluble Phospholipid Polymers Conjugated with Papain on the Enzymatic Stability. *Biomaterials* **2004**, *25*, 71−76.
(477) Seo, J.-H.; Matsuno, R.; Lee, Y.; Takai, M.; Ishihara, K. Conformational Recovery and Preservation of Protein Nature from Heat-Induced Denaturation by Water-Soluble Phospholipid Polymer Conjugation. *Biomaterials* **2009**, *30*, 4859−4867.
(478) Seo, J.-H.; Matsuno, R.; Lee, Y.; Konno, T.; Takai, M.; Ishihara, K. Effect of Hydrophilic Polymer Conjugation on Heat-Induced Conformational Changes in a Protein. *Acta Biomater.* **2011**, *7*, 1477−1484.
(479) Lewis, A.; Tang, Y. Q.; Brocchini, S.; Choi, J. W.; Godwin, A. Poly(2-methacryloyloxyethyl phosphorylcholine) for Protein Conjugation. *Bioconjugate Chem.* **2008**, *19*, 2144−2155.
(480) Liu, S.; Jiang, S. Zwitterionic Polymer-Protein Conjugates Reduce Polymer-Specific Antibody Response. *Nano Today* **2016**, *11*, 285−291.
(481) Li, B. W.; Yuan, Z. F.; Hung, H. C.; Ma, J. R.; Jain, P.; Tsao, C.; Xie, J. Y.; Zhang, P.; Lin, X. J.; Wu, K.; et al. Revealing the Immunogenic Risk of Polymers. *Angew. Chem., Int. Ed.* **2018**, *57*, 13873−13876.
(482) Richter, A. W.; Åkerblom, E. Antibodies against Polyethylene Glycol Produced in Animals by Immunization with Monomethoxy Polyethylene Glycol Modified Proteins. *Int. Arch. Allergy Immunol.* **2004**, *70*, 124−131.
(483) Tsao, C.; Zhang, P.; Yuan, Z.; Dong, D.; Wu, K.; Niu, L.; McMullen, P.; Luozhong, S.; Hung, H.-C.; Cheng, Y.-H.; et al. Zwitterionic Polymer Conjugated Glucagon-Like Peptide-1 for Prolonged Glycemic Control. *Bioconjugate Chem.* **2020**, *31*, 1812−1819.
(484) Selis, F.; Schrepfer, R.; Sanna, R.; Scaramuzza, S.; Tonon, G.; Dedoni, S.; Onali, P.; Orsini, G.; Genovese, S. Enzymatic Mono-PEGylation of Glucagon-Like Peptide 1 towards Long Lasting Treatment of Type 2 Diabetes. *Results Pharma Sci.* **2012**, *2*, 58−65.
(485) Xie, J.; Lu, Y.; Wang, W.; Zhu, H.; Wang, Z.; Cao, Z. Simple Protein Modification Using Zwitterionic Polymer to Mitigate the Bioactivity Loss of Conjugated Insulin. *Adv. Healthcare Mater.* **2017**, *6*, 1601428.
(486) Bhattacharjee, S.; Liu, W.; Wang, W.-H.; Weitzhandler, I.; Li, X.; Qi, Y.; Liu, J.; Pang, Y.; Hunt, D. F.; Chilkoti, A. Site-Specific Zwitterionic Polymer Conjugates of a Protein Have Long Plasma Circulation. *ChemBioChem.* **2015**, *16*, 2451−2455.
(487) Hu, J.; Wang, G.; Zhao, W.; Gao, W. In Situ Growth of a C-Terminal Interferon-Alpha Conjugate of a Phospholipid Polymer That Outperforms PEGASYS in Cancer Therapy. *J. Controlled Release* **2016**, *237*, 71−77.
(488) Tsao, C.; Yuan, Z.; Zhang, P.; Liu, E.; McMullen, P.; Wu, K.; Hung, H.-C.; Jiang, S. Enhanced Pulmonary Systemic Delivery of Protein Drugs via Zwitterionic Polymer Conjugation. *J. Controlled Release* **2020**, *322*, 170−176.
(489) Li, B.; Yuan, Z.; He, Y.; Hung, H.-C.; Jiang, S. Zwitterionic Nanoconjugate Enables Safe and Efficient Lymphatic Drug Delivery. *Nano Lett.* **2020**, *20*, 4693−4699.
(490) Li, B.; Yuan, Z.; Jain, P.; Hung, H.-C.; He, Y.; Lin, X.; McMullen, P.; Jiang, S. De Novo Design of Functional Zwitterionic Biomimetic Material for Immunomodulation. *Sci. Adv.* **2020**, *6*, No. eaba0754.
(491) Su, C.; Correa, F.; Liang, H.; Jacobson, R.; Perlroth, V.; Pham, L. Characterization of Antibody Biopolymer Conjugate Reveals Superior Biophysical Properties Compared to Naked Antibodies. *Invest. Ophthalmol. Vis. Sci.* **2020**, *61*, 4237.
(492) Patel, S. S.; Janer, D.; Miller, B.; Ehrlich, J. S.; Perlroth, V.; Velazquez-Martin, J. P. Updated Results of Phase 1b Study of KSI-301, an Anti-VEGF Antibody Biopolymer Conjugate with Extended Durability, in wAMD, DME, and RVO. *Invest. Ophthalmol. Vis. Sci.* **2020**, *61*, 4286.
(493) Turecek, P. L.; Bossard, M. J.; Schoetens, F.; Ivens, I. A. PEGylation of Biopharmaceuticals: A Review of Chemistry and Nonclinical Safety Information of Approved Drugs. *J. Pharm. Sci.* **2016**, *105*, 460−475.
(494) Zhang, P.; Jain, P.; Tsao, C.; Yuan, Z.; Li, W.; Li, B.; Wu, K.; Hung, H.-C.; Lin, X.; Jiang, S. Polypeptides with High Zwitterion Density for Safe and Effective Therapeutics. *Angew. Chem., Int. Ed.* **2018**, *57*, 7743−7747.
(495) Banskota, S.; Yousefpour, P.; Kirmani, N.; Li, X.; Chilkoti, A. Long Circulating Genetically Encoded Intrinsically Disordered Zwitterionic Polypeptides for Drug Delivery. *Biomaterials* **2019**, *192*, 475−485.
(496) McMullen, P.; Qiao, Q.; Luozhong, S.; Cai, L.; Fang, L.; Shao, Q.; Jiang, S. Motif-based zwitterionic peptides impact their structure and immunogenicity. *Chem. Sci.* **2022**, *13*, 10961.
(497) McMullen, P.; Fang, L.; Qiao, Q.; Shao, Q.; Jiang, S. Impacts of a Zwitterionic Peptide on its Fusion Protein. *Bioconjugate Chem.* **2022**, *33* (8), 1485−1493.
(498) Li, B. W.; Yuan, Z. F.; Zhang, P.; Sinclair, A.; Jain, P.; Wu, K.; Tsao, C.; Xie, J. Y.; Hung, H. C.; Lin, X. J.; et al. Zwitterionic

https://doi.org/10.1021/acs.chemrev.2c00344
Chem. Rev. 2022, 122, 17073−17154

Nanocages Overcome the Efficacy Loss of Biologic Drugs. *Adv. Mater.* **2018**, *30*, 1705728.
(499) Liang, S.; Liu, Y.; Jin, X.; Liu, G.; Wen, J.; Zhang, L.; Li, J.; Yuan, X.; Chen, I. S. Y.; Chen, W.; et al. Phosphorylcholine Polymer Nanocapsules Prolong the Circulation Time and Reduce the Immunogenicity of Therapeutic Proteins. *Nano Res.* **2016**, *9*, 1022−1031.
(500) Zhao, M.; Xu, D.; Wu, D.; Whittaker, J. W.; Terkeltaub, R.; Lu, Y. Nanocapsules of Oxalate Oxidase for Hyperoxaluria Treatment. *Nano Res.* **2018**, *11*, 2682−2688.
(501) Zhang, P.; Jain, P.; Tsao, C.; Sinclair, A.; Sun, F.; Hung, H.-C.; Bai, T.; Wu, K.; Jiang, S. Butyrylcholinesterase Nanocapsule as a Long Circulating Bioscavenger with Reduced Immune Response. *J. Controlled Release* **2016**, *230*, 73−78.
(502) Zhang, P.; Liu, E. J.; Tsao, C.; Kasten, S. A.; Boeri, M. V.; Dao, T. L.; DeBus, S. J.; Cadieux, C. L.; Baker, C. A.; Otto, T. C.; et al. Nanoscavenger Provides Long-Term Prophylactic Protection against Nerve Agents in Rodents. *Sci. Transl. Med.* **2019**, *11*, No. eaau7091.
(503) Park, S. M.; Aalipour, A.; Vermesh, O.; Yu, J. H.; Gambhir, S. S. Towards Clinically Translatable in Vivo Nanodiagnostics. *Nat. Rev. Mater.* **2017**, *2*, 17014.
(504) Dominguez-Medina, S.; Kisley, L.; Tauzin, L. J.; Hoggard, A.; Shuang, B. D. S.; Indrasekara, A. S.; Chen, S.; Wang, L.-Y.; Derry, P. J.; Liopo, A.; et al. Adsorption and Unfolding of a Single Protein Triggers Nanoparticle Aggregation. *ACS Nano* **2016**, *10*, 2103−2112.
(505) Ohyanagi, T.; Nagahori, N.; Shimawaki, K.; Hinou, H.; Yamashita, T.; Sasaki, A.; Jin, T.; Iwanaga, T.; Kinjo, M.; Nishimura, S.-I. Importance of Sialic Acid Residues Illuminated by Live Animal Imaging Using Phosphorylcholine Self-Assembled Monolayer-Coated Quantum Dots. *J. Am. Chem. Soc.* **2011**, *133*, 12507−12517.
(506) Wang, W.; Ji, X.; Kapur, A.; Zhang, C.; Mattoussi, H. A Multifunctional Polymer Combining the Imidazole and Zwitterion Motifs as a Biocompatible Compact Coating for Quantum Dots. *J. Am. Chem. Soc.* **2015**, *137*, 14158−14172.
(507) Yang, W.; Ella-Menye, J.-R.; Bai, T.; Sinclair, A.; Jiang, S. Stable and Functionalizable Quantum Dots with a Thin Zwitterionic Carboxybetaine Layer. *Langmuir* **2017**, *33*, 8784−8789.
(508) Zahid, M. U.; Ma, L.; Lim, S. J.; Smith, A. M. Single Quantum Dot Tracking Reveals the Impact of Nanoparticle Surface on Intracellular State. *Nat. Commun.* **2018**, *9*, 1830.
(509) Rouhana, L. L.; Jaber, J. A.; Schlenoff, J. B. Aggregation-Resistant Water-Soluble Gold Nanoparticles. *Langmuir* **2007**, *23*, 12799−12801.
(510) Zhou, Z. J.; Wang, L. R.; Chi, X. Q.; Bao, J. F.; Yang, L. J.; Zhao, W. X.; Chen, Z.; Wang, X. M.; Chen, X. Y.; Gao, J. H. Engineered Iron-Oxide-Based Nanoparticles as Enhanced T_1 Contrast Agents for Efficient Tumor Imaging. *ACS Nano* **2013**, *7*, 3287−3296.
(511) Zhan, N.; Palui, G.; Safi, M.; Ji, X.; Mattoussi, H. Multidentate Zwitterionic Ligands Provide Compact and Highly Biocompatible Quantum Dots. *J. Am. Chem. Soc.* **2013**, *135*, 13786−13795.
(512) Feng, Z.; Li, Q.; Wang, W.; Ni, Q.; Wang, Y.; Song, H.; Zhang, C.; Kong, D.; Liang, X.-J.; Huang, P. Superhydrophilic Fluorinated Polymer and Nanogel for High-Performance 19F Magnetic Resonance Imaging. *Biomaterials* **2020**, *256*, 120184.
(513) Yang, W.; Zhang, L.; Wang, S.; White, A. D.; Jiang, S. Functionalizable and Ultra Stable Nanoparticles Coated with Zwitterionic Poly(carboxybetaine) in Undiluted Blood Serum. *Biomaterials* **2009**, *30*, 5617−5621.
(514) Liang, G.; Han, J.; Hao, Q. Gram-Scale Preparation of Iron Oxide Nanoparticles with Renal Clearance Properties for Enhanced T_1-Weighted Magnetic Resonance Imaging. *ACS Appl. Bio Mater.* **2018**, *1*, 1389−1397.
(515) Kim, D.; Chae, M. K.; Joo, H. J.; Jeong, I.-h.; Cho, J.-H.; Lee, C. Facile Preparation of Zwitterion-Stabilized Superparamagnetic Iron Oxide Nanoparticles (ZSPIONs) as an MR Contrast Agent for in Vivo Applications. *Langmuir* **2012**, *28*, 9634−9639.
(516) Nowinski, A. K.; White, A. D.; Keefe, A. J.; Jiang, S. Biologically Inspired Stealth Peptide-Capped Gold Nanoparticles. *Langmuir* **2014**, *30*, 1864−1870.
(517) Han, Y.; Zhou, X.; Qian, Y.; Hu, H.; Zhou, Z.; Liu, X.; Tang, J.; Shen, Y. Hypoxia-Targeting Dendritic MRI Contrast Agent Based on Internally Hydroxy Dendrimer for Tumor Imaging. *Biomaterials* **2019**, *213*, 119195.
(518) Zhou, Z. J.; Wu, C. Q.; Liu, H. Y.; Zhu, X. L.; Zhao, Z. H.; Wang, L. R.; Xu, Y.; Ai, H.; Gao, J. H. Surface and Interfacial Engineering of Iron Oxide Nanoplates for Highly Efficient Magnetic Resonance Angiography. *ACS Nano* **2015**, *9*, 3012−3022.
(519) Ma, D.; Chen, J. W.; Luo, Y.; Wang, H.; Shi, X. Y. Zwitterion-Coated Ultrasmall Iron Oxide Nanoparticles for Enhanced T_1-Weighted Magnetic Resonance Imaging Applications. *J. Mater. Chem. B* **2017**, *5*, 7267−7273.
(520) Zhou, C.; Long, M.; Qin, Y. P.; Sun, X. K.; Zheng, J. Luminescent Gold Nanoparticles with Efficient Renal Clearance. *Angew. Chem., Int. Ed.* **2011**, *50*, 3168−3172.
(521) Liu, J.; Yu, M.; Zhou, C.; Yang, S.; Ning, X.; Zheng, J. Passive Tumor Targeting of Renal-Clearable Luminescent Gold Nanoparticles: Long Tumor Retention and Fast Normal Tissue Clearance. *J. Am. Chem. Soc.* **2013**, *135*, 4978−4981.
(522) Xiong, Z. J.; Wang, Y.; Zhu, J. Y.; Li, X.; He, Y.; Qu, J.; Shen, M. W.; Xia, J. D.; Shi, X. Y. Dendrimers Meet Zwitterions: Development of a Unique Antifouling Nanoplatform for Enhanced Blood Pool, Lymph Node and Tumor CT Imaging. *Nanoscale* **2017**, *9*, 12295−12301.
(523) Ranneh, A. H.; Takemoto, H.; Sakuma, S.; Awaad, A.; Nomoto, T.; Mochida, Y.; Matsui, M.; Tomoda, K.; Naito, M.; Nishiyama, N. An Ethylenediamine-Based Switch to Render the Polyzwitterion Cationic at Tumorous pH for Effective Tumor Accumulation of Coated Nanomaterials. *Angew. Chem., Int. Ed.* **2018**, *57*, 5057−5061.
(524) Pons, T.; Bouccara, S.; Loriette, V.; Lequeux, N.; Pezet, S.; Fragola, A. In Vivo Imaging of Single Tumor Cells in Fast-Flowing Bloodstream Using Near-Infrared Quantum Dots and Time-Gated Imaging. *ACS Nano* **2019**, *13*, 3125−3131.
(525) Choi, H. S.; Liu, W.; Liu, F.; Nasr, K.; Misra, P.; Bawendi, M. G.; Frangioni, J. V. Design Considerations for Tumour-Targeted Nanoparticles. *Nat. Nanotechnol.* **2010**, *5*, 42−47.
(526) Wei, H.; Insin, N.; Lee, J.; Han, H.-S.; Cordero, J. M.; Liu, W.; Bawendi, M. G. Compact Zwitterion-Coated Iron Oxide Nanoparticles for Biological Applications. *Nano Lett.* **2012**, *12*, 22−25.
(527) Muro, E.; Pons, T.; Lequeux, N.; Fragola, A.; Sanson, N.; Lenkei, Z.; Dubertret, B. Small and Stable Sulfobetaine Zwitterionic Quantum Dots for Functional Live-Cell Imaging. *J. Am. Chem. Soc.* **2010**, *132*, 4556−4557.
(528) Tasso, M.; Giovanelli, E.; Zala, D.; Bouccara, S.; Fragola, A.; Hanafi, M.; Lenkei, Z.; Pons, T.; Lequeux, N. Sulfobetaine-Vinylimidazole Block Copolymers: A Robust Quantum Dot Surface Chemistry Expanding Bioimaging's Horizons. *ACS Nano* **2015**, *9*, 11479−11489.
(529) Debayle, M.; Balloul, E.; Dembele, F.; Xu, X.; Hanafi, M.; Ribot, F.; Monzel, C.; Coppey, M.; Fragola, A.; Dahan, M.; et al. Zwitterionic Polymer Ligands: An Ideal Surface Coating to Totally Suppress Protein-Nanoparticle Corona Formation? *Biomaterials* **2019**, *219*, 119357.
(530) Gao, C.; Li, G.; Xue, H.; Yang, W.; Zhang, F.; Jiang, S. Functionalizable and Ultra-Low Fouling Zwitterionic Surfaces via Adhesive Mussel Mimetic Linkages. *Biomaterials* **2010**, *31*, 1486−1492.
(531) Sun, F.; Hung, H.-C.; Sinclair, A.; Zhang, P.; Bai, T.; Galvan, D. D.; Jain, P.; Li, B.; Jiang, S.; Yu, Q. Hierarchical Zwitterionic Modification of a SERS Substrate Enables Real-Time Drug Monitoring in Blood Plasma. *Nat. Commun.* **2016**, *7*, 13437.
(532) Rocchitta, G.; Spanu, A.; Babudieri, S.; Latte, G.; Madeddu, G.; Galleri, G.; Nuvoli, S.; Bagella, P.; Demartis, M. I.; Fiore, V.; et al. Enzyme Biosensors for Biomedical Applications: Strategies for

https://doi.org/10.1021/acs.chemrev.2c00344
Chem. Rev. 2022, 122, 17073−17154

Safeguarding Analytical Performances in Biological Fluids. *Sensors* **2016**, *16*, 780.
(533) Xu, J.; Lee, H. Anti-Biofouling Strategies for Long-Term Continuous Use of Implantable Biosensors. *Chemosensors* **2020**, *8*, 66.
(534) Ladd, J.; Taylor, A. D.; Piliarik, M.; Homola, J.; Jiang, S. Label-Free Detection of Cancer Biomarker Candidates Using Surface Plasmon Resonance Imaging. *Anal. Bioanal. Chem.* **2009**, *393*, 1157−1163.
(535) Vaisocherová, H.; Yang, W.; Zhang, Z.; Cao, Z.; Cheng, G.; Piliarik, M.; Homola, J.; Jiang, S. Ultralow Fouling and Functionalizable Surface Chemistry Based on a Zwitterionic Polymer Enabling Sensitive and Specific Protein Detection in Undiluted Blood Plasma. *Anal. Chem.* **2008**, *80*, 7894−7901.
(536) Brault, N. D.; White, A. D.; Taylor, A. D.; Yu, Q.; Jiang, S. Directly Functionalizable Surface Platform for Protein Arrays in Undiluted Human Blood Plasma. *Anal. Chem.* **2013**, *85*, 1447−1453.
(537) Sun, F.; Ella-Menye, J.-R.; Galvan, D. D.; Bai, T.; Hung, H.-C.; Chou, Y.-N.; Zhang, P.; Jiang, S.; Yu, Q. Stealth Surface Modification of Surface-Enhanced Raman Scattering Substrates for Sensitive and Accurate Detection in Protein Solutions. *ACS Nano* **2015**, *9*, 2668−2676.
(538) Yang, W.; Xue, H.; Carr, L. R.; Wang, J.; Jiang, S. Zwitterionic Poly(carboxybetaine) Hydrogels for Glucose Biosensors in Complex Media. *Biosens. Bioelectron.* **2011**, *26*, 2454−2459.
(539) Hu, Y.; Liang, B.; Fang, L.; Ma, G.; Yang, G.; Zhu, Q.; Chen, S.; Ye, X. Antifouling Zwitterionic Coating via Electrochemically Mediated Atom Transfer Radical Polymerization on Enzyme-Based Glucose Sensors for Long-Time Stability in 37 °C Serum. *Langmuir* **2016**, *32*, 11763−11770.
(540) Wu, H.; Lee, C.-J.; Wang, H.; Hu, Y.; Young, M.; Han, Y.; Xu, F.-J.; Cong, H.; Cheng, G. Highly Sensitive and Stable Zwitterionic Poly(sulfobetaine-3,4-ethylenedioxythiophene) (PSBEDOT) Glucose Biosensor. *Chem. Sci.* **2018**, *9*, 2540−2546.
(541) Liu, X.; Xiao, T.; Wu, F.; Shen, M.-Y.; Zhang, M.; Yu, H.-h.; Mao, L. Ultrathin Cell-Membrane-Mimic Phosphorylcholine Polymer Film Coating Enables Large Improvements for in Vivo Electrochemical Detection. *Angew. Chem., Int. Ed.* **2017**, *56*, 11802−11806.
(542) Feng, T.; Ji, W.; Zhang, Y.; Wu, F.; Tang, Q.; Wei, H.; Mao, L.; Zhang, M. Zwitterionic Polydopamine Engineered Interface for in Vivo Sensing with High Biocompatibility. *Angew. Chem., Int. Ed.* **2020**, *59*, 23445−23449.
(543) Zhu, Y.; Xu, X.; Brault, N. D.; Keefe, A. J.; Han, X.; Deng, Y.; Xu, J.; Yu, Q.; Jiang, S. Cellulose Paper Sensors Modified with Zwitterionic Poly(carboxybetaine) for Sensing and Detection in Complex Media. *Anal. Chem.* **2014**, *86*, 2871−2875.
(544) Sun, F.; Wu, K.; Hung, H.-C.; Zhang, P.; Che, X.; Smith, J.; Lin, X.; Li, B.; Jain, P.; Yu, Q.; et al. Paper Sensor Coated with a Poly(carboxybetaine)-Multiple DOPA Conjugate via Dip-Coating for Biosensing in Complex Media. *Anal. Chem.* **2017**, *89*, 10999−11004.
(545) Huang, C.-J.; Li, Y.; Jiang, S. Zwitterionic Polymer-Based Platform with Two-Layer Architecture for Ultra Low Fouling and High Protein Loading. *Anal. Chem.* **2012**, *84*, 3440−3445.
(546) Brault, N. D.; Sundaram, H. S.; Huang, C.-J.; Li, Y.; Yu, Q.; Jiang, S. Two-Layer Architecture Using Atom Transfer Radical Polymerization for Enhanced Sensing and Detection in Complex Media. *Biomacromolecules* **2012**, *13*, 4049−4056.
(547) Gao, M.; Wang, P.; Jiang, L.; Wang, B.; Yao, Y.; Liu, S.; Chu, D.; Cheng, W.; Lu, Y. Power Generation for Wearable Systems. *Energy Environ. Sci.* **2021**, *14*, 2114−2157.
(548) Peng, X.; Liu, H.; Yin, Q.; Wu, J.; Chen, P.; Zhang, G.; Liu, G.; Wu, C.; Xie, Y. A Zwitterionic Gel Electrolyte for Efficient Solid-State Supercapacitors. *Nat. Commun.* **2016**, *7*, 11782.
(549) Tiyapiboonchaiya, C.; Pringle, J. M.; Sun, J.; Byrne, N.; Howlett, P. C.; MacFarlane, D. R.; Forsyth, M. The Zwitterion Effect in High-Conductivity Polyelectrolyte Materials. *Nat. Mater.* **2004**, *3*, 29−32.
(550) Diao, W.; Wu, L.; Ma, X.; Zhuang, Z.; Li, S.; Bu, X.; Fang, Y. Highly Stretchable, Ionic Conductive and Self-Recoverable Zwitterionic Polyelectrolyte-Based Hydrogels by Introducing Multiple Supramolecular Sacrificial Bonds in Double Network. *J. Appl. Polym. Sci.* **2019**, *136*, 47783.
(551) Lei, Z.; Wu, P. A Highly Transparent and Ultra-Stretchable Conductor with Stable Conductivity During Large Deformation. *Nat. Commun.* **2019**, *10*, 3429.
(552) Lei, Z.; Wu, P. A Supramolecular Biomimetic Skin Combining a Wide Spectrum of Mechanical Properties and Multiple Sensory Capabilities. *Nat. Commun.* **2018**, *9*, 1134.
(553) Lei, Z.; Wu, P. Zwitterionic Skins with a Wide Scope of Customizable Functionalities. *ACS Nano* **2018**, *12*, 12860−12868.
(554) Lei, Z.; Zhu, W.; Zhang, X.; Wang, X.; Wu, P. Bio-Inspired Ionic Skin for Theranostics. *Adv. Funct. Mater.* **2021**, *31*, 2008020.
(555) Zhang, W.; Wu, B.; Sun, S.; Wu, P. Skin-Like Mechanoresponsive Self-Healing Ionic Elastomer from Supramolecular Zwitterionic Network. *Nat. Commun.* **2021**, *12*, 4082.
(556) Guo, H.; Bai, M.; Wen, C.; Liu, M.; Tian, S.; Xu, S.; Liu, X.; Ma, Y.; Chen, P.; Li, Q.; et al. A Zwitterionic-Aromatic Motif-Based Ionic Skin for Highly Biocompatible and Glucose-Responsive Sensor. *J. Colloid Interface Sci.* **2021**, *600*, 561−571.
(557) He, K.; Liu, Z.; Wan, C.; Jiang, Y.; Wang, T.; Wang, M.; Zhang, F.; Liu, Y.; Pan, L.; Xiao, M.; et al. An on-Skin Electrode with Anti-Epidermal-Surface-Lipid Function Based on a Zwitterionic Polymer Brush. *Adv. Mater.* **2020**, *32*, 2001130.
(558) Spadafora, A.; Korogiannaki, M.; Sheardown, H. Antifouling Silicone Hydrogel Contact Lenses via Densely Grafted Phosphorylcholine Polymers. *Biointerphases* **2020**, *15*, 041013.
(559) Willis, S. L.; Court, J. L.; Redman, R. P.; Wang, J.-H.; Leppard, S. W.; O'Byrne, V. J.; Small, S. A.; Lewis, A. L.; Jones, S. A.; Stratford, P. W. A Novel Phosphorylcholine-Coated Contact Lens for Extended Wear Use. *Biomaterials* **2001**, *22*, 3261−3272.
(560) Goda, T.; Konno, T.; Takai, M.; Ishihara, K. Synthesis and Characterization on Polydimethylsiloxane Grafted with Poly(2-methacryloyloxyethyl phosphorylcholine) by Photo-Induced Radical Polymerization. *54th SPSJ Symposium on Macromolecules*; The Society of Polymer Science, Japan: 2005; abstract 4207.
(561) Goda, T.; Ishihara, K. Soft Contact Lens Biomaterials from Bioinspired Phospholipid Polymers. *Expert Rev. Med. Devices* **2006**, *3*, 167−174.
(562) Shi, X.; Cantu-Crouch, D.; Sharma, V.; Pruitt, J.; Yao, G.; Fukazawa, K.; Wu, J. Y.; Ishihara, K. Surface Characterization of a Silicone Hydrogel Contact Lens Having Bioinspired 2-Methacryloyloxyethyl Phosphorylcholine Polymer Layer in Hydrated State. *Colloids Surf., B* **2021**, *199*, 111539.
(563) Ishihara, K.; Fukazawa, K.; Sharma, V.; Liang, S.; Shows, A.; Dunbar, D. C.; Zheng, Y.; Ge, J.; Zhang, S.; Hong, Y.; et al. Antifouling Silicone Hydrogel Contact Lenses with a Bioinspired 2-Methacryloyloxyethyl Phosphorylcholine Polymer Surface. *ACS Omega* **2021**, *6*, 7058−7067.
(564) Shi, X.; Sharma, V.; Cantu-Crouch, D.; Yao, G.; Fukazawa, K.; Ishihara, K.; Wu, J. Y. Nanoscaled Morphology and Mechanical Properties of a Biomimetic Polymer Surface on a Silicone Hydrogel Contact Lens. *Langmuir* **2021**, *37*, 13961−13967.
(565) Goda, T.; Shimizu, T.; Ishihara, K. 10 - Bioinspired Biomaterials for Soft Contact Lenses. In *Biomaterials and Regenerative Medicine in Ophthalmology*; Woodhead Publishing: 2010; pp 263−279.
(566) Selan, L.; Palma, S.; Scoarughi, G. L.; Papa, R.; Veeh, R.; Di Clemente, D.; Artini, M. Phosphorylcholine Impairs Susceptibility to Biofilm Formation of Hydrogel Contact Lenses. *Am. J. Ophthalmol.* **2009**, *147*, 134−139.
(567) Shimizu, T.; Goda, T.; Minoura, N.; Takai, M.; Ishihara, K. Super-Hydrophilic Silicone Hydrogels with Interpenetrating Poly(2-methacryloyloxyethyl phosphorylcholine) Networks. *Biomaterials* **2010**, *31*, 3274−3280.
(568) Kiritoshi, Y.; Ishihara, K. Preparation of Cross-Linked Biocompatible Poly(2-methacryloyloxyethyl phosphorylcholine) Gel and Its Strange Swelling Behavior in Water/Ethanol Mixture. *J. Biomater. Sci., Polym. Ed.* **2002**, *13*, 213−224.

https://doi.org/10.1021/acs.chemrev.2c00344
Chem. Rev. 2022, 122, 17073−17154

(569) Kiritoshi, Y.; Ishihara, K. Synthesis of Hydrophilic Cross-Linker Having Phosphorylcholine-Like Linkage for Improvement of Hydrogel Properties. *Polymer* **2004**, *45*, 7499−7504.
(570) Xu, C.; He, R. Y.; Xie, B. B.; Ismail, M.; Yao, C.; Luan, J.; Li, X. S. Silicone Hydrogels Grafted with Natural Amino Acids for Ophthalmological Application. *J. Biomater. Sci., Polym. Ed.* **2016**, *27*, 1354−1368.
(571) Zhang, W. L.; Li, G. J.; Lin, Y. L.; Wang, L. Y.; Wu, S. Q. Preparation and Characterization of Protein-Resistant Hydrogels for Soft Contact Lens Applications via Radical Copolymerization Involving a Zwitterionic Sulfobetaine Comonomer. *J. Biomater. Sci., Polym. Ed.* **2017**, *28*, 1935−1949.
(572) Zhang, J.; Qian, S.; Chen, L.; Wu, M.; Cai, Y.; Mou, X.; Feng, J. Antifouling and Antibacterial Zwitterionic Hydrogels as Soft Contact Lens against Ocular Bacterial Infections. *Eur. Polym. J.* **2022**, *167*, 111037.
(573) Han, Y. M.; Xu, X.; Tang, J. M.; Shen, C. H.; Lin, Q. K.; Chen, H. Bottom-up Fabrication of Zwitterionic Polymer Brushes on Intraocular Lens for Improved Biocompatibility. *Int. J. Nanomed.* **2017**, *12*, 127−135.
(574) He, B. B.; Yang, J. H.; Liu, Y.; Xie, X. H.; Hao, H. J.; Xing, X. L.; Liu, W. G. An in Situ-Forming Polyzwitterion Hydrogel: Towards Vitreous Substitute Application. *Bioact. Mater.* **2021**, *6*, 3085−3096.
(575) Thiele, J.; Ma, Y.; Bruekers, S. M. C.; Ma, S.; Huck, W. T. S. 25th Anniversary Article: Designer Hydrogels for Cell Cultures: A Materials Selection Guide. *Adv. Mater.* **2014**, *26*, 125−148.
(576) Annabi, N.; Tamayol, A.; Uquillas, J. A.; Akbari, M.; Bertassoni, L. E.; Cha, C.; Camci-Unal, G.; Dokmeci, M. R.; Peppas, N. A.; Khademhosseini, A. 25th Anniversary Article: Rational Design and Applications of Hydrogels in Regenerative Medicine. *Adv. Mater.* **2014**, *26*, 85−124.
(577) Chien, H. W.; Tsai, W. B.; Jiang, S. Direct Cell Encapsulation in Biodegradable and Functionalizable Carboxybetaine Hydrogels. *Biomaterials* **2012**, *33*, 5706−5712.
(578) Chien, H.-W.; Xu, X.; Ella-Menye, J.-R.; Tsai, W.-B.; Jiang, S. High Viability of Cells Encapsulated in Degradable Poly(carboxybetaine) Hydrogels. *Langmuir* **2012**, *28*, 17778−17784.
(579) Lin, C.-Y.; Wang, Y.-R.; Lin, C.-W.; Wang, S.-W.; Chien, H.-W.; Cheng, N.-C.; Tsai, W.-B.; Yu, J. Peptide-Modified Zwitterionic Porous Hydrogels for Endothelial Cell and Vascular Engineering. *BioRes. Open Access* **2014**, *3*, 297−310.
(580) Dong, D.; Li, J.; Cui, M.; Wang, J.; Zhou, Y.; Luo, L.; Wei, Y.; Ye, L.; Sun, H.; Yao, F. In Situ "Clickable" Zwitterionic Starch-Based Hydrogel for 3D Cell Encapsulation. *ACS Appl. Mater. Interfaces* **2016**, *8*, 4442−4455.
(581) Zhang, Y.; Liu, S.; Li, T.; Zhang, L.; Azhar, U.; Ma, J.; Zhai, C.; Zong, C.; Zhang, S. Cytocompatible and Non-Fouling Zwitterionic Hyaluronic Acid-Based Hydrogels Using Thiol-Ene "Click" Chemistry for Cell Encapsulation. *Carbohydr. Polym.* **2020**, *236*, 116021.
(582) Villa-Diaz, L. G.; Nandivada, H.; Ding, J.; Nogueira-de-Souza, N. C.; Krebsbach, P. H.; O'Shea, K. S.; Lahann, J.; Smith, G. D. Synthetic Polymer Coatings for Long-Term Growth of Human Embryonic Stem Cells. *Nat. Biotechnol.* **2010**, *28*, 581−583.
(583) Bai, T.; Sun, F.; Zhang, L.; Sinclair, A.; Liu, S.; Ella-Menye, J.-R.; Zheng, Y.; Jiang, S. Restraint of the Differentiation of Mesenchymal Stem Cells by a Nonfouling Zwitterionic Hydrogel. *Angew. Chem., Int. Ed.* **2014**, *53*, 12729−12734.
(584) Bai, T.; Sinclair, A.; Sun, F.; Jain, P.; Hung, H.-C.; Zhang, P.; Ella-Menye, J.-R.; Liu, W.; Jiang, S. Harnessing Isomerization-Mediated Manipulation of Nonspecific Cell/Matrix Interactions to Reversibly Trigger and Suspend Stem Cell Differentiation. *Chem. Sci.* **2016**, *7*, 333−338.
(585) Dong, D.; Hao, T.; Wang, C.; Zhang, Y.; Qin, Z.; Yang, B.; Fang, W.; Ye, L.; Yao, F.; Li, J. Zwitterionic Starch-Based Hydrogel for the Expansion and "Stemness" Maintenance of Brown Adipose Derived Stem Cells. *Biomaterials* **2018**, *157*, 149−160.
(586) Bai, T.; Li, J.; Sinclair, A.; Imren, S.; Merriam, F.; Sun, F.; O'Kelly, M. B.; Nourigat, C.; Jain, P.; Delrow, J. J.; et al. Expansion of Primitive Human Hematopoietic Stem Cells by Culture in a Zwitterionic Hydrogel. *Nat. Med.* **2019**, *25*, 1566−1575.
(587) Wahl, M.; Goecke, F.; Labes, A.; Dobretsov, S.; Weinberger, F. The Second Skin: Ecological Role of Epibiotic Biofilms on Marine Organisms. *Front. Microbiol.* **2012**, *3*, 292.
(588) Dobretsov, S. Marine Biofilms. In *Biofouling*; Wiley-Blackwell: 2010; pp 123−136.
(589) Vinagre, P. A.; Simas, T.; Cruz, E.; Pinori, E.; Svenson, J. Marine Biofouling: A European Database for the Marine Renewable Energy Sector. *J. Mar. Sci. Eng.* **2020**, *8*, 495.
(590) Blackwood, D. J.; Lim, C. S.; Teo, S. L. M.; Hu, X.; Pang, J. Macrofouling Induced Localized Corrosion of Stainless Steel in Singapore Seawater. *Corros. Sci.* **2017**, *129*, 152−160.
(591) Fitridge, I.; Dempster, T.; Guenther, J.; de Nys, R. The Impact and Control of Biofouling in Marine Aquaculture: A Review. *Biofouling* **2012**, *28*, 649−669.
(592) Yukihira, H.; Lucas, J. S.; Klumpp, D. W. Comparative Effects of Temperature on Suspension Feeding and Energy Budgets of the Pearl Oysters Pinctada Margaritifera and P. Maxima. *Mar. Ecol.: Prog. Ser.* **2000**, *195*, 179−188.
(593) Mao Che, L.; Le Campion-Alsumard, T.; Boury-Esnault, N.; Payri, C.; Golubic, S.; Bézac, C. Biodegradation of Shells of the Black Pearl Oyster, Pinctada Margaritifera Var. Cumingii, by Microborers and Sponges of French Polynesia. *Mar. Biol.* **1996**, *126*, 509−519.
(594) Oppedal, F.; Dempster, T.; Stien, L. H. Environmental Drivers of Atlantic Salmon Behaviour in Sea-Cages: A Review. *Aquaculture* **2011**, *311*, 1−18.
(595) Dai, G.; Xie, Q.; Ai, X.; Ma, C.; Zhang, G. Self-Generating and Self-Renewing Zwitterionic Polymer Surfaces for Marine Anti-Biofouling. *ACS Appl. Mater. Interfaces* **2019**, *11*, 41750−41757.
(596) Li, C.; Xia, Y.; Liu, C.; Huang, R.; Qi, W.; He, Z.; Su, R. Lubricin-Inspired Loop Zwitterionic Peptide for Fabrication of Superior Antifouling Surfaces. *ACS Appl. Mater. Interfaces* **2021**, *13*, 41978−41986.
(597) Li, Y.; Liu, C.-M.; Yang, J.-Y.; Gao, Y.-H.; Li, X.-S.; Que, G.-H.; Lu, J. R. Anti-Biofouling Properties of Amphiphilic Phosphorylcholine Polymer Films. *Colloids Surf., B* **2011**, *85*, 125−130.
(598) Ventura, C.; Guerin, A. J.; El-Zubir, O.; Ruiz-Sanchez, A. J.; Dixon, L. I.; Reynolds, K. J.; Dale, M. L.; Ferguson, J.; Houlton, A.; Horrocks, B. R.; et al. Marine Antifouling Performance of Polymer Coatings Incorporating Zwitterions. *Biofouling* **2017**, *33*, 892−903.
(599) Yang, W.; Lin, P.; Cheng, D.; Zhang, L.; Wu, Y.; Liu, Y.; Pei, X.; Zhou, F. Contribution of Charges in Polyvinyl Alcohol Networks to Marine Antifouling. *ACS Appl. Mater. Interfaces* **2017**, *9*, 18295−18304.
(600) Koschitzki, F.; Wanka, R.; Sobota, L.; Koc, J.; Gardner, H.; Hunsucker, K. Z.; Swain, G. W.; Rosenhahn, A. Amphiphilic Dicyclopentenyl/Carboxybetaine-Containing Copolymers for Marine Fouling-Release Applications. *ACS Appl. Mater. Interfaces* **2020**, *12*, 34148−34160.
(601) Zhang, J.; Liu, Y.; Wang, X.; Zhang, C.; Liu, H.; Yang, W.; Cai, M.; Pei, X.; Zhou, F. Self-Polishing Emulsion Platforms: Eco-Friendly Surface Engineering of Coatings toward Water Borne Marine Antifouling. *Prog. Org. Coat.* **2020**, *149*, 105945.
(602) Su, X.; Yang, M.; Hao, D.; Guo, X.; Jiang, L. Marine Antifouling Coatings with Surface Topographies Triggered by Phase Segregation. *J. Colloid Interface Sci.* **2021**, *598*, 104−112.
(603) Zhang, Z.; Guo, L.; Hao, J. Emulsion-Based Organohydrogels with Switchable Wettability and Underwater Adhesion toward Durable and Ecofriendly Marine Antifouling Coatings. *ACS Appl. Polym. Mater.* **2021**, *3*, 3060−3070.
(604) Quintana, R.; Jańczewski, D.; Vasantha, V. A.; Jana, S.; Lee, S. S. C.; Parra-Velandia, F. J.; Guo, S.; Parthiban, A.; Teo, S. L.-M.; Vancso, G. J. Sulfobetaine-Based Polymer Brushes in Marine Environment: Is There an Effect of the Polymerizable Group on the Antifouling Performance? *Colloids Surf., B* **2014**, *120*, 118−124.
(605) Yang, W. J.; Neoh, K.-G.; Kang, E.-T.; Teo, S. L.-M.; Rittschof, D. Polymer Brush Coatings for Combating Marine Biofouling. *Prog. Polym. Sci.* **2014**, *39*, 1017−1042.

https://doi.org/10.1021/acs.chemrev.2c00344
Chem. Rev. 2022, 122, 17073−17154

(606) Kardela, J. H.; Millichamp, I. S.; Ferguson, J.; Parry, A. L.; Reynolds, K. J.; Aldred, N.; Clare, A. S. Nonfreezable Water and Polymer Swelling Control the Marine Antifouling Performance of Polymers with Limited Hydrophilic Content. *ACS Appl. Mater. Interfaces* **2019**, *11*, 29477−29489.
(607) Del Grosso, C. A.; Leng, C.; Zhang, K.; Hung, H.-C.; Jiang, S.; Chen, Z.; Wilker, J. J. Surface Hydration for Antifouling and Bio-Adhesion. *Chem. Sci.* **2020**, *11*, 10367−10377.
(608) Tan, J.; Xu, J.; Wang, D.; Yang, J.; Zhou, S. Seawater-Responsive SiO_2 Nanoparticles for in Situ Generation of Zwitterionic Polydimethylsiloxane Antifouling Coatings with Underwater Superoleophobicity. *J. Mater. Chem. A* **2020**, *8*, 24086−24097.
(609) Wang, D.; Xu, J.; Tan, J.; Yang, J.; Zhou, S. In Situ Generation of Amphiphilic Coatings Based on a Self-Catalytic Zwitterionic Precursor and Their Antifouling Performance. *Chem. Eng. J.* **2021**, *422*, 130115.
(610) Zhang, Z.; Finlay, J. A.; Wang, L.; Gao, Y.; Callow, J. A.; Callow, M. E.; Jiang, S. Polysulfobetaine-Grafted Surfaces as Environmentally Benign Ultralow Fouling Marine Coatings. *Langmuir* **2009**, *25*, 13516−13521.
(611) Aldred, N.; Li, G.; Gao, Y.; Clare, A. S.; Jiang, S. Modulation of Barnacle (Balanus Amphitrite Darwin) Cyprid Settlement Behavior by Sulfobetaine and Carboxybetaine Methacrylate Polymer Coatings. *Biofouling* **2010**, *26*, 673−683.
(612) Zhang, L.; Sha, J.; Chen, R.; Liu, Q.; Liu, J.; Yu, J.; Zhang, H.; Lin, C.; Wang, J. Three-Dimensional Flower-Like Shaped Bi5o7i Particles Incorporation Zwitterionic Fluorinated Polymers with Synergistic Hydration-Photocatalytic for Enhanced Marine Antifouling Performance. *J. Hazard. Mater.* **2020**, *389*, 121854.
(613) Zhang, L.; Sha, J.; Chen, R.; Liu, Q.; Liu, J.; Yu, J.; Zhang, H.; Lin, C.; Zhou, W.; Wang, J. Surface Plasma Ag-Decorated Bi5o7i Microspheres Uniformly Distributed on a Zwitterionic Fluorinated Polymer with Superfunctional Antifouling Property. *Appl. Catal., B* **2020**, *271*, 118920.
(614) Dai, G.; Ai, X.; Mei, L.; Ma, C.; Zhang, G. Kill-Resist-Renew Trinity: Hyperbranched Polymer with Self-Regenerating Attack and Defense for Antifouling Coatings. *ACS Appl. Mater. Interfaces* **2021**, *13*, 13735−13743.
(615) Mohan, A.; Ashraf, P. M. Biofouling Control Using Nano Silicon Dioxide Reinforced Mixed-Charged Zwitterionic Hydrogel in Aquaculture Cage Nets. *Langmuir* **2019**, *35*, 4328−4335.
(616) Pu, Y.; Hou, Z.; Khin, M. M.; Zamudio-Vázquez, R.; Poon, K. L.; Duan, H.; Chan-Park, M. B. Synthesis and Antibacterial Study of Sulfobetaine/Quaternary Ammonium-Modified Star-Shaped Poly[2-(dimethylamino)ethyl methacrylate]-Based Copolymers with an Inorganic Core. *Biomacromolecules* **2017**, *18*, 44−55.
(617) Zhao, J.; Zhu, Y.; He, G.; Xing, R.; Pan, F.; Jiang, Z.; Zhang, P.; Cao, X.; Wang, B. Incorporating Zwitterionic Graphene Oxides into Sodium Alginate Membrane for Efficient Water/Alcohol Separation. *ACS Appl. Mater. Interfaces* **2016**, *8*, 2097−2103.
(618) Sun, Z.; Wu, Q.; Ye, C.; Wang, W.; Zheng, L.; Dong, F.; Yi, Z.; Xue, L.; Gao, C. Nanovoid Membranes Embedded with Hollow Zwitterionic Nanocapsules for a Superior Desalination Performance. *Nano Lett.* **2019**, *19*, 2953−2959.
(619) Dobosz, K. M.; Kolewe, K. W.; Schiffman, J. D. Green Materials Science and Engineering Reduces Biofouling: Approaches for Medical and Membrane-Based Technologies. *Front. Microbiol.* **2015**, *6*, 196.
(620) Pan, J. R.; Su, Y.-C.; Huang, C.; Lee, H.-C. Effect of Sludge Characteristics on Membrane Fouling in Membrane Bioreactors. *J. Membr. Sci.* **2010**, *349*, 287−294.
(621) Mansouri, J.; Harrisson, S.; Chen, V. Strategies for Controlling Biofouling in Membrane Filtration Systems: Challenges and Opportunities. *J. Mater. Chem.* **2010**, *20*, 4567−4586.
(622) Hoek, E. M. V.; Bhattacharjee, S.; Elimelech, M. Effect of Membrane Surface Roughness on Colloid-Membrane Dlvo Interactions. *Langmuir* **2003**, *19*, 4836−4847.
(623) Coker, S.; Sehn, P. Four Years Field Experience with Fouling Resistant Reverse Osmosis Membranes. *Desalination* **2000**, *132*, 211−215.
(624) Avlonitis, S. A.; Kouroumbas, K.; Vlachakis, N. Energy Consumption and Membrane Replacement Cost for Seawater Ro Desalination Plants. *Desalination* **2003**, *157*, 151−158.
(625) Van Houdt, R.; Michiels, C. W. Biofilm Formation and the Food Industry, a Focus on the Bacterial Outer Surface. *J. Appl. Microbiol.* **2010**, *109*, 1117−1131.
(626) Hadidi, M.; Zydney, A. L. Fouling Behavior of Zwitterionic Membranes: Impact of Electrostatic and Hydrophobic Interactions. *J. Membr. Sci.* **2014**, *452*, 97−103.
(627) Li, Q.; Bi, Q.-Y.; Zhou, B.; Wang, X.-L. Zwitterionic Sulfobetaine-Grafted Poly(vinylidene fluoride) Membrane Surface with Stably Anti-Protein-Fouling Performance via a Two-Step Surface Polymerization. *Appl. Surf. Sci.* **2012**, *258*, 4707−4717.
(628) Li, M.-Z.; Li, J.-H.; Shao, X.-S.; Miao, J.; Wang, J.-B.; Zhang, Q.-Q.; Xu, X.-P. Grafting Zwitterionic Brush on the Surface of PVDF Membrane Using Physisorbed Free Radical Grafting Technique. *J. Membr. Sci.* **2012**, *405−406*, 141−148.
(629) Zhu, J.; Su, Y.; Zhao, X.; Li, Y.; Zhao, J.; Fan, X.; Jiang, Z. Improved Antifouling Properties of Poly(vinyl chloride) Ultrafiltration Membranes via Surface Zwitterionicalization. *Ind. Eng. Chem. Res.* **2014**, *53*, 14046−14055.
(630) Ma, T.; Su, Y.; Li, Y.; Zhang, R.; Liu, Y.; He, M.; Li, Y.; Dong, N.; Wu, H.; Jiang, Z. Fabrication of Electro-Neutral Nanofiltration Membranes at Neutral pH with Antifouling Surface via Interfacial Polymerization from a Novel Zwitterionic Amine Monomer. *J. Membr. Sci.* **2016**, *503*, 101−109.
(631) Yang, R.; Xu, J.; Ozaydin-Ince, G.; Wong, S. Y.; Gleason, K. K. Surface-Tethered Zwitterionic Ultrathin Antifouling Coatings on Reverse Osmosis Membranes by Initiated Chemical Vapor Deposition. *Chem. Mater.* **2011**, *23*, 1263−1272.
(632) Sun, H.; Zhang, Y.; Sadam, H.; Ma, J.; Bai, Y.; Shen, X.; Kim, J.-K.; Shao, L. Novel Mussel-Inspired Zwitterionic Hydrophilic Polymer to Boost Membrane Water-Treatment Performance. *J. Membr. Sci.* **2019**, *582*, 1−8.
(633) Chakrabarty, T.; Shahi, V. K. (3-Glycidoxypropyl) Trimethoxy Silane Induced Switchable Zwitterionic Membrane with High Protein Capture and Separation Properties. *J. Membr. Sci.* **2013**, *444*, 77−86.
(634) Liu, G.; Zhang, L.; Mao, S.; Rohani, S.; Ching, C.; Lu, J. Zwitterionic Chitosan-Silica-Pva Hybrid Ultrafiltration Membranes for Protein Separation. *Sep. Purif. Technol.* **2015**, *152*, 55−63.
(635) Azari, S.; Zou, L. Using Zwitterionic Amino Acid L-DOPA to Modify the Surface of Thin Film Composite Polyamide Reverse Osmosis Membranes to Increase Their Fouling Resistance. *J. Membr. Sci.* **2012**, *401−402*, 68−75.
(636) Zhou, Q.; Lei, X.-P.; Li, J.-H.; Yan, B.-F.; Zhang, Q.-Q. Antifouling, Adsorption and Reversible Flux Properties of Zwitterionic Grafted PVDF Membrane Prepared via Physisorbed Free Radical Polymerization. *Desalination* **2014**, *337*, 6−15.
(637) Kaner, P.; Dudchenko, A. V.; Mauter, M. S.; Asatekin, A. Zwitterionic Copolymer Additive Architecture Affects Membrane Performance: Fouling Resistance and Surface Rearrangement in Saline Solutions. *J. Mater. Chem. A* **2019**, *7*, 4829−4846.
(638) Tran, T.; Pan, S.; Chen, X.; Lin, X.-C.; Blevins, A. K.; Ding, Y.; Lin, H. Zwitterionic Hydrogel-Impregnated Membranes with Polyamide Skin Achieving Superior Water/Salt Separation Properties. *ACS Appl. Mater. Interfaces* **2020**, *12*, 49192−49199.
(639) Wang, A.; Fang, W.; Zhang, J.; Gao, S.; Zhu, Y.; Jin, J. Zwitterionic Nanohydrogels-Decorated Microporous Membrane with Ultrasensitive Salt Responsiveness for Controlled Water Transport. *Small* **2020**, *16*, 1903925.
(640) Li, Y.; Wu, H.; Yin, Y.; Cao, L.; He, X.; Shi, B.; Li, J.; Xu, M.; Jiang, Z. Fabrication of Nafion/Zwitterion-Functionalized Covalent Organic Framework Composite Membranes with Improved Proton Conductivity. *J. Membr. Sci.* **2018**, *568*, 1−9.

https://doi.org/10.1021/acs.chemrev.2c00344
Chem. Rev. 2022, 122, 17073−17154

(641) Yang, R.; Gleason, K. K. Ultrathin Antifouling Coatings with Stable Surface Zwitterionic Functionality by Initiated Chemical Vapor Deposition (iCVD). *Langmuir* **2012**, *28*, 12266−12274.
(642) Yang, R.; Jang, H.; Stocker, R.; Gleason, K. K. Synergistic Prevention of Biofouling in Seawater Desalination by Zwitterionic Surfaces and Low-Level Chlorination. *Adv. Mater.* **2014**, *26*, 1711−1718.
(643) Yang, R.; Goktekin, E.; Gleason, K. K. Zwitterionic Antifouling Coatings for the Purification of High-Salinity Shale Gas Produced Water. *Langmuir* **2015**, *31*, 11895−11903.
(644) He, K.; Duan, H.; Chen, G. Y.; Liu, X.; Yang, W.; Wang, D. Cleaning of Oil Fouling with Water Enabled by Zwitterionic Polyelectrolyte Coatings: Overcoming the Imperative Challenge of Oil-Water Separation Membranes. *ACS Nano* **2015**, *9*, 9188−9198.
(645) Zhu, Y.; Xie, W.; Zhang, F.; Xing, T.; Jin, J. Superhydrophilic In-Situ-Cross-Linked Zwitterionic Polyelectrolyte/PVDF-Blend Membrane for Highly Efficient Oil/Water Emulsion Separation. *ACS Appl. Mater. Interfaces* **2017**, *9*, 9603−9613.
(646) Venault, A.; Chang, C.-Y.; Tsai, T.-C.; Chang, H.-Y.; Bouyer, D.; Lee, K.-R.; Chang, Y. Surface Zwitterionization of PVDF VIPS Membranes for Oil and Water Separation. *J. Membr. Sci.* **2018**, *563*, 54−64.
(647) Zang, L.; Zheng, S.; Wang, L.; Ma, J.; Sun, L. Zwitterionic Nanogels Modified Nanofibrous Membrane for Efficient Oil/Water Separation. *J. Membr. Sci.* **2020**, *612*, 118379.
(648) Venault, A.; Chen, L.-A.; Maggay, I. V.; Marie Yap Ang, M. B.; Chang, H.-Y.; Tang, S.-H.; Wang, D.-M.; Chou, C.-J.; Bouyer, D.; Quémener, D.; et al. Simultaneous Amphiphilic Polymer Synthesis and Membrane Functionalization for Oil/Water Separation. *J. Membr. Sci.* **2020**, *604*, 118069.
(649) Zhu, Y.; Wang, J.; Zhang, F.; Gao, S.; Wang, A.; Fang, W.; Jin, J. Zwitterionic Nanohydrogel Grafted PVDF Membranes with Comprehensive Antifouling Property and Superior Cycle Stability for Oil-in-Water Emulsion Separation. *Adv. Funct. Mater.* **2018**, *28*, 1804121.
(650) Zhu, Y.; Zhang, F.; Wang, D.; Pei, X. F.; Zhang, W.; Jin, J. A Novel Zwitterionic Polyelectrolyte Grafted PVDF Membrane for Thoroughly Separating Oil from Water with Ultrahigh Efficiency. *J. Mater. Chem. A* **2013**, *1*, 5758−5765.
(651) Liang, B.; Zhang, G.; Zhong, Z.; Sato, T.; Hozumi, A.; Su, Z. Substrate-Independent Polyzwitterionic Coating for Oil/Water Separation Membranes. *Chem. Eng. J.* **2019**, *362*, 126−135.
(652) Zhou, L.; Xiao, G.; He, Y.; Wu, J.; Shi, H.; Zhong, F.; Yin, X.; Li, Z.; Chen, J. Multifunctional Filtration Membrane with Anti-Viscous-Oils-Fouling Capacity and Selective Dyes Adsorption Ability for Complex Wastewater Remediation. *J. Hazard. Mater.* **2021**, *413*, 125379.
(653) Yang, R.; Moni, P.; Gleason, K. K. Ultrathin Zwitterionic Coatings for Roughness-Independent Underwater Superoleophobicity and Gravity-Driven Oil-Water Separation. *Adv. Mater. Interfaces* **2015**, *2*, 1400489.
(654) Li, C.; Li, X.; Tao, C.; Ren, L.; Zhao, Y.; Bai, S.; Yuan, X. Amphiphilic Antifogging/Anti-Icing Coatings Containing POSS-PDMAEMA-*b*-PSBMA. *ACS Appl. Mater. Interfaces* **2017**, *9*, 22959−22969.
(655) Tao, C.; Bai, S.; Li, X.; Li, C.; Ren, L.; Zhao, Y.; Yuan, X. Formation of Zwitterionic Coatings with an Aqueous Lubricating Layer for Antifogging/Anti-Icing Applications. *Prog. Org. Coat.* **2018**, *115*, 56−64.
(656) Liang, B.; Zhang, G.; Zhong, Z.; Huang, Y.; Su, Z. Superhydrophilic Anti-Icing Coatings Based on Polyzwitterion Brushes. *Langmuir* **2019**, *35*, 1294−1301.
(657) Qi, H.; Zhang, C.; Guo, H.; Zheng, W.; Yang, J.; Zhou, X.; Zhang, L. Bioinspired Multifunctional Protein Coating for Antifogging, Self-Cleaning, and Antimicrobial Properties. *ACS Appl. Mater. Interfaces* **2019**, *11*, 24504−24511.
(658) Sui, X. J.; Guo, H. S.; Chen, P. G.; Zhu, Y. N.; Wen, C. Y.; Gao, Y. H.; Yang, J.; Zhang, X. Y.; Zhang, L. Zwitterionic Osmolyte-Based Hydrogels with Antifreezing Property, High Conductivity, and Stable Flexibility at Subzero Temperature. *Adv. Funct. Mater.* **2020**, *30*, 1907986.
(659) Sui, X.; Guo, H.; Cai, C.; Li, Q.; Wen, C.; Zhang, X.; Wang, X.; Yang, J.; Zhang, L. Ionic Conductive Hydrogels with Long-Lasting Antifreezing, Water Retention and Self-Regeneration Abilities. *Chem. Eng. J.* **2021**, *419*, 129478.
(660) Wen, C.; Guo, H.; Bai, H.; Xu, T.; Liu, M.; Yang, J.; Zhu, Y.; Zhao, W.; Zhang, J.; Cao, M.; et al. Beetle-Inspired Hierarchical Antibacterial Interface for Reliable Fog Harvesting. *ACS Appl. Mater. Interfaces* **2019**, *11*, 34330−34337.
(661) Liu, X.; Cheng, P. Dropwise Condensation Theory Revisited Part II. Droplet Nucleation Density and Condensation Heat Flux. *Int. J. Heat Mass Transfer* **2015**, *83*, 842−849.
(662) Wen, C.; Guo, H.; Zhu, Y.; Bai, H.; Zhao, W.; Wang, X.; Yang, J.; Cao, M.; Zhang, L. Fully Superhydrophilic, Self-Floatable, and Multi-Contamination-Resistant Solar Steam Generator Inspired by Seaweed. *Engineering* **2022**, DOI: 10.1016/j.eng.2021.06.029.
(663) Wen, C.; Guo, H.; Yang, J.; Li, Q.; Zhang, X.; Sui, X.; Cao, M.; Zhang, L. Zwitterionic Hydrogel Coated Superhydrophilic Hierarchical Antifouling Floater Enables Unimpeded Interfacial Steam Generation and Multi-Contamination Resistance in Complex Conditions. *Chem. Eng. J.* **2021**, *421*, 130344.
(664) Yuan, Y. L.; Ai, F.; Zhang, J.; Zang, X. B.; Shen, J.; Lin, S. C. Grafting Sulfobetaine Monomer onto the Segmented Poly(ether-urethane) Surface to Improve Hemocompatibility. *J. Biomater. Sci., Polym. Ed.* **2002**, *13*, 1081−1092.
(665) Yuan, J.; Zhang, J.; Zhou, J.; Yuan, Y. L.; Shen, J.; Lin, S. C. Platelet Adhesion onto Segmented Polyurethane Surfaces Modified by Carboxybetaine. *J. Biomater. Sci., Polym. Ed.* **2003**, *14*, 1339−1349.

https://doi.org/10.1021/acs.chemrev.2c00344
Chem. Rev. 2022, 122, 17073−17154